RELIABILITY:
THEORY&APPLICATIONS

RELIABILITY

RISK ANALYSIS

Vol.16
No.1 (61)
•
March
2021

MAINTENANCE

SAFETY

San Diego

RELIABILITY:

THEORY & APPLICATIONS

San Diego
2021

Editorial Board

Kaminsky, Mark (USA)
PhD, principal reliability engineer at the NASA Goddard Space Flight Center
e-mail: mkaminskiy@hotmail.com

Krivtsov, Vasiliy (USA)
PhD. Director of Reliability Analytics at the Ford Motor Company. Associate Professor of Reliability Engineering at the University of Maryland (USA)
e-mail: VKrivtso@Ford.com, krivtsov@umd.edu

Lemeshko Boris (Russia)
Doctor of Sci., Professor, Novosibirsk State Technical University, Professor of Theoretical and Applied Informatics Department
e-mail: Lemeshko@ami.nstu.ru

Lesnykh, Valery (Russia)
Doctor of Sci. Director of Risk Analysis Center, 20-8, Staraya Basmannaya str., Moscow, Russia, 105066, LLC "NIIGAZECONOMIKA" (Economics and Management Science in Gas Industry Research Institute)
e-mail: vvlesnykh@gmail.com

Levitin, Gregory (Israel)
PhD, The Israel Electric Corporation Ltd. Planning, Development & Technology Division. Reliability & Equipment Department, Engineer-Expert; OR and Artificial Intelligence applications in Power Engineering, Reliability.
e-mail: levitin@iec.co.il

Limnios, Nikolaos (France)
Professor, Université de Technologie de Compiègne, Laboratoire de Mathématiques, Appliquées Centre de Recherches de Royallieu, BP 20529, 60205 COMPIEGNE CEDEX, France
e-mail: Nikolaos.Limnios@utc.fr

Papic, Ljubisha (Serbia)
PhD, Professor, Head of the Department of Industrial and Systems Engineering Faculty of Technical Sciences Cacak, University of Kragujevac, Director and Founder The Research Center of Dependability and Quality Management (DQM Research Center), Prijevor, Serbia
e-mail: dqmcenter@mts.rs

Zio, Enrico (Italy)
PhD, Full Professor, Direttore della Scuola di Dottorato del Politecnico di Milano, Italy.
e-mail: Enrico.Zio@polimi.it

e-Journal *Reliability: Theory & Applications* publishes papers, reviews, memoirs, and bibliographical materials on Reliability, Quality Control, Safety, Survivability and Maintenance.

Theoretical papers have to contain new problems, finger <u>practical applications</u> and should not be overloaded with clumsy formal solutions.

Priority is given to descriptions of case studies.
General requirements for presented papers

1. Papers have to be presented in English in MS Word or LaTeX format.
2. The total volume of the paper (with illustrations) can be up to 15 pages.
3. A presented paper has to be spell-checked.
4. For those whose language is not English, we kindly recommend using professional linguistic proofs before sending a paper to the journal.

The manuscripts complying with the scope of journal and accepted by the Editor are registered and sent for external review. The reviewed articles are emailed back to the authors for revision and improvement.

The decision to accept or reject a manuscript is made by the Editor considering the referees' opinion and taking into account scientific importance and novelty of the presented materials. Manuscripts are published in the author's edition. The Editorial Board are not responsible for possible typos in the original text. The Editor has the right to change the paper title and make editorial corrections.

The authors keep all rights and after the publication can use their materials (re-publish it or present at conferences).

Publication in this e-Journal is equal to publication in other International scientific journals.

Papers directed by Members of the Editorial Boards are accepted without referring.
The Editor has the right to change the paper title and make editorial corrections.

The authors keep all rights and after the publication can use their materials (re-publish it or present at conferences).

Send your papers to Alexander Bochkov, e-mail: a.bochkov@gmail.com

Table of Contents

V. S. Kharchenko, M. A. Yastrebenetsky

Concept of Big Safety (BS) is discussed. BS is a result of crossing of the following 10Big: Big property (nuclear safety, radiation safety, functional safety, information (cyber) security, fire safety ,physical safety, infection safety, safety from natural hazards, etc.); Big/complex environment (a lot of factors of influence and parameters); Big/complex system; Big value of a fatal failure or event; Big number of causes of failure; Big data which should be processed; Big number of requirements to safety; Big time and process complexity of development of systems; Big toolbox for safety assessment and assurance; Big resources for assurance and recovery. General principles and methods for assessing and assurance of Big Safety are described considering experience of different critical domains, first of all, NPPs. Some well-known accidents in context of Black Swan theory are analyzed. The strategies of Black Swan tolerance are proposed.

Nafisatu Muhammad Usman, Ibrahim Yusuf

The paper deals with modeling and performance assessment of a series-parallel with independent failures using the Markov Birth-Death method and the probabilistic approach. The system consists of five subsystems arranged in series and parallel configurations with three possible states of operation, reduced capacity and failure. First-order systems of ordinary differential equations are developed and recursively resolved using a probabilistic approach via the transition diagram. The state probabilities for the proposed scheme are derived. Using state probabilities, system availability expressions, busy repairman probabilities due to minor and major failures as well as benefit feature are calculated. Profit and availability matrices for each subsystem have been computed to provide various output values for different combinations of parameters. The finding of this paper will boost the efficiency of the system and will be useful for timely maintenance progress, decision-making, preparation and optimization.

Eesha Mishra, Santosh Kumar

Blockchain is inalterable and simple confirmable framework that has a noteworthy potential to be an option in contrast to customary races. It carries savvy answers for focal power issue as far as squares having all information in blockchain. In past decades customary races neither fulfill the residents nor government official. The democratic isn't completely made sure about, compromises security and straightforwardness of voters alongside having an excess of time to check the vote. In this paper, we proposed a model that giving the arrangement utilizing the blockchain to dispense with all drawbacks of customary decisions. The security of information, votes and voter is guaranteed in the framework. The sitting tight an ideal opportunity for result diminished fundamentally through the proposed model.

Evaluation of reliability is most important when we have to check the availability of supply in any distribution system. A basic reliability index which is of importance is failure rate of the distribution system. In this paper evaluation of system data i.e. failure rate which is one of the important basic reliability indices of Roy Billinton test system (RBTS) Bus-2 distribution system for educational purpose is done. This paper also evaluates the reliability of each and every feeder section of the RBTS. The mean time to failure (MTTF) of the feeders is also evaluated for each and every feeder section of the distribution system of the RBTS Bus-2 distribution system. The evaluated system data and various reliability indices can be used for educational purpose.

In Germany an App has been introduced to cope with the Corona epidemic. In this paper we describe, how the app works and analyze the semi-quantitative risk model that has been used in the app, because a large number of semi-quantitative risk models are known that are not consistent. Further we discuss in how far the Corona app in its current state can contribute to mitigate the pandemic. The risk model of the German Corona warning app has several interesting, somewhat puzzling properties. In this paper we describe the analysis and its results related to the underlying risk model.

The article discusses some common mathematical models of counterterrorism and acts of unlawful interference with protected objects. The use of methods of queuing theory of Markov and non-Markov types for modeling the counteraction of security personnel by a malicious group with a random number of criminals in a group and different ways of organizing the actions of such personnel is proposed.

One of the basic problems of electro power systems is absence of the normative documents regulating operation, maintenance service and repair of the capital equipment, which service life exceeds normative value. We shall name them «oldtech» (OT). The essence of the difficulties demanding overcoming is reduced to absence of methodologies a quantitative estimation of operative reliability and safety of OT, with the subsequent benchmarking of OT. Considering the science-intensive, bulkiness and labour input of the decision of this problem indisputable becomes necessity of development of the corresponding automated systems. In present article, some features of an estimation of an integrated indicator and benchmarking unique objects are resulted. To unique objects, which analogues on the set combination of versions of significant attributes are absent concern. For an illustration of recommended methods and algorithms technical and economic parameters of power units with SGI-400 are used.

Mohd Arif Khan, Ahteshamul Haq, Aquil Ahmed

In this paper, we present the development of a daily diet model using fuzzy multi-objective goal programming (GP) to satisfy daily nutrient. We have designed the objective function as minimize the cost of diet, Saturated Fat and carbohydrate. This paper consists of ten consumed foodstuffs as the decision variable. The daily diet's tolerable lower and upper intake level is given for the Protein, Vit. B6, Vit. C and Calcium. This paper aims to present a stepwise solution procedure based on fuzzy GP to obtain the compromise solution of the diet problem. Finally, a numerical example is illustrated to compare the daily diet plan with weighted GP, pre-emptive GP and fuzzy GP.

Kamlesh Kumar Shukla

In this paper, new lifetime distribution has been proposed which is an inverse of Ishita distribution Shanker and Shukla (2017). Its statistical and mathematical properties including Reneyi entropy and Stress-strength reliability measure have been discussed. Maximum likelihood estimation method has been used to estimate its parameter. Simulation study has also been carried out to check the behavior of maximum likelihood estimator. Finally, proposed distribution has been applied on lifetime datasets and compares its superiority over other inverse lifetime distributions.

Deepthi K. S., Chacko V. M

In this paper, increasing convex (concave) Total Time on Test (TTT) transform of a lifetime random variable is considered. In order to identify the failure rate model of functions of random variables, the TTT of transformed data can be used. Some properties of the transforms are derived. Some examples are given.

Neena Krishna P K, Dr S Jayalakshmi

Acceptance Sampling performs a major role in industry for monitoring process and assessing complains for reducing the cost and inspection time. A truncated life test may be conducted to determine the smallest sample size to ensure certain percentile life time of an items. The operating characteristic function values are obtained according to different quality levels and the minimum ratios of the true average life to the specified average life at the specified producer's risk are derived. Useful tables are provided for the proposed sampling plan.

M. L. Soujanya, P. Vijaya Laxmi, E. Sirisha

In this paper we analyzed an inventory model with two-suppliers, finite life times, multiple working vacations and customers who arrive according to RCE process. Perishable and replenishment rates of two-suppliers are exponentially distributed. The server takes exponential working vacations when the queue is empty. Arrival process follows Poisson distribution and the probability for an ordinary customer is p and for negative customer is q. Limiting distribution of the assumed model is obtained. Numerical results are presented for cost function and various system performance parameters. The impact of two-suppliers on the optimal reorder points will be useful in developing strategies for handling various perishable inventory problems with replenishment rates.

Zinovi Krougly

Numerical Laplace transform and inverse Laplace transform is a challenging task in queueing theory and others probability models. A double transformation approach is used to find stable, accurate, and computationally efficient methods for performing the numerical Laplace and inverse Laplace transform. To validate and improve the inversion solution obtained, direct Laplace transforms are taken of the numerically inverted transforms to compare with the original function. Algorithms provide increasing accuracy as precision level increases. The most promising methods were applied to computational probability models, when there are no closed-form solutions of the Laplace transform inversion. The computational efficiency compared to precision levels is demonstrated for different service models in $M/G/1$ queuing systems.

Yogesh Pal Singh, Santosh Kumar, Madhulika Singh

The revolutionary discovery in forensic investigation in DNA fingerprinting that helps to identify individuals it is an important tool for molecular research that support the human breeding. DNA fingerprinting model played an important role in identifying an individual in millions of people by looking in unique patterns in their DNA. DNA fingerprinting is a technique that simultaneously detects lots of minisatellites in genome to produce a pattern unique to an individual. In this research work, we analyzed DNA fingerprinting based identification and designed a DNA fingerprinting based identification model along with DNA database management system for 360 degree interlinking i.e. all services and progresses will be progressed by DNAFIDs and database.

Rakesh Kumar, Bhavneet Singh Soodan, Sapana Sharma

In this paper, we study a finite capacity single server queuing model with balking and correlated reneging and discuss its application in queues at health care facilities. The reneging considered so far in the queuing literature is a function of system-state. In many practical situations, reneging may depend on factors other than the system-state. For instance, in health care systems the reneging of patients at two consecutive time marks may be correlated in a sense that if a patient reneges at a time mark then there is a probability that a patient may renege at the next time mark due to the factors like improper check-up, sluggish management, unnecessary costly prescription by doctors, etc. The steady-state solution of the model is derived by using matrix-decomposition method. Finally, the transient performance analysis of the model is performed using Runge-Kutta method.

Albin Paul, K.K. Jose

In this paper we consider an extension of the linear exponential distribution based on the Harris generalization method, which includes some of the life time distribution as sub models. Along with the four parameter generalization namely Harris generalized linear exponential distribution, we derive some of its properties such as moments, quantiles and moment generating function. A compound form expression of the density function is given. For the given model the R´enyi entropy, mean residual life and the distribution of order statistics is derived. The problem of estimation of parameters is considered and validated with respect to two real data sets.

Neelesh Gupta, A. R. Nigwal, U. K. Khedlekar

In this article, we have developed an imperfect production system under the following four different cases. The first one is imperfect production with rework, and without disruption, second one is imperfect production with rework and disruption, third one is imperfect production with rework, disruption, and without backlogging, fourth one is imperfect production with rework, disruption and backlogging. For these all cases, we have optimized the regular production time, rework production time, backlog time and backlog quantity. In this article we have considered the demand rate, production rate defective item's production rate and deteriorating rate are all constant. We have also considered the production rate is always grater than the demand rate. The model is illustrated by numerically and analyzed by graphically.

K. H. Ibrahim, M. S. Isa, M. I. Abubakar, I. Yusuf, I. Tukur

In relation to types and advantages of computer network topologies, in this research work, availability and cost analysis of complex computer network is considered to focus on a tree topology network that has four subsystems A,B,C and D and all the subsystems are figured in series and parallel configuration, the subsystem A and B served as computer servers together with two units each and are working 1-out-of-2: G/F policy while C and D subsystems both has three units and are working in 2-out-of-3: G/F scheme, A and B attached to subsystems C and D respectively. The system has two types of failure, degraded (partial failure) or complete failed states. The system is analyzed using supplementary variables techniques and Laplace transform. Copula family and general distribution are employed to restore the complete failed and partial failed states respectively. Computed results have been highlighted by the means of tables and graphs.

Dhruv Raghav, D.K. Rawal, Ibrahim Yusuf, Rabiu Hamisu Kankarofi, V.V. Singh

The present paper intends to design and development reliability models for the analysis of distributed hardware-software system. For the determination of reliability and system performance, the study analyzed a distributed system consisting of a single host with two heterogeneous software running on the host and two identical servers configured as series-parallel system. Both client (host), software and server's failure time are to be exponentially distributed while repairs follow two forms of distributions that are general and Gumbel-Hougaard family copula. The system is analyzed using supplementary variable technique with implications of Laplace transforms. The results are presented in tables and graphs. Some important measures of reliability such as availability of system, reliability of the system, MTTF and cost analysis have been discussed. Some particular cases have also been derived and examined to see the practical effect of the model.

Naijun Sha

Copula is a powerful tool to describe dependence among variables and has gained significant attention in many fields of research. In this paper, we study modeling the lifetimes of two fundamental hybrid systems: series-parallel and parallel-series by copula functions to reflect the effect on dependence of working components in the systems. We consider Farlie-Gumbel-Morgenstern (FGM) and Clayton copula functions to represent dependent structures in parallel and series configuration, respectively. A flexible lifetime distribution, the extended exponential distribution, is applied to the components of system. The explicit expressions of the reliability and mean time to failure (MTTF) of both hybrid systems are obtained. For the purpose of illustration, the effect of different degrees on dependence among components is analyzed and presented for various parameter settings in the lifetime distribution.

About Conception of Big Safety

V.S. Kharchenko

●

National Aerospace University "KhAI", Kharkiv, Ukraine
v.kharchenko@csn.khai.edu

M.A. Yastrebenetsky

●

State Scientific and Technical Center for Nuclear and
Radiation Safety, Kharkiv, Ukraine
ma_yastreb@mail.ru

Abstract

Concept of Big Safety (BS) is discussed. BS is a result of crossing of the following 10Big: Big property (nuclear safety, radiation safety, functional safety, information (cyber) security, fire safety ,physical safety, infection safety, safety from natural hazards, etc.); Big/complex environment (a lot of factors of influence and parameters); Big/complex system; Big value of a fatal failure or event; Big number of causes of failure; Big data which should be processed; Big number of requirements to safety; Big time and process complexity of development of systems; Big toolbox for safety assessment and assurance; Big resources for assurance and recovery. General principles and methods for assessing and assurance of Big Safety are described considering experience of different critical domains, first of all, NPPs. Some well-known accidents in context of Black Swan theory are analyzed. The strategies of Black Swan tolerance are proposed.

Keywords: Big safety, safety, infection safety, diversity, defense-in-depth, Black Swan

I. Introduction

The global news trend of the last 12 months is related to the Covid-19 pandemic, which affects hundreds of thousands of people every day on all continents. The pandemic has caused a serious economic crisis, the effects of which have yet to be assessed, survived and returned to the growth point. It certainly affects the stable functioning of entire industries and industrial facilities, including those commonly referred to as critical, including aviation, maritime and railway transport, chemical plants and oil and gas utilities, nuclear power plants, etc. These circumstances make it necessary to address the safety of critical objects and the systems that control them in the face of new Covid-19-related and non-Covid-19-related challenges.

This paper is an elaboration of the ideas of the [1] written at the beginning of the coronavirus quarantine and dealt with the safety of nuclear power plants (NPP) and the so-called big safety in the time of Covid-19. The authors began to develop the concept of big safety (BS), which integrates different kinds of safety of information and control systems (ICS), controlled objects and infrastructures, and formulated some provisions of big safety taking into account its new component - infectious safety. We had some doubts as to whether such issues would be relevant in the context of coronavirus in a few months' time. Unfortunately, it is even more urgent now given,

first, the dynamics of the pandemic and, second, the global safety challenges that have developed before and during the pandemic.

In addition, this paper is a natural extension of the results obtained over, the past decades and published in two books by US publisher IGI Global in 2014 and 2020 [2,3]. They focus on the functional and information (cyber) safety aspects of NPP ICS. NPPs and their multiple control systems are perhaps one of the most complex, critical and well developed from safety point of view objects. NPPs, in turn, are part of the critical energy infrastructure and the critical infrastructure of the state as a whole, and are therefore an excellent case study for understanding big safety.

An additional motivation was also that this problem is now being addressed in many online events. In particular, at the 11th International IEEE Conference Dependable Systems, Services and Technologies Professor A. Rucinski [4] held a Round Table "Trusted Dependability, Safety and Safety in Covid-19 Time", which started the formation of a platform dedicated to the discussion of BS by experts from Ukraine, USA, UK, France, FRG, Poland, Bulgaria and other countries.

There are two trends in every science - centrifugal (aimed at clarifying and justifying ways of solving problems related to specific classes of objects and their individual properties, in particular safety components) and centripetal (aimed at combining and generalizing the results obtained to a broader class of objects). Colossal number of works have been produced on various aspects of safety. The number of references to the word Safety on the Internet was 3.010.000.000, to the word Security was 6.630.000.000 at the end of 2020. It should be said that the number of works and references on the Internet, to word combinations of these terms with such popular ones as Bid Data, Internet of Things, Artificial Intelligence is growing very fast - only for 2017-2019 their number has increased tenfold [5], For example, the numbed of citations for phrases Big Data for safety has increased 7.2-fold (123000000 citation in 2018), and for phrases safety of Big Data - 11.5-fold (215000000 citations in 2018). Some aspects of application of Internet of Things, Big Data technologies for safety of critical systems, in particular NPPs. were considered in [6,7].

There are disproportionately fewer works on general safety issues, to which this article is devoted. The closest to the authors of this paper is the book by Y. Rudenko and I. Ushakov "Reliability of power systems" [8], where a methodical approach to the analysis of reliability of various power systems, including coal, oil and gas. etc., is developed. Besides, many papers research aspects of complex safety considering different types of influence on systems and complexity of the systems, for example [9,10]. The papers [11-13] discuss directions of safety science and describe methods of scientometric mapping for the safety science community taking into account huge number of publications.

This paper supports the centripetal trend. Methodological aspects of safety analysis of large critical systems, such as rocket and space complexes, have been studied by NASA specialists, in particular by its leading expert N. Levenson [14]. She proposed the concept of comprehensive functional safety of such complexes and even patented a special term safeware. It similarly with hardware, software and the other X-ware defines a set of measures and tools to ensure safety including systems and computer safety. It should be noted that aspects of cybersafety and some other types of BS big safety have not been addressed in this methodology.

A separate direction in safety theory has developed in the last 20 years in relation to critical infrastructures - energy grids, transport complexes, etc. [15-17], including in the context of building resilient systems [18]. Many works are devoted to human activities in emergency situations, where natural disasters and accidents of various man-made objects and methods of disaster and accident tolerance analysis and assurance are described [19-21]).

Note that the term 'Big Safety' was mentioned in the context of big data analysis and the development of the SIEM (Safety information and event management) concept [22] and implied primarily aspects of integrity, confidentiality and other attributes of information security and its

management. In this work we try to change the methodology of approach to the analysis of safety, namely to go to its cognition not only, and maybe not so much cased on the prevalence of scale of the analyzed object, when a pair of concepts "big system" and "safety" automatically generates the concept "big safety". We believe that it is necessary to be based on the prevalence of scale, multidimensionality of safety itself in all its manifestations for different systems, which allow using the adjective "big". This makes it advisable to form general concept of BS, taking into account different types of objects and different types of safety.

An important approach in shaping and making sense of BS is the use of the principle of comparativistics, i.e. comparing methods for assessing and ensuring the safety of objects of different purposes for selection and dissemination. Such studies have been conducted previously for control systems of NPP and carrier rockets [23], and later for NPP and rocket-space complexes [24]. It is also important to consider the impact of Covid-19 on the emergence of new safety deficits in the context of modern technology [25].

Thus, the purpose of this research is to develop the concept of BS, analyze its attributes and interconnection of safety types, some principles and methods for its assessment and assurance, based on the experience gained in the nuclear power industry, in particular in the digital ICS of NPP, which form their IT infrastructure.

The paper is structured as follows. The second section analyses the concept of BS, describes its attributes and classifies the objects and types of BS. The third section discusses the principles and methods of BS analysis and assurance, taking into account the experience of providing functional and cyber safety of NPP ICS. The fourth section discusses the important black swan phenomenon in terms of BS and considers some principles for mitigating its effects. The fifth section concludes the article and describes directions for further research.

II. Conception and Features of Big Safety

I. 10 B Attributes of Big Safety

By BS we will understand the multi-species (informational, functional, physical, infectious, etc.) safety of technical and organization -technical systems in which: many functions are performed and many safety-critical processes are carried out; a significant amount of heterogeneous, rapidly changing and safety-critical data is generated, transmitted, stored and processed; disruption of functioning processes and data circulating in systems can cause a transition to a critical emergency state, which can lead to significant material losses, risks to human health and life, and environmental disasters.

.Big Safety is a result of crossing of the following 10 "Big":

1. Big/Complex Property (BPR). Big safety combines different types of safety such as
   - nuclear safety (NS),
   - radiation safety (RS),
   - functional safety (FnS),
   - information (cyber) safety (InS),
   - fire safety (FrS),
   - physical safety (PS),
   - infection safety (IfS),
   - safety from natural hazards (disasters): seismic safety (SsS), flooding safety (FIS) etc.,
   - transport safety (TS),
   - ecological safety (ES),
   - chemical safety (ChS),

- food safety (FdS), etc.

The different types of safety for different critical systems interact with each other in different combinations. A typical example of an object where different types of safety interact is a NPP, for which the first 9 safety types listed are essential. Note that transport safety is important because of the need to transport fresh and spent nuclear fuel. By definition NPP safety is the property of not exceeding the established limits of radiation impact on personnel, the public and the environment during normal operation of a NPP, operational disturbances and design basis accidents, as well as limiting radiation impact during beyond design basis accidents [26].

The set of NPP BS types is shown on Figure 1. The narrows illustrate the influence of BS types one to one.
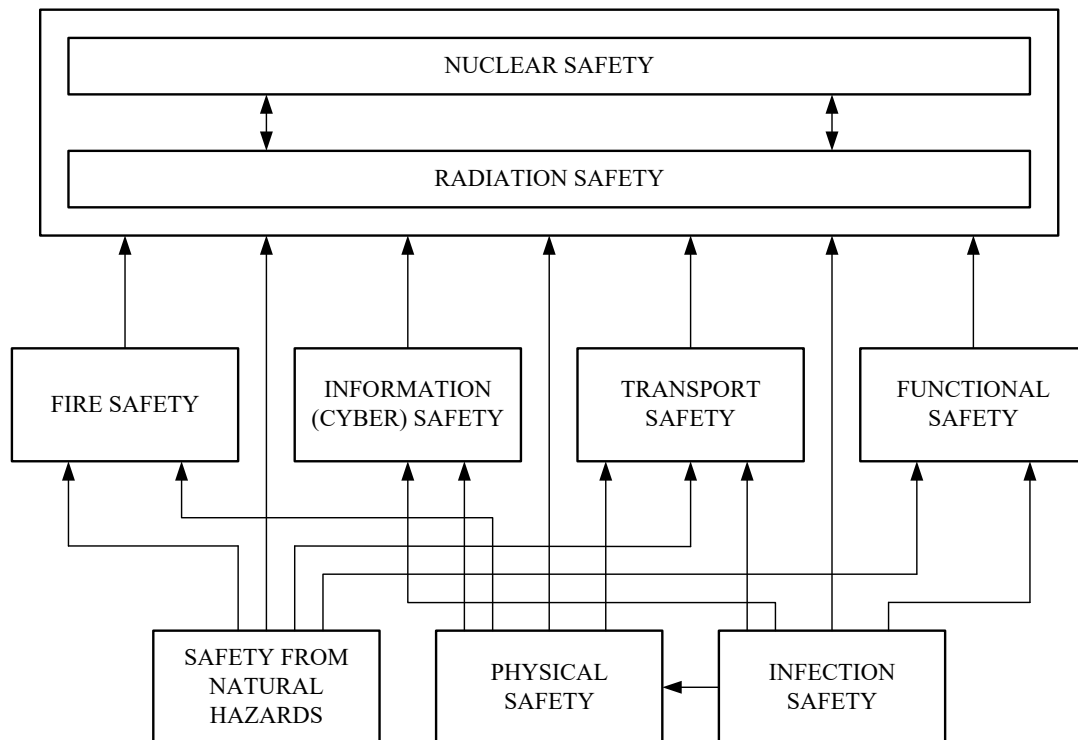
Figure 1: *Interconnection of Big Safety properties for NPP*

The hierarchy of big safety properties depends on the scope of critical systems such as safety critical, security critical, availability critical and so on.

2. Big/Complex Environment (BEN). The concept of BS is characterised by the fact that the behaviour of a (large) system is considered in a complex environment which influences the system - carries out impacts - of various types: physical (with a large number of different parameters - temperature and humidity, vibration, seismic, electromagnetic, radiation....), informational (changing input data, unauthorised impacts through data entry, changes in control panel elements, attacks on vulnerabilities...), nuclear and radiological, biological (induction of the system to a potentially dangerous or dangerous - emergency state). Each of these impacts or combinations of impacts can result in the system entering a potentially dangerous or hazardous - emergency state.

3. Big/Complex System (BSS). Most often, BS is characteristic of a large/complex system, which consists of a large number or complex interrelated software, technical, ergative components and subsystems/systems. Each of these components, subsystems is characterised by a certain level of reliability and safety. In this case, we can talk about positive or negative safety synergies at the component-subsystem-system level, which are assessed by different indicators.

In large systems, the object of safety is divided into two parts: controlled (e.g. process

equipment, level of operation technologies, OT) and controlling (level of information technologies. IT) which have become more and more convergent recent years. Controlling (or instrumentation and control) systems are generally man-machine systems, and personal is a very important part of the systems in terms of safety and security. A control system can be categorised as a big system too.

4. Big Failure/ Big or Huge Value of a Fatal Failure or Event (BFV). BS is characterised by the fact that it is considered in relation to so-called critical objects - critical failures or other events with serious material loss, loss of health or threat to human life. That is, such objects and their control systems are systems of great responsibility.

5. Big Number of Reasons/ Causes of Fatal Failure (BRF). A large number of causes usually lead to a large number of breaches of safety. The various safety violations often overlap over time ("trouble does not come alone") or are disrupted by a domino effect.

6. Big Data (BDT). To safety ensure and control, large amounts of data from tens or hundreds of thousands of sensors, other sources of information that can change dynamically, have high variability, etc., must be analysed. They are described by number of letters V (from 3 to 7). They are described by a metric where number has a value between three and seven. In order to obtain, process this data, safety control systems are built into the object of analysis and maintenance of safety, which are based on cybernetic, principles and big data processing, implementing predictive analytics methods.

7. Big Requirements to Safety (BRQ). Today's safety-critical systems must comply with hundreds and thousands of requirements of branch, national and international standards that are designed for different domains and common to all systems. Examples of such "universal" standards are: IEC 61508 [27], ISO/IEC 15408 [28], ISO 62443 [29].

8. Big Time and Process Complexity of Development Implementation and Operation of Safe Systems (BTP). A distinctive feature of the critical systems in question is that they are built over a long period of time, involving a large number of engineers, managers and auditors. Reliability of systems is built up during development, ensured during production and maintained during application. In the case of a high level of safety. this is incorporated into, produced and maintained during development, production and use. Regulatory, (independent) verification and validation processes are also mandatory here.

9. Big Toolbox (set of methods, techniques and tools) for Safety Assessment and Assurance (BMT). A large number of different methods techniques and tools are used for safety assessment and assurance at different stages of the life cycle of systems. Universal methods and techniques used for safety assessment include failure modes and effects criticality analysis, block diagram based assessment fault tree analysis, Markov's chain based assessment and others [3, 30].

10. Big Resources for Assurance and Recovery (BRR). BS requires colossal resources. The cost of developing and implementing safety systems for facilities such as AEC is in the tens and hundreds of millions of dollars. However, it will cost even more in the event of a breach. Japan's economy, trade, and industry ministry recently (as of 2016) estimated the total cost of dealing with the Fukushima disaster at ¥21.5 trillion (US$187 billion), almost twice the previous estimate of ¥11 trillion (US$96 billion) [31].

In our opinion BPR, BEN, BFV, BRF are key attributes among 10B.

II. Objects of Big Safety

BS objects are divided into global and local depending on the size of the object and the consequences of safety violations.

Global **Objects**. In this case there may be dangers to humanity as whole. Examples are infections, volcanic eruptions and earthquakes, a celestial body falling to earth, a nuclear disaster

(war with nuclear weapons). The most pressing hazard that has affected and continues to affect humanity as a whole is Covid-19. According to research the COVID-19 pandemic will likely end up costing between S8.1 trillion and S15.8 trillion worldwide [31]. As of 1/01/2021, some 1.8 million people had died of Covid-19.

Local **Objects**. For these objects, the impact is on a group of people of a specific area. Examples: accidents at nuclear power plants, hydroelectric plants (dams, hydroelectric power plants), chemical, oil and gas production facilities, transport accidents. One of the most recent accidents was a nitrate explosion in Beirut that destroyed a large part of the city.

Note that the boundary between BS for global and local objects is difficult to delineate. The consequences of accidents at local facilities, such as NPP, can take on a national and cross-national character.

III. Analysis of Big Safety Types

The concept of BS consists in its representation taking into account the scale and importance of the system, the volume and sensitivity of the data in the system, the variety of factors and channels of unacceptable violations of the system. The formation and implementation of the BS concept should take into account concepts that are already in use and are defined in standards (in particular [28]):

- system assets (AoS), i.e. its resources that are critical in terms of various types of BS and to be protected;
- safety space (SoS) and perimeter (PoS). The former defines a multi-dimensional space characterised by the values of information, signalling, physical and other parameters at which the system is in a safe state; the SoS is the space in which AoSs are embedded. PoS is characterized by the limit values of these parameters;
- threats, causes, factors, channels of disruption of different types of BS (ToS). Each type of BS is characterised by a different set of threats;
- The consequences of a safety violations (EoS) - determined by the amount of loss due to such a violation (failure, unauthorised access and deformation of assets, accident).

Table 1 provides a description of some types of BS using the concepts discussed for local objects. Thus, the BS concept includes the definition, attributes (10B), types and additional concepts of assets, space, perimeter, causes and consequences of violation of BS or its types.

III. General principles and methods for assessing and assurance of BS
I. BS assessment

To assess Big Safety and its types using by qualitative or quantitative approaches the most widely used methods of assessing functional safety and cyber safety can be applied. There are a lot of safety/security assessment techniques [1,9,27-29] that can be generalized for BS assessment by the following way.

Technique TE. **X** Modes and Effects C/D (Criticality/Diagnostics) Analysis abbreviated as **X**ME(C/D)A), where **X** = {Failure, Software failure, Intrusion,...}. In general **X** can be interpreted as an event which is reason for the violation of one or another type of BS. So this method analyses events X (failures, intrusions/attacks, infections etc.), its modes and effects, possibilities of detection, identification or diagnosis and criticality (probability and severity) of the events.

Technique TD. **X** Block Diagrams (**X**BD), where **X** = {Reliability, Safety, Security, Trustworthiness....}. The most known assessment method is based on reliability block diagrams (RBD). It can generalized as XBD depending on assessed BS type or subtype X.

Technique TT. **X** Tree Analysis (**X**TA), where **X** = {Failure, Attack, Non-availability,...}. In this

case X can be presented as an event similar XME(C/D)A and other events considering anomalies of BS properties.

Technique TI. **X** Injection/insertion Testing (**X**IT), where **X** = {Fault, Software fault, Vulnerability,...}. The method is based on injection into analysed system anomalies X to assess one of the BS types.

Table 1: *Analysis of types of big safety*

BS types	AoS	SoS	PoS	ToS	EoS
Information	Data, information and knowledge critical to the system	Information space (cyberspace for cyber safety)	The information perimeter is defined by the entry and exit points for data as well as access to system assets	Violations, unauthorised access, blocking of data or functions in progress	Material damage from loss or disruption of data, **accident**
Functional	ICS. sensors and actuators, personnel	Parameter and signal space, describes the safe functioning of the ICS	Maximum permissible values of parameters, determining the safe operation of the ICS	Untimely system actuation, resulting in an accident	Material losses from failures, accident
Physical	Premises, equipment, personnel	The physical space in which the systems, personnel	Physical boundaries of the area, facilities where systems, personnel are located	Trespassing on protected equipment, destruction, threat to personnel	Material losses from intrusion, can lead to an emergency situation, loss of assets
Infectious	Personnel	Space to which person-nel have access and through which they can become infected	A perimeter that ensures that no infection can occur	Threat to the health and life of staff, inability to perform duties	Loss of health and life, can increase the risks of an accident

Technique TH. Hazard Operation Analysis (HAZOP(**X**)), where **X** = {Safety. Security,...}. The method allows to assess hazards of system operation and can be applied for analysis in point of different types X of BS.

Technique TC. Common Cause **X** Analysis (CC(**X**)A), where **X**={Failure, Vulnerability, Intrusion,...}. The method is aimed at identifying the reasons and events X why and when there may be a simultaneous violation of BS or its types of several redundant systems used for BS assurance.

Technique TM. Markov's Models (MM(**X**)), where **X** = {Availability, Dependability, **Safety, Security}. Well-known Markov's model based method can be applied to assess different types of BS. Main restriction of MM or semi-MM techniques application to assess BS is correctness of conditions and representativeness of the initial data for obtaining such models.**

There are other techniques based on model checking, formal methods and so on which can be adapted as well. The described set of techniques ST = {TE, TD, TT, TI, TC, TM} can be aggregated using a special framework FW ={SI, F, SO} [3]. Each technique Ti ϵ ST is presented by sets of input SIi and output SOi information and transformer Fi. It transforms input information, for example, set of components and functional structure of system to reliability block diagram presented as a scheme of connected components considering influence on up/down states (output information).

The techniques can be joined using a directed graph G = {N, L}, where a set of nodes N is described by set of the techniques ST (and transformers F) and set of edges L are links between the

same outputs and inputs of the corresponding techniques. Thus, the graph G allows getting:
- a set of the possible paths SP = {Pj} to provide the required output information of final technique using available input information of initial technique. For example the techniques TE can be initial and its outputs can be inputs for the techniques TD, TI, TT and so on;
- a set of pairs of the paths Pj. Pk ϵ SP to compare the results obtained when using combinations of techniques corresponding to different paths. If allows improving trustworthiness of assessment.

II. BS assurance

For all the different objects and the dissimilarity of BS types, there are a number of general principles for its ensuring which have already been tested for functional, information and other types of safety, including for NPP. This is further supported by the [25] on the role of the Internet of Things, artificial intelligence, drones and other modern technologies in addressing Covid-19. Table 2 provides a comparison of some types and common principles of BS safety assurance.

Redundancy. *Redundancy is* the most common principle for ensuring the reliability, and subsequently the safety, of a wide class of local objects. Let's note, that one of the authors of the first handbook on reliability, where different ways of redundancy are considered, was published in 1966 by I.A. Ushakov [33], the founder of Gnedenko-Forum https://gnedenko.net/. This handbook was subsequently reprinted and expanded many times and translated into several languages.

Table 2: *Types and principles of safety assurance*

BS assurance principles	Types of Big Safety						
	NRS	FnS .	InS	FrS	PS	IfS	SsS, FIS and others
Redundancy	+	+	+	+	+	+	-
Diversity	+	+	+	+	+	+	-
Defence-in-Depth	+	+	+	+	+	+	-
Reserves of resistance	+	+	+/-	+	+	+	+
Independent verification and validation	+	+	+	+	-	+	+
Platform based decisions	+/-	+	+	+/-	+/-	+	-

Diversity. Due to the fact that common cause failures have become one of the main hazards, particularly in computer (software) based systems, the principle of diversity has been widely developed in the last 40 years. It is based on the simple idea "the same products/processes have the same anomalies, the different product/processes have different anomalies" [34,35]. "Different" means that products have the same functionality and processes have the same goals but are developed and implemented by different ways. Diversity is a principle of multi-version computing based on the following concepts [36]:
- version is an option of different product or/and process realization of function(s); version redundancy (VR) is a type of redundancy when different versions are used: diversity or

multiversity is provided using several versions multi-version system (MVS) is a system in which redundant channels implement two or more versions; multi-version technology (MVT) is a set of the rules and design actions in which a few versions-processes leading to development of two or more intermediate or end-products are used;

- strategy of diversity is a collection of general criteria, metrics and rules defining principles of formation and selection of version redundancy types and volume or MVTs; diversity metric is indicator to assess level of diversity.

There are the following types of diversity [34-36]:

- design (different technologies, design approaches, architectures);

- equipment (different manufacturers and design technologies) etc;

- functional (different underlying mechanisms, logics, actuators);

- human (different design companies; different managers, designers, programmers, testers and maintenance teams);

- signal (different sensed parameters, physical effects, different manufacturers and sensor designs, different set and location of sensors);

- software (different algorithms, operating systems, languages) etc.

Tabie 3 illustrates domains for diversity principle application according with this classification. MVSs are used in space (Shuttle, International Space Station (ISS)), aviation (Airbus and Boeing on-board systems), railway automatics (signalling, centralization and blocking systems, SCB), chemical industry (Center for Chemical Process Safety, CCPS), defense systems (military information and control systems, MICS), power plants (electrical grid), NPPs (reactor trips systems, RTS and Engineered Safety Features and Auxialiary Systems, ESFAS), e-commerce (web-service-oriented architecture based systems, WSOA with diverse target web-services) [3,35,36].

Table 3: *Application of diversity principle*

Kinds of diversity (NUREG 6303 [28])	Diversity application domains										
	Space		Aviation		Rail-way	Chemical industry	Defense	Power Plants	NPP		e-Com-merce
	Shuttle	ISS	Airbus A380	Boeing 777	SCB	CCPS	MICS	Electrical Grid	RTS	ESFAS	WSOA
Design			■			■			■	■	■
Equipment		■	■	■	■				■	■	■
Function	■	■	■	■	■	■	■		■	■	■
Human	■	■	■	■	■	■	■	■	■	■	■
Signal					■	■			■	■	
Software	■	■	■	■	■	■			■	■	■
Others	■	■			■						

It can be assumed that, for infectious safety, diversification is realised through a variety of vaccines developed by different organisations and countries and implemented according to different principles.

Defense-in-Depth. Defense-in-Depth includes a set of consistent physical barriers to the spread of hazards (e.g. radioactive substances and ionizing radiation) combined with technical means and organizational measures aimed at preventing deviations from normal operating conditions], preventing accidents and limiting their consequences. Thus, for nuclear and radiation safety of NPPs, the system of consecutive physical barriers includes fuel matrix, fuel element cladding, boundary of reactor compartment (RC) coolant circuit, containment of RC. biological

protection. The strategy of NPP Defense-in-Depth is implemented at five levels:
- prevention of operational disruptions;
- ensuring safety in the event of disturbances and preventing emergencies:
- prevention and elimination of accidents;
- management of beyond design basis accidents;
- emergency preparedness and response.

For infectious safety, a system of consistent physical barriers includes state borders, regional borders, city borders, and company borders. For information and physical safety, consistent barriers include control of access to territory or premises, safety systems, control of access to information resources, etc.

Independent Verification and Validation (IV&V). The introduction of Independent Verification and Validation, as well as multiple techniques to assess the functional and information safety of NPP Instrumentation and Control systems has enabled the implementation of another echelon of verification and protection of these systems against residual software and systems in general, in fact, IV&V is another option to implement process diversion and protection in depth to reduce risks of undetected defects and CCF in general. This experience is very important in an environment where safety systems for critical facilities have become digital and software-driven.

Thus the principles diversity, Defense-in-Depth (D3) and IV&V can be presented as a common approach to decreasing of CCF risks (Figure 2) on the stages creation and operation of system [24]. Techniques IV&V of developed or modernized l&C systems and hardware, software, FPGA components, platforms etc. allow minimizing risks of undetected design and physical faults and vulnerabilities. D3 is a horizontal/vertical echelon consisting of n sub echelons e_i and m version redundancy types vr_i and providing protection of critical assets.
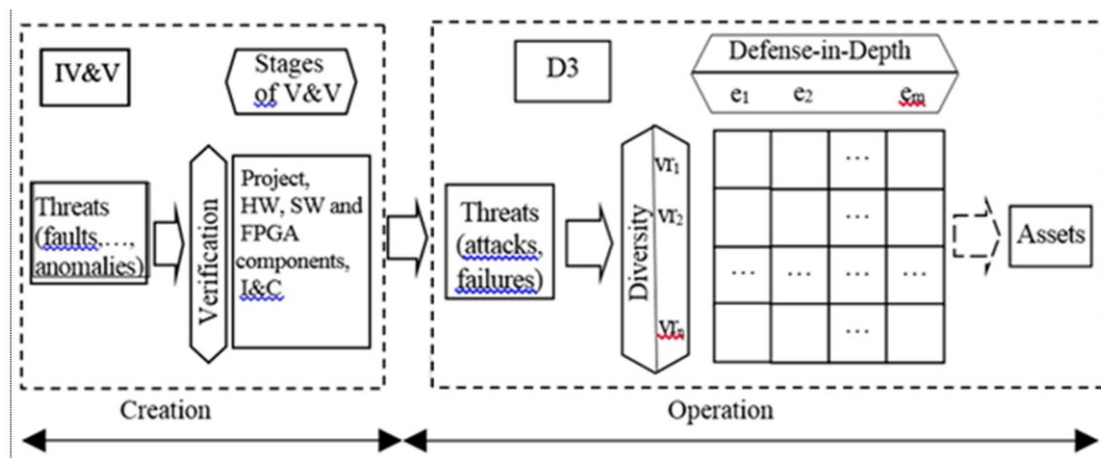
Figure 2: *Two echelons of CCF protection: independent verification and validation and D3 (Defense-in-Depths and diversity) approach: ei - echelons of protection in depth, vr - types of version redundancy*

Reserves of resistance. Reserves of resistance against external impacts (seismic, flooding, hurricanes, falling aircraft and other aircraft etc.) are probably the most obvious safety principle for a number of impacts. Unfortunately, this principle has not always been used to its full potential (as evidenced, for example, by the Fukushima accident). Its implementation is associated with high additional costs.

Platform based decisions. The concept of "*platform* (family of equipment)" has become widespread in recent years for the development of NPP control systems [3]. A platform is a set of hardware and software components that can work together in one or more defined configurations (structures) designed to implement a predefined set of specific control systems of different purposes. A feature of the platform is functional, structural and design completeness for the main

application area.

The completeness of the platform is determined by the possibility *to* create on its basis a variety of information and control systems, which by the composition of performed functions, structure, constructive realization, technical parameters and characteristics in advance can satisfy the requirements of a wide enough, though limited range of specific customers. Such approach allows during development, introduction and justification of safety of each concrete system to concentrate its applied functions, relying at realization of basic functions on the technical decisions accepted at creation of the platform and tested in the course of its application [3].

To the surprise of the authors - nuclear and radiation safety specialists the concept of "platform" was used in vaccine development, including against COVID-19, when previously tested antiviral platforms were used to develop vaccines against new infectious diseases, greatly simplifying and accelerating their development.

III. BS regulation

The term 'regulation' in relation to the activities and names of organisations implementing governmental safety policies is now commonly used for a number of types of safety. The term has been adopted by legislation in many countries, e.g., in the United States - US Nuclear Regulatory Commission, Ukraine - State Nuclear Regulatory Inspectorate, international organizations (for example, Regulatory Committee on Nuclear Activities (CNRA) is an international committee of Nuclear Energy Agency (NEA) including in OECD- Organization for Economic Co-operation and Development. It was created in 1989 to guide the NEA programmes concerning the regulation, licensing and inspection of nuclear installations with regard to safety).
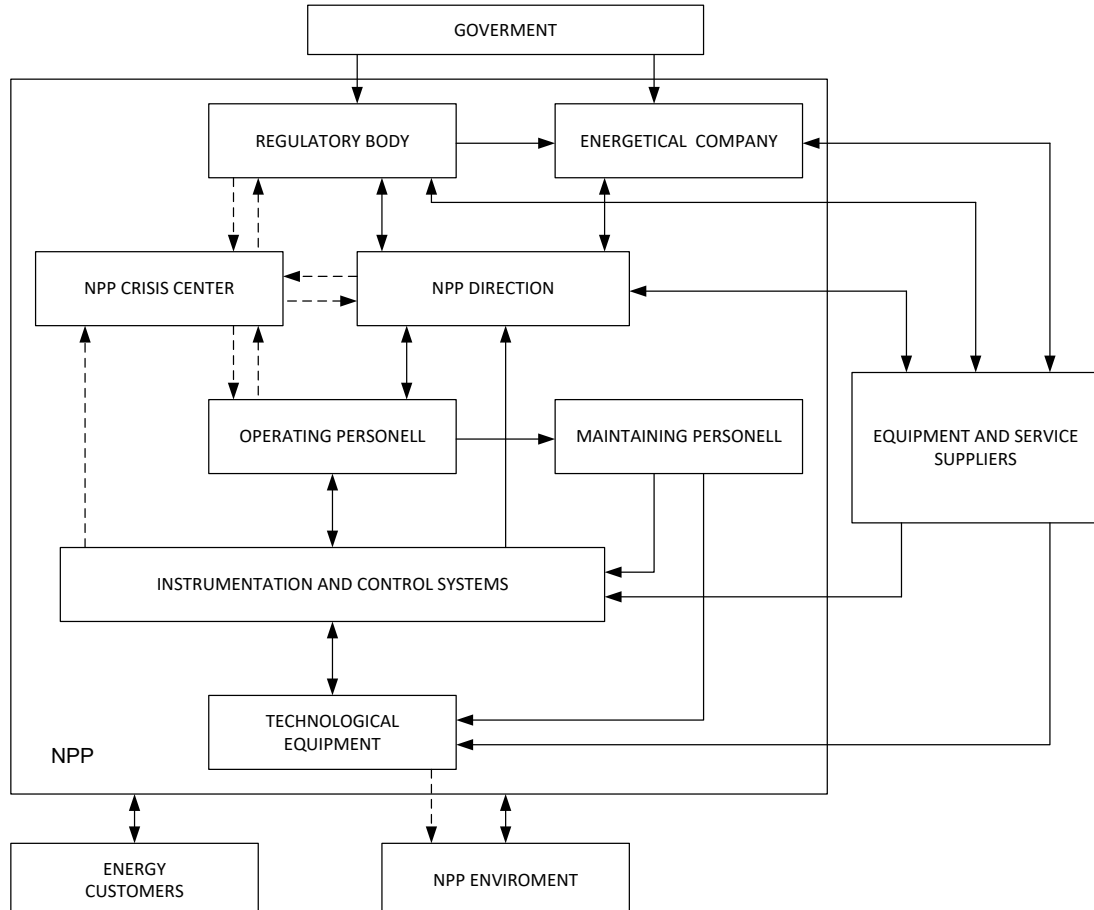
Figure 3: *Example of NPP big safety control scheme*

Safety regulation includes:

- safety standardisation (development of international, national and industry standards, regulations, rules and guidelines with safety requirements). Safety requirements are specified in the form of quantitative safety indicators (probabilistic and deterministic, e.g. limits on external influences) and in the form of regulations and rules;

- safety licensing, consisting of the examination, verification and assessment of compliance with safety requirements for the granting of licences (permits for all safety-related activities);

- monitoring compliance with safety requirements in accordance with the terms of the issued licences.

Regulatory features:

- the independence of the regulator from either the designers of the facility equipment or the operator of the facility;
- the Regulatory Body (RB) is usually a state organization;
- the existence, in some cases, of inter-state regulatory organisations.

An example of a big safety control scheme for a NPP (involving RB) is given in Figure 3.

The RB which reports only to the government, has two types of impacts on the NPP:

- during normal operation - documents (safety standards and regulations, licences, temporary operating permits, various ordinances, etc.);
- in case of an accident and emergency- instructions coming to the NPP crisis centre (these links are shown as dotted lines in Figure 3).

The RB receives information from NPPs that describes the safety of the plant and from suppliers of equipment and services.

IV. Big Safety and Problem of Black Swan

I. Accidents as a Black Swan

The BS concept, the experience gained in the field of ensuring the safety of NPP and other critical systems can be used to find solutions to another methodological problems. Large man-made accidents in general and accidents at NPP's, in particular, are considered by many experts in the context of the Black Swan effect [37, 38]. According to this theory, the author of which is Nassim Taleb [39], events with the following features are called 'black swans":

- Ch1: these events are anomalous, as nothing in the past has foreshadowed them;
- Ch2: they have a significant impact because they are characterised by large material consequences, threats to the health and lives of many people;
- Ch3: An explanation for an event is found ('invented') after it has happened.

Let us analyse examples of events that could be considered as candidates for Black Swan recognition [1,5]. Table 4 summarises the results of the analysis in terms of identifying causes and assessing these events in terms of Ch1-Ch3 attributes. The markings "+" and "−" indicate the presence or absence of a relevant cause or attribute, "+/−" and "−/+" indicates a preponderance of positive or negative responses. This table was constructed taking into account expert judgement [5].

Add comments on the coronavirus pandemic.

Ch1. During the influenza epidemic of 1918-1919 years, 22 million people died worldwide. The world learned nothing from epidemics of lesser consequences. A number of countries lacked dedicated infectious disease hospitals and public anti-infection services. Global solutions must be

implemented to control infection.

Ch2. The impact of the coronavirus infection is well known - a pandemic began and within a few months had spread to more than 200 countries on all continents. The death toll is approaching 2 million. Many countries are partially paralysed. Losses amount to tens of trillions of dollars.

Ch3. There is still no unequivocal explanation for the cause and mechanism. Note that Nassim Taleb himself did not refer to the coronavirus as a "black swan" because, in his view, the consequences of the pandemic were predicted at its inception and could have been prevented on this scale [40].

Table 4: *Accidents in context of Black Swan*

Accident	Country	Accident reasons				Is it Black Swan?			
		Complexity	Design anomaly	Human factor	Environment	Ch1	Ch2	Ch3	Yes/No
Three Mile Island. 1979	USA	-/+	+	+	-	+	-/+	-/+	Rather No
Chemo-byl. 1986	Formed USSR (Ukraine)	-/+	+	+	-	+/-	+	+	Rather Yes
Fuku-shima 2011	Japan	-/+	+/-	+/-	+	+/-	+	+	Rather Yes
Covid-19	218 countries	-	-	+/-	-/+	+	+	+	Yes

II. The strategies of Black Swan tolerance assurance

Many authors have analysed possible strategies to reduce the effects of the Black Swan effect [37]. "Black swans" become a kind of dataset that is used to train a "world" neuro-model for (support) decision-making systems. After receiving each new dataset, the "intelligence" of the model is increased, however, it is limited to the appearance of a predictable and intelligent response of the system to the arrival of a similar "black swan".

There are several strategies for Black Swan tolerance (StrT) [1].

A posteriori strategy (AsStrT). It is based on a comprehensive and detailed analysis of causes and effects, developing measures to reduce the risks of occurrence and minimise damage from the "black swan" that has "arrived". The results are formation and implementation of a set or set of sets for neuro-model training.

A priori, proactive strategy (ApStrT). The strategy consists of classifying and object-orienting analysis of "black swans" to form scenarios for future behaviour (earth meeting a major asteroid, a worldwide flood, the arrival of aggressive aliens, etc.). It is clear that the attempt to be proactive based on predictions of new black s wans runs counter to their very nature and Ch1 attribute, and is an attempt to erase the boundary between the part of probability theory that deals with rare events and the fundamental (by definition) unpredictability of these events. What is at stake here, however, is not an attempt to find a mathematical solution to the problem or to come close to solving it, but to typify the solution procedure itself. A "set" is then formed for another "neuro-model", which will support decisions to improve this procedure.

A 'colour change' strategy (CStrT). In this it is worth revisiting Nassim Taleb's characterisation

of the coronavirus as a ''White swan''. It is worth highlighting a construct in his judgement that relates to the very possibility of a change of "colour" and the formation of an appropriate strategy on this basis. If consists of analysing, predicting, devising and implementing mitigation measures, i.e. changing the colour from black to grey or white, in the event of a time-bound event that may have the characteristics of a "black swan".

Swarming or swarming strategy (FStrT). The above strategies are based on the assumption of "ordinariness" of the black swan flow. A more complex situation is when two or more black swans arrive at the same time or with a delay that makes it impossible to react to the consequences of the previous black swan. At the same time, they can be from the same "swarm" (i.e. of the same type. e.g. a NPP accident), or from different ones (accident and pandemic). A combination of actions based on the strategies discussed above, taking into account the negative synergy of Black Swans from the swarms, is needed here. If situation "a Black Swan by Black Swan" happens, i.e. a known domino effect with Black Swans occurs, people should try to change the colour of at least the next Swan.

It is clear that implementing such strategies will involve enormous costs. However, dealing with the consequences of Black Swans is always immeasurably greater than the cost of defending against them.

V. Conclusions

1. The introduction of the concept and formation of the BS concept is an objective necessity related to trends in the development of critical systems in various areas of human activity and stimulated by the emergence of the coronavirus pandemic. It is not a tribute to fashion in the use of the word BIG. For all the different objects of safety and diversity of types of BS, there are a number of common principles for its assurance and assessment.

2. The BS problem becomes a global one because:
   • has global causes and consequences;
   • cannot be predicted and warned about outside the global context:
   • cannot be solved by a single organization, region or country;
   • consequences cannot be dealt with by local efforts.

It requires a global organizational and technical platform based on the BS concept, its legal and financial support, and teams of analysts and experts - "strategists and tacticians" (the experience of the Fukushima Daiichi accident in 2011 demonstrated this).

3. In the 2000s, the sustainable development movement began in the world. The coronavirus pandemic seems to be interrupting sustainable development trends. However, the lessons to be learned will help return to sustainable development with 'greater sustainability'.

4. Nuclear power plant is an example of a local BS object. The nuclear power industry has accumulated invaluable experience in evaluating and providing various types of BS, which should be used by other critical areas. The same lessons learned in these areas need to be analyzed and applied to the safety of nuclear power plants and other critical objects consequently, it is important to develop comparative approach in framework of BS.

5. When analyzing and improving the BS concept, the importance of the human factor should be noted once again. The coronavirus situation already allows us to draw a simple conclusion: we should always take care of people, because people are both the object and the instrument of safety assurance.

6. It must be taken into account that information and communication technology and software are often the vectors of "danger". Sometimes accidents in different systems are caused by failures of their IT component. There is a need for an "amplifier of positives" and a "filter" of safety deficits caused by the introduction of new technologies (Internet of Things, artificial intelligence, man-

machine cooperation, Big data, etc.) and concepts (Industry 4.0, 5.0...). Thus, it is important to rule out a situation that could be called as "the technology coronavirus" when new technologies can become reason of cyber or other kinds of threats and effects in point of global point view.

7. It is important to rule out the formation of any myths related to BS. Since the introduction of digital technology, the closed systems of nuclear power plants and other critical objects have led to a persistent judgment that cyber attacks are impossible, which has been debunked more than once. Now it is time to analyze the infectious safety with which the threats of creating bio-channels of influence on such systems, their human component, are linked.

8. BS is a safety without borders that are geographical, informational, technological, human. Its concept needs to be refined and filled in the face of new threats. It requires refinement and expansion of the set of countermeasures to counter additional threats in line with the strategies considered. It is necessary to make sure that "black swans" in the sphere of BS do not become absolutely black, to change their color towards grey or white, ensuring black swans-resilience of humanity, which should be proactive.

9. During last year a few papers have been published which discuss problems of safety of structurally complex systems [10], future of safety science [11] in general. The increase in the number of critical industries, the globalization of BS problems requires the development of a theory of big safety. This need is also related to the growing damage caused by hazards. The history of humanity, at least in the 21st century, has probably never known greater damage than that caused by COVID-19.

Notes. The authors understand the discussion nature of some provisions of the paper and, first of all, the very concept of Big Safety. The paper reflects our views on this problem, which are also being formed and developed, taking into account its multidimensional issue. We would be grateful for any feedback and comments.

References

[1] V. Kharchenko, M. Yastrebenetsky (2020). NPP Safety and big Safety in the Time of Covid-19. *Nuclear and Radiation Safety*, 3(87): 74-87.

[2] M. Yastrebenetsky, V. Kharchenko (edits), Nuclear Power Plant Instrumentation and Control Systems for Safety and Safety, Hershey, Pennsylvania, United States of America, IGI Global, 2014, 450 p.

[3] M. Yastrebenetsky, V. Kharchenko (edits), Safety and Safety of Nuclear Power Plant Instrumentation and Control Systems, Hershey, Pennsylvania, United States of America, IGI Global, 2020, 501 p.

[4] A. Rucinski. Global Trusted Dependability as a Grand Challenge. Proceedings of the 11th IEEE Conference on Dependable Systems, Services and Technologies, DESSERT2020, Ukraine, Kyiv, May 14-18, 2020: 9-10.

[5] V. Kharchenko (2018). Big Data and Internet of Things for Safety Critical Applications: Challenges, Methodology and Industrial Cases. *International Journal on Information Technologies and Safety*, 4: 3-16.

[6] Yastrebenetsky, M., Dybach, O. (2019). Prospects of using Big Data Technologies in nuclear energy of Ukraine. *Nuclear and Radiation Safety*, 2(82), 9-13.

[7] Illiashenko, O., Kolisnyk, M., Strielkina, A., Kotsiuba, I., Kharchenko, V. (2020). Conception and

Application of Dependable Internet of Things Based Systems. Radio electronics, *Computer Science and Control*. 4 (57): 139-150.

[8] Rudenko, Y., Ushakov, I, Reliability of Power Systems. Science, Moscow. 1986, 254.

[9] Bochkov A.V. (2020).On the method of risk synthesis in the safety management of structurally complex systems. *Dependability*. 20(1): 57-67.

[10] Bochkov A.V. On the methods of qualitative estimation of the safety state of structurally complex systems (2020). *Dependability*. 20(3): 34-46. https://doi.org/10.21683/1729-2646-2020-20-3-34-46.

[11] Paul Swuste, Jop Groeneweg, Coen van Gulijk, Walter Zwaard, Saul Lemkowitz, Yvette Oostenthdorp (2020). The future of safety science. *Safety Science*. 125(3):104593: 1-9.

[12] A. Ian Glendon (2021). Safety Science directions: The journal. *Safety Science*. 135(3):105127: 1-8.

[13] Jie Li, Floris Goerlandt, Genserik Reniers (2021). An overview of scientometric mapping for the safety science community: Methods, tools, and framework. *Safety Science*. 134(2):105093: 1-11.

[14] Leveson N. Safeware: System Safety and Computers. – Addison–Wesley, 1995, 680.

[15] Alcaraz, C., Zeadally, S. (2015). Critical infrastructure protection: Requirements and challenges for the 21st century. *International Journal of Critical Infrastructure Protection*, 8: 53–66.

[16] Harvey, C., Stanton, N., Safety in System-of-Systems: Ten key challenges (2014). *Safety Science, 70,* December: 58-366.

[17] Kharchenko, V., Sklyar, V., Brezhnev, E. Safety of Information and Control Systems and Infrastructures: Models, Methods and Technologies. Palmarium Academic Publishing. Germany, 2013. 529.

[18] Rehak, D., P. Senovsky, P., Slivkova, S. (2018), Resilience of Critical Infrastructure Elements and Its Main Factors. *Systems*, 6(2): 21-32.

[19] Severe accident management programs for nuclear power plants: safety guide. — Vienna, International Atomic Energy Agency, 2008.

[20] Shropshire, J. and C. Kadlec, Developing the IT Disaster Recovery Planning Construct. Journal of Information Technology Management, 2009. 20(4): p. 37.

[21] Charit, I. Accident Tolerant Nuclear Fuels and Cladding Materials. JOM 70, 173–175 (2018). https://doi.org/10.1007/s11837-017-2701-3

[22] The SIEM Buyer's Guide for 2021, Splunk, 2020 https://www.splunk.com/en_us/form/the-siem-buyers-guide.html.

[23] Isenberg, J., Yastrebenetsky, M. (2002). Comparing of principles of safety assurance of control systems for carrier rockets and NPPs. *Space Science and Technology*, 8, № 1: 4–8.

[24] Sklyar, V., Kharchenko, V., Yastrebenetsky, M. (2004).   Digital Instrumentation and Control Systems of NPPs and Rocket-Space Complexes: Comparative Analysis, Tendencies of Development, Safety Assurance. *Nuclear and Radiation Safety*, 10 (2): 12–16.

[25] V. Chamola, V. Hassija, V. Gupta and M. Guizani, A Comprehensive Review of the COVID-19 Pandemic and the Role of IoT, Drones, AI, Blockchain, and 5G in Managing its Impact," n *IEEE Access*, vol. 8: 90225-90265.

[26] NP 306.2.141-2008. Nuclear and Radiation Safety Standards and Regulations. General Safety Regulations for Nuclear Power Plants, Ukraine, Kyiv, 2008.

[27] IEC 61508. Functional safety of Electrical/Electronic/Programmable Electronic safety-related systems.

[28] IEC 15408 ISO / IEC 15408-1: 2005 Information technology-Safety techniques-Evaluation criteria for IT safety - Part 1: Introduction and general model.

[29] IEC 62443-1-1: 2009 Industrial communication networks - Network and system safety - Part 1-1: Terminology, concepts and models.

[30] Kharchenko, V. Independent Verification and Diversity: The Echelons for Assurance of Cyber Physical Systems Safety, Proceedings of the 2nd International Workshop on Information-Communication Technologies and Embedded Systems (ICTES 2020), Mykolaiv, Ukraine, November 12, 2020: 19-29.

[31] 2.4 trillion yen in Fukushima crisis compensation costs to be tacked onto power bills // December 10, 2016 (Mainichi Japan) https://mainichi.jp/english/articles/20161210/p2a/00m/0na/002000c

[32] Jeremy Schwab. Fighting COVID-19 could cost 500 times as much as pandemic prevention measures World Economic Forum, August 03, 2020 https://www.weforum.org/agenda/authors/jeremy-schwab

[33] Kozlov, B., Ushakov, I., Manual on estimation of radio-electronic and automatics equipment, Moscow, 1975, 472.

[34] NUREG/CR-6303. Method for Performing Diversity and Defense-in-Depth Analyses of Reactor Protection Systems. Lawrence Livermore National Laboratory, Livermore, CA, USA. 1994

[35] NUREG/CR-7007. Diversity Strategies for Nuclear Power Plant Instrumentation and Control Systems. ORNL/TM-2009/302. 2008.

[36] Kharchenko, V., Siora, A., Sklyar, V., Volkoviy, A., Bezsaliy, V. Multi-Diversity Versus Common Cause Failures: FPGA-based Multi-Version NPP I&C Systems. Proceedings of the 7th International Topical Meeting on Nuclear Plant Instrumentation, Control, and Human-Machine Interface Technologies (NPIC&HMIT 2010). Las Vegas, USA, November 7-11, 2010: 1081-1093.

[37] Avinash M. Nafday, Strategies for Managing the Consequences of Black Swan Events. Leadership Manage. Eng., 2009, No. 9(4): 191–197.

[38] Barry Brook. Black Swan theory and the anti-nuclear sentiment https://bravenewclimate.com /2012/02/01/black-swan-anti-nuclear/

[39] Nassim Nicholas Taleb. The Black Swan: Second Edition: The Impact of the Highly Improbable. Random House Trade Paperbacks, Retrieved November 5, 2017.

[40] Nassim Taleb Says 'White Swan' Coronavirus Pandemic Was Preventable. Bloomberg. July 10, 2020. URL: https://www.bloomberg.com/news/videos/2020-03-30/nassim-taleb-says-white-swan-coronavirus-pandemic-was-preventable-video.

Introducing Probabilistic Models for Cost Analysis of Sachet Water Plant

Nafisatu Muhammad Usman

•

Department of Arts and Humanity, School of General Studies,
Kano State Polytechnic, Kano, Nigeria
mamankhairat2015@gmail.com

Ibrahim Yusuf

•

Department of Mathematical Sciences, Bayero University, Kano, Nigeria
iyusuf.mth@buk.edu.ng

Abstract

The paper deals with modeling and performance assessment of a series-parallel with independent failures using the Markov Birth-Death method and the probabilistic approach. The system consists of five subsystems arranged in series and parallel configurations with three possible states of operation, reduced capacity and failure. First-order systems of ordinary differential equations are developed and recursively resolved using a probabilistic approach via the transition diagram. The state probabilities for the proposed scheme are derived. Using state probabilities, system availability expressions, busy repairman probabilities due to minor and major failures as well as benefit feature are calculated. Profit and availability matrices for each subsystem have been computed to provide various output values for different combinations of parameters. The finding of this paper will boost the efficiency of the system and will be useful for timely maintenance progress, decision-making, preparation and optimization.

Keywords: *Availability, modelling, probability, sachet water plant*

I. Introduction

Reliability, availability and profit are some of the most important factors in any successful sachet water system. Like other systems, sachet water systems are exposed to different types of failures such as common cause, partial, human and complete failure. Proper maintenance planning plays a role in achieving high system reliability, availability and production output. Availability and profit of a sachet water system may be enhanced through adequate maintenance planning, regular inspection, fault tolerant units or subsystems, reliable structural design of the system or subsystem of higher reliability.

Systems are typically analyzed with a view to determining their reliability metrics. High productivity and full income from process plants are important for their survival. In order to do this, the efficiency and reliability of the equipment in the process must be ensured in the highest order. In order to increase the efficiency and reliability of the related development curriculum, more emphasis needs to be put on operational management. The most common weakness of our technical capabilities has been our inability to pay adequate attention to process technology. In the

manufacturing phase, inputs are: raw materials, electricity, machinery, information and technology, labor, etc. In order to achieve quality and quantity, efficient plant management is necessary to monitor the conversion process and the variables affecting output. The development of a mathematical model is one of the ways of plant management. The modeling method is commonly used in the technology world. This method is used in the oil and milling industries, etc.

A large volume of literature exists on the issue of predicting performance evaluation of various manufacturing and industrial systems configured as series-parallel system. For instance; Kadiyan et al. (2012) analyzed the reliability and availability of uncaser system of brewery plant. Khanduja et al. (2012) discussed the maintenance planning of bleaching system of paper plant. Gupta and Tewari (2011) focuses on simulation of availability in thermal plant. Garg et al. (2010b) analyzed the availability of crankcase manufacturing of two-wheeler automobile industry. Garg et al. (2010a) analyzed the availability of a cattle feed plant using matrix method. Arvind et al. (2013) dealt with behavioral study of piston manufacturing plant through stochastic models. Aggarwal et al. (2014) presented Markov analysis of urea synthesis system of a fertilizer plant. Aggarwal et al. (2017) focuses on fuzzy availability analysis for serial processes in the crystallization system of a sugar plant. Kumar and Lata (2012) discussed the evaluation of reliability of condensate system using fuzzy Markov Model. Kumar et. al. (2011) dealt with performance modelling of furnace draft air cycle in a thermal plant. Kumar and Tewari (2011) presented modelling and performance optimization of CO2 cooling system of a fertilizer plant. Kumar and Mudgil (2014) presented an optimization of availability of ice cream making unit of milk plant using genetic algorithm.

Mathematical modelling of industrial and manufacturing systems may prove beneficial by analyzing the performance of the system/ subsystems through reliability, availability as well as generated profit and by identifying the combination of the problem that may result in increasing the risk of a complete breakdown which may lead to high corrective maintenance cost, low reliability, availability and profit. Through this mathematical model, the optimal profit level in which the profit is maximum can be identified and the corresponding subsystem that enable the maximum profit in order to lay emphasis on its preventive maintenance as well as the most critical subsystem leading to drop in profit.

One of the key sources of drinking water for low and medium class is sachet water. Knowing that water is an essential resource for the continued life of all living things, including man, sufficient supply of fresh and safe drinking water in abundance is an absolute necessity for all human beings. As such, the implementation of the modeling method in the water sector would play a vital role in ensuring a sufficient supply of fresh and safe water in society. As a result, individuals who can afford water are now sinking holes and selling it, some of them suffering from less efficient machinery to an ever-growing population. In some less developed countries, water is manufactured in a variety of products, such as bottled water, sachet wine, etc. Sachet water is commercially processed water, developed, packaged and distributed for sale in sealed polythene containers for human consumption. The development of sachet water began in the late 1990s, and today the progress of scientific technology has made the development of sachet water one of the fastest growing industries in the less developed countries. Many individuals and corporate bodies are now engaged in packaging water in polythene bags of about 50-60cl, which they sell to the public. Drinking water is therefore commercially available in a bag that is so easy to open.

The marketing and consumption of sachet water has increased enormously. The majority of producers are less concerned about increasing the availability, profit and reliability of their machinery. The continuous increase in the population and the indiscriminate consumption of sachet water demand an increase in production, as it is difficult for the most underprivileged citizens to obtain. Sachet water is seen to be a good addition to other types of packaged water and

can be purchased at a cheaper price. It is a source of drinking water for low and middle class. The needs of this research are motivated by the increasing pressures on the demand of sachet water industries and their reliability modelling in order to meet the challenges of meeting water demand of the populace.

II. Notations and Description of the System

The System consists of five dissimilar subsystems which are:
1. Subsystem A (storage tank): Single units in series whose failure cause complete failure of the entire system.
2. Subsystem B (filter): Consists of two cold standby units. Failure of one unit, the system will work in full capacity. Complete failure occurs when both units failed.
3. Subsystem C (tank): consisting of single unit whose failure cause complete failure of the entire system.
4. Subsystem D (booster):): Consists of two cold standby units. Failure of one unit, the system will work in full capacity. Complete failure occurs when both units failed.
5. Subsystem E: A single unit in series whose failure cause complete failure of the entire system.

Notations

☐   Indicate the system is in failed state
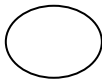
◯   Indicate the system is in full working state

A, B, C,D,E: represent full working state of subsystem
B2   denote that the subsystem B is working in reduced capacity
C1   denote subsystem is working on standby unit
a, b, c,d,e   represent failed state of subsystem

$\lambda_1, \lambda_2, \lambda_3, \lambda_4, \lambda_5$ represent failure rates of subsystems A, B,C,D and E

$\mu_1, \mu_2, \mu_3, \mu_4, \mu_5$:   represent repair rates of subsystems A,B,C,D and E

$h_m(t), m = 0,1,2,3$:   Probability of the system working with full capacity at time t

$h_m(t), \ m = 4,5,6,...,19$: Probability of the system in failed state

$A_V(\infty)$:   Steady state availability of the system

$B_{S1}(\infty)$: **Busy period probability of repairman due to type I failure**

$B_{S2}(\infty)$: **Busy period probability of repairman due to type II failure**

$P_F(\infty)$: **Profit function**

k_0: Total revenue generated

k_1: Cost due to partial failure

k_2: Cost due to complete failure
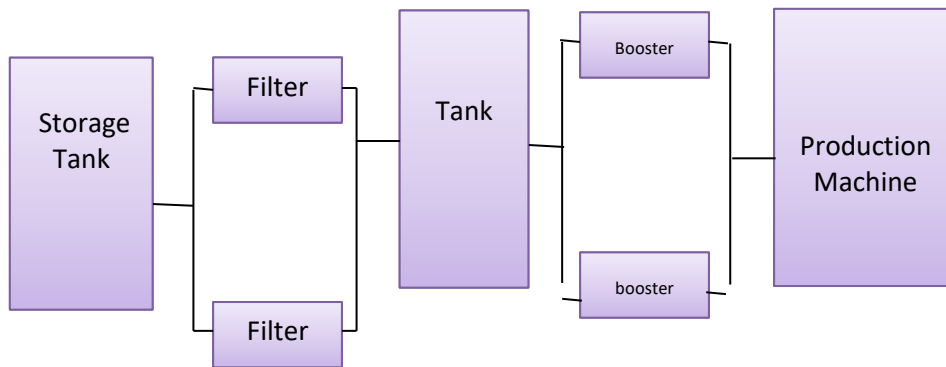
Figure 1: *reliability block diagram of the system*
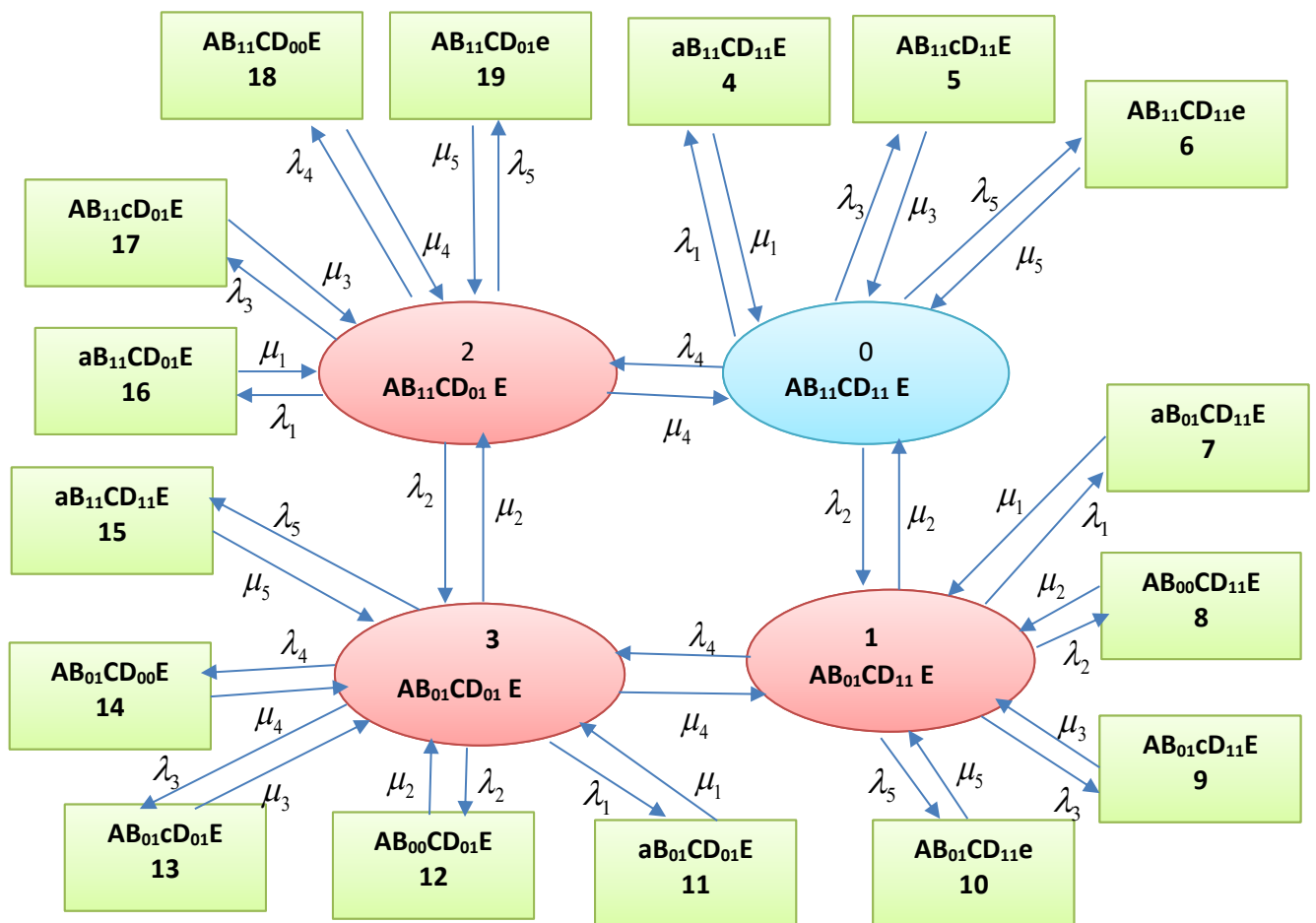
Figure 2: *Transition diagram of the system*

III. Mathematical Model Formulation

System of first order ordinary differential difference equations are derived using Markov birth-death process from Figure 2 above:

$$\left(\frac{d}{dt} + \sum_{k=1}^{5} \lambda_k\right) h_0(t) = \mu_2 h_1(t) + \mu_4 h_2(t) + \mu_1 h_4(t) + \mu_3 h_5(t) + \mu_5 h_6(t)$$

(1)

$$\left(\frac{d}{dt} + \mu_2 + \sum_{k=1}^{5} \lambda_k\right) h_1(t) = \lambda_2 h_0(t) + \mu_4 h_3(t) + \mu_1 h_7(t) + \mu_2 h_8(t) + \mu_3 h_9(t) + \mu_5 h_{10}(t) \qquad (2)$$

$$\left(\frac{d}{dt} + \mu_4 + \sum_{k=1}^{5} \lambda_k\right) h_2(t) = \lambda_4 h_0 + \mu_2 h_3(t) + \mu_1 h_{16}(t) + \mu_3 h_{17}(t) + \mu_4 h_{18}(t) + \mu_5 h_{19}(t) \qquad (3)$$

$$\left(\frac{d}{dt} + \mu_2 + \mu_4 + \sum_{k=1}^{5} \lambda_k\right) h_3(t) = \lambda_4 h_1(t) + \lambda_2 h_2(t) + \mu_1 h_{11}(t) + \mu_2 h_{12}(t) + \mu_3 h_{13}(t) + \mu_4 h_{14}(t) + \mu_5 h_{15}(t) \quad (4)$$

$$\left(\frac{d}{dt} + \mu_1\right) h_4(t) = \lambda_1 h_0(t) \qquad (5)$$

$$\left(\frac{d}{dt} + \mu_3\right) h_5(t) = \lambda_3 h_0(t) \qquad (6)$$

$$\left(\frac{d}{dt} + \mu_5\right) h_6(t) = \lambda_5 h_0(t) \qquad (7)$$

$$\left(\frac{d}{dt} + \mu_1\right) h_7(t) = \lambda_1 h_1(t) \qquad (8)$$

$$\left(\frac{d}{dt} + \mu_2\right) h_8(t) = \lambda_2 h_1(t) \qquad (9)$$

$$\left(\frac{d}{dt} + \mu_3\right) h_9(t) = \lambda_3 h_1(t) \qquad (10)$$

$$\left(\frac{d}{dt} + \mu_5\right) h_{10}(t) = \lambda_5 h_1(t) \qquad (11)$$

$$\left(\frac{d}{dt} + \mu_1\right) h_{11}(t) = \lambda_1 h_3(t) \qquad (12)$$

$$\left(\frac{d}{dt} + \mu_2\right) h_{12}(t) = \lambda_2 h_3(t) \qquad (13)$$

$$\left(\frac{d}{dt} + \mu_3\right) h_{13}(t) = \lambda_3 h_3(t) \qquad (14)$$

$$\left(\frac{d}{dt} + \mu_4\right) h_{14}(t) = \lambda_4 h_3(t) \qquad (15)$$

$$\left(\frac{d}{dt} + \mu_5\right) h_{15}(t) = \lambda_5 h_3(t) \qquad (16)$$

$$\left(\frac{d}{dt} + \mu_1 \right) h_{16}(t) = \lambda_1 h_2(t) \tag{17}$$

$$\left(\frac{d}{dt} + \mu_3 \right) h_{17}(t) = \lambda_3 h_2(t) \tag{18}$$

$$\left(\frac{d}{dt} + \mu_4 \right) h_{18}(t) = \lambda_4 h_3(t) \tag{19}$$

$$\left(\frac{d}{dt} + \mu_5 \right) h_{19}(t) = \lambda_5 h_2(t) \tag{20}$$

With initial condition $h_i(t) = \begin{cases} 1, & i = 0 \\ 0, & i = 1, 2, 3, ..., 19 \end{cases}$

$$\tag{21}$$

The steady state availability, busy period due to partial failure and complete failure are respectively given by:

$$A_V(\infty) = h_0(\infty) + h_1(\infty) + h_2(\infty) + h_3(\infty) \tag{22}$$

$$B_{p1}(\infty) = h_1(\infty) + h_2(\infty) + h_3(\infty) \tag{23}$$

$$B_{p2}(\infty) = h_4(\infty) + h_5(\infty) + h_6(\infty) + ... + h_{19}(\infty) \tag{24}$$

To compute the states probabilities $h_k(t)$ $k = 0, 1, 2, ..., 19$, the derivatives of states probabilities are set equal to 0 in (1) to (20) and solving them recursively using (21), the steady state probabilities given Table 1 below:

Table 1: States Probabilities

$h_0(\infty) = \dfrac{1}{1 + \delta_0 + \delta_1\delta_2 + \delta_3\delta_4}$	$h_1(\infty) = \dfrac{y_2}{1 + \delta_0 + \delta_1\delta_2 + \delta_3\delta_4}$	$h_2(\infty) = \dfrac{y_4}{1 + \delta_0 + \delta_1\delta_2 + \delta_3\delta_4}$
$h_3(\infty) = \dfrac{y_2 y_4}{1 + \delta_0 + \delta_1\delta_2 + \delta_3\delta_4}$	$h_4(\infty) = \dfrac{y_1}{1 + \delta_0 + \delta_1\delta_2 + \delta_3\delta_4}$	$h_5(\infty) = \dfrac{y_3}{1 + \delta_0 + \delta_1\delta_2 + \delta_3\delta_4}$
$h_6(\infty) = \dfrac{y_5}{1 + \delta_0 + \delta_1\delta_2 + \delta_3\delta_4}$	$h_7(\infty) = \dfrac{y_1 y_2}{1 + \delta_0 + \delta_1\delta_2 + \delta_3\delta_4}$	$h_8(\infty) = \dfrac{y_2^2}{1 + \delta_0 + \delta_1\delta_2 + \delta_3\delta_4}$
$h_9(\infty) = \dfrac{y_2 y_3}{1 + \delta_0 + \delta_1\delta_2 + \delta_3\delta_4}$	$h_{10}(\infty) = \dfrac{y_2 y_5}{1 + \delta_0 + \delta_1\delta_2 + \delta_3\delta_4}$	$h_{11}(\infty) = \dfrac{y_1 y_2 y_4}{1 + \delta_0 + \delta_1\delta_2 + \delta_3\delta_4}$
$h_{12}(\infty) = \dfrac{y_2^2 y_4}{1 + \delta_0 + \delta_1\delta_2 + \delta_3\delta_4}$	$h_{13}(\infty) = \dfrac{y_2 y_3 y_4}{1 + \delta_0 + \delta_1\delta_2 + \delta_3\delta_4}$	$h_{14}(\infty) = \dfrac{y_2 y_2^4}{1 + \delta_0 + \delta_1\delta_2 + \delta_3\delta_4}$
$h_{15}(\infty) = \dfrac{y_2 y_4 y_5}{1 + \delta_0 + \delta_1\delta_2 + \delta_3\delta_4}$	$h_{16}(\infty) = \dfrac{y_1 y_4}{1 + \delta_0 + \delta_1\delta_2 + \delta_3\delta_4}$	$h_{17}(\infty) = \dfrac{y_3 y_4}{1 + \delta_0 + \delta_1\delta_2 + \delta_3\delta_4}$
$h_{18}(\infty) = \dfrac{y_4^2}{1 + \delta_0 + \delta_1\delta_2 + \delta_3\delta_4}$	$h_{19}(\infty) = \dfrac{y_4 y_5}{1 + \delta_0 + \delta_1\delta_2 + \delta_3\delta_4}$	

Where $m_k = \dfrac{\lambda_k}{\mu_k}$, $k = 1, 2, 3, 4, 5$

$\delta_0 = y_2^2 + y_4^2$, $\delta_1 = (y_1 + y_2 + y_3 + y_4 + y_5)$, $\delta_2 = (1 + y_2 y_4)$, $\delta_3 = (y_1 + y_3 + y_5)$ and $\delta_4 = (y_2 + y_4)$

Equations (22) to (24) are now:

$$A_V(\infty) = \frac{(1 + y_2 + y_4 + y_2 y_4)}{1 + \delta_0 + \delta_1 \delta_2 + \delta_3 \delta_4} \tag{25}$$

$$B_{S1}(\infty) = \frac{y_2 + y_4 + y_2 y_4}{1 + \delta_0 + \delta_1 \delta_2 + \delta_3 \delta_4} \tag{26}$$

$$B_{S2}(\infty) = \frac{(y_1 + y_3 + y_4)(y_2 + y_4 + y_2 y_4) + \delta_0 + y_2 y_4 (y_2 + y_4)}{1 + \delta_0 + \delta_1 \delta_2 + \delta_3 \delta_4} \tag{27}$$

The units/subsystems are exposed to corrective maintenance due to partial and complete failure, while the repairman is busy performing maintenance action to the failed units. Let C_0, C_1 and C_2 be the revenue generated when the system is in working state and no income when in failed state, cost of each repair due to partial and complete failure respectively. The expected total profit of system per unit time incurred to the system in the steady-state is given by:

Profit =total revenue generated – cost incurred by the repair man due to partial failure – cost incurred due to complete failure.

$$P_F(\infty) = k_0 A_V(\infty) - k_1 B_{S1}(\infty) - k_2 B_{S2}(\infty) \tag{28}$$

IV. Results and Discussion

In this section, numerical examples are presented using
MATLAB package. The following cases are used in the simulations.

The following parameter values are used in this case: $\lambda_1 = 0.003$; $\lambda_2 = 0.003$; $\lambda_3 = 0.001$; $\lambda_4 = 0.002$; $\lambda_5 = 0.002$; $\mu_1 = 0.8$; $\mu_2 = 0.7$; $\mu_3 = 0.6$; $\mu_4 = 0.6$; $\mu_5 = 0.9$; $k_0 = 10,500,000$; $k_1 = 550$; $k_2 = 1250$;

(a)   (b)
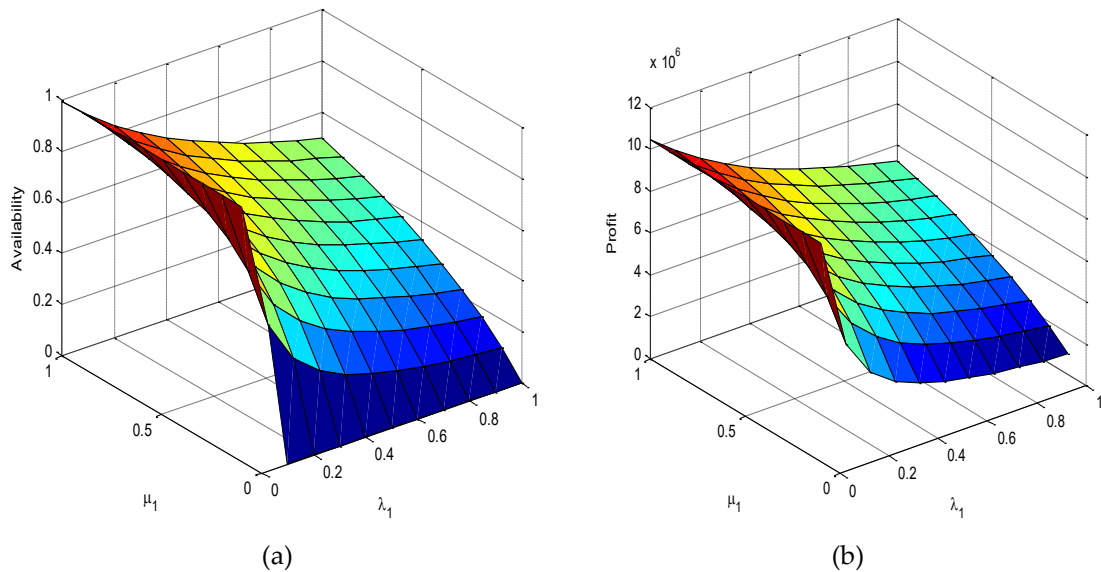
Figure 3: Availability and Profit with respect to failure and rates of subsystem A
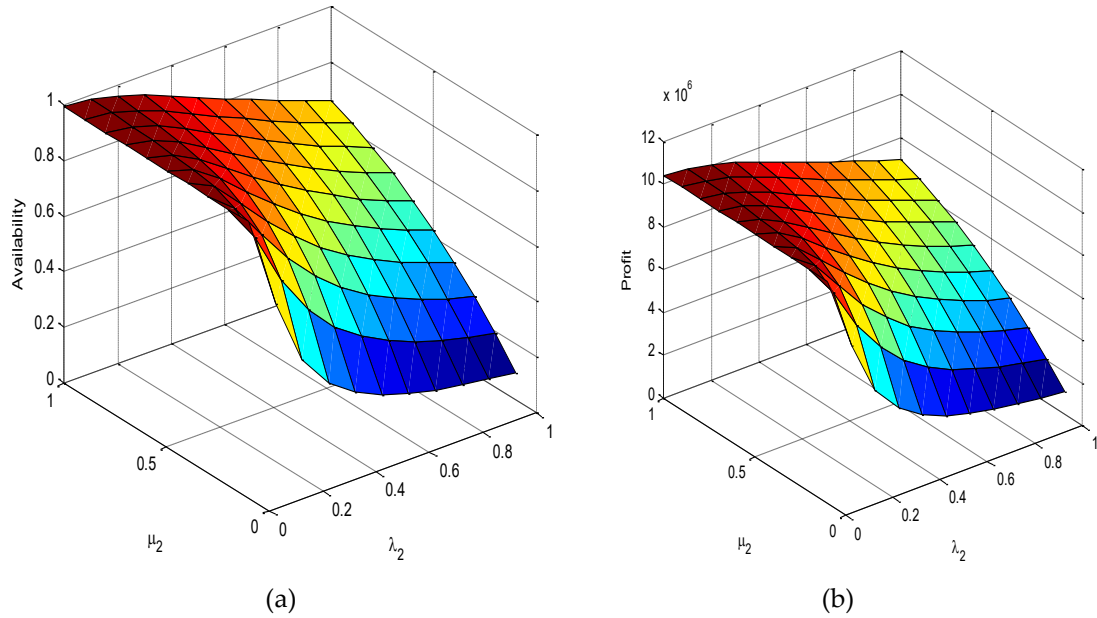
Figure 4: Availability and Profit with respect to failure and rates of subsystem B
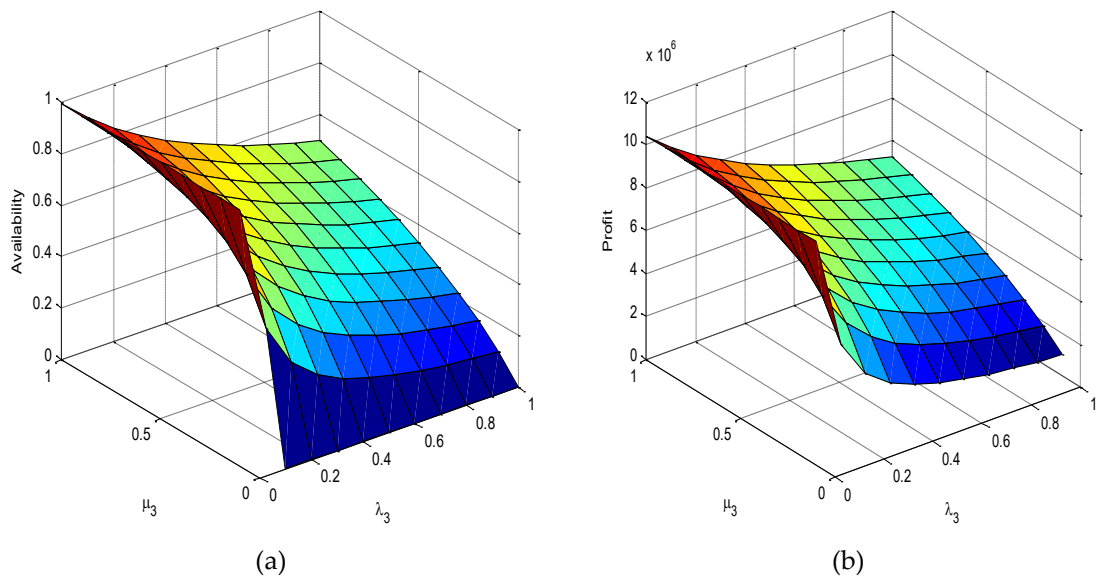
Figure 5: Availability and Profit with respect to failure and rates of subsystem C
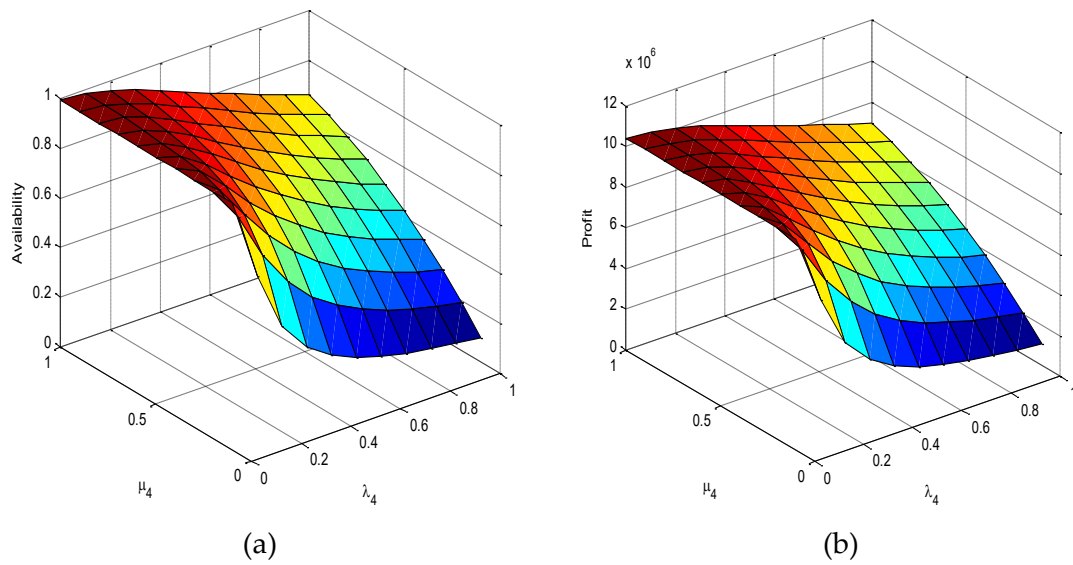
Figure 6: Availability and Profit with respect to failure and rates of subsystem D
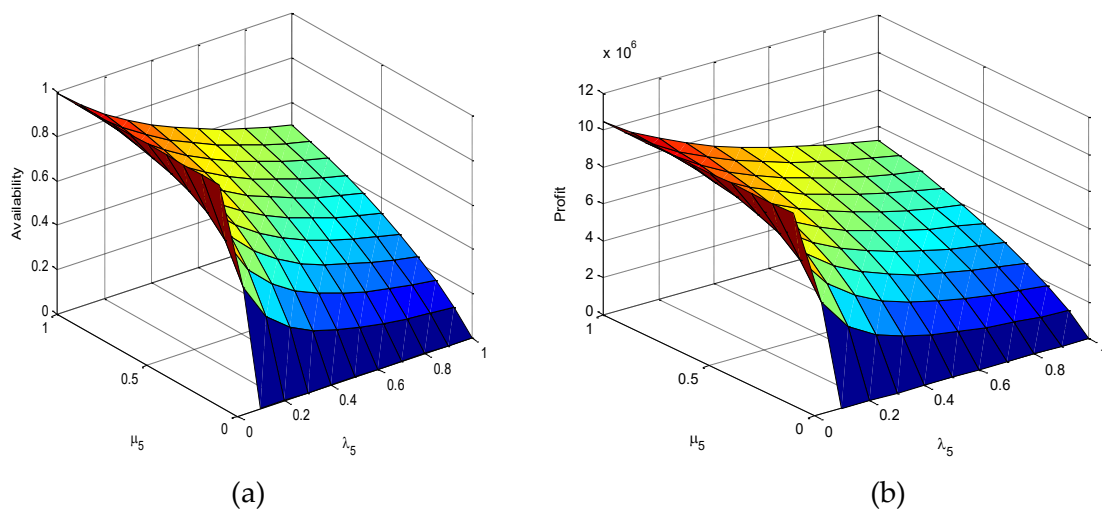
Figure 7: Availability and Profit with respect to failure and rates of subsystem E

From the surface plots in Figures 3 to 7 availability and profit decreases as the failure rate increases λ_m and increases as repair rate μ_m increases for $m = 1, 2, 3, 4, 5$. These plots indicate that, availability and profit of the system are higher for higher values of μ_m and lower values of λ_m. From these plots it can be observe that reducing the occurrence of failure earlier or practicing perfect repair will lead to higher values of availability and profit as well as the expected life time of the system. This indicate that adequate maintenance action such as inspection, perfect repair or replacement should be practice to enhance the availability and profit.

Table 2: Variation of Availability and Profit with respect to failure and rates of subsystem A

λ_1	Availability $\mu_1 \in [0.45 : 0.05 : 0.7]$						Profit $*10^7$ $\mu_1 \in [0.45 : 0.05 : 0.7]$					
0.0005	0.9950	0.9951	0.9952	0.9953	0.9953	0.9954	1.0448	1.0449	1.0450	1.0450	1.0451	1.0452
0.001	0.9939	0.9941	0.9943	0.9945	0.9946	0.9947	1.0436	1.0438	1.0440	1.0442	1.0443	1.0444
0.0015	0.9928	0.9931	0.9934	0.9936	0.9938	0.9940	1.0425	1.0428	1.0431	1.0433	1.0435	1.0437
0.002	0.9917	0.9922	0.9925	0.9928	0.9931	0.9933	1.0413	1.0418	1.0421	1.0425	1.0427	1.0429
0.0025	0.9906	0.9912	0.9916	0.9920	0.9923	0.9926	1.0402	1.0407	1.0412	1.0416	1.0419	1.0422
0.003	0.9895	0.9902	0.9907	0.9912	0.9916	0.9919	1.0390	1.0397	1.0403	1.0407	1.0411	1.0415

Table 3: Variation of Availability and Profit with respect to failure and rates of subsystem B

λ_2	Availability $\mu_2 \in [0.5 : 0.05 : 0.8]$						Profit $*10^7$ $\mu_2 \in [0.5 : 0.05 : 0.8]$					
0.03	0.9898	0.9902	0.9906	0.9908	0.9910	0.9912	1.0393	1.0397	1.0401	1.0403	1.0406	1.0408
0.04	0.9878	0.9885	0.9891	0.9896	0.9899	0.9902	1.0372	1.0379	1.0385	1.0390	1.0394	1.0397
0.05	0.9853	0.9864	0.9873	0.9880	0.9885	0.9890	1.0345	1.0357	1.0366	1.0373	1.0379	1.0384
0.06	0.9823	0.9838	0.9851	0.9860	0.9868	0.9875	1.0314	1.0330	1.0343	1.0353	1.0362	1.0369
0.07	0.9788	0.9809	0.9825	0.9838	0.9849	0.9858	1.0277	1.0299	1.0316	1.0330	1.0341	1.0351
0.08	0.9749	0.9776	0.9796	0.9813	0.9827	0.9838	1.0237	1.0264	1.0286	1.0304	1.0318	1.0330

Table 4: Variation of Availability and Profit with respect to failure and rates of subsystem C

λ_3	Availability $\mu_3 \in [0.4 : 0.05 : 0.65]$						Profit $*10^7$ $\mu_3 \in [0.4 : 0.05 : 0.65]$					
0.005	0.9818	0.9832	0.9843	0.9851	0.9859	0.9865	1.0309	1.0323	1.0335	1.0344	1.0352	1.0358
0.01	0.9699	0.9726	0.9747	0.9764	0.9778	0.9791	1.0184	1.0212	1.0234	1.0252	1.0267	1.0280
0.015	0.9583	0.9622	0.9653	0.9678	0.9699	0.9718	1.0062	1.0103	1.0135	1.0162	1.0184	1.0203
0.02	0.9470	0.9520	0.9560	0.9594	0.9622	0.9645	0.9943	0.9996	1.0038	1.0073	1.0103	1.0128
0.025	0.9359	0.9420	0.9470	0.9511	0.9545	0.9574	0.9827	0.9891	0.9943	0.9986	1.0022	1.0053
0.03	0.9251	0.9323	0.9381	0.9429	0.9470	0.9504	0.9713	0.9789	0.9850	0.9901	0.9943	0.9980

Table 5: Variation of Availability and Profit with respect to failure and rates of subsystem D

λ_4	Availability $\mu_4 \in [0.5 : 0.05 : 0.75]$						Profit $*10^7$ $\mu_4 \in [0.5 : 0.05 : 0.75]$					
0.02	0.9910	0.9913	0.9915	0.9916	0.9917	0.9918	1.0406	1.0409	1.0411	1.0412	1.0413	1.0414
0.045	0.9855	0.9867	0.9876	0.9883	0.9888	0.9893	1.0347	1.0360	1.0369	1.0377	1.0383	1.0388
0.07	0.9763	0.9789	0.9810	0.9826	0.9839	0.9850	1.0251	1.0278	1.0300	1.0317	1.0331	1.0342
0.095	0.9640	0.9686	0.9721	0.9749	0.9772	0.9790	1.0122	1.0170	1.0207	1.0236	1.0260	1.0280
0.12	0.9494	0.9561	0.9613	0.9655	0.9689	0.9717	0.9969	1.0038	1.0093	1.0137	1.0173	1.0203
0.145	0.9329	0.9418	0.9489	0.9546	0.9593	0.9631	0.9795	0.9889	0.9963	1.0023	1.0072	1.0113

Table 6: Variation of Availability and Profit with respect to failure and rates of subsystem E

λ_5	Availability $\mu_4 \in [0.5 : 0.05 : 0.75]$						Profit $*10^7$ $\mu_4 \in [0.5 : 0.05 : 0.75]$					
0.0145	0.9600	0.9667	0.9713	0.9745	0.9770	0.9789	1.0080	1.0150	1.0198	1.0232	1.0258	1.0279
0.0170	0.9543	0.9621	0.9673	0.9711	0.9740	0.9763	1.0020	1.0102	1.0157	1.0197	1.0227	1.0251
0.0195	0.9486	0.9575	0.9635	0.9678	0.9711	0.9736	0.9960	1.0053	1.0116	1.0162	1.0196	1.0223
0.022	0.9430	0.9529	0.9596	0.9644	0.9681	0.9710	0.9902	1.0005	1.0076	1.0127	1.0165	1.0195
0.0245	0.9375	0.9484	0.9558	0.9611	0.9652	0.9684	0.9844	0.9958	1.0036	1.0092	1.0135	1.0168
0.027	0.9320	0.9439	0.9520	0.9579	0.9623	0.9658	0.9786	0.9911	0.9996	1.0057	1.0104	1.0141
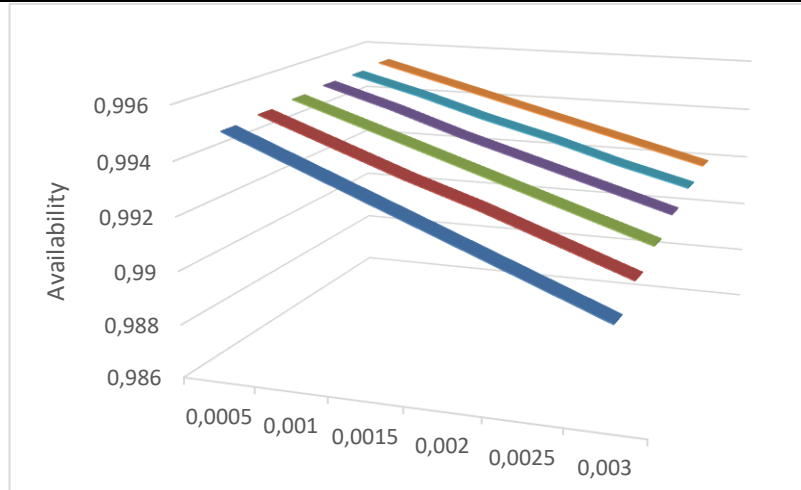
Figure 8a: Availability against λ_1 for $\mu_1 \in [0.45 : 0.05 : 0.7]$
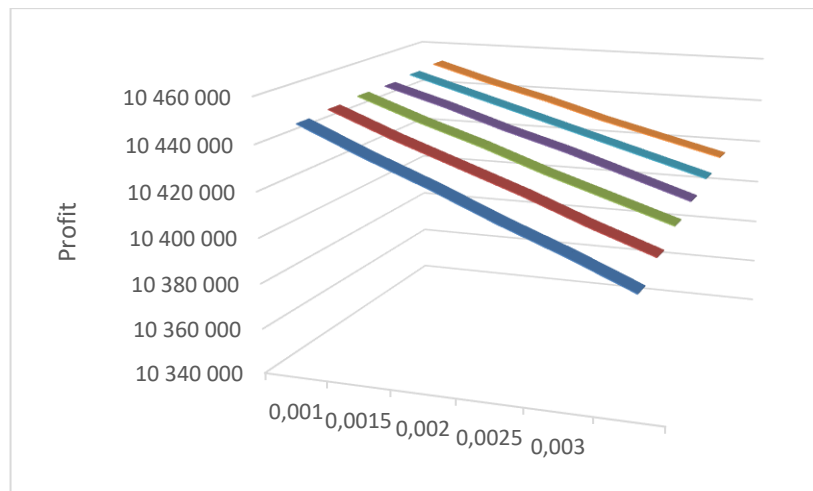
Figure 8b: Profit against λ_1 for $\mu_1 \in [0.45 : 0.05 : 0.7]$
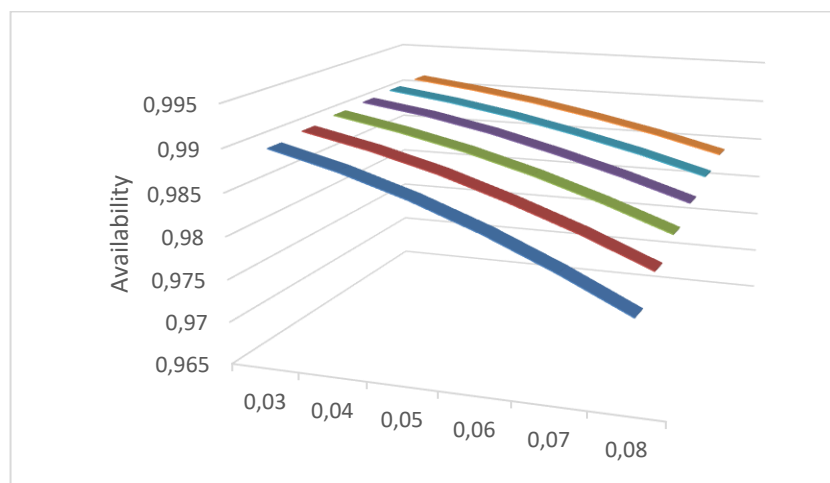
Figure 9a: Availability against λ_2 for $\mu_2 \in [0.5 : 0.05 : 0.8]$
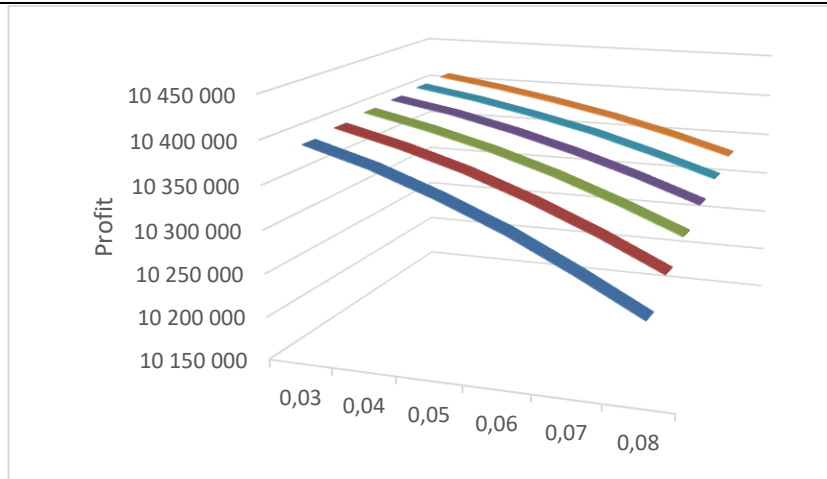
Figure 9b: Profit against λ_2 for $\mu_2 \in [0.5 : 0.05 : 0.8]$
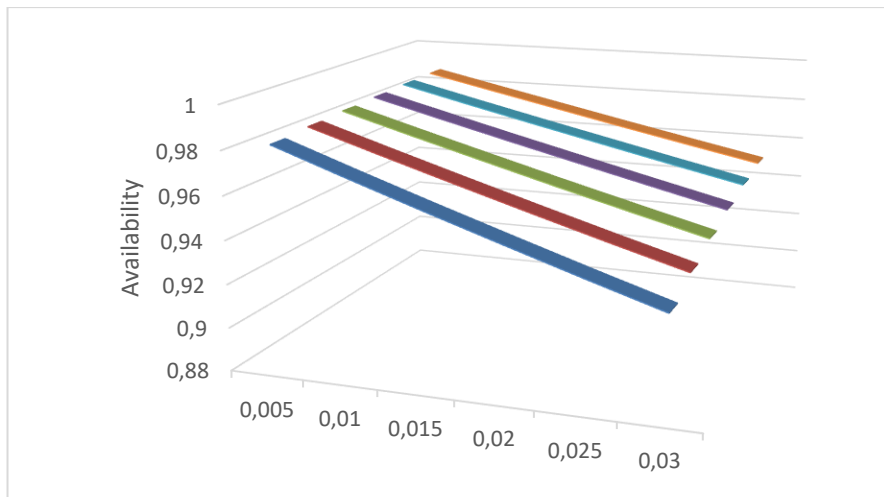
Figure 10a: Availability against λ_3 for $\mu_3 \in [0.4 : 0.05 : 0.65]$
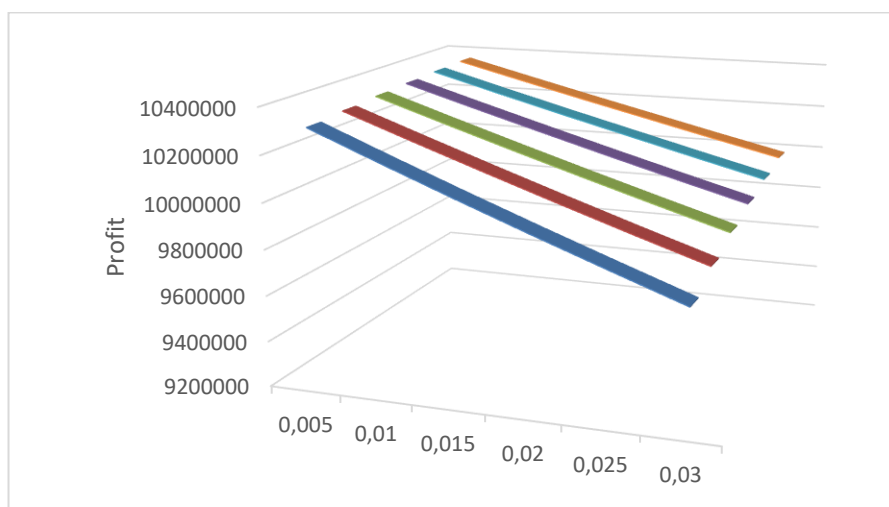
Figure 10b: Profit against λ_3 for $\mu_3 \in [0.4:0.05:0.65]$
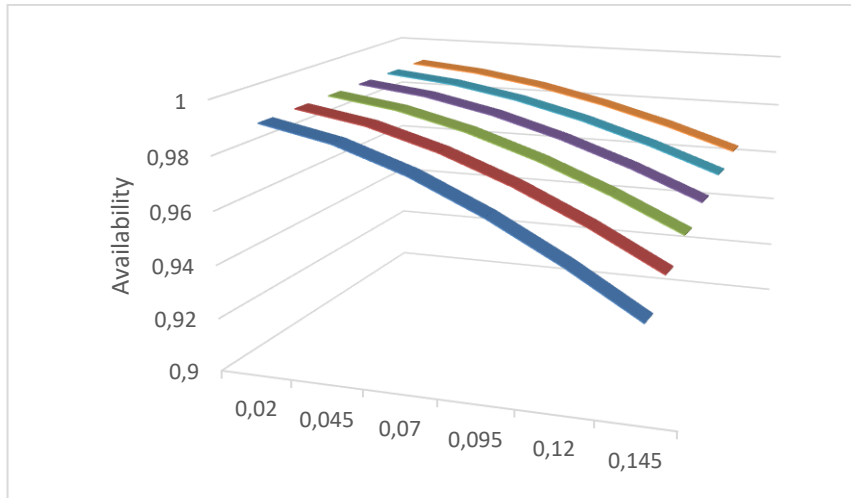
Figure 11a: Availability against λ_4 for $\mu_4 \in [0.5:0.05:0.75]$
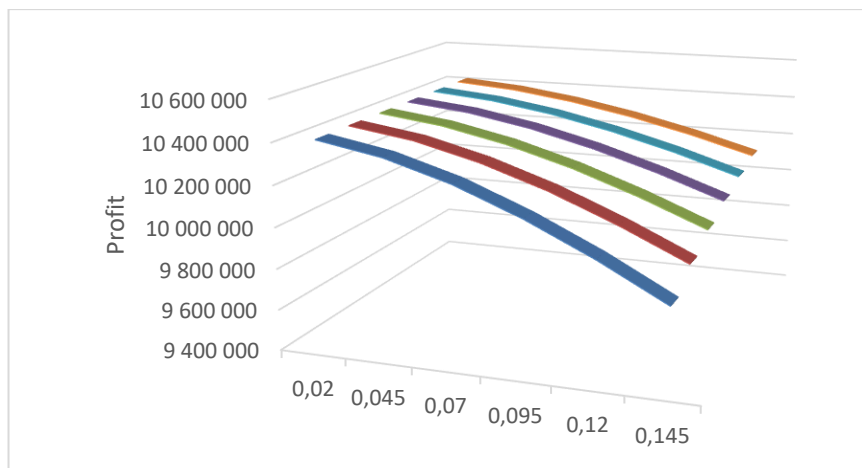
Figure 11b: Profit against λ_4 for $\mu_4 \in [0.5:0.05:0.75]$
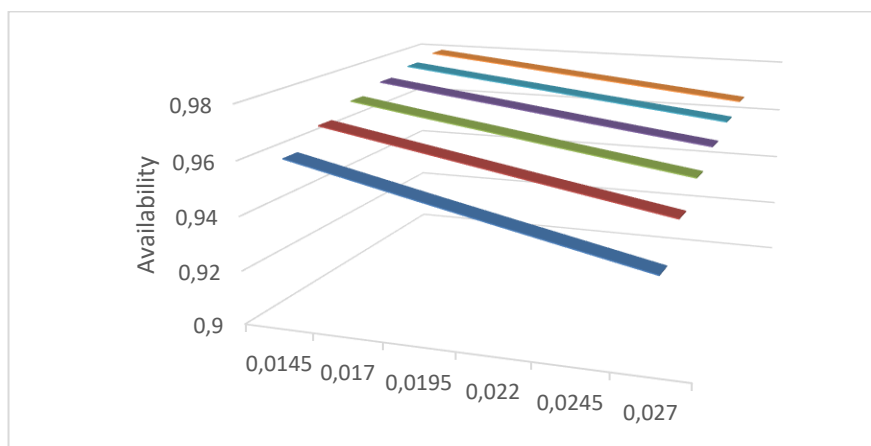
Figure 12a: Availability against λ_5 for $\mu_5 \in [0.0145:0.0025:0.027]$
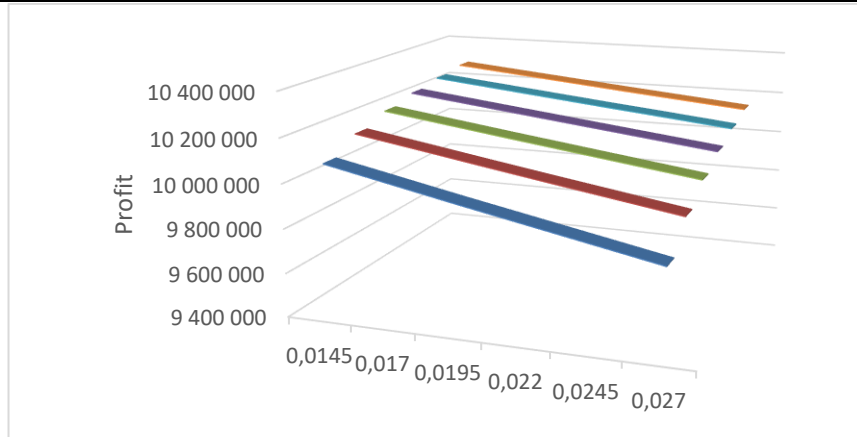
Figure 12b: Profit against λ_5 for $\mu_5 \in [0.0145:0.0025:0.027]$

Table 2 and Figures 8a and 8b present the impact of failure and repair rates of subsystem A against the availability and profit for different values of parameters λ_1 and μ_1. It is evident from Table 2 and Figure 8a and 8b that availability and profit shows increasing pattern with respect to repair rate μ_1 and decreasing pattern with respect to failure rate λ_1. It is clear that availability and profit are higher with the higher value of μ_1 **and lower with higher value of** λ_1.

Table 3 and Figures 9a and 9b display the effect of failure and repair rates of subsystem B against the profit for different values of parameters λ_2 and μ_2. It is evident from Table 3 and Figure 9a and 9b that the availability and profit shows increasing pattern with respect to repair rate μ_2 and decreasing pattern with respect to failure rate λ_2. It is clear that availability and profit are higher with the higher value of μ_2 **and lower with higher value of** λ_2.

Results from Table 4 and Figures 10a and 10b present the impact of failure and repair rates of subsystem C against availability and profit for different values of parameters μ_3 and λ_3. It is evident from Table 4 and Figure 5a that the profit shows increasing pattern with respect to repair rate μ_3 and decreasing pattern with respect to failure rate λ_3. It is clear that availability and profit are higher with the higher value of μ_3 **and lower with higher value of** λ_3.

It is evident from Table 5 and Figures 11a and 11b that availability and profit increases and decreases with increase in the values of parameters μ_4 and λ_4. It is evident from Table 5 and Figure 11a and 11b that availability and profit shows increasing pattern with respect to repair rate μ_4 and decreasing pattern with respect to failure rate λ_4. It is clear that availability and profit are higher with the higher value of μ_4 **and lower with higher value of** λ_4.

Table 6 and Figures 12a and 12b present the impact of failure and repair rates of subsystem E against the availability and profit for different values of parameters μ_5 and λ_5. It is evident from Table 6 and Figure 12a and 12b that availability and profit shows increasing pattern with respect to repair rate μ_5 and decreasing pattern with respect to failure rate λ_5. It is clear that profit is higher with the higher value of μ_5 **and lower with higher value of** λ_5.

V. Conclusion

In this paper, we constructed a series-parallel system configuration consisting of five subsystems to study the cost analysis of the system. Explicit expressions for steady-state availability, busy period and profit function for the system are derived. In this research work, mathematical models of availability and profit are developed and validated for each of the subsystem operation in a sachet water system. Numerical results presented have shown the effect of both failure and repair rates on profit. From the analysis, it is evident that profit can be enhancing through:

- ✓ Proper maintenance planting to avoid the occurrence of catastrophic failure.
- ✓ Maintaining the system availability at the highest order.
- ✓ Adding more fault tolerant redundant units/subsystem

Mathematical models of the system are developed in the form of availability, busy period of repairman due to minor and major failure and as well as profit function. Availability and Profit generated are presented in the Tables 2 to 6. The effects of failure and repair rates of all the subsystems are presented in the form of profit matrices. It is evident from the availability and profit matrices that as failure/repair rates increases, availability and profit tend to decrease/increase.

With modifications and assumptions, the model in this paper will plant management to avoid an incorrect reliability assessment and consequent erroneous decision making, which may lead to unnecessary expenditures. The present work can extend to incorporate failure dependency, condition monitoring to enable management in determining the optimal maintenance/ replacement time.

On the basis of the surface plots, tables and figures, it is evident that the availability and profit can be enhanced through higher values of repair rates together with lower values of failure rates. Thus, higher system availability and revenue can be achieved through repair of early failure of units, individual subsystem replacement, and proper maintenance planning to avoid the occurrence of catastrophic failure, and by adding fault tolerant units/subsystems. The present work can be extended further for a system to containing multi-subsystems with multi units and solve using human reliability analysis techniques

References

[1] Aggarwal A. K, Kumar S, Singh V, Garg TK, 2014. Markov modelling and reliability analysis of urea synthesis system of a fertilizer plant. Journal of Industrial Engineering International, 11, 1-14, DOI 10. 1007/s40092-014-0091-5.

[2] Aggarwal, A. K.,Kumar, S. and Singh, V, 2017. Mathematical modeling and fuzzy availability analysis for serial processes in the crystallization system of a sugar plant, Journal of Industrial Engineering International, 13:47–58, DOI 10.1007/s40092-016-0166-6.

[3] Arvind K Lal, A. K., Manwinder Kaur M and Lata, S. (2013). Behavioral study of piston manufacturing plant through stochastic models, Journal of Industrial Engineering International, 9(24), 1-10. http://www.jiei-tsb.com/content/9/1/24.

[4] Fadi N. Sibai, F.N. (2014). Modelling and output power evaluation of series parallel photovoltaic modules, International Journal of Advanced Computer Science and Applications,5(1),129-136.

[5] Garg D, Kumar K, and Singh J., 2010a. Availability analysis of a cattle feed plant using matrix method. Int J Eng 3(2):201–219

[6] Garg S, Singh J and Singh D. V., 2010b. Availability analysis of crankcase manufacturing in a

two-wheeler automobile industry. Appl Math Model 34:1672–1683

[7] Garg H and Sharma S.P., 2011. Multi-objective optimization of crystallization unit in a fertilizer plant using particle swarm optimization. Int J Appl Sci Eng 9(4):261–276

[8] Gupta S, and Tewari P.C., 2011. Simulation modeling in a availability thermal power plant. J Eng Sci Technol Rev 4(2):110–117.

[9] Khanduja R, Tewari PC, Kumar D., 2012. Steady state behaviour and maintenance planning of bleaching system in a paper plant. Int J Ind Eng 7(12):39–44

[10] Kadiyan S, Garg RK, Gautam R., 2012. Reliability and availability analysis of uncaser system in a brewery plant. Int J Res Mech Eng Technol 2(2):7–11.

[11] Kumar, A., Saini, M. and Malik, S. C., 2014. Stochastic modelling of a concrete mixture plant with preventive maintenance, Application and Applied Mathematics, 9(1): 13-27.

[12] Kumar V and Mudgil V., 2014. Availability optimization of ice cream making unit of milk plant using genetic algorithm, IntManag Bus Stu, 4(3), 17-19.

[13] Kumar S, and Tewari PC., 2011. Mathematical modelling and performance optimization of CO2 cooling system of a fertilizer plant. Int J IndustEng Comp, 2, 689-698

[14] Kumar R, Sharma AK, Tewari PC., 2011. Performance modelling of furnace draft air cycle in a thermal plant. Int J EngSci Tech, 3(8), 6792-6798.

[15] Kumar, A and Lata, S., 2012. Reliability evaluation of condensate system using fuzzy Markov Model, Annals of Fuzzy Mathematics and Informatics, 4(2), 281-291.

[16] Ram, M and Manglik, M., 2016. An analysis to multi-state manufacturing system with common cause failure and waiting repair strategy, Cogent Engineering 3: 1266185, 1-20, http://dx.doi.org/10.1080/23311916.2016.1266185

[17] Tewari PC, Khaduja R, and Gupta, M., 2012 Performance enhancement for crystallization unit of a sugar plant using genetic algorithm technique. J Ind Eng Int 8(1):1–6

[18] Yusuf, I., Sani, B and Yusuf, B. (2019). Profit analysis of a series-parallel system under partial and complete failures, Journal of Applied Sciences, 19(6),565-574.

Eesha Mishra, Santosh Kumar
PERFORMANCE COMPUTATION MODEL AND TIME LATENCY
IMPROVEMENT FOR BLOCKCHAIN-BASED VOTING SYSTEM

RT&A, No 1 (61)
Volume 16, March 2021

Performance Computation Model and Time Latency Improvement for Blockchain-Based Voting System for Elections in India

Eesha Mishra

●

*Research Scholar, School of Computer Science, Maharishi University
of Information Technology, Lucknow
Eeshamishra786@gmail.com*

Santosh Kumar

●

*Associate Professor, School of Computer Science, Maharishi University
of Information Technology, Lucknow
Sant7783@hotmail.com*

Abstract

Blockchain is inalterable and simple confirmable framework that has a noteworthy potential to be an option in contrast to customary races. It carries savvy answers for focal power issue as far as squares having all information in blockchain. In past decades customary races neither fulfill the residents nor government official. The democratic isn't completely made sure about, compromises security and straightforwardness of voters alongside having an excess of time to check the vote. In this paper, we proposed a model that giving the arrangement utilizing the blockchain to dispense with all drawbacks of customary decisions. The security of information, votes and voter is guaranteed in the framework. The sitting tight an ideal opportunity for result diminished fundamentally through the proposed model.

Keywords: Blockchain, Voting, Electronic Voting.

1. Introduction

Elections are one of the significant instrument to got the vote based system any nation. Elections give the opportunity to choose your preferred individual for lead the country. In this manner, it is a lot of significant for each individual of the nation to included and take part in Elections to assemble the eventual fate of the country. In any case, this is a lot of significant that political decision system must be a lot of conspicuous and reliable in its inclination. The administration association that engaged with Elections need to guarantee individuals' protection and vote's security. In addition, the political decision commission is answerable for checking the votes and delivering the outcomes however there is an opportunity of robbery or control of votes and results if commission setting aside long effort to tally the votes. The reliability of any elections is a questionable issues which depends on the territories of the elections. Particularly, those zones where the paper elections are overseen by the political elections commission. Along these lines, there is an extraordinary danger of security and protection of political elections and the votes during checking them effectively while the time is another significant factor to report the political

Eesha Mishra, Santosh Kumar
PERFORMANCE COMPUTATION MODEL AND TIME LATENCY
IMPROVEMENT FOR BLOCKCHAIN-BASED VOTING SYSTEM

RT&A, No 1 (61)
Volume 16, March 2021

elections result convenient. Subsequently, in this paper an endeavor is made to elevate the security, protection and execution of the electronic democratic framework.

This is a way to deal with expel the escape clauses or disadvantages of the customary elections frameworks and attempt to profited by web based democratic framework to computerise the entire procedure. There are a few issues in traditional democratic just as electronic democratic that can be settled by the utilising the blockchain instrument that has capacity to make sure about the voter's protection and information (votes).

A blockchain instrument takes a shot at the dispersed and undeniable system framework that conjures the extremely secure exchange of squares with no go between. In this system the enlightening qualities trade carefully that can't be modify at any stage. Because of these such usefulness a blockchain can possibly turn into an option of the conventional decisions and give a savvy answer for the political elections commission where all the squares have all the information (votes) as chain that is difficult to change a data of the square which increment the security of the data that put away in it. As in conventional elections there is a lot of time required to declare the consequence of the democratic however blockchain resolve this issue by its tendency on the grounds that the last hub of the blockchain has all the data which is sufficient for checking the vote simply look the last hub and get all the data and this lessens the holding up time exponentially. In this manner, this paper proposed the arrangement explicitly for issues of customary paper elections in INDIA. Security and protection of votes and voters and the speed of checking votes and reporting the outcomes are talked about in the arrangement. An agent model of the framework is introduced in Proposed Solution segment.

2. Related Works

As the blockchain based democratic framework is secure and safe democratic component still it isn't broadly received by the few nations because of some exhibition and time inactivity issues in casting a ballot framework. Hence, there are a few analysts have done parcel of exploration to improve the presentation and time inertness. Let us first quickly examined some exploration works identified with blockchain based democratic framework. F. P. Hjálmarsson [1] et al have proposes a novel electronic democratic framework dependent on blockchain that tends to a portion of the impediments in existing frameworks and assesses a portion of the mainstream blockchain structures to build a blockchain-based e-casting a ballot framework and assess the capability of circulated record advances through the depiction of a contextual analysis; specifically, the procedure of a political race, and the execution of a blockchain-based application, which improves the security and diminishes the expense of facilitating an across the country political decision. A. Barne et al [2] have proposed to fathom the issues of advanced democratic by utilizing blockchain innovation. M. Pawlak et al [3] have portrayed the utilization of shrewd operators and multi-specialist framework idea for Auditable Blockchain Voting System (ABVS), which coordinates e-casting a ballot procedure with blockchain innovation into one regulated non-far off web casting a ballot framework which is start to finish unquestionable. P. Tarasov and H. Tewari [4] have introduced a methodology that included a convention created on blockchain innovation. The basic innovation utilized in the democratic framework is an installment plot, which offers secrecy of exchanges, an attribute not seen in blockchain conventions to date. Bartolucci et al [5] have talked about potential employments of the blockchain innovation to execute a protected and reasonable democratic framework and presented a mystery share-put together democratic framework with respect to the blockchain, the supposed SHARVOT convention. B. Wang et al [6] have proposed homomorphic ElGamal encryption and ring signature, an electronic democratic plan dependent on blockchain for enormous scope casting a ballot. R. Hanifatunnisa and B. Rahardjo [7] have talks about the chronicle of casting a ballot result utilizing blockchain calculation from each spot of political race and proposed a strategy dependent on a foreordained turn on the framework for

Eesha Mishra, Santosh Kumar
PERFORMANCE COMPUTATION MODEL AND TIME LATENCY
IMPROVEMENT FOR BLOCKCHAIN-BASED VOTING SYSTEM

RT&A, No 1 (61)
Volume 16, March 2021

every hub in the worked of blockchain. R. Krimmer et al [8] have talked about the utilization of e-deciding in favor of the decisions to the Austrian Federation of understudies.

3. Experimental Study

Electronic Voting is the new period of the election of any nation which is broadly considered however embraced by certain nations in nowadays wherein INDIA is one of them. There are casting a ballot is done through electronic democratic machine. The way toward casting a ballot through the EVM is extremely straightforward, the voter go to the surveying stall as per their surveying territory alongside voter ID gave by the legislature of INDIA. The voter ID is confirmed by the surveying official and permit the voter to give the vote through the Electronic Voting Machine (EVM) and not permitted if the voter ID isn't checked. The vote is put away in the memory that is introduced in the democratic machine. The checking of casting a ballot is start after certain days when all the EVM have been gathered by the administration to its focal Wearhouse and the aftereffects of casting a ballot is reported subsequent to finishing the tallying of votes. The checking of votes is done physically so there are as yet an opportunity to miscalculating the votes or altering the votes during the tallying. Subsequently, handle these dangers of miscalculating or abusing the votes another democratic methodology is prepared to begin for example I-casting a ballot (web casting a ballot) which is blockchain based election approach.

3.1. Blockchain Based Election System

The blockchain based election framework has not been applied generally yet. This methodology is applied in constrained nations, South Korea is one of them which applied this methodology of election and reach to an effective resolutions in year 2017. Thusly, it is an endeavor to present another methodology of I-Voting a ballot (Blockchain based elections) in INDIA. The working instrument of Blockchain Based elections is represented in figure 3.1.1.
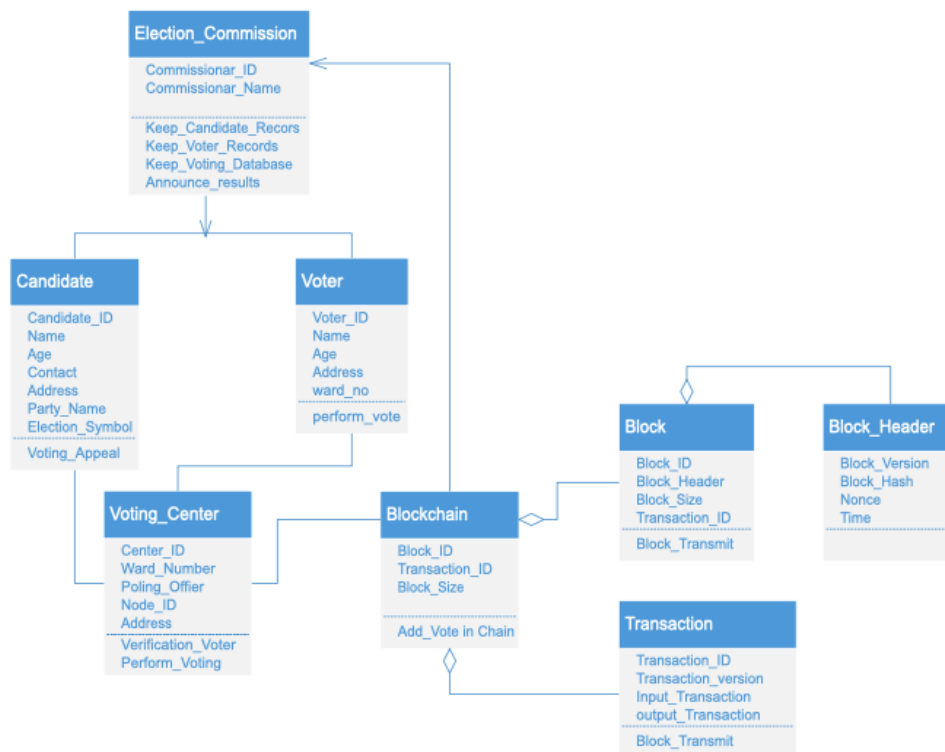
Figure 3.1. 1. Class Diagram for i-Voting System (Blockchain Based Election)

Eesha Mishra, Santosh Kumar
PERFORMANCE COMPUTATION MODEL AND TIME LATENCY
IMPROVEMENT FOR BLOCKCHAIN-BASED VOTING SYSTEM

RT&A, No 1 (61)
Volume 16, March 2021

In current innovation, blockchain is the most noticeable option of the conventional races for protection, security and consistency. For planning a protected blockchain in a vigorously populated nations think about numerous angles. First factor is human for such a framework, human impedance is completely precluded. In this manner, there are number of hubs (PCs) are viewed as that are near human interface. There no other information is considered aside from the vote that framework invigorate the to prevent from taking votes or evolving votes. The subsequent factor is to shielding the framework from programmers and ensured that one voter can cast a ballot just one time. As the vote is projected by the voter, the political race commission will be educated about the vote without uncovering the data about the vote. At that point political race commission award the consent to voter cast the vote. It is preposterous to expect to cast a ballot over and over by the voter in light of the fact that the elections commission give an electorate information of voters. Albeit a programmer is gotten the resident data and entered to the framework, he can't cast a ballot more than one time. It is beyond the realm of imagination to anybody to change in the acknowledged exchange in the blockchain on the grounds that in blockchain each exchange is associated or identified with the past exchange. In this manner, the democratic is a lot of dependable in blockchain innovation instead of conventional decisions in light of the fact that the blockchain is so much predictable. On the off chance that the programmers hacked the framework for controlling in casting a ballot distinguished promptly because of an incredible synchronization between hubs.

3.2. State Transitions of Blockchain Based Election System (i-Voting)

The Government (election commission) in this framework gives the approval to the residents of the nation that they can play out the vote at the democratic focuses. Additionally, the election commission and residents of the nation's decide the up-and-comers that will be taking an interest in that political decision. The voting booth data, up-and-comers and resident polling station connection will be given by the election commission which is the confided in party in the races. After resident's vote, it is added to the blockchain that is proposed in this examination work and any vote has an assurance from the framework about being changeless. Since a chain contains all the resident votes namelessly toward the finish of the elections, the official outcomes will be reported inside minutes after the election ends. Any concerning outsider can get the chain and tally the decisions in favor of being certain that casting a ballot is truly trusted.

The state transition or state chart diagram is represented here in the figure 3.1.2. that shows the transition of states at any time. The citizen/voter is an initial or starting state where the voter went to the voting center where the citizens are verified by checking the pooling officer if the citizen found right the voter allowed to perform the vote by choosing their favorite candidate and the choice of the voters are saved in the blockchain and send to send to central voting warehouse for counting at same time and announcing the result of the election in a quick time.

Eesha Mishra, Santosh Kumar
PERFORMANCE COMPUTATION MODEL AND TIME LATENCY
IMPROVEMENT FOR BLOCKCHAIN-BASED VOTING SYSTEM

RT&A, No 1 (61)
Volume 16, March 2021
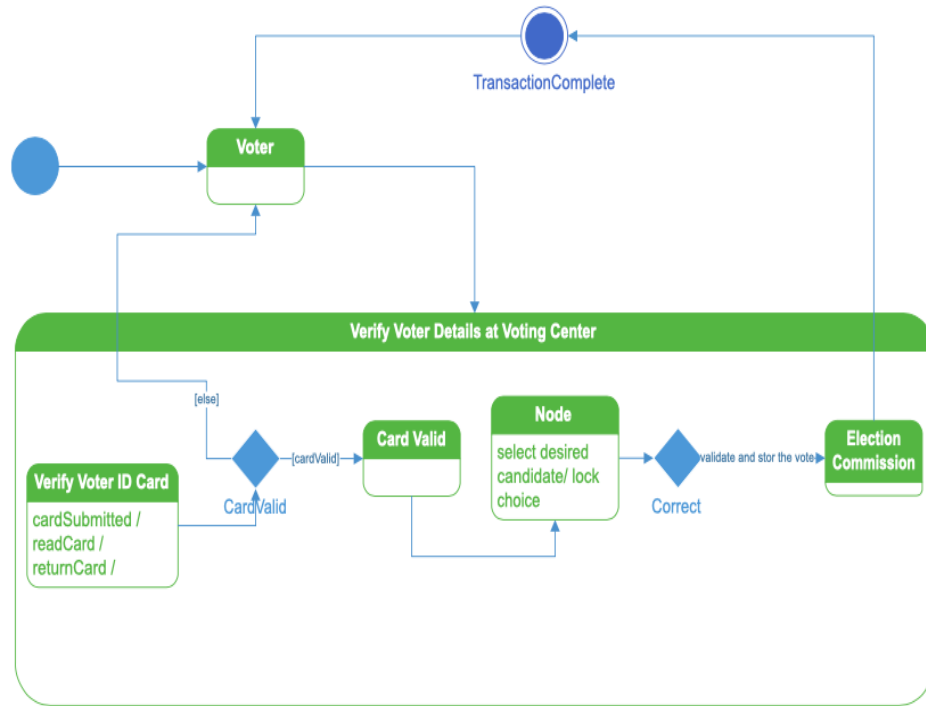
Figure 3.1.2. State Diagram for Blockchain Based Election System

3.3. Layered Architecture and Time Latency

A system is proposed here that has a layered structure. The layers of the system are dependent on the necessity of the country; for providing a fast, consistent and secure system, designed it into a layered manner. Reasons behind using a layered architecture are explained below in detail. Suppose the whole country represented the voting on a single blockchain, the performance of the system would affected because of huge number of ballots and the distances of the voting centers. These factors causes the latency, the time latency is the major problem when the country under the same blockchain. In INDIA the expected time latency would be much more higher than the expected time because INDIA is a Highly populated country that consists of thousands of voting centers where voting is performed at the same time at each center. Therefore, synchronization of the system would take lots of time. So, in order to decrease time latency, the blockchains are distributed over the states or stages of voting. From initial state/stage to final state/stage, there will be different chains at each state/stage, and connections between state/stage will be provided with a secure system.

Eesha Mishra, Santosh Kumar
PERFORMANCE COMPUTATION MODEL AND TIME LATENCY
IMPROVEMENT FOR BLOCKCHAIN-BASED VOTING SYSTEM

RT&A, No 1 (61)
Volume 16, March 2021
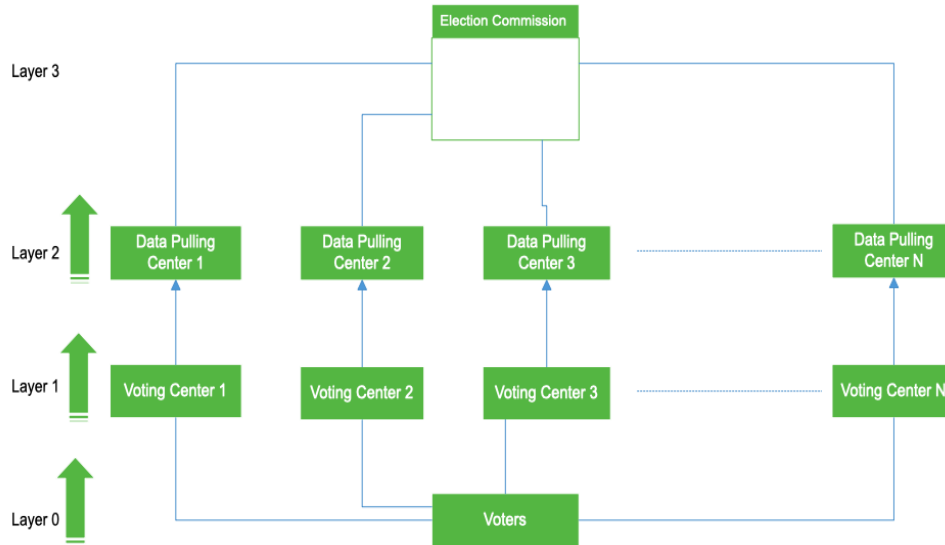
Figure 3.3.1. 3-Layer Architecture for I-Voting System

A 3-layer architecture for i-voting system is represented in figure 3.3.1. at the first layer there will be a chain that containing the several nodes known as voting centers. The voters perform their vote here after the verification by the polling officer. As there are limited numbers of nodes in every voting center and there are many voting centers in all the country. So synchronization will take adequate amount of time on that the chain will perform the voting without any latency. For that arranged the number of nodes in good patter. A system is try to build here which working on the government system that hold the voting data that was performed by the voter into Central voting data warehouse. In that system only those voters can vote who have authenticated ID proof issued by the government and one voter can give one vote only at a time, no proxy voting and tampering voting is done. When the voting process authenticated and satisfied, the voter can perform the vote otherwise voter has the choice to not give the vote anybody.

At the second layer, a cluster of chains is taken here that stored the data which coming from the first layer where blockchain technology used to make system consistent. At the second layer there are adequate numbers of nodes according to the country's population. Therefore, huge improvement in performance of the system due to increased number of nodes decreases the time latency. Hence the performance improved exponentially as the number of nodes are increased at layer 1 and layer 2.
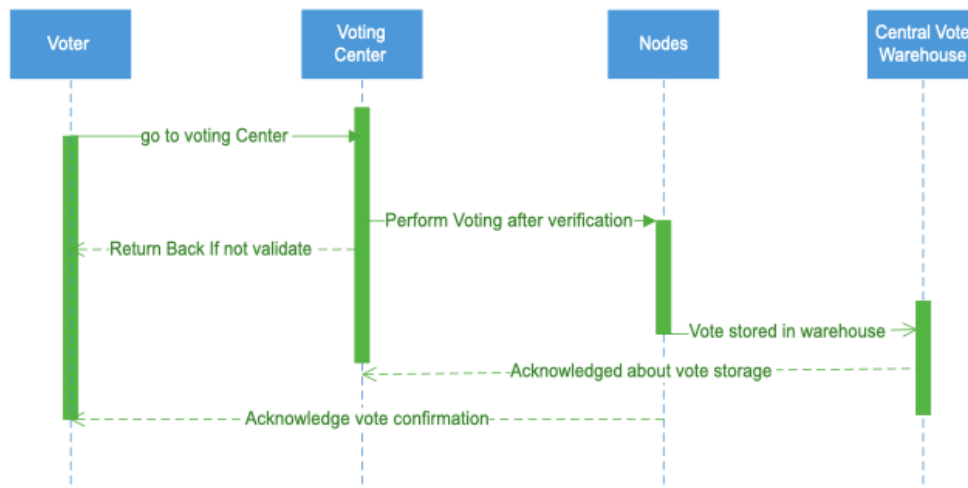
Figure 3.3.2. Sequence Diagram for Blockchain Based Election System

Eesha Mishra, Santosh Kumar
PERFORMANCE COMPUTATION MODEL AND TIME LATENCY
IMPROVEMENT FOR BLOCKCHAIN-BASED VOTING SYSTEM

RT&A, No 1 (61)
Volume 16, March 2021

The communication between these layers are done periodically through the communication protocols, so there is a time delay between each synchronization of layers because a huge complexity between these synchronization layers if every vote consider at the same time, a deadlock situation may arise. For country like India the synchronization time of voting more than 5 minutes i.e. each node send the chain data to the upper layer nodes (voting centers) through a synchronization algorithm.

3.2.   Algorithm for Synchronization

The nodes (Voting Centers) of the selected area using the same blockchain, so each node having a file that store the numbers of votes accepted from the upper layer at previous synchronization step. The voting is stopped for very short time due to voter is verified by the polling officer this took some time almost 3 to 5 minutes and then resynchronize the blockchain data between layers. The consistency of data is verified which is arrived from the lower layer to upper chain. If the consistency is confirmed the data (vote) is accepted and updated this into the file attached with this node. The nodes always know that how many votes are accepted at both layers and update the blockchain which is further considered as a transaction block.

The inconsistent data arrived from various machines to the upper layer considered with extra care. If the data not satisfying the consensus the data will not accepted and liable to decline. For the safe side the same data send to the upper layer for consistency satisfaction. This process continue until the consistency of votes are satisfied at each layers. Therefore, the election related data are stored in blocks which are categorized into two type such as: first one for building blockchain at lower layer that stored voter information, ballot box information and prev_hash info that is used when creating block which is added to blockchain. The block synchronization algorithm is represented below:

Step 1: Authentication of voter
- *Nodes (Voting Centers) gets the login details of voter and send them the central voting warehouse system along with voting center ID..*
- *Central Voting warehouse System (Government) validate the voter details (login details, voter info, node_id).*

Step 2: Voting
- *Let vote → Block, vote= (voter_id + election candidate)*
- *add(vote, chain) Block is added to blockchain*
- *Block information is updated to all the nodes (voting Centers)*
- *Acknowledged the vote and update the voter's information(voter_id, voter List, update) in central voting warehousing system.*

Step 3: Vote Counting Process
- *Get the candidates list*
- *Count the votes (Blocks) and determine the results*
  Result → Count (Blocks, Candidates)
- *Recheck the final blockchain by third party for any anomalies in blocks counting.*

Step 4: Exit

4. Conclusion and Future Scope

Democracies depend on trusted elections and citizens should trust the election system for a strong democracy. However traditional paper based elections do not provide trustworthiness. In this paper, we proposed a blockchain based e-voting system which provides trusted, secure and fast voting system for India. Proposed system is suitable to apply in another country whereas

Eesha Mishra, Santosh Kumar
PERFORMANCE COMPUTATION MODEL AND TIME LATENCY
IMPROVEMENT FOR BLOCKCHAIN-BASED VOTING SYSTEM

RT&A, No 1 (61)
Volume 16, March 2021

integration is a hard work since each country has different laws and election system changes between countries. For the future work, system can be applied for a use case and measurements can be taken to compare if the calculations hold. Synchronization and consensus algorithms can be discussed and improved for better performance and security.

Acknowledgments

References

[1]. F. Þ. Hjálmarsson, G. K. Hreiðarsson, M. Hamdaqa and G. Hjálmtýsson, "Blockchain-Based E-Voting System," 2018 IEEE 11th International Conference on Cloud Computing (CLOUD), San Francisco, CA, 2018, pp. 983-986.

[2]. A. Barnes, C. Brake, and T. Perry, "Digital Voting with the use of Blockchain Technology," Available: https://www.economist.com/sites/default/files/plymouth.pdf, Nov. 20, 2018.

[3]. M. Pawlak, A. Poniszewska-Marańda and N. Kryvinska, "Towards the intelligent agents for blockchain e-voting system," Science , vol. 141, pp. 239-246, 2018.

[4]. P. Tarasov and H. Tewari, "The Future of e-Voting", IADIS International Journal on Computer Science and Information Systems, vol. 12, no. 2, pp. 148-165.

[5]. Bartolucci, S., Bernat, P., & Joseph, D. SHARVOT: Secret SHARe-Based VOTing on the Blockchain. 2018 IEEE/ACM 1st International Workshop on Emerging Trends in Software Engineering for Blockchain (WETSEB), 30-34, 2018.

[6]. B. Wang, J. Sun, Y. He, D. Pang and N. Lu, "Large-scale Election Based On Blockchain", Procedia Computer Science, vol. 129, pp. 234- 237, 2018.

[7]. R. Hanifatunnisa and B. Rahardjo, "Blockchain based e-voting recording system design," 2017 11th International Conference on Telecommunication Systems Services and Applications (TSSA), Lombok, 2017, pp. 1-6.

[8]. R. Krimmer, A. Ehringfeld, and M. Traxl, "The Use of E-Voting in the Austrian Federation of Students Elections 2009," Internet: https://pdfs.semanticscholar.org/6b8f/34a5bd3e7eabc7e3a9a3f008187e4415e26a.pdf, Nov. 26, 2018.

Aditya Tiwary, Swati Tiwary
EVALUATION OF RELIABILITY INDICES OF ROY BILLINTON TEST
SYSTEM (RBTS) BUS-2 DISTRIBUTION SYSTEM FOR EDUCATIONAL
PURPOSE

RT&A, No 1 (61)
Volume 16, March 2021

Evaluation of Reliability Indices of Roy Billinton Test System (RBTS) Bus-2 Distribution System for Educational Purpose

Aditya Tiwary, Swati Tiwary

●

Entrepreneur, Vijay Nagar, Indore, India
raditya2002@gmail.com

Abstract

Evaluation of reliability is most important when we have to check the availability of supply in any distribution system. A basic reliability index which is of importance is failure rate of the distribution system. In this paper evaluation of system data i.e. failure rate which is one of the important basic reliability indices of Roy Billinton test system (RBTS) Bus-2 distribution system for educational purpose is done. This paper also evaluates the reliability of each and every feeder section of the RBTS. The mean time to failure (MTTF) of the feeders is also evaluated for each and every feeder section of the distribution system of the RBTS Bus-2 distribution system. The evaluated system data and various reliability indices can be used for educational purpose.

Keywords: Roy Billinton Test System (RBTS) Bus-2 Distribution System; Reliability; Failure Rate; Mean Time to Failure.

I. Introduction

Reliability evaluation of distribution system is an important issue. Allan et al. [1] proposed modelling and evaluation of the distribution system reliability. Wojczynski et al. [2] discussed distribution system simulation studies which investigate the effect of interruption duration distributions and cost curve shapes on interruption cost estimates. New indices to reflect the integration of probabilistic models and fuzzy concepts was proposed by Verma et al. [3]. Zheng et al. [4] developed a model for a single unit and derived expression for availability of a component accounting tolerable repair time. Distributions of reliability indices resulting from two sampling techniques are presented and analyzed along with those from MCS by Jirutitijaroen and Singh [5]. Dzobe et al. [6] investigated the use of probability distribution function in reliability worth analysis of electric power system. Bae and Kim [7] presented an analytical technique to evaluate the reliability of customers in a microgrid including distribution generations. Reliability network equivalent approach to distribution system reliability assessment is proposed by Billinton and Wang [8]. It also described a new method of planning for power distribution system. Bhowmik et al. [9] developed an algorithm to obtain an optimal solution by considering a non-linear objective function with linear and non-linear constraints for a large scale radial distribution system. A Markov cut-set composite approach to the reliability evaluation of transmission and distribution systems involving dependent failures was proposed by Singh et al. [10]. The reliability indices have been determined at any point of composite system by conditional probability approach by Billinton et al. [11]. Distributions of reliability indices resulting from two sampling techniques are

Aditya Tiwary, Swati Tiwary
EVALUATION OF RELIABILITY INDICES OF ROY BILLINTON TEST
SYSTEM (RBTS) BUS-2 DISTRIBUTION SYSTEM FOR EDUCATIONAL
PURPOSE

RT&A, No 1 (61)
Volume 16, March 2021

presented and analyzed along with those from MCS by Jirutitijaroen and Singh [12].

Customer and energy based indices consideration for reliability enhancement of distribution system using Improved Teaching Learning based optimization is discussed [13]. An Innovative Self-Adaptive Multi-Population Jaya Algorithm based Technique for Evaluation and Improvement of Reliability Indices of Electrical Power Distribution System, Tiwary et al. [14]. Jirutitijaroen et al. [15] developed a comparison of simulation methods for power system reliability indexes and their distribution. Determination of reliability indices for distribution system using a state transition sampling technique accounting random down time omission is discussed [16]. Tiwary et al. [17] proposed a methodology based on Inspection-Repair-Based Availability Optimization of Distribution System Using Bare Bones Particle Swarm Optimization. Bootstrapping based technique for evaluating reliability indices of RBTS distribution system neglecting random down time was evaluated [18].

Volkanavski et al. [19] proposed application of fault tree analysis for assessment of the power system reliability. Li et al. [20] studies the impact of covered overhead conductors on distribution reliability and safety. Reliability enhancement of distribution system using Teaching Learning based optimization considering customer and energy based indices was obtained [21]. Self-Adaptive Multi-Population Jaya Algorithm based Reactive Power Reserve Optimization Considering Voltage Stability Margin Constraints was obtained [22]. A smooth bootstrapping based technique for evaluating distribution system reliability indices neglecting random interruption duration is developed [23]. Tiwary et al. [24] have developed an inspection maintenance based availability optimization methodology for feeder section using particle swarm optimization. The impact of covered overhead conductors on distribution reliability and safety is discussed [25]. A methodology for reliability evaluation of an electrical power distribution system, which is radial in nature is proposed [26]. Sarantakos et al. [27] introduced a method to include component condition and substation reliability into distribution system reconfiguration. This paper has discussed a methodology for evaluation of customer orientated indices and reliability of a meshed power distribution system [28]. Reliability evaluation of engineering system is discussed [29]. Battu et al. [30] discussed a method for reliability compliant distribution system planning using Monte Carlo simulation. Application of non-parametric bootstrap technique for evaluating MTTF and reliability of a complex network with non-identical component failure laws is discussed [31]. Tiwary and Tiwary [32] have developed an innovative methodology for evaluation of customer orientated indices and reliability study of electrical feeder system.

In this paper the value of failure rate per year is evaluated for the Roy Billinton test system (RBTS) Bus-2 distribution system for educational purpose [33]. The criteria of the failure rate and the length of the feeder sections are provided by Allan et al. [33]. This paper also evaluates the reliability of each and every distribution section of the RBTS Bus-2 distribution system. Mean time to failure (MTTF) is also obtained for the distribution system.

II. Reliability evaluation of series and parallel system and its implementation

The system is having a constant failure rate and therefore the reliability of the system having constant failure rate is evaluated by using the following relation.

$$R(t)=e^{(-\lambda t)} \tag{1}$$

Where R(t) represents the reliability of each and every distribution section. λ represents the failure rate per year of the feeder section under consideration and t represents time period which is taken as one year.

The mean time to failure (MTTF) can be obtained as follows:

$$MTTF = \frac{1}{\lambda} \tag{2}$$

Aditya Tiwary, Swati Tiwary
EVALUATION OF RELIABILITY INDICES OF ROY BILLINTON TEST
SYSTEM (RBTS) BUS-2 DISTRIBUTION SYSTEM FOR EDUCATIONAL
PURPOSE

RT&A, No 1 (61)
Volume 16, March 2021

If system fails even if a single component fails or system survives if all the components are working successfully then that type of system or network is known as series reliability system or network. If one assumes time independent reliability r1, r2...rn, then reliability of series system is given as:

$$R_s = \prod_{i=1}^{n} r_i$$

(3)

The system or network fails, if all components fail and the system will perform its function even if a single component is working, such a system or network is known as parallel reliability system or network.

The reliability of parallel system (Rp) is given as:

$$R_p = 1 - \prod_{i=1}^{n} (1 - r_i)$$

(4)

Where ri represents the reliability of components from i=1….n.

III. Evaluation of reliability indices of Roy Billinton test system (RBTS) Bus-2 distribution system

Allan et al. [33] have provided reliability test system for educational purposes. This paper contains various distribution system configuration and various values of different parameters related to the system.

Fig.-1 Standard RBTS-Bus-2 distribution system [33].

Aditya Tiwary, Swati Tiwary
EVALUATION OF RELIABILITY INDICES OF ROY BILLINTON TEST
SYSTEM (RBTS) BUS-2 DISTRIBUTION SYSTEM FOR EDUCATIONAL
PURPOSE

RT&A, No 1 (61)
Volume 16, March 2021
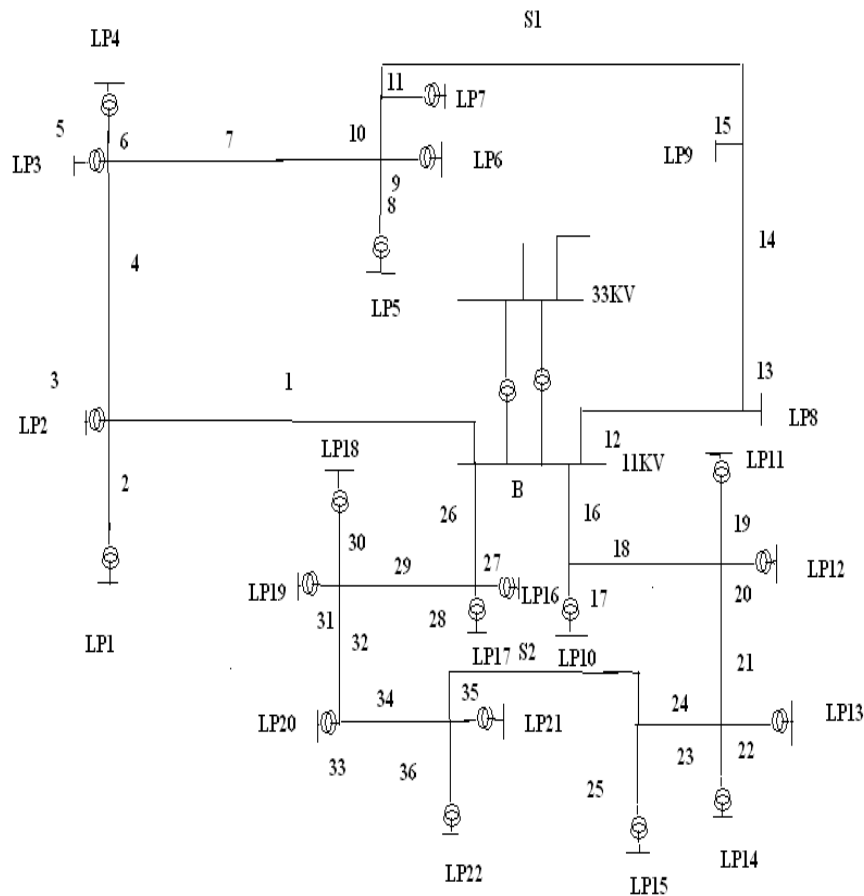
In present study evaluation of the failure rate of the Roy Billinton test system (RBTS) Bus-2 distribution system is done. Two parameters are of importance to evaluate the failure rate for each and every feeder section of the RBTS Bus-2 distribution system. First parameter is the failure rate as suggested in the paper [33] and second is the line length of each and every feeder in distribution system. Based on the parameters suggested by Allan et al. [33] failure rate for each and every feeder section is evaluated in this study. Fig. 1 represents the Standard Roy Billinton test system (RBTS) Bus-2 distribution system [33]. It consists of 36 distributor segments and 22 load points from LP-1 to LP-22. For each and every load point series path is considered from source to that load point. Table 1 provides the evaluated failure rate per year for each and every feeder section of RBTS-Bus-2 distribution system.

Table 1. Evaluated system data for standard RBTS-Bus-2 distribution system

Feeder section	Failure rate /year	Length of the feeder section	Feeder section	Failure rate /year	Length of the feeder section
#1	0.04875	0.75	#19	0.04875	0.75
#2	0.03900	0.60	#20	0.05200	0.80
#3	0.05200	0.80	#21	0.03900	0.60
#4	0.04875	0.75	#22	0.04875	0.75
#5	0.05200	0.80	#23	0.05200	0.80
#6	0.03900	0.60	#24	0.04875	0.75
#7	0.04875	0.75	#25	0.03900	0.60
#8	0.05200	0.80	#26	0.05200	0.80
#9	0.04875	0.75	#27	0.04875	0.75
#10	0.03900	0.60	#28	0.03900	0.60
#11	0.05200	0.80	#29	0.04875	0.75
#12	0.04875	0.75	#30	0.03900	0.60
#13	0.05200	0.80	#31	0.05200	0.80
#14	0.03900	0.60	#32	0.04875	0.75
#15	0.05200	0.80	#33	0.05200	0.80
#16	0.04875	0.75	#34	0.03900	0.60
#17	0.03900	0.60	#35	0.04875	0.75
#18	0.05200	0.80	#36	0.05200	0.80

Table 2 provides the evaluated reliability for each and every feeder section of the distribution system under study. Table 3 provides mean time to failure for the feeder sections.

Table 2. Evaluated reliability of the feeder section of standard RBTS-Bus-2 distribution system

Feeder section	Evaluated reliability	Feeder section	Evaluated reliability
#1	0.952419205	#19	0.952419205
#2	0.961750709	#20	0.949328867
#3	0.949328867	#21	0.961750709
#4	0.952419205	#22	0.952419205
#5	0.949328867	#23	0.949328867
#6	0.961750709	#24	0.952419205
#7	0.952419205	#25	0.961750709
#8	0.949328867	#26	0.949328867
#9	0.952419205	#27	0.952419205
#10	0.961750709	#28	0.961750709
#11	0.949328867	#29	0.952419205
#12	0.952419205	#30	0.961750709
#13	0.949328867	#31	0.949328867
#14	0.961750709	#32	0.952419205
#15	0.949328867	#33	0.949328867
#16	0.952419205	#34	0.961750709
#17	0.961750709	#35	0.952419205
#18	0.949328867	#36	0.949328867

Aditya Tiwary, Swati Tiwary
EVALUATION OF RELIABILITY INDICES OF ROY BILLINTON TEST
SYSTEM (RBTS) BUS-2 DISTRIBUTION SYSTEM FOR EDUCATIONAL
PURPOSE

RT&A, No 1 (61)
Volume 16, March 2021

Table 3. Evaluated mean time to failure of the feeder section of standard RBTS-Bus-2 distribution system

Feeder section	Evaluated mean time to failure	Feeder section	Evaluated mean time to failure
#1	20.51282051	#19	20.51282051
#2	25.64102564	#20	19.23076923
#3	19.23076923	#21	25.64102564
#4	20.51282051	#22	20.51282051
#5	19.23076923	#23	19.23076923
#6	25.64102564	#24	20.51282051
#7	20.51282051	#25	25.64102564
#8	19.23076923	#26	19.23076923
#9	20.51282051	#27	20.51282051
#10	25.64102564	#28	25.64102564
#11	19.23076923	#29	20.51282051
#12	20.51282051	#30	25.64102564
#13	19.23076923	#31	19.23076923
#14	25.64102564	#32	20.51282051
#15	19.23076923	#33	19.23076923
#16	20.51282051	#34	25.64102564
#17	25.64102564	#35	20.51282051
#18	19.23076923	#36	19.23076923

Fig. 2 provides the magnitude of evaluated reliability of the feeder section of standard RBTS-Bus-2 distribution system. Fig. 3 shows the magnitude of evaluated mean time to failure of the feeder section of standard RBTS-Bus-2 distribution system.

Fig. 2 Magnitude of evaluated reliability of the feeder section
of standard RBTS-Bus-2 distribution system

Aditya Tiwary, Swati Tiwary
EVALUATION OF RELIABILITY INDICES OF ROY BILLINTON TEST
SYSTEM (RBTS) BUS-2 DISTRIBUTION SYSTEM FOR EDUCATIONAL
PURPOSE

RT&A, No 1 (61)
Volume 16, March 2021
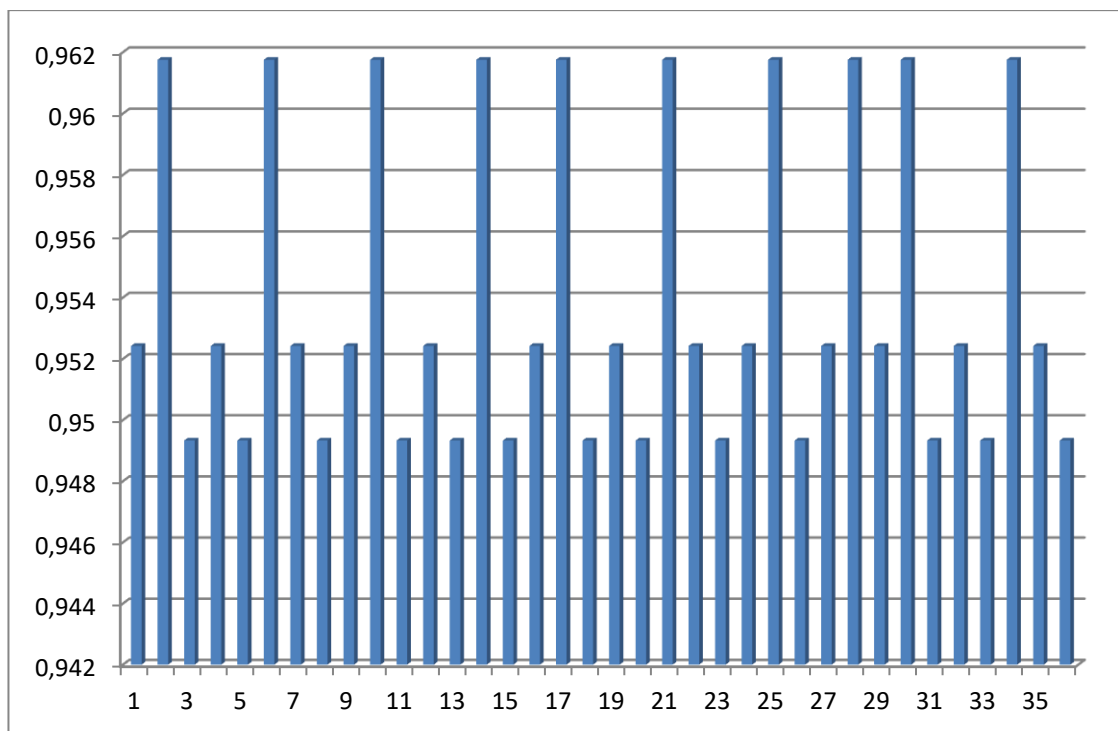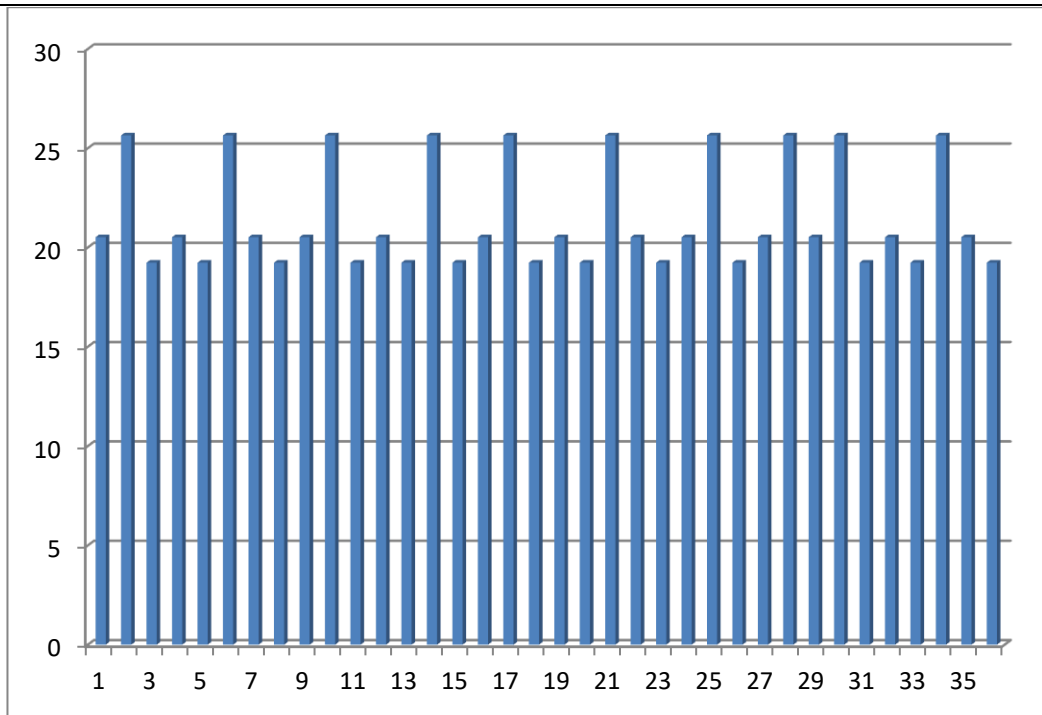
Fig. 3 Magnitude of evaluated mean time to failure of the feeder section
of standard RBTS-Bus-2 distribution system

IV. Conclusion

Identifying various values of reliability is most important when we have to check the availability of supply in any distribution system. Failure rate of the distribution system is a basic reliability index which is of importance. The value of failure rate per year is evaluated for each and every feeder section of the Roy Billinton test system (RBTS) Bus-2 distribution system for educational purpose. This paper also evaluates the reliability of each and every distribution section of the RBTS Bus-2 distribution system. Mean time to failure (MTTF) is also obtained for each and every feeder section of the distribution system under study.

References

1. R. N. Allan, E. N. Dialynas, I. R. Homer. (1979). Modelling and evaluating the reliability of distribution systems. IEEE Trans. on Power Apparatus and Systems, 98: 2181-2189.
2. E. Wojczynski, R. Billinton. (1985). Effects of distribution system reliability index distributions upon interruption cost/reliability worth estimates. IEEE Trans. on Power Apparatus and Systems, 11: 3229-3235.
3. A. K. Verma, A. Srividya, H. M. R. Kumar. (2002). A framework using uncertainties in the composite power system reliability evaluation. Electric Power Components and Systems, 30: 679-691.
4. Z. Zheng, L. Cui, Alan G. Hawkes. (2006). A study on a single-unit Markov repairable system with repair time omission. IEEE Trans. on Reliability, 55: 182-188.
5. P. Jirutitijaroen, C. singh. (2008). Comparison of simulation methods for power system reliablity indexes and their distributions. IEEE Trans. on Power Systems, 23: 486-493.

Aditya Tiwary, Swati Tiwary
EVALUATION OF RELIABILITY INDICES OF ROY BILLINTON TEST
SYSTEM (RBTS) BUS-2 DISTRIBUTION SYSTEM FOR EDUCATIONAL
PURPOSE

RT&A, No 1 (61)
Volume 16, March 2021

6. O. Dzobe, C. T. Gaunt, R. Herman. (2012). Investigating the use of probability distribution functions in reliability-worth analysis of electric power systems. Int. J. of Electrical Power and Energy Systems, 37: 110-116.

7. I. S. Bae, J. O. Kim. (2008). Reliability evaluation of customers in a microgrid. IEEE Trans. on Power Systems, 23: 1416-1422.

8. R. Billinton, P. Wang. (1998). Reliability-network-equivalent approach to distribution-system-reliability evaluation. IEE Proc. generation, transmission and distribution, 145: 149-153.

9. S. Bhowmik, S. K. Goswami, P. K. Bhattacherjee. (2000). A New power distribution system planning through reliability evaluation technique. Electric Power Systems Research, 54: 169-179.

10. C. Singh. (1981). Markov cut-set approach for the reliability evaluation of transmission and distribution systems. IEEE Trans. on Power Apparatus and Systems, 100: 2719-2725.

11. R. Billinton. (1969). Composite system reliability evaluation. IEEE Trans. on Power Apparatus and Systems, 88: 276-281.

12. P. Jirutitijaroen, C. singh. (2008). Comparison of simulation methods for power system reliability indexes and their distributions. IEEE Trans. on Power Systems, 23: 486-493.

13. A. Tiwary. (2017). Customer and energy based indices consideration for reliability enhancement of distribution system using Improved Teaching Learning based optimization. International Journal of Latest Trends in Engineering and Technology, 9: 254-258.

14. Aditya Tiwary. (2018). An Innovative Self-Adaptive Multi-Population Jaya Algorithm based Technique for Evaluation and Improvement of Reliability Indices of Electrical Power Distribution System. International Journal on Future Revolution in Computer Science & Communication Engineering, 4: 299-302.

15. Jirutitijaroen P, singh C. (2008). Comparison of simulation methods for power system reliability indexes and their distribution. IEEE Trans Power Syst, 23: 486–92.

16. Aditya Tiwary, R. Arya, S. C. Choube and L. D. Arya. (2013). Determination of reliability indices for distribution system using a state transition sampling technique accounting random down time omission. Journal of The Institution of Engineers (India): series B (Springer), 94: 71-83.

17. A. Tiwary. (2019). Inspection-Repair-Based Availability Optimization of Distribution System Using Bare Bones Particle Swarm Optimization. Chapter in Book Series Computational Intelligence: Theories, Applications and Future Directions – Volume II, Advances in Intelligent Systems and computing, 799.

18. Aditya Tiwary, R. Arya, L. D. Arya, S. C. Choube. (2017). Bootstrapping based technique for evaluating reliability indices of RBTS distribution system neglecting random down time. The IUP Journal of Electrical and Electronics Engineering, X: 48-57.

19. Volkanavski, Cepin M, Mavko B. (2009). Application of fault tree analysis for assessment of the power system reliability. Reliab Eng Syst Safety, 94: 1116-27.

20. Li BM, Su CT, Shen CL. (1989). The impact of covered overhead conductors on distribution reliability and safety. Int J Electr Power Energy Syst, 32: 281–9.

21. Aditya Tiwary. (2017). Reliability enhancement of distribution system using Teaching Learning based optimization considering customer and energy based indices. International Journal on Future Revolution in Computer Science & Communication Engineering, 3: 58-62.

22. A. Tiwary. (2018). Self-Adaptive Multi-Population Jaya Algorithm based Reactive Power Reserve Optimization Considering Voltage Stability Margin Constraints. International Journal on Future Revolution in Computer Science & Communication Engineering, 4: 341-345.

23. R. Arya , A. Tiwary , S. C. Choube, L. D. Arya. (2013). A smooth bootstrapping based technique for evaluating distribution system reliability indices neglecting random interruption duration. Int. J. of Electrical Power and Energy System, 51: 307-310.

Aditya Tiwary, Swati Tiwary
EVALUATION OF RELIABILITY INDICES OF ROY BILLINTON TEST
SYSTEM (RBTS) BUS-2 DISTRIBUTION SYSTEM FOR EDUCATIONAL
PURPOSE

RT&A, No 1 (61)
Volume 16, March 2021

24. A. Tiwary. (2018). Inspection–Maintenance-Based Availability Optimization of Feeder Section Using Particle Swarm optimization. Soft Computing for Problem Solving-Advances in Intelligent Systems and Computing, 816: 257-272.

25. M. Bin Li, C. Tzong Su, C. Lung Shen. (2010). The impact of covered overhead conductors on distribution reliability and safety. Int. J. of Electrical Power and Energy System, 32: 281-289.

26. Aditya Tiwary. (2019). Reliability evaluation of radial distribution system – A case study. Int. J. of Reliability: Theory and Applications, 14, 4(55): 9-13.

27. I. Sarantakos, D. M. Greenwood, J. Yi, S. R. Blake, P. C. Taylor. (2019). A method to include component condition and substation reliability into distribution system reconfiguration. Int. J. of Electrical Power and Energy System, 109: 122-138.

28. Aditya Tiwary. (2020). Customer orientated indices and reliability evaluation of meshed power distribution system. Int. J. of Reliability: Theory and Applications, 15, 1(56):10-19.

29. A. Tiwary, P. Patel. (2020). Reliability Evaluation of Hose Reel System - A Practical Approach. Journal of Industrial Safety Engineering, 7: 30-34.

30. N. R. Battu, A. R. Abhyankar, N. Senroy. (2019). Reliability Compliant Distribution System Planning Using Monte Carlo Simulation. Electric power components and systems, 47: 985-997.

31. Aditya Tiwary. (2020). Application of Non-Parametric Bootstrap Technique for evaluating MTTF and Reliability of a Complex Network with Non-Identical Component Failure Laws. Reliability: Theory and Applications, 15: 62-69.

32. Aditya Tiwary, Swati Tiwary. (2020). Evaluation of Customer Orientated Indices and Reliability Study of Electrical Feeder System. Reliability: Theory and Applications, 15: 36-43.

33. R. N. Allan, R. Billinton, I. Sjarief, L. Goel, K. S. So. (1991). A reliability test system for educational purposes-basic distribution system data and results. IEEE Trans. on Power Systems, 6: 813-820

Analysis of the Risk Model of German Corona Warning App

Jens Braband

•

TU Braunschweig, Germany
j.braband@*tu-braunschweig*.de

Hendrik Schäbe

•

TÜV Rheinland
schaebe@de.tuv.com

Abstract

In Germany an App has been introduced to cope with the Corona epidemic. In this paper we describe, how the app works and analyze the semi-quantitative risk model that has been used in the app, because a large number of semi-quantitative risk models are known that are not consistent. Further we discuss in how far the Corona app in its current state can contribute to mitigate the pandemic. The risk model of the German Corona warning app has several interesting, somewhat puzzling properties. In this paper we describe the analysis and its results related to the underlying risk model.

Keywords: risk model, Corona app, risk calculation

I. Introduction

In Germany, the so-called Corona Warning App has been introduced to cope with the Corona epidemic. This app computes an individual infections risk based on contacts with infected persons. In this paper we describe, how the app version 1.7 works and analyzes the semi-quantitative risk model that has been used in the app, because a large number of semi-quantitative risk models are known that are not consistent. Further we discuss in how far the Corona app version 1.7 in its current state can contribute to mitigate the pandemic. Not that the current version of the app is 1.9 and changes are ongoing.

II. How the app works

First a simplified overview is given in order to understand the risk model. More details are given in [1][2].
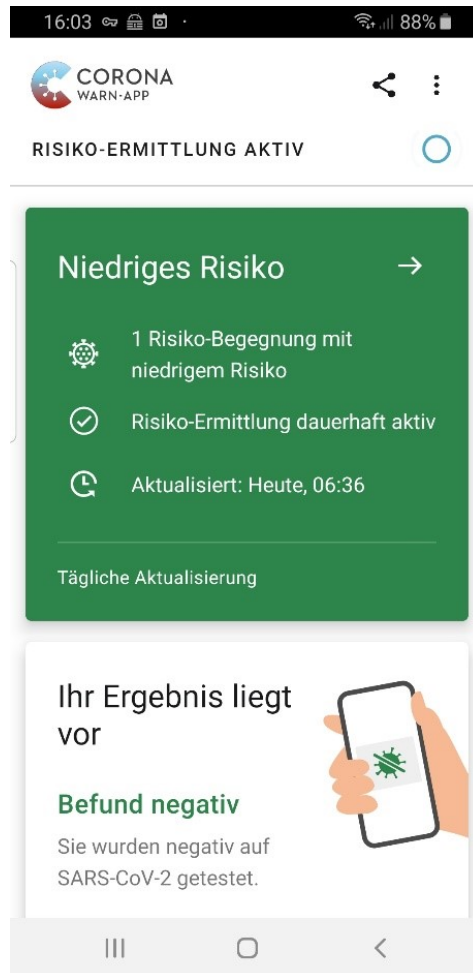
Figure 1: *Screenshot of the Corona Warning App indicating a low risk and a negative test result*

After a user has installed the app, each day a new anonymous ID is created. Every few minutes the environment is scanned for Bluetooth signals emitted from other apps. Data like ID, signal attenuation, duration etc. are collected and aggregated for each day.

If the user receives a positive test result and agrees to publish it, then the anonymous ID for the preceding 14 days are transmitted to the central server, from which it is transmitted to all subscribers. The actual risk evaluation is performed decentralized by each app.

Figure 1 shows a screenshot of the app, with an indication of a low risk because of one encounter with an infected person. However the date of the encounter or a more detailed risk estimate is not given, although such data are known.

III. The Basic Risk Model

The basic model is defined by four parameters [2], which in a first step are evaluated on a semi-quantitative scale each ranging from 0-8 for each day for each ID that reported a positive test result (see figure 2):

- The Days since Exposure (DE) is the time since exposure to the infected person, a value between 0 and 14, durations longer than 14 days are not considered.
- The Exposure Duration (ED) is the cumulative time of exposure on the day, takes values between 0 and 8.
- The Bluetooth Signal Attenuation (SA) is used as a measure of the distance to the infected person, takes values between 0 and 8.
- The Transmission Risk (TR) estimates the level of infectiosity of the person on that day, takes values between 0 and 8.

Then the Total Risk Score (TRS) is evaluated by multiplication of DE, ED, SA and TR, theoretically resulting in scores between 0 and 7168.

This resembles the approach known as Risk Priority Numbers (RPN) and suffers from the same limitations and flaws, which are known for about two decades [5][6]. For some application sectors the use of RPN is even deprecated [7].

The major problem is that the scores for the parameters are often only ordinal scale or rank numbers, for which operations like multiplication or division are not well-defined. As a consequence, the results may lead to under- or overestimation of the related risk [8].

However, in the practical implementation of the Corona warning app today the model is simplified and the coinciding ranges are limited [3] by

- Days since Exposure (DE) is set to 5 for values below 14 days, and 0 for above, leading to
  $\delta_{ED} = 5*I(DE \leq 14)$
- Exposure Duration (ED) is set to 0 for all values up to 10 minutes, and 1 for above, yielding
  $\delta_{DE} = I(ED > 10)$
- Signal Attenuation (SA) is set to 0 above 73 dB, and 2 for all values below, i.e.
  $\delta_{SA} = 2* I(SA \leq 73dB)$
- Transmission Risk (TR) is set to (6, 8, 8, 8, 5, 3, 1, 1, 1, 1, 1, 1, 1) [4], depending on DE, e. g. TR is 6 if DE=1, 8 if DE=2 etc., and 0, if DE=14 or above

Here, I(.) denotes the indicator function, which take value 1 if the expression in brackets holds true, and zero otherwise.

So, most of the parameters are only used as binary indicator variables and in the current configuration the Total Risk Score for a particular day and a particular ID is given by

$$TRS = 10 \cdot \delta_{ED} \cdot \delta_{SA} \cdot \delta_{DE}TR \qquad (1)$$

So, with the current implementation [3] there are only six possible scores: 0, 10, 30, 50, 60, 80. But also a Minimum Risk Score (MRS) of 11 is defined and all risks below are discarded. But the parametrization of the app may be changed.

So, as of today, we can conclude that the basic risk model as implemented is more a dosimetric model, depending on the estimated virus concentration, rather than on exposure and other parameters (but for some threshold values). It is not even a risk model as per the definition of many standards. Moreover, the risk model has been heavily discretized.
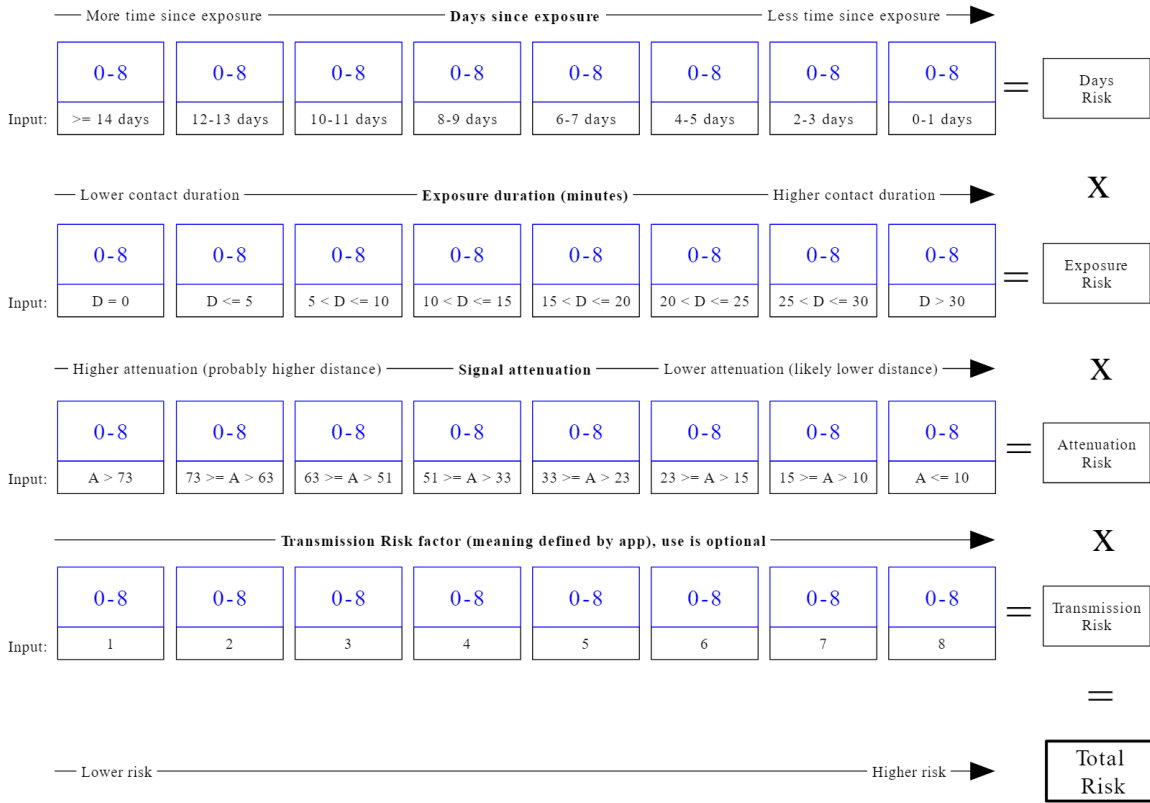
Figure 2: *Basic Risk Calculation [2]*

Example:

- Alice receives a positive test result on the 20th of the month, which she reports immediately.
- Bob is often taking the same bus as Alice. A ride takes 10 minutes and he has met her on the 16th (two rides) and the 9th (one ride). They have sat together with a distance of about 1m.
- For the 16th DE=4 and so TR=8. Both SA and ED are above the threshold and set to 2 and 1, respectively, so TRS=80.
- For the 9th DE=11 and so TR=1. However, ED is below the threshold and set to 0. So TRS=0. Otherwise the TRS would have been 5, which is below the MRS and would have been discarded anyhow.

IV. Combined Risk Model

In a second step each app combines the scores for different encounters calculated by the basic risk model. Let R_1, R_2, …R_n denote the individual TRS for different days and different IDs that are above the MRS.

In a first step the maximum value R_{max} of the different TRS is determined. Then the ED of all the n encounters are summed up into three different classes: close, medium and far. Let their durations be t_1, t_2 and t_3, respectively. For each of the classes a weight is defined and additionally a weight offset, which are denoted by w_1, w_2, w_3 and w_4, respectively. Note that in practice the weights for the close and medium classes outweigh the others. Also, an Average Risk Score (ARS), currently 50 [3], is defined. Then the Total Combined Risk (TCR) is calculated as (see figure 3)

$$TCR = (t_1 w_1 + t_2 w_2 + t_3 w_3 + w_4)\frac{R_{max}}{ARS} \qquad (2)$$
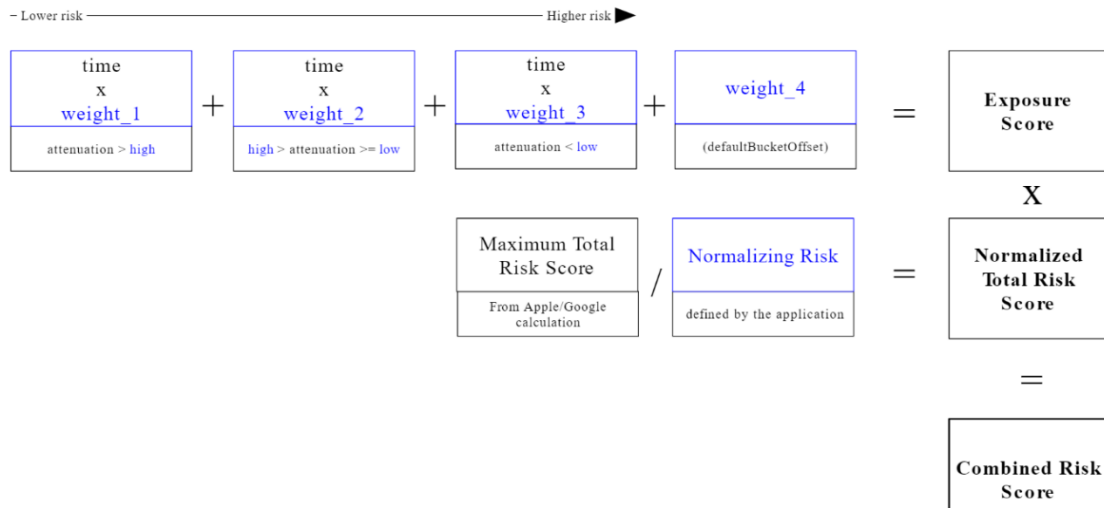
Figure 3: *Combined Risk Calculation [2]*

Surprisingly the TCR is in fact not a risk, but an exposure as the result is in minutes. The first term (in brackets) is a weighted exposure time which is adjusted by a relative factor (dimensionless) which depends on the maximum virus concentration compared with some average.

So overall, without full mathematical exactness, we can characterize the approach used today [3] by the German Corona warning app as

$$TCR = (t_1 w_1 + t_2 w_2 + t_3 w_3 + w_4) \frac{max\{10 \cdot \delta_{ED} \cdot \delta_{DE} \delta_{SA} \cdot TR\}}{ARS} \approx (t_1 + t_2/2) \frac{10 max\{TR\}}{ARS} \quad (3)$$

Basically this is not a risk in the narrow sense, it is a weighted exposure duration, the units of TCR are not expected damage per time or similar, but just minutes of exposure. And the weight applied is just a measure of relative infectiosity, which expresses the size of TR relative to a normalizing factor of 5, which is assumed as average infectiosity. And the impact of the factor is limited, the highest possible value being 1.6.

And, if we take additionally into account the uncertainty and spread of all the input parameters, e. g. noise in the signal attenuation, uncertainty in the exposure duration and infectiosity [4], or arbitrariness of the weights chosen, then the model boils down to a quite simple formula and decision procedure:

$$TCR \approx \frac{maxTR}{5} \sum ED \quad (4)$$

- Estimate the minutes that the person was exposed closely to infected persons ($\sum ED$)
- Weight the exposure ED by the infectiosity of the most infected person (max TR/5)
- Take action if the result is HIGH

Example (continued)
- Additionally, Charlie has received a positive test result on the 20th, but he reported it only on the 21st. But he has installed the app only a week ago.
- He has been on the same bus on the same days, but with some larger distance to Bob (2m)
- For the 16th, DE=5 (evaluated on the 21st) and so TR=5. Both SA and ED are above the threshold and set to 2 and 1, so TRS=50.
- For the 9th, Charlie had not installed the app yet, so there are no data.

- As Alice set close to Bob, and Charlie in medium distance, t1=t2=20 minutes. The weights are currently set [3] to w1=1, w2=0.5, w3=w4=0, and so the weighted sum results in 30 minutes
- So, the TCR amounts to 30 x 80 / 50, which gives 48 minutes.
- The warnings of the app are issued based on the TCR, which are configured [3] as LOW for values up to 15, and HIGH from 15 onwards. So finally, Bob would get a HIGH risk warning.

Note that the TCR is almost independent of the distance measured by Bluetooth Signal Attenuation. There is only a loose threshold defined and the exposure duration is weighted into two distance classes. However, it is known, see e. g. the FAQ by RKI [9], that transmission is mainly by aerosols, and the risk increases when the exposure distance decreases. Close contact to infected persons is also known to be a factor in superspreading events. The importance of the distance is also supported by the fact that it is a major factor in the German Corona rules AHA, where the first letter stands for Abstand (distance).

V. Naive Risk Model

Unfortunately, the derivation of the Risk Model described above seems only partially published [4]. But we may formulate a general risk model stimulated by similar models from dosimetry.

The similarity that we exploit here is that we have sources of activity (the infected persons), here transmission of virus material with a certain intensity I (which is assumed to be constant at least temporarily e. g. over a day). The exposed persons are assumed to be exposed at a fixed (or average) distance D and time T.

The intensity I could be defined e. g. by virus material per volume or surface e. g. $[M/m^2]$, D would be measured by [m] and T by [min]. For the risk model we would have to take some assumptions how the intensity decreases with distance to the source.

Several assumptions on the dependence of concentration depending on distance can be made:
a. Thinning of the virus in a volume. The concentration of the virus is the amount of the virus per volume unit, assuming more or less equal distribution. Then the concentration would decrease with R^3, where R is the distance between the source (infected person) and the receiver. This assumption would only hold, if there is sufficient convection.
b. The virus is emitted as a spherical wave, e.g. as a result of playing a brass instrument, sneezing etc. Then the virus is approximately present on the surface of a sphere. So, the concentration would decrease with R^2.
c. The virus is emitted as a cylindrical wave. Then the concentration would decrease proportional to R. This can be the case if e.g. infected singers are standing on a stage, emitting their virus into a large room.
d. The virus is spread in the room, reflected from the walls, so that an equal concentration occurs in the entire room. Then, distancing would not decrease the virus concentration.

Therefore, we think that assuming a dependence of the intensity I on 1/R is a plausible assumption, which should cover typical cases or be conservative.

We may also define a nominal virus intensity I0 at a given distance, say 1 m. This would still depend on the infectiousness of the person.

As the exposure to virus material increases proportional to exposure time, we may define the dose for a particular encounter with an infectious person

$$R \approx \frac{TI_0}{D} \tag{5}$$

Note that these parameters directly reflect parameters ED, SA and TR, while DE is not needed. Interestingly it is defined, but not used in the basic risk model, currently it is just a constant. And in the definition of many standards the dose R is not a risk.

Example (continued):

- Let's try to evaluate Alice's and Bob's encounter on the 16th by this approach. D=1 and T=20 mins. The absolute I0 value is not known, but it was the highest possible value. For the sake of simplicity, we take the same value of 8, which is also justified by the construction of the TR vector [4]. So, R=160 would result.
- For the 9th we have D=1 and T=10. I0 is at the lowest value, let's assume 1 and we get R=10.
- Now let's look at Charlie. He is at D=2m distance exposing Bob for T=20 min. His TR value was 5, thus resulting in R=50. The Combined Risk is just the sum of the partial risk and gives 220.

Note that in this model the influence of the distance is explicit and influential. E. g. if we assume that Charlie and Alice had close contact, e. g. at a party instead of on the bus ride, we might assume D=0.5, which would result then in R=200. Note that in the original model the TCR would only rise from 48 to 64 as Bob's 20 minutes of exposure to Charlie would now fall into the close distance category.

VI. Other influences and limitations

Besides the risk model – or to be precise the dose model - inside the app we also would need to consider influences that can be identified outside the app.

Currently only 19.3 million persons in Germany have the app [10], out of 83.2 million inhabitants [11]. That means, that with a probability of 23% a person has the app installed. Now, this might have different reasons:

a. Some person do not own a smartphone. This holds for very young children or for elderly people.
b. Some persons have not yet installed the app, e. g. because their phone is not compatible or outdated
c. Some persons refuse to install the app.

Then, the probability that two persons meet that have both installed the app is 23%*23% =5.4%.

This computation is very rough, since there are correlations in different population groups with mobility and owning a smartphone. On the one hand side, elderly people who might not own a smartphone would on the other hand be less mobile or even be in an pensioner's home and would also be part of a group with high risk of fatality. On the other hand, small children do not own a smartphone, have many contacts but seem not to play a great role in transmitting infections.

In any case, the figure above gives a rough indication that the app overall would miss about 95% of all encounters between persons. However, for a person that has installed the app, it rises to 23%

Assume now that a person is infected but has no symptoms. There is a growing number of persons with no or light symptoms [12]. A precise number is hard to give. In [13] a number of 43% is given. Now, even if a person has no symptoms, Corona can be detected by a test. End of August 2020 a weekly number of tests of about 1 million has been carried out in Germany [12]. Assuming now a typical period of 14 days, i.e. two weeks that are relevant, the probability of being detected by mass tests as infected during the two weeks period is

$$1-(1-1/83.2)^2 = 2.4\%. \tag{6}$$

So, finally a person that is infected with Corona will only be detected by a test with probability

$$57\% + 43\%*2.4\% = 58\%. \tag{7}$$

Here we have even assumed that all persons with symptoms are tested and a Corona infection

is detected by test.

The infected and tested person has to register herself in the Corona app as infected. Assume now, that even everyone would do so.

We can now compute the probability that the Corona app would detect and handle such an encounter of an infected person with another. The result is

$$58\% * 5.4\% = 3.1\% \tag{8}$$

Only in this fraction of cases of encounters the risk or dose model described above would come to work and help to protect persons.

However, there is another serious influence when computing the overall dose or risk according to

$$TCR \approx \frac{maxTR}{5} \sum ED, \tag{9}$$

This value would be underestimated. The sum will run only over those encounters with another person also having the app, i.e. 23% and knowing that he / she is infected, i.e. 58%. That means, that in the sum above only

$$23\% * 58\% = 13\% \tag{10}$$

of all dangerous encounters will be considered so that the TCR value statistically heavily underestimate this value.

So we see that there are two influences on the risk or dose values currently computed by the Corona app:

1) Only a small number of encounters is handled in the app with a risk model that is more or less a dose model
2) A cumulative TCR value computed by the app is heavily biased and indicates too small values.

To make the use of the app more efficient it is important to increase the number of users. Since the fraction of users has a quadratic influence on the probability that an encounter of persons is analyzed, this is the most important possibility. For analyzing the accumulated risk, one needs to take into account the fraction of use of the app, too. The TCR value depends linearly on the fraction of persons that have installed the app. Possible target values on this value need to be adapted when the fraction of app users in the population grows.

Another approach to make the estimations more precise would be to allow the infected person to voluntarily release more or more precise data. E. g. the infected person might be asked to enter the date of the test instead of the day when she releases the test result. Also, the number of daily encounters with small distance could be shown by the app in order to increase the awareness for keeping distance. Additionally the user may voluntarily keep a contact diary in the app so that in case of infection the tracing of contacts may be easier.

VII. Summary

The risk model of the German Corona warning app has several interesting, somewhat puzzling properties:

1. In the narrow definition of many standards it is not a complete risk model, as it estimates only single parameters of risk, but not a comprehensive risk. A partial explanation can be based on the decentralized architecture of the app and the incomplete and inaccurate information it uses, often explained by data privacy concerns
2. Out of four parameters defined in the basic risk model only one parameter, the transmission risk is fully evaluated, others are only used as binary parameters
3. While in the basic risk model the result could be expressed as an infectiosity or dose of infectious particles to which the individual is exposed, the resulting combined risk is expressed as an exposure time. This is very uncommon that the combination of

several similar risks is expressed in different measurement units.

4. The estimated distance to the infected person is only compared to a threshold and as a means to weight different exposure times, but it has a minor influence in the model compared to the other parameters, while distance keeping plays a major role in infection prevention.

Finally, the authors would not recommend using the full parameter set for the basic risk model as this would lead to the same problems encountered with risk priority numbers. It would be reasonable to develop a full risk model and not only a partial risk model based on a weighted exposure duration only. Some parameters could be collected voluntarily from the user, like the age as the predominant factor for serious consequences or the health status. Other important parameters could be estimated by data from other smartphone sensors like GPS, e. g. environmental parameters like indoor or outdoor.

Moreover, the authors have seen that the effectivity of the app is still small, since the action of persons using it is also limited.

References

[1]   RKI: So   funktioniert   die   Corona-Warn-App   im   Detail, https://www.rki.de/DE/Content/InfAZ/N/Neuartiges_Coronavirus/WarnApp/Funktio n_Detail.pdf, last retrieval 2020-10-06

[2]   CWA Team: Corona-Warn-App Solution Architecture, https://github.com/corona-warn-app/cwa-documentation/blob/master/solution_architecture.md, last retrieval 2020-10-06

[3]   CWA   Team: Wie   ermittelt   die   Corona-Warn-App   ein   erhöhtes   Risiko ?, https://github.com/corona-warn-app/cwa-documentation/blob/master/translations/cwa-risk-assessment.de.md, last retrieval 2020-10-06

[4]   CWA Team: Epidemiological Motivation of the Transmission Risk Level, 2020-06-15, https://github.com/corona-warn-app/cwa-documentation/blob/master/transmission_risk.pdf, last retrieval 2020-10-06

[5]   J. Bowles: An Assessment of RPN Prioritization in a Failure Modes Effects and Criticality Analysis. In: Proc. RAMS2003, Tampa, January 2003

[6]   J. Braband: Improving the Risk Priority Number Concept. In: Journal of System Safety. 3, 2003, S. 21–23

[7]   Durivage, M.: Is It Time To Say Goodbye To FMEA Risk Priority Number (RPN) Scores?, in: Pharmaceutical   Online,   https://www.pharmaceuticalonline.com/doc/is-it-time-to-say-goodbye-to-fmea-risk-priority-number-rpn-scores-00012020-04-27

[8]   J. Braband: Beschränktes Risiko. In: Qualität und Zuverlässigkeit. 53(2), 2008, S. 28–33.

[9]   Robert-Koch-Institut: SARS-Cov-2 Steckbrief, https://www.rki.de/DE/Content/InfAZ/N/ Neuartiges_Coronavirus/Steckbrief.html, last retrieval 2020-10-06

[10]   https://de.statista.com/statistik/daten/studie/1125951/umfrage/downloads-der-corona-warn-app/, accessed on 23.10.2020

[11]   https://de.statista.com/statistik/daten/studie/1217/umfrage/entwicklung-der-gesamtbevoelkerung-seit-2002/, accessed on 23.10.2020

[12]   https://www.aerzteblatt.de/nachrichten/116077/Wenig-Schwerkranke-trotz-gestiegener-Infektionszahlen

[13]   https://www.faz.net/aktuell/wissen/wie-viele-corona-infizierte-frei-von-symptomen-bleiben-16816959.html

Approach to Determining the Parameters of Physical Security Units for a Critical Infrastructure Facility

M.D. Katsman

•

Doctor of Sci., Associate Professor, Security Department of JSC "Ukrainian Railways",
Iezhy Hedroitsa str. 5, 03680, Kyiv, Ukraine, e-mail: katsman@uz.gov.ua

V.K. Myronenko

•

Doctor of Sci., Professor, Head of Department of Railway commercial activities management,
Faculty of Railway transport management, State University of infrastructure and technologies,
04071, Kyiv, Ukraine, e-mail: pupil7591@gmail.com

V.I. Matsiuk

•

Doctor of Sci., Professor, Department of transport technology and traffic process control,
Faculty of Railway Transport Operation, State University of Infrastructure and Technology,
Ivan Ogienko str., 19, Kyiv, 03049, Ukraine, e-mail: vimatsiuk@gmail.com

P.V. Lapin

•

M.D., PhD, MPH, Security Department of JSC "Ukrainian Railways",
Iezhy Hedroitsa str. 5, 03680, Kyiv, Ukraine, e-mail: pavlolapin@gmail.com

Abstract

The article discusses some common mathematical models of counterterrorism and acts of unlawful interference with protected objects. The use of methods of queuing theory of Markov and non-Markov types for modeling the counteraction of security personnel by a malicious group with a random number of criminals in a group and different ways of organizing the actions of such personnel is proposed.

Keywords: security object, queuing system (QS), nonordinary stream of malefactor groups, random number of malefactors in the group, non-Markov type QS, security personnel.

I. Introduction

Many scientific works are currently devoted to the problem of counter-terrorism and acts of illegal interference in the activities of critical infrastructure.
The classification of counter-terrorism models is reflected in [1], which provides an overview of current work on modeling the counter-terrorism system and proposes a classification of terrorism

and counter-terrorism models.

According to this paper the conceptual models include models developed by specialists in the subject area, political scientists, psychologists, sociologists. As an example, work is given [2], which provides empirical data on the decision-making patterns of members of terrorist organizations at different levels: strategic, tactical and operational, as well as at the level of the individual terrorist.

Models of analysis and synthesis are usually mathematical or physical models. In the review [3] more such works are characterized. In particular, in [4] the basis for the development of classification of terrorist groups using chemical, biological, radiological and nuclear weapons the heuristic method of pattern recognition, the method of classification trees and discriminant analysis were proposed. With regard to transport safety systems, a number of works are devoted to the analysis of devices to increase the probability of detection and reduce the intensity of false alarms. In [5], using Bayesian analysis, a method of threat ranking and prioritization of security measures for facilities is presented.

The complexity of real-world security situations requires the universality of the mathematical models used.

These requirements inevitably contradict the commonality and validity of the simulation results, so when solving models in the form of hierarchy (usually lower levels of hierarchy corresponds to a higher level of detail of the modeled systems description) or a horizontal chain, each element of which is approximately the same [6].

In [1] the levels of modeling (hierarchy of models) of counteraction to terrorism are considered in detail. Theoretical game models of counter-terrorism are presented in [7,8,9]. In [10], an approach to creating a mathematical model of the physical protection systems functioning of objects as a process of interaction of sets based on the theory of ordinary sets, fuzzy set theory and the analysis of hierarchies.

In [11], a mathematical model of describing the nature of the interaction between the components of the "defender - attacker" system as components of the "predator - victim" system is proposed. The model is a modified classic model of Lotki-Volterra competition, which allows you to assess changes in the level of danger for the object with a change in its security.

The use of fuzzy cognitive modeling to prevent risk situations in conditions of fuzzy source data at critical infrastructure facilities is considered in [12]. It proposes the management structure of NPPs in the form of a fuzzy cognitive model, scenarios of risk situations and their analysis.

In [13] the possibilities of application of models of operations research methods for planning of protection of objects of critical infrastructure are considered. Adaptation of these models includes taking into account the stochastic, informational and behavioral uncertainties of terrorists. In this paper, in particular, the generalizations of the tasks of the antagonistic game of attack and defense and the optimal distribution of protective resources are considered.

An example of the use of complex models with parameters measured on different scales is the game-theoretic model for security at Los Angeles international airport, on the basis of which the automated system "Assistant for randomized route control" (ARMOR) was developed and put into operation. [14]. Security is a very important factor in the protection of this facility, given the terrorist threat. However, limited resources do not allow security forces to monitor all facilities and routes around the clock. Terrorists are able to monitor and select unprotected routes and targets if security forces do not use randomized monitoring and patrol tactics.

II. Results and discussion

The authors formulate the basic requirements for ARMOR:

1. The system must take into account the weight of the protected objects. If an attack on the first object leads to economic damage and on the second to human casualties, more weight is given

to the second object. Weights are evaluated by experts and expressed on an ordinal scale.

2. The system must take into account all information about the enemy that is in the security service.

3. The system should not offer a strict service schedule, taking into account additional information, the security service may make adjustments to this schedule. In [15] presented is a description of tests for ARMOR testing, which has been in operation since 2007. Such tests include:

- analysis on the basis of game theory (type of test Mathematic): with known matrices of winnings, the gain of the attacker and the probability of refusal to attempt an offense is calculated;

- resource allocation (test type - Mathematic): game theory helps to find the expected gain of the attacker in different security strategies;

- cost of protection (type of test - Mathematic): game theory helps to find the expected gain of the parties at change of security technologies (due to introduction of new technical means of protection, new technology of check of passengers and luggage);

- simulation of the attack (test type - Simulation): the use of additional simulation models;

- conducting exercises using "educational" criminals;

- Expert assessment (type of test - Qualitative): security specialists are able to assess many factors for their further consideration in the model as their parameters.

Since 2009, ARMOR has been used to plan air patrol services with the task of optimal distribution of 3000-4000 patrols on 29000 daily flights.

Thus, a wide range of mathematical models are used to model the physical security systems of objects.

In our opinion, in order to determine the effectiveness of the actions of the unit of protection of critical infrastructure, it is advisable to use the mathematical tools of the queuing theory.

Consider an object guarded by a security unit of n people as a queuing system. Groups of intruders with an intensity of λ try to enter the object in order to endanger its safe operation. In general, the number of a group of attackers can be random, in other words, with a probability of as, the group can consist of s attackers.

That is, the n-channel queuing system (QS) receives a stream of λ [groups / units of time] of group demands with a random number of demands in the group.

Such QS have found their application in mathematical models of information technology, which is reflected in the works [16-18].

One of the features of the QS under consideration is that the time $\bar{t}_{int}$ of intruders on the object is limited, it is a random variable that is subject to the exponential law with the parameter $\eta = \frac{1}{\bar{t}_{int}}$.

The parameter η is the intensity of demands leaving the QS service channel due to the restriction of their stay in the system.

The parameter μ characterizes the system of counteraction $\mu = \frac{1}{\bar{t}_{ca}}$ [malefactor / unit of time], where $\bar{t}_{ca}$ is the average time of the guard's use of counteraction means to the malefactor.

Counteraction to intruders by the security unit can be organized in different ways, which determines the type of queuing system. The first group of QS includes:

1. M / M / n / m type QS with restriction ($\eta \neq 0$), without mutual assistance (h = n, g = 1), non-ordinary demands and a random number of demands in the group. Here, h is a value equal to the ratio of the total number of n guards (service channels) to the number of g guards, which are combined into a group to counter one attacker, ie n = n / g.

2. M / M / n / m type QS with restriction ($\eta \neq 0$), full mutual assistance (h = 1; g = n), non-ordinary demands and random number of demands in the group.

3. M / M / n / m type QS with restriction ($\eta \neq 0$), with partial mutual assistance (h = n / g), non-ordinary demands and a random number of demands in the group.

The second group includes QSs of the non-Markov type, which simulate the conditions

when the forces and means of protection are not on the site, for example, when it is necessary to concentrate additional forces and means. That is, the counteraction process consists of two phases lasting respectively $\bar{t}_1$ - concentration time and $\bar{t}_{gr}$ - time of counteraction means application, where $\bar{t}_1$ has an exponential distribution with the parameter $\mu_1 = \frac{1}{\bar{t}_1}$ [guard / unit time], and $\bar{t}_2$ - with parameter $\mu_2 = \frac{1}{\bar{t}_{gr}}$ [malefactor / unit time].

That is, the total resistance time has a generalized Erlang distribution with parameters $\mu 1$ and $\mu 2$.

Such QS have limitations $\eta \neq 0$, can be with different characteristics of mutual assistance, there is a queuing system with heterogeneous demands and a random number of demands in the group.

Some aspects of mathematical models of these QS are considered in [19-22].

Consider in more detail the QS of the first group.

1.1 M / M / n / m type QS with restriction ($\eta \neq 0$), without mutual assistance (h = n, g = 1), non-ordinary applications and random number of applications in the group.

Kolmogorov differential equations for the probabilities of states of these QS are:

$$\frac{dP_0(t)}{dt} = -\lambda P_0(t) + (\mu + \eta)P_1(t);$$
$$\frac{dP_0(t)}{dt} = -(\lambda + \mu + \eta)P_1(t) + \lambda a_1 P_0(t) + 2(\mu + \eta)P_2(t);$$

(1)

$$\frac{dP_2(t)}{dt} = -(\lambda + 2\mu + 2\eta)P_2(t) + \lambda \sum_{s=1}^{2} sa_s P_{2-s}(t) + 3(\mu + \eta)P_2(t);$$
………………………………………………………………………

$$\frac{dP_k(t)}{dt} = -(\lambda + k\mu + k\eta)P_k(t) + \lambda \sum_{s=1}^{k} sa_s P_{k-s}(k+1)(\mu + \eta)P_{k+1}(t);$$

At $1 \leq k < n$

………………………………………………………………………

$$\frac{dP_k(t)}{dt} = -(\lambda + n\mu + k\eta)P_k(t) + \lambda \sum_{s=1}^{n} sa_s P(t)_{n-s}(t) + [n\mu + (k+1)\eta]P_{k+1}(t);$$

At $k \geq n$.

For stationary conditions the system of linear equations will be:
$$0 = -\lambda P_0 + (\mu + \eta)P_1;$$
$$0 = -(\lambda + \mu + \eta)P_1 + \lambda a_1 P_0 + 2(\mu + \eta)P_2;$$
…………………………………………………………

$$0 = -(\lambda + k\mu) + k\eta)P_k + \lambda \sum_{s=1}^{k} sa_s P_{k-s} + (k+1)(\mu + \eta)P_{k+1}$$

(2)

At $1 \leq k < n$;

………………………………………………………………………

$$0 = -(\lambda + n\mu) + k\eta)P_k + \lambda \sum_{s=1}^{k} sa_s P_{k-s} + [n\mu+)k+1)\eta]P_{k+1}$$

At $k \geq n$

Normalizing condition

$$\sum_{k=0}^{\infty} P_k = 1.$$

1.2. M / M / n / m type QS with restriction ($\eta \neq 0$), full interaction (h = 1, g = n), non-ordinary demands and random number of demands in the group.

The peculiarities of this QMS functioning, and hence the organization of counteraction is:
- the first demand is served by all service channels with intensity $\mu = n\mu + \eta$;
- the next demand is served by part of the service channels, others continue to service the previous demand, if it was not completed;
- after the completion of the service of any demand, the group of channels that has been vacated is connected to the service of demands that are in the system;
- in the Markov (Poisson) QS, the characteristics of the service do not depend on the distribution of channels between demands, only it would be uniform and all channels would participate in the service simultaneously [20];
- if there are already n applications in the system, then (n + 1) application stands in the queue.
The system of differential equations of states probabilities has the form:

$$\frac{dP_0(t)}{dt} = -\lambda P_0(t) + \mu^* P_1(t);$$

$$\frac{dP_1(t)}{dt} = -(\lambda + \mu^*)P_1(t) + \lambda a_1 P_0(t) + 2\mu^* P_2(t);$$

$$\frac{dP_2(t)}{dt} = -(\lambda + 2\mu^*)P_2(t) + \lambda \sum_{s=1}^{2} sa_s P_{2-s}(t) + 3\mu^* P_3(t); \qquad (3)$$

$$\dotsb$$

$$\frac{dP_k(t)}{dt} = -(\lambda + k\mu^*)P_k(t) + \lambda \sum_{s=1}^{k} sa_s P_{k-s}(t) + (k+1)\mu^* P_{k+1}(t);$$

При $1 \leq k < n$;

$$\dotsb$$

$$\frac{dP_k(t)}{dt} = -(\lambda + n\mu^* + k\eta)P_k(t) + \lambda \sum_{s=1}^{n} sa_s P_{n-s}(t) + [n\mu^* + (k+1)\eta]P_{k+1}(t);$$

At $k \geq n$.

1.3. M / M / n / m type QS with restriction ($\eta \neq 0$), partial interaction (h = n / g), extraordinary applications and random number of applications in the group.

The system of differential equations of probabilities of states of the system will be as follows:

$$\frac{dP_0(t)}{dt} = -\lambda P_0(t) + \mu_g^* P_1(t);$$

$$\mu_g^* = g\mu + \eta;$$

$$\frac{dP_1(t)}{dt} = -(\lambda + \mu_g^*)P_1(t) + \lambda a_1 P_0(t) + 2\mu_g^* P_2(t);$$

$$\frac{dP_2(t)}{dt} = -(\lambda + 2\mu_g^*)P_2(t) + \lambda \sum_{s=1}^{2} sa_s P_{2-s}(t) + 3\mu_g^* P_3(t);$$

$$\dotsb$$

$$\frac{dP_i(t)}{dt} = -(\lambda + i\mu_g^*)P_i(t) + \lambda \sum_{s=1}^{i} sa_s P_{i-s}(t) + (i+1)\mu_g^* P_{i+1}(t); \qquad (4)$$

At $0 < i < h$

$$\dotsb$$

$$\frac{dP_h(t)}{dt} = -(\lambda + n\mu_g^*)P_h(t) + \lambda \sum_{s=1}^{h} sa_s P_{h-s}(t) + (n\mu + (h+1)\eta)P_{h+1}(t);$$

$$\dotsb$$

$$\frac{dP_{h+1}(t)}{dt} = -(\lambda + h\mu_g^* + \eta)P_{h+1}(t) + \lambda \sum_{s=1}^{h+1} sa_s P_{(h+1)-s}(t) + (h\mu_g^* + 2\eta)P_{h+2}(t)$$

…………...……………………………………………………………………….

$$\frac{dP_j(t)}{dt} = -(\lambda + h\mu_g^*(j - h)\eta)P_j(t) + \lambda \sum_{s=1}^{j} sa_s\, P_{j-s}(t) + (h\mu_g^* + (j - h + 1)\eta)P_{j+1}(t)$$

At $h < j < n$

…………...……………………………………………………………………….

$$\frac{dP_k(t)}{dt} = -(\lambda + n\mu_g^*)P_n(t) + \lambda \sum_{s=1}^{k} sa_s\, P_{n-s}(t) + (n\mu_g^* + \eta)P_{n+1}(t)$$

At $k \geq n$.

The probability of intruders entering the object due to the fact that the guards do not have time to counter intruders can be calculated from the formula:

$$P_{int} = \frac{\eta \sum_{k=1}^{\infty} kP_k}{\lambda \sum_{k=1}^{\infty} ka_k} \qquad (5)$$

The probability that the intruders will be neutralized will be:

$$P_{neut} = 1 - P_{int}. \qquad (6)$$

We will consider the QS of the second type on the example of the queuing system M / E2 / n / m with restriction ($\eta \neq 0$), without mutual assistance, with non-ordinary demands and a random number of demands in the group.

The system of differential equations of probabilities of states of these QS has the form:

$$\frac{dP_{00}(t)}{dt} = -\lambda P_{00}(t) + \mu_2^* P_{21}(t);$$

$$\frac{dP_{11}(t)}{dt} = -(\lambda + \mu_1^*)P_{11}(t) + \lambda a_1 P_{00}(t) + 2\mu_2^* P_{22}(t);$$

$$\frac{dP_{21}(t)}{dt} = -(\lambda + \mu_2^*)P_{21}(t) + \mu_1^* P_{11}(t);$$

$$\frac{dP_{12}(t)}{dt} = -(\lambda + 2\mu_1^*)P_{12}(t) + \lambda a_1 P_{11}(t) + 2\lambda a_2 P_{00}(t) + 3\mu_2^* P_{23}(t) + \lambda P_{21}(t);$$

$$\frac{dP_{22}(t)}{dt} = -(\lambda + 2\mu_2^*)P_{22}(t) + 2\mu_1^* P_{12}(t); \qquad (7)$$

…………...………………………………..…………………………………………

$$\frac{dP_{1k}(t)}{dt} = -(\lambda + k\mu_1^*)P_{1k}(t) + \lambda \sum_{s=1}^{k} sa_s P_{1(k-s)}(t) +$$

$$+[(k + 1)\mu_2^* + \eta]P_{2(k+1)}(t) + \lambda P_{2(k-1)}(t)$$

$$\frac{dP_{2k}(t)}{dt} = -(\lambda + k\mu_2^*)P_{2k}(t) + k\mu_1^* P_{1k}(t);$$

At $k = n$

…………...…………………………………………………………………...…

$$\frac{dP_{1k}(t)}{dt} = -(\lambda + \eta\mu_1^* + k\eta)P_{1k}(t) + \lambda \sum_{s=1}^{k} sa_s P_{1(k-s)}(t) + \lambda P_{2(k-1)}(t) +$$

$$+(\eta\mu_2^* + k\eta)P_{2(k+1)}$$

$$\frac{dP_{2k}(t)}{dt} = -(\lambda + n\mu_2^* + k\eta)P_{2k}(t) + (n\mu_1^* + k\eta)P_{1k}(t)$$

At $k > n$

The mathematical model of SMO M / E2 / n / m is considered in detail in [22].

The queuing system, which consists of QS of the first and second types, simulates a multi-stage counteraction to groups of attackers.

The probabilities of penetration and neutralization of attackers can be calculated from the formulas (5) and (6). A multistage counteraction QS structure is shown in Fig.1.
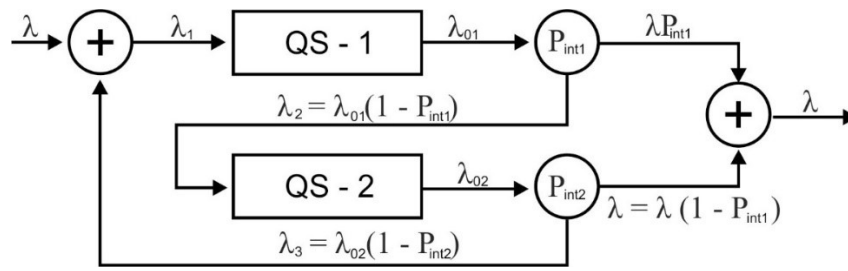
Figure 1: *Multistage counteraction QS*

The following equations will take place in stationary mode:

$\lambda 1 = \lambda 01$; $\lambda 2 = \lambda 02$;

$\lambda 2 = \lambda 01 (1 - Pneut) = \lambda(1 - Pneut1) = \lambda Pint1$; $\quad\quad\quad\quad\quad$ (8)

$\lambda 01 = \lambda 01 (1 - Pneut1) \cdot P_{int2}^{-1} = \lambda Pint1 \cdot P_{int2}^{-1}$;

$\lambda 2 = \lambda 02 (1 - Pneut2) = \lambda(1 - Pneut1)(1 - Pneut2) \cdot P_{neut2}^{-1} = \lambda Pint1 \cdot \lambda Pint2 \cdot P_{neut2}^{-1}$

Conditions of QS stationary work:

$$\omega_1 = \frac{\lambda}{n_1(\mu_1 + \eta_1)} < 1;$$

$$\omega_2 = \frac{\lambda P_{int1}}{n_2(\mu_2 + \eta_2)} < 1; \quad\quad\quad\quad (9)$$

Total mathematical expectation of the demand staying in the QS:

$$\bar{t} = (\bar{t}_{QS1} + \bar{t}_{QS2})P_{int2}^{-1}.$$

Consider an example.

An object guarded by a three-person security unit (n = 3) is attacked by a group of intruders with a rate of $\lambda = 1$ [group / unit time]. Each group with a probability of as can have a different number of attackers. The distribution law of the number of malefactors in the group is uniform, i.e. with a probability of 0.2 in the group there can be 1,2,3,4 or 5 malefactors: a1 = a2 = a3 = a4 = a5 = 0.2. The time spent by intruders on the object $\bar{t}_{int}$ is a limited random variable that is subject to the exponential law with the parameter $\eta = \frac{1}{\bar{t}_{int}}$.

Intensity of counteraction by guards is $\mu = \frac{1}{\bar{t}_{gr}}$ [malefactors neutralized by guard / unit of time].

It is necessary to determine the probability of neutralizing intruders/ malefactors by protecting the object at different ratios $\lambda: \mu: \eta$.

Figure 2 shows the object protection QS for the example under consideration.
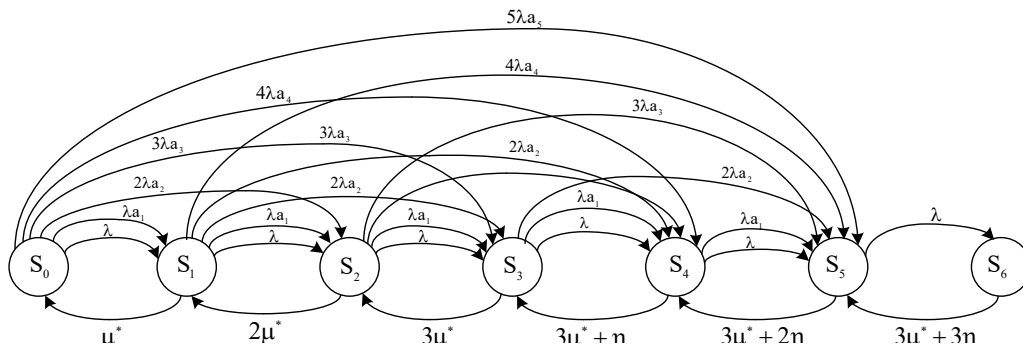
Figure 3: *Object protection QS for the example under consideration*

Kolmogorov's differential equations for the probabilities of the states of these QS will be:

$$\frac{dP_1(t)}{dt} = -\lambda P_0(t) + \mu^* P_1(t) \; ;$$

$$\frac{dP_1(t)}{dt} = -(\lambda + \mu^*)P_1(t) + \lambda a_1 P_0(t) + 2\mu^* P_2(t) \; ;$$

$$\frac{dP_2(t)}{dt} = -(\lambda + 2\mu + 2\eta)P_2(t) + \lambda a_1 P_1(t) + 2\lambda a_2 P_0(t) + 3\mu^* P_3(t) \; ;$$

$$\frac{dP_3(t)}{dt} = -(\lambda + 3\mu + 3\eta)P_3(t) + \lambda a_1 P_2(t) + 2\lambda a_2 P_1(t) + 3\lambda a_3 P_1(t) + 3\lambda a_3 P_0(t) + (3\mu + 4\eta)P_4(t)$$

$$\frac{dP_4(t)}{dt} = -(\lambda + 3\mu + 4\eta)P_4(t) + \lambda a_1 P_3(t) + 2\lambda a_2 P_2(t) + 3\lambda a_3 P_1(t) + 4\lambda a_4 P_0(t) + (3\mu + 5\eta)P_5(t)$$

$$\frac{dP_5(t)}{dt} = -(\lambda + 3\mu + 5\eta)P_5 + \lambda a_1 P_4(t) + 2\lambda a_2 P_3(t) + 3\lambda a_3 P_2(t) + 4\lambda a_4 P_1(t) + 5\lambda a_5 P_0(t) + (3\mu + 6\eta)P_6(t)$$

(10)

Normalizing condition $\sum_{k=0}^{6} = 1; \mu^* = \mu + \eta$.

For stationary operating conditions of these QS, the linear equations have the form

$$0 = -\lambda P_0(t) + \mu^* P_1 \; ;$$

$$0 = -(\lambda + \mu^*)P_1 + \lambda a_1 P_0 + 2\mu^* P_2 \; ;$$

$$0 = -(\lambda + 2\mu^*)P_2 + \lambda a_1 P_1 + 2\lambda a_2 P_0 + 3\mu^* P_3 \; ;$$

(11)

$$0 = -(\lambda + 3\mu^*)P_3 + \lambda a_1 P_2 + 2\lambda a_2 P_1 + 3\lambda a_3 P_1 + 3\lambda a_3 P_0 + (3\mu^* + \eta)P_4 \; ;$$

$$0 = -(\lambda + 3\mu^* + \eta)P_4 + \lambda a_1 P_3 + 2\lambda a_2 P_2 + 3\lambda a_3 P_1 + 4\lambda a_4 P_0 + (3\mu^* + 2\eta)P_5 \; ;$$

$$0 = -(\lambda + 3\mu^* + 2\eta)P_5 + \lambda a_1 P_4 + 2\lambda a_2 P_3 + 3\lambda a_3 P_2 + 4\lambda a_4 P_1 + 5\lambda a_5 P_0 + (3\mu^* + 3\eta)P_6 \; .$$

The P_{ntr} probability was determined from formulas (5,6). Figure 3 shows the graph of the dependence of the P_{ntr} probability at different values of μ and η.
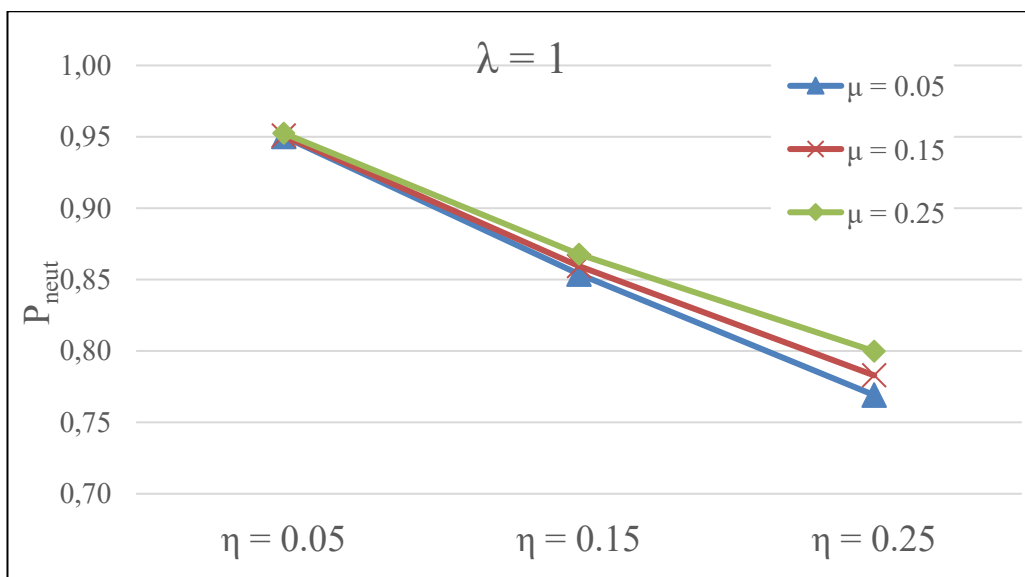
Figure 3: *Probability of attackers' neutralization against the counteraction intensity*

From Figure 3 it is seen that with increasing the counteraction intensity, the value of the P_{ntr} probability increases even with a decrease in the time spent by intruders on the protected object.

III. Conclusion

The use of models of protection of critical infrastructure from unauthorized interference acts will determine the rational ratios of the quantitative composition of security units, the intensity of countermeasures and concentration of additional security forces against the intensity of penetration of malicious groups with a random number of attackers, ensuring an acceptable probability of detection, prevention and neutralization of such groups.

References

[1] Shumov V.V. Models against terrorism: classification. Trudy ISA RAN. Vol 62, 3/2012, pp.106-115 (In Russian).

[2] Social Science for Counterterrorism. Putting the Pieces Together/Davis P.K., Cragin K., Editors. RAND Corporation, 2009.

[3] Wright P.D, Liberatore M.I., Nydick R.L, A Survey of Operations Reserch Models and Application in Homeland Security/Interfaces, 2006.V.36, №6, pp.514-529.

[4] Sullivan T.J., Perry W.L. Identifying indicators of chemical, biological, radiological and nuclear (CBRN) Weapons development activity in sub-national terrorist group/ J. Oper. Res. Soc. 2004, N 55 (4), PP. 361-374.

[5] Pate-Cornell E. Fusion of intelligence information: A Bayesian approach/ Risk Anal. 2002, N 22(3), pp. 445-454.

[6] Novikov D.A. Hierarchical models of military action/ Management of Large systems. Vol. 37. Moscow: Institute for Management Problems of Russian Academy of Sciences, 2012, C.25-62 (In Russian).

[7] Bachrach Y., Draief V., Goyal S. Security games with contagion/University of Cambridge, 2011.

[8] Bier V., Oliveros S., Samuelson L. Choosing what to protect: Strategic defensive allocation against an unknown attacker//Journal of Public Economic Theory, 2006, N9, pp. 1-25.

[9] Kiekintveld C., Tambe M., Marecki J. Robust Bayesian Methods for Stackelberg Security Games//Conference: Autonomous Agents & Multiage Systems/Agent Theories, Architectures and Languages – ATAL, pp. 1467-1468, 2010.

[10] Borovsky A.S., Tarasov A.D. An integrated approach to the development of a general model for the functioning of physical protection systems of objects // Trudy ISA RAN. Vol. 61. 1/2011, pp. 3-13 (In Russian).

[11] Dormidontov A.V., Mironova L.V., Mironov V.S. On the possibility of applying the countermeasures model to assessing the security level of transport infrastructure facilities // Naichny Vestnik MGTU. Vol 21, № 03, 2018, pp.67-77 (In Russian).

[12] Ginis L.A., Kolodenkova A.Ye. Fuzzy modeling to prevent risk situations at critical infrastructure facilities / Vestnik UGATU, Vol. 21, № 4(78), 2017, pp. 113-1120 (In Russian).

[13] Norkin V.I., Gaivoronsky A.A., Zaslavsky V.A., Knopov P.S. Optimal Resource Allocation Models for Critical Infrastructure Protection / Cybernetic I and System Analysis. Vol. 54 № 5, 2018, pp.13-26 (in Russian).

[14] Pita J., Jain M., Western C., Portway C., Tambe M., Ordonez F., Kraus S., Paruchuri P. Deployed ARMOR protection: The application of a games theoretic model for security at the

Los Angeles International Airport/In Proc. Of AAMAS,2008.

[15] Taylor M.E., Kiekintveld C., Western C., Tambe M. Beyond Runtimes and Optimality: Challenges and Opportunities in Evaluating Deployed Security Sistems/ In Proceeding of the AAMAS – 09 Workshop on Agent Design: Advancing from Practice to Theory, May 2009.

[16] Ryzhikov Yu.I. Simulation modeling. Theory and technology. S.-Petersburg: Korona Print, 2004, 384 p. (In Russian).

[17] Ryzhikov Yu.I. Calculation of service systems with group arrival of requests /Information and Control systems № 2. 2007, pp.39-49 (In Russian).

[18] Monsik V.B., Skrypnikov A.A., Fedotov A.Yu. Queuing systems for indivisible group claims with a queue of unlimited length / Nauchnyi Vestnik MGTU GA № 184, 2012, p. 108-112 (In Russian).

[19] Gnedenko B.V., Kovalenko I.N. Introduction to queuing theory. – Moscow: Nauka, 1987. – 336 p (In Russian).

[20] Shuenkin V.A., Donchenko V.S. Applied models of queuing theory. Kyiv: NMKVO, 1992, 398 p (In Russian).

[21] Ventsel E.S., Ovcharov L.A. The theory of stochastic processes and its engineering applications. – 2nd edition., Moscow: Vysshaya Shkola, 2000. — 383 p (In Russian).

[22] Katsman M. D., Mathematical models of ecologically hazardous rail traffic accidents / M. D. Katsman, V. K., Myronenko, V. I. Matsiuk // Reliability: theory&applications. – Vol. 10, № 1(36). – San Diego, USA – 2015. – P. 28–39.

Farhadzadeh E.M., Muradaliyev A.Z., Ashurova U.K.
METHODICAL BASES OF BENCHMARKING UNIQUE.....

RT&A, No 1 (61)
Volume 16, March 2021

Methodical Bases of Benchmarking Unique Objects of Electric Power Systems

Farhadzadeh E.M., Muradaliyev A.Z., Ashurova U.K.

•

Azerbaijan Scientific-Research and Design-Prospecting
Institute of Energetic, *e-mail: elmeht@rambler.ru*

Abstract

One of the basic problems of electro power systems is absence of the normative documents regulating operation, maintenance service and repair of the capital equipment, which service life exceeds normative value. We shall name them «oldtech» (OT). The essence of the difficulties demanding overcoming is reduced to absence of methodologies a quantitative estimation of operative reliability and safety of OT, with the subsequent benchmarking of OT. Considering the science-intensive, bulkiness and labour input of the decision of this problem indisputable becomes necessity of development of the corresponding automated systems. In present article, some features of an estimation of an integrated indicator and benchmarking unique objects are resulted. To unique objects, which analogues on the set combination of versions of significant attributes are absent concern. For an illustration of recommended methods and algorithms technical and economic parameters of power units with SGI-400 are used.

Keywords. Benchmarking, oldtech, unique object, operative efficiency, integrated indicator, analysis, synthesis, technical condition

I. Introduction

One of the main problems of electric power systems (EPS) is to increase the operative efficiency of work (OEW) of the main equipment, devices and installations (objects), which service life is approximately equal to or even exceeds the calculated (nominal, park). We shall agree to name them «oldtech» (OT). This problem is far from new. Suffice it to refer to the publications of well-known specialists [1,2,3]. And, despite the fact that there is a systematic increase in many EPS in the relative number of OT (today this value exceeds 60%), "and the problem is still there." Why? After all, the unacceptable consequences of system accidents, initiated by OT, are well known. Of course, the death and injury of EPS personnel, environmental damage and large material costs attributed to climate change. Therefore, they often also speak. But why this problem is not solved anywhere?

To realize this, we need to agree that:

❖ The efficiency of EPS facilities in the modern sense is no longer economic efficiency. This is a complex (integral) concept that includes, along with efficiency of operation, reliability and safety of service. So what? These properties always been taken into account (the reader will say). Sure. But only the economic component of the OEW was quantified;

❖ There was no quantitative assessment of operational reliability and maintenance hazards. "Within the guaranteed period, the manufacturer (supplier) is responsible for hidden, and in the cases provided for by the contract, and for obvious defects" [4];

❖ At the end of the guaranteed service life of the object, our attitude to the OEW characteristic does not change. And how can it change if there is no corresponding regulatory framework for the maintenance and repair of OT? After all, we are accustomed to calculating reliability indicators on the basis at the design stage of objects based on a priori information about failures, defects and the duration of damage recovery in many objects of the same type. Now it is required to assess the operational reliability of work over the past month, week, day and even shift. But, if we are able to assess a quantitative assessment of the reliability of work at least at the design stage, then the danger of maintenance has always, including during design, been assessed only at a qualitative level;

❖ By the way, it is not safety that needs to quantified, but the hazard of maintenance. Security is either there or not. Only the danger changes;

❖ Quantifying the efficiency and reliability of work, as well as the risks of maintenance, is not an end in itself. It is necessary for operational comparison and ranking of EPS objects. In economics, this analysis usually called benchmarking, when specialists compare numerous properties of objects and, because of this comparison, increase the efficiency of their work. The number of compared indicators calculated in tens. The ranking results here are largely subjective, and the risk of making a wrong decision is great;

❖ Comparison and ranking of the OEW of EPS objects significantly simplified in the transition to the integral indicator. But reducing the risk of an erroneous decision is achieved only if the integral indicator characterizes the technical condition of the object;

❖ The use of Harrington's integral indicator [5] has become widespread in many branches of material production and in the service sector, which indicates the relevance of integral assessment. But Harrington's integral exponent is calculated as the geometric mean of the probabilities of realizations of a set of indicators, and therefore it has no physical meaning. "The calculation methodology, noted in [6], becomes a black box that gives out numbers that not have physical meaning."

Some of the features of the problem, briefly listed above, cause difficulties in solving it by the efforts of the EPS personnel. One of the possible ways to partially overcome these difficulties are the recommendations [3], the essence of which boils down to organizing centers for providing the OEW of EPS facilities at the branch research institutes of energy. The Center carries out: collection and analysis of statistical data on the technical condition of equipment, failures, repairs; identification of factors influencing the ERM; development of measures to increase the OEW; organization of staff training; conducting benchmarking. The practical implementation of these recommendations would undoubtedly have positive results. But they could not solve the problem for two reasons: there are no methods for quantitative assessment of the integral indicator of the OEW of objects and criteria for testing hypotheses about the nature of the discrepancy between these indicators.

II. Methodical bases of synthesis of integral indicators of the OEW and benchmarking of OT.

We will distinguish between same tipe, similar and unique EES objects. Objects that characterized by the same set of varieties of significant features will be referred to as "the same type". "Similar" considered objects that characterized by the same samples of varieties of significant features from their totality. We will refer to "unique" objects, as there are no analogues for the given types of features.

An example of same objects can be power units of power plants, their main equipment, devices and installations, an example of "similar" objects - switchgear switches (linear, block), and an example of a "unique" object - the only 500 MW steam turbine power installation in the EPS. This classification of objects is not given by chance. First of all, it testifies to the fact that there are numerous benchmarking tasks, methods and algorithms for their solution. And this feature

Farhadzadeh E.M., Muradaliyev A.Z., Ashurova U.K.
METHODICAL BASES OF BENCHMARKING UNIQUE…..

RT&A, No 1 (61)
Volume 16, March 2021

determines one of the difficulties in solving the problem of improving the management of the OEW EPS. But all these methods and algorithms have a lot in common. To them concern:

❖ Ensuring the infallibility of the information base is one of the most important tasks of the automated system for operational benchmarking of objects. Information on the technical condition of EPS facilities formed according to the monthly reports of EPS enterprises (for example, form 3-TECH (energy)), test and repair protocols and dispatch logs. Naturally, these data differ significantly from the list of calculated indicators used in benchmarking, and the transformation of the initial data is one of the possible sources of errors. The recommended methods and algorithms for ensuring the error-freeness of the initial data, as well as the error-freeness of the database as a whole, are given in [7], and for the control of the accuracy of the calculated technical and economic indicators (TEI) - in [8].

❖ _Requirements for the estimates of integral indicators_. Along with the infallibility of the initial data, the calculation method should ensure objectivity, physical essence, and the availability of practical use of the integral indicator.

One of the main reasons for distorting the assessment of the integral indicator based on error-free initial data is the presence of interconnected TEI. In other words, some specific property of an object represented by several integral indicators. Thus, the significance (relative value characterizing the technical condition) of this property is unjustifiably increased, which leads to a distortion of the integral indicator and benchmarking. The solution to this problem would not present difficulties, bearing in mind the mathematical apparatus of the theory of correlation, if not one "but" - these methods are developed for one-dimensional random variables and a number of restrictions. Constraints include the correspondence of the distribution of random variables to the normal law and a considerable number of implementations.

The multidimensional character of the TEI realizations determines their difference from the normal distribution law. And if for any TEI the statistical distribution function resembles a normal distribution law, then on an adjacent time interval the assumption of such a correspondence will be erroneous with a high probability. As for the number of TEI, even in the presence of similar EPS objects, their number is naturally limited, and when classifying integral indicators, calculated in units. Overcoming these difficulties in [9] proposes to carry out the transition from constant critical values of TEI to "local" ones, calculated by simulation modeling of possible realizations of the correlation coefficients for fiducial distributions of TEI.

❖ _Providing the physical essence of the integral indicator_. Obviously, the recommendations for benchmarking EPS facilities should be objective and, as a rule, understandable to a specialist. Specific recommendations among a number of possible ones should not cause a smile. Inconsistency of recommendations with real possibilities not excluded, since in this complex system it is almost impossible to take into account all external factors. An example is the lack of spare nodes necessary for the repair of an object due to an accidental delay in their delivery. But with proper organization of maintenance and repair, such reasons can appear, but of course, far, not monthly. Since, in fact, it is necessary to compare the technical condition of objects the most important for OT are indicators characterizing the degree of "wear" of individual properties.

In reality, TEI vary from the nominal to the maximum permissible value. It is proposed to represent this interval as the interval of the possibility of the EPS object to meet the requirements for the technical state. Over time, as a result, of aging, these opportunities decrease. The change can be continuous or discontinuous. A relative portion of the utilized capacity referred to as "wear and tear", and the remainder referred to as "residual resource".

The amount of wear varies within [0;1], and the residual resource - within [1;0]. The transition to relative values of TEI called rationing. The advantage of rationing is also overcoming the difficulties of differences in the dimensions and scales of TEI, which does not allow for the possibility of their joint consideration. As random variables, wear estimates most fully characterized by statistical parameters. The methodology for overcoming the difficulties of joint consideration of TEI is given in [10].

Farhadzadeh E.M., Muradaliyev A.Z., Ashurova U.K.
METHODICAL BASES OF BENCHMARKING UNIQUE…..

RT&A, No 1 (61)
Volume 16, March 2021

❖ *Varieties of integral indicators of operational efficiency.* The transition from multiple TEI to integral indicators undoubtedly simplifies benchmarking if we can answer the following questions: how are integral indicators calculated how to choose integral indicators from a variety of possible ones, and how to compare these indicators taking into account their random nature.

It is known, that the number of indicators characterizing the average values TEI realizations and their scatter about 10. If, in addition, take into account complex indicators (similar to the coefficient of variation K_v), their total number may exceed the number of TEI. Thus, refusing to compare the set of possible TEI realizations and moving on to integral indicators, we encountered the problem of choosing from a set of possible types of integral indicators. Overcoming this difficulty is supposed to be carried out by assessing the analysis of the possibility of practical use and the relationship of integral indicators. The analysis made it possible to establish that the technical state of the object represented by two integral indicators that characterize the average wear and the degree of misalignment of the technical state of the object, and most independent. This is the arithmetic average of the normalized values of the calculated TEI and their coefficient of variation;

❖ Since the recommended benchmarking methodology based on comparing and ranking random wear values, conclusions and recommendations for increasing the OEW of objects cannot fail to consider this feature. Objects of the same type, for example, power generating units of power plants of the same type, and completely different ones, for example, steam and hydraulic turbines, compared in terms of wear. In both cases, the comparison is associated with an assessment of the appropriateness of the classification and is quite accessible, since the values of average wear compared. And the difficulties in solving this problem are again associated with the multidimensional nature of these indicators and the high risk of using a mathematical algorithm for testing hypotheses about the nature of the discrepancy between statistical parameters. The risk of an erroneous decision is due to the inadmissibility of applying to multidimensional values criteria that involve the comparison of statistical parameters of one-dimensional random variables. Overcoming these difficulties achieved by comparing two fiducial distributions, the first of which reflects the distribution of a set of normalized TEI realizations, and the second - a sample of TEI realizations for a given combination of varieties of features. At the same time, proposed to agree that if the statistical distribution functions differ randomly, then their distribution parameters also randomly differ.

❖ Science-intensive, cumbersome and labor-intensive, the high risk of an erroneous decision in manual counting necessitate the transition to automated systems for the synthesis of integral OEW and benchmarking of operational tasks of maintenance and repair. It noted that the above difficulties and ways to overcome them categorized as "explicit". "Implicit" difficulties appear during the implementation of an automated system and are caused by numerous external factors specific to each EPS.

This article presents the features of the methodology for analyzing the error-freeness of TEI, assessing the integral indicator of the OEW (synthesis of TEI), benchmarking the maintenance and repair system and taking into account the random nature of the integral indicators using the example of a number of TEI of the SGI-400 combined cycle plant.

Farhadzadeh E.M., Muradaliyev A.Z., Ashurova U.K.
METHODICAL BASES OF BENCHMARKING UNIQUE…..

RT&A, No 1 (61)
Volume 16, March 2021

III. Features of the methodology of analysis, synthesis
and comparison of TEI SGI -400.

Table 1 shows some average monthly TEI, that characterize the OEW of SGI -400 in the analyzed (t_j) and the previous month ($t_{(j-1)}$).

Table 1. Implementation of the average monthly TEI SGI -400

i	TEI name	Symbol	unit of measurement	Months of year	
				t_j	t_{j-1}
1	EE generation (total)	E_Σ	кWh10^3	241322,8	89617,9
2	EE release from the trunks of station	$E_\text{т}$	кWh10^3	235541,2	86858,1
3	Energy consumption in system of ON	E_on	кWh10^3	5781,6	2759,8
4	Natural gas consumption	B_g	t.м^3	45310,9	17077,5
5	Equivalent fuel consumption	B_f	t.e.f.	51783,8	19517,1
6	Specific consumption of equivalent fuel	b_f	g/кWh	219,85	224,7
7	Average power	P_av	MW	342,7	322,7
8	Efficiency (gross)	η_g	%	55,9	51,68
9	Feed water temperature	T_f	^{0}C	150,5	151,8
10	Flue gas temperature	T_fg	^{0}C	113,2	113,4
11	Vacuum	K_v	%	95,8	95,7

As follows from table 1, the reported indicators are not always convenient for comparing the OEW of the SGI. For example, these TEI do not answer the question about the reasons for a sharp decline in total electricity generation (EE), or a sharp decline in consumption EE in system of own needs (OW). On the other hand, the TEI "natural gas consumption" (B_g), "equivalent fuel consumption" (B_f) and "Specific consumption of equivalent fuel" (b_f) characterize economic efficiency quite fully. But they do not take into account that $b_f \cdot \eta_g$=const, i.e. TEI efficiency (gross) η_g as objectively characterizes the economic efficiency of a SGI unit, as well as TEI b_f. To take into account this discrepancy for the synthesis and benchmarking of TEI, it proposed slightly modify the list of analyzed TEI.

Namely:

❖ TEI E_Σ and $E_\text{т}$. replace with TEI "coefficient of use of nominal performance" $K_P = E_\Sigma / P_n \cdot t_j$;

❖ TEI E_on should be presented in relative units (%) according to the formula $\varepsilon E_\text{on} = 100 \cdot E_\text{on} / E_\Sigma$;

❖ instead of TEI P_av, introduce TEI "coefficient of use of installed capacity" $K_c = 100 P_\text{av} / P_n$;

❖ enter the TEI "coefficient of technical use", calculated by the formula $K_\text{т} = 100 E_\Sigma / P_\text{av} \cdot t_j$.

Indicators K_P, εE_on, K_c and $K_\text{т}$ will agree to call calculated. The results of the automated transformation of the reporting TEI of the SGI -400 into calculated TEI shown in table 2. It is easy to see that the transformation of TEI reduced to the input of the indicators K_P, K_c and $K_\text{т}$, well known in the theory of reliability.

Moreover, since $K_P = K_c \cdot K_\text{т}$ - this ratio can be used to control the accuracy of their calculation.

Table 2. Implementation of the recommended list of average monthly TEI SGI -400

i	TEI name	Symbol	unit of measurement	Months of year	
				t_j	t_{j-1}
1	Coefficient of use of nominal energy	K_P	o.e.	0,84	0,30
2	Consumption in system of ON	εE_on	%	2,39	3,08
3	Coefficient of use of installed capacity	K_c	o.e.	0,86	0,81
4	Coefficient of technical use	$K_\text{т}$	o.e.	0,98	0,37
5	Efficiency (gross)	η_g	%	55,9	54,7
6	Feed water temperature	T_f	^{0}C	150,5	151,8
7	Flue gas temperature	T_fg	^{0}C	113,2	113,4
8	Vacuum	K_v	%	95,8	95,7

Farhadzadeh E.M., Muradaliyev A.Z., Ashurova U.K.
METHODICAL BASES OF BENCHMARKING UNIQUE…..

RT&A, No 1 (61)
Volume 16, March 2021

The next stage of the analysis (when the automated system is put into operation) is to determine the change interval of possible TEI realizations. For unique objects, these intervals are established and adjusted according to the monthly average TEI realizations for a number of years of observation. It should be borne in mind that the width of the interval increases with time (with a constant number of realizations) from the initial to the maximum permissible value, since TEI implementations vary from the nominal to the maximum permissible value. For illustrative purposes,

Table 3 shows the results of calculations of these intervals for each of the last four years and the width of the interval for four years. When analyzing these data, one should take into account the direction of the TEI change.

Table 3. Interval of changes in TEI SGI -400 realizations

		TEI		Change interval				
i	Symbol	unit of measurement	Estimation	On years (j)				Maximum
				1	2	3	4	
1	K_P	o.e.	min	0,232	0,179	0,450	0,210	0,179
			max	0,699	0,747	0,787	0,875	0,875
2	εE_{on}	%	min	2,60	2,40	2,31	2,32	2,31
			max	3,23	3,15	3,71	4,68	4,68
3	K_c	o.e.	min	0,58	0,59	0,48	0,39	0,39
			max	0,73	0,78	0,79	0,88	0,88
4	$K_т$	o.e.	мин	0,37	0,27	0,60	0,37	0,27
			max	1,0	1,0	1,0	1,0	1,0
5	η_g	%	min	50,8	50,0	47,0	42,7	47,0
			max	54,3	54,6	54,3	56,8	56,8
6	T_f	^0C	min	152,0	153,2	156,2	149,7	149,7
			max	155,1	158,4	158,9	158,2	158,9
7	T_{fg}	^0C	min	113,3	112,9	112,5	113,1	112,5
			max	119,7	121,7	123,2	124,8	124,8
8	K_v	%	min	87,5	87,3	85,7	85,7	85,7
			max	96,8	96,4	93,5	96,3	96,8

Under the "direction of change», we mean the direction of change in TEI with an increase in the service life and wear of the object. For example, with an increase in the wear of a SGI TPS, the value of K_P decreases, and the value of εE_{on} increases.

The boundary values of the TEI change intervals serve not only as the basis for the interval method for monitoring the TEI error-freeness, but also as a necessary condition for the transition from the actual TEI values to the normalized values. For an arbitrary TEI (P_i) i=1,mp, the normative value will be denoted as $Iz(P_i)$.

There are a lot ways to normalized TEI of EE objects. It is proposed [9] to carry out standardization, as a result of which the normalized estimate of the TEI will reflect the technical condition of the SGI, that is, the amount of wear (Iz).

Let us consider the sequence of calculations of the normalized TEI values for the coefficient of utilization of the nominal capacity K_P, which decreases with increasing service life of the SGI. In accordance with Table 2, K_P in the j-th month is equal to $K_P(t_j)=0,84$:

❖ according to table 3, we determine the interval of possible realizations

$$\Delta K_P=(K_{P,max}-K_{P,min})=0,696;$$

❖ the normalized value of K_P is calculated by the formula:

$$Iz[K_P(t_j)]=[K_{P,max} - K_{P,min}(t_j)]/\Delta K_P=0,05.$$

Thus, the wear rate does not exceed 5%.

Farhadzadeh E.M., Muradaliyev A.Z., Ashurova U.K.
METHODICAL BASES OF BENCHMARKING UNIQUE…..

RT&A, No 1 (61)
Volume 16, March 2021

Let us now consider the sequence for calculating the normalized value of the TEI εE_{on}, which increases with the service life of the SGI. According to table 2, εE_{on} in the j-th month is equal to $\varepsilon E_{on}(t_j) =2,39\%$:

❖ according to the data in table 3, we determine the interval of possible realizations $\Delta(\varepsilon E_{on})=2,37\%$;

❖ the normalized value εE_{on} is calculated by the formula:

$$Iz\ [\varepsilon E_{on}(t_j)]=[\varepsilon E_{on,max} - \varepsilon E_{on,min}(t_j)]/\Delta(\varepsilon E_{on})=0,034.$$

The results of similar calculations are shown in table 4. It also shows the estimates (*) of integral indicators ($M^*(Iz)$ and $K_v^*(Iz)$), characterizing the technical condition of SGI -400 for the j-th and for comparison - for (j-1) month according to the data tables 2 and 3.

Table 4. The results of calculating the normalized values of TEI

TEI		Month of year	
i	tip	j	j-1
1	$Iz(K_P)$	0.050	0.826
2	$Iz\ \varepsilon E_{on})$	0.034	0.629
3	$Iz(K_c)$	0.036	0.127
4	$Iz(K_T)$	0.027	0.863
5	$Iz(\eta_g)$	0.092	0.214
6	$Iz(T_f)$	0.087	0.228
7	$Iz(T_{fg})$	0.057	0.073
8	$Iz(K_v)$	0.090	0.099
$M^*(Iz)$		0.079	0.313
$K_v^*(Iz)$		0.42	1.093

Comparison of quantitative estimates of TEI SGI-400 in the j-th and preceding (j-1) month allows us to conclude:

❖ six TEI $Iz(K_P)$, $Iz(\varepsilon E_{on})$, $Iz(K_c)$, $Iz(K_t)$, $Iz(\eta_g)$ and $Iz(T_f)$ indicate that as a result of average repair of SGI-400 in (j-1) month significantly improved their quantitative estimates in the j-th month;

❖ two TEI $Iz\ (T_{fg})$ and $Iz(Kv)$ - practically did not change;

The transition to integral TEI $M^*(Iz)$ and $Kv(Iz)$ also indicates a significant improvement in the technical condition of SGI-400 after repair.

The apparent simplicity of the synthesis and benchmarking of the TEI SGI-400 is deceptive, since far from all TEI are taken into account, and the SGI -400 is not represented by a set of main equipment, devices, installations and their units. Comparing them (benchmarking) manually would be extremely cumbersome and time consuming. But there is one more feature that is not always taken into account in calculations.

Since the normalized TEI values, as well as the actual TEI values themselves, are random variables, and the number of TEI realizations for the given types of features may be quite small, the observed discrepancy of the integral indicators may be random, and the risk of making an erroneous decision is great.

As an example of solving this problem, we can consider the nature of the discrepancy between the integral indicators in the j-th and (j-1) -th months. However:

❖ because benchmarking is multidimensional (many comparison options);

❖ comparison in the framework of the theory of testing statistical hypotheses of one-dimensional random variables is associated with a high risk of erroneous decisions;

❖ assessment of critical values of integral indicators based on simulation is specific;

Comparison of random implementations of integral indicators, due to the high labor intensity, cumbersomeness and science intensity, should carry out automatically.

Farhadzadeh E.M., Muradaliyev A.Z., Ashurova U.K.
METHODICAL BASES OF BENCHMARKING UNIQUE…..

RT&A, No 1 (61)
Volume 16, March 2021

Conclusion

1. If the replacement of OT with modern facilities is currently impossible, and funds for their complete modernization are not enough, and at the same time, the occurrence of system accidents caused by OT is unacceptable, it is advisable to carry out partial modernization, eliminating the identified defects, with mandatory operational control of the technical state of the OT and clarification of the maximum permissible load values;

2. Centers for ensuring operational efficiency at branch research institutes of energy collect and formalize data on the technical state of OT, automated analysis and synthesis of this data, benchmarking, preparation of operational recommendations to improve work efficiency, development of appropriate methodological guidelines, professional development of personnel of launches in on-line mode;

3. Development of automated systems for monitoring the technical condition of OT, taking into account specific external factors. Improving the objectivity of recommendations on the effectiveness of the OT requires the approval of the form of the output documents with the management;

4. Some features of the formalization of data on the technical state of OT, ensuring the infallibility of the initial data, performing the standardization of technical and economic indicators, assessing integral indicators and some benchmarking results indicate the possibility of an objective assessment of the operational efficiency of OT and thereby reducing the risk of unacceptable consequences.

References

[1]   Dyakov A.F., Isamukhammedov Y.Sh., Molodyuk B.D. Problems and ways of increasing the reliability of the UES of Russia / Methodological issues of researching the reliability of large power systems. Issue 64 / Reliability of energy systems: achievements, problems, prospects // Ed. ed. N.I. Voropai ISEM SO RAN, 2014, p.8-16.

[2]   Aminov R.Z., Shkret A.F., Garievsky M.V. Calculation of the equivalent development of the resource of TPS power units. Power stations No.8, 2014, p.16-18

[3]   Rezinsky V.F. Once again about the reserve of power equipment. Energy reliability and safety. No.4, 2009, p.9-13

[4]   STO 70238424.27.040.007-2009. Steam turbine installations. Organization of operation and maintenance. Norms and requirements. M., ORGRES, 2010, 165 p.

[5]   Zaznobina N.I. Assessment of the ecological situation in a large industrial center using the Harrington generalized desirability function.//Bulletin of the Nizhny Novgorod University, 2007, No.2, p.115-118

[6]   Loseva P. Counterclockwise. What is aging and how to deal with it. M., "Alpina non-fikish", 2020, 500 p.

[7]   Farhadzadeh E.M., Muradaliyev A.Z., Farzaliyev Yu.Z., Ismailova S.M. Database security and integrity management system. M .: Energetik No.3, 2008, p.33-35.

[8]   Farhadzadeh E.M., Farzaliyev Y.Z., Muradaliyev A.Z. Assessment of the quality of restoration of deterioration of TPS power units. Minsk, Energy No.1, 2016, p.4-24.

[9]   Farhadzadeh E.M., Muradaliyev A.Z., Farzaliyev Yu.Z., Rafiyeva T.K., Abdullayeva S.A. Assessment of the relationship of technical and economic indicators of EPS facilities. Kiev Electronic modeling №6, 2017, p.93-106

[10]   Farhadzadeh E.M., Farzaliyev Yu.Z., Muradaliyev A.Z. Method and algorithm for ranking boiler plants of block power plants by the criterion of reliability and efficiency of operation. M. Heat Power Engineering No.10, 2015, p.22-29

Multi-objective Model for Daily Diet Planning

[1]Mohd Arif Khan, [2,*]Ahteshamul Haq, and [3]Aquil Ahmed

•

Department of Statistics & Operations Research
Aligarh Muslim University, Aligarh-202002, Uttar Pradesh, India
[1]mohdarifkhan4012@gmail.com, [2,*]a.haq@myamu.ac.in, [3]aquilstats@gmail.com
*Corresponding author

Abstract

In this paper, we present the development of a daily diet model using fuzzy multi-objective goal programming (GP) to satisfy daily nutrient. We have designed the objective function as minimize the cost of diet, Saturated Fat and carbohydrate. This paper consists of ten consumed foodstuffs as the decision variable. The daily diet's tolerable lower and upper intake level is given for the Protein, Vit. B$_6$, Vit. C and Calcium. This paper aims to present a stepwise solution procedure based on fuzzy GP to obtain the compromise solution of the diet problem. Finally, a numerical example is illustrated to compare the daily diet plan with weighted GP, pre-emptive GP and fuzzy GP.

Keywords: Diet Planning, Multi-objective, Weighted goal programming, Pre-emptive Goal Programming, Fuzzy Goal Programming

I. Introduction

It is a severe problem throughout life to meet their health goals based on the daily diet. Researcher and scientists have been using different types of mathematical programming to solve this type of question. With the assist of operations research techniques, it is quite viable to discover a listing of foodstuffs in an appropriate quantity which can grant all nutrient pointers in a day. Firstly, the diet problem by using linear programming was solved by Smith [1]. Anderson and Earle [2] have done the comparative study of diet planning through linear programming and GP approach for daily nutritional requirements of Thais. Nutritionists are turning into extra conscious about the overdoses of vitamins and want for a balanced consumption of all nutrient. The essential traits of the real-world decision-making problems going through human beings at present are multidimensional and have multiple objectives which include economics, social, environmental and technical ones. Hence, it appears natural that the consideration of many objectives in the actual decision-making process requires multi-objective approaches rather than a single objective.

Linear GP is one of many techniques for dealing with the modelling, solution, and analysis of multiple and conflicting objective by reducing it to a single (or sequential) objective one. Since Charnes and Cooper [3] introduced the concept of GP. Pre-emptive GP is a particular case of GP in which the more critical (upper level) goals are optimized before lower-level goals. Once complication concerned the weighting of goals in the objective function, Ignizio [4] demonstrated the use of weighted GP in diet planning and presented the results of the problem involving the selection of foodstuffs for improvement in nutritional balance by minimizing the cost of foodstuffs. Many authors have been worked on diet planning, some of them are listed in Table 1.

Table 1. Research Review Summary

Authors	Model Objective		Techniques used					Remarks
	Single	Multi	LP	IP	WGP	FGP	PGP	
Eghbali et al. [5]		✓				✓		Multi-objective Fuzzy Linear Programming, Diet Model
Nath et al. [6]	✓		✓					Trial and Error Method, Nutritional model
Eghbali et al. [7]		✓				✓		Multi-objective Fuzzy Programming, Diet Problem
Mamat [8]		✓				✓		Diet Planning, nutritional requirements, Fuzzy Programming
Eghbali-Zarch et al. [9]		✓				✓		Mixed Integer Linear Programming, Diet Plan, Jimenez and Epsilon-constraint Method
Sheng and Sufahani [10]	✓			✓				Diet Planning, Integer Programming
Ali et al. [11]	✓			✓				diet planning for boarding schools, Zero One Integer Programming
Bhargava et al. [12]	✓				✓			weighted GP, Diet planning
Proposed model		✓			✓	✓	✓	Diet plan, pre-empty GP, weighted GP, fuzzy programming

Decerle et al. [13] highlight the relationship between working time, quality of service and route balancing for the home health care problem by using Pareto based approach. The objectives of the model are the minimization of the total working time of the caregivers while maximizing the quality of service and minimizing the maximal working time difference among nurses and auxiliary nurses. Nguyen and Montemanni, [14] propose mixed linear programming to find the best schedule minimizing the costs due to the non-respect of patients' time windows and exceeded hours of caregivers. En-nahli et al. [15] develop a multi-objective optimization problem in which the model tries to satisfy the Home Health Care Services objectives. On the other hand, 'patients and caregivers' objectives that satisfy all patients by assigning their wished caregiver, help to get solutions taking into account the priority of a patient and the affinity patient-caregiver. Mutingi & Mbohwa [16] present a multi-agent architecture that facilitates decision making characterised with multiple objectives and the capabilities of a multi-agent system and Web services as to facilitate effective decisions for home healthcare services by using genetic algorithm. Niakan & Rahimi [17] presents a multi-objective mathematical model to address a Healthcare Inventory Routing Problem for medicinal drug distribution to healthcare facilities. The first part of objective function minimizes total inventory and transportation costs, while satisfaction is maximized by minimizing forecast error which caused by product shortage and the number of expired drugs; Greenhouse Gas emissions are also minimized. A hybridized possibilistic method is applied to cope with uncertainty, and an interactive fuzzy approach is considered to solve an auxiliary crisp multi-objective model and find optimal solutions. Othman et al. [18] composed two phases: the first one is an assignment procedure based on fuzzy logic and the second phase is based on an evolutionary method to solve the problem of medical staff scheduling which improves the performance of the scheduling system in order to help physicians to manage the organization better. Turgay & Taşkın [19] presents fuzzy GP using exponential membership function, which uses the modelling, and solving of health care system for optimal, efficient management and prioritized for the strategic

planning and resource allocation. Zhang et al. [20] examine the health-care facilities that should be located to improve the equity of accessibility, reduce the population that falls outside the coverage range, raise the total accessibility for the entire population, and decrease the cost of building new facilities and use genetic algorithm-based multi-objective optimization approach to yield a set of Pareto solutions. The multi-objective optimization approach is used to optimize the location of new health-care facilities which provides a set of different plans that compare the values of the objectives and comparing the Pareto solutions with other solutions.

In this paper, we present the development of a multi-objective daily diet model using pre-emptive and fuzzy GP to satisfy daily nutrients with an example. The objective function is designed to minimize the cost of the diet, Saturated Fat and carbohydrate. The objective of this approach is to select diets to meet specific nutritional requirements. The comparison for the daily diet plan with weighted GP, pre-emptive GP and Fuzzy GP is also shown.

II. Formulation of the Diet Model

A diet is required to propose by the dietician for the special needs of the patient. An integer number of units of the diet can be composed as ten basic foodstuffs termed as Food 1, Food 2, …, Food 10. The nutrients that are used in the model are Saturated Fat, Carbohydrate, Protein, Vitamin C, Vitamin B$_6$ and Calcium. The lower and upper levels of Protein, Vitamin C, Vitamin B$_6$ and Calcium are used as constraints.

In the diet model, $x_j (j = 1,2,..., n)$ represents the different types of food items that work as a decision variable and the cost of food, Saturated Fat, and Carbohydrates for each food are $C_{Dj}, S_{Flj}, C_{dj} (j = 1,2,..., n)$. Then the objective function will be

$$Min\ Z_1 = \sum_{j=1}^{10} C_{Dj} x_j \ , \ Min\ Z_2 = \sum_{j=1}^{10} S_{Fj} x_j \ , \ Min\ Z_3 = \sum_{j=1}^{10} C_{dj} x_j$$

The constraints of the model satisfy the nutrients requirements. The nutrient contents of the food items in respect to the diet concerning nutrients are represented on the left-hand side of the constraints, and the right-hand side of the constraint is lower and upper demand of each nutrient (Protein, Vitamin B$_6$, Vitamin C, and Calcium). The upper requirement of Saturated Fat also works as a constraint. Then the constraints are as follow:

$$\sum_{j=1}^{n} P_j x_j \geq P_{Min} \ , \ \sum_{j=1}^{n} P_j x_j \leq P_{Max} \quad ; \text{for Protein}$$

$$\sum_{j=1}^{n} V_{Bj} x_j \geq V_{BMin} \ , \ \sum_{j=1}^{n} V_{Bj} x_j \leq V_{BMax} \quad ; \text{for Vitamin B}_6$$

$$\sum_{j=1}^{n} V_{Cj} x_j \geq V_{CMin} \ , \ \sum_{j=1}^{n} V_{Cj} x_j \leq V_{CMax} \quad ; \text{for Vitamin C}$$

$$\sum_{j=1}^{n} C_{lj} x_j \geq C_{lMin} \ , \ \sum_{j=1}^{n} C_{lj} x_j \leq C_{lMax} \quad ; \text{for Calcium}$$

$$\sum_{j=1}^{n} S_{Fj} x_j \leq S_{FMax} \quad ; \text{for Saturated Fat}$$

$$x_j \geq 0, \quad x_j \leq 4, \quad x_j \in \text{Integer} \quad \forall j = 1, 2,..., n$$

III. Procedure for Solving Multi-Objective Problem

Fuzzy GP is flexible and powerful techniques that can be applied to a variety of decision-making problems that have multiple objectives. Therefore, we can use this approach to obtain the optimal compromise solution for the formulated models. The stepwise solution procedure is given as follows:

Step 1: Solve the multiple objective problems by considering a single objective at a time and ignoring the others with the given set of constraints. The solution thus obtained is the idle solution. The payoff matrix constructs using idle solutions. Finally, the payoff matrix helps to construct the aspiration level to each objective function.

Step 2: The aspiration level of the objective function is set as the goal value $\left(g_k, k = 1, 2, 3 \right)$.

Find $X = (x_1, x_2, ..., x_n)$ to optimize the following fuzzy goals

$$Z_1(X) \precsim g_1, \ Z_2(X) \precsim g_2, Z_3(X) \precsim g_3$$

Subject to the constraint

$$\sum_{j=1}^{10} P_j x_j \geq P_{Min} , \ \sum_{j=1}^{10} P_j x_j \leq P_{Max}, \sum_{j=1}^{10} V_{Bj} x_j \geq V_{BMin} , \ \sum_{j=1}^{10} V_{Bj} x_j \leq V_{BMax}$$

$$\sum_{j=1}^{10} V_{Cj} x_j \geq V_{CMin} , \ \sum_{j=1}^{10} V_{Cj} x_j \leq V_{CMax}, \sum_{j=1}^{10} C_{lj} x_j \geq C_{lMin} , \ \sum_{j=1}^{10} C_{lj} x_j \leq C_{lMax}$$

$$\sum_{j=1}^{n} S_{Fj} x_j \leq S_{FMax} \quad x_j \geq 0, \quad x_j \leq 4 \quad \forall j = 1, 2, ..., 10$$

where, $\left(g_1 \right) = Min \left(Z_1(x) \right) \left(g_2 \right) = Min \left(Z_2(x) \right)$ and $\left(g_3 \right) = Min \left(Z_3(x) \right)$. The symbol '$\precsim$' (the type of fuzzy-min) referring to that $Z_1(X), Z_2(X)$ and $Z_3(X)$ should be approximately less than or equal to the aspiration level g_1, g_2 and g_3 up to the specified tolerance limit.

Step 3: Construct the fuzzy linear membership function the membership function of the fuzzy goal of $Z_1(X) \precsim g_1$ (*i.e.*, fuzzy-min) as:

$$\mu_1(Z_1(X)) = \begin{cases} 1, & if \ Z_1(X) \leq g_1 \\ \dfrac{U_1 - Z_1(X)}{U_1 - g_1}, & if \ g_1 \leq Z_1(X) \leq U_1 \\ 0, & if \ Z_1(X) \geq U_1 \end{cases}$$

where, the upper tolerance limit for the fuzzy goal $Z_1(x)$ is U_1 .

Similarly, the membership function for the fuzzy goal $Z_2 \precsim g_2$ (*i.e.*, fuzzy-min)

$$\mu_2(Z_2(X)) = \begin{cases} 1, & if \ Z_2(X) \leq g_2 \\ \dfrac{U_2 - Z_2(X)}{U_2 - g_2}, & if \ g_2 \leq Z_2(X) \leq U_2 \\ 0, & if \ Z_2(X) \geq U_2 \end{cases}$$

where, the upper tolerance limit for the fuzzy goal $Z_2(x)$ is U_2 .

Similarly, the membership function for the fuzzy goal $Z_3 \precsim g_3$ (*i.e.*, fuzzy-min)

$$\mu_3(Z_3(X)) = \begin{cases} 1, & if \ Z_3(X) \le g_3 \\ \dfrac{U_3 - Z_3(X)}{U_3 - g_3}, & if \ g_3 \le Z_3(X) \le U_3 \\ 0, & if \ Z_3(X) \ge U_3 \end{cases}$$

Where the upper tolerance limit for the fuzzy goal $Z_3(x)$ is U_3.

Step 4: Finally, the mathematical form of all the above-given steps are summarised as:

$$Max \ D(\mu) = \mu_1(Z_1(X)) + \mu_2(Z_2(X)) + \mu_3(Z_3(X))$$

subject to constraint

$$\sum_{j=1}^{10} P_j x_j \ge P_{Min} \ , \ \sum_{j=1}^{10} P_j x_j \le P_{Max}, \sum_{j=1}^{10} V_{Bj} x_j \ge V_{BMin} \ , \ \sum_{j=1}^{10} V_{Bj} x_j \le V_{BMax}$$

$$\sum_{j=1}^{10} V_{Cj} x_j \ge V_{CMin} \ , \ \sum_{j=1}^{10} V_{Cj} x_j \le V_{CMax}, \sum_{j=1}^{10} C_{lj} x_j \ge C_{lMin} \ , \ \sum_{j=1}^{10} C_{lj} x_j \le C_{lMax}$$

$$\mu_1(Z_1(X)) = \frac{U_1 - Z_1(X)}{U_1 - g_1}, \ 0 \le \mu_1(Z_1(X)) \le 1, \mu_2(Z_2(X)) = \frac{U_2 - Z_2(X)}{U_2 - g_2}, 0 \le \mu_2(Z_2(X)) \le 1$$

$$\mu_3(Z_3(X)) = \frac{U_3 - Z_3(X)}{U_3 - g_3}, 0 \le \mu_3(Z_3(X)) \le 1, x_j \ge 0, \quad x_j \le 4, \quad x_j \in Integer \quad \forall j = 1, 2, ..., n$$

$D(\mu)$ is called the fuzzy achievement function. Finally, we have a single objective problem that can be solved by using a suitable classical optimization technique.

IV. Numerical case study

A diet is required to propose by the dietician for the special needs of the patient. An integer number of units of the diet can be composed as ten basic foodstuffs termed as Food 1, Food 2, …, Food 10. The values of protein, vitamin C, vitamin B6, saturated fat and calcium ideally fall between the bounds which are given in Table 2. The data is taken from Bhargava et al. [12].

Table 2: Nutritional and cost of the foodstuffs

Nutritions	Food Types										Daily Demand	
	1	2	3	4	5	6	7	8	9	10		
Protein (g)	3.3	25.5	2.5	11.0	27.3	3.3	1.2	1.2	2.6	0.4	40.0	15.0
Vit B₆ (mg)	0.06	0.10	0.02	0.22	0.29	0.11	0.29	0.05	0.07	0.06	1.0	2.0
Vit C (mg)	1	0	0	0	0	44	11	7	10	6	50	100
Calcium(mg)	120	720	11	35	7	40	6	20	18	4	700	1000
Sat. Fat (g)	1.0	21.7	0.6	0.4	5.2	0.2	0.1	0.1	0.3	0.0	-	15
Carbohydrates (g)	5.0	0.1	0.0	75.7	0.0	1.1	23.2	2.6	30.9	11.8		
Cost (Rs.)	2.5	15.0	3.3	1.8	20.0	2.5	1.5	6.0	1.5	1.6		

The bounds for the three objective functions are as: $29.9 \le Z_1 \le 54.5,\ 5.7 \le Z_2 \le 7.8,$ and $161.3 \le Z_3 \le 366.7.$ Using these bounds, the corresponding linear membership functions for the three objective functions are constructed as follows:

$$\mu_1(Z_1(X)) = \begin{cases} 1, & \text{if } Z_1(X) \leq 29.9 \\ \dfrac{54.5 - Z_1(X)}{54.5 - 29.9}, & \text{if } 29.9 \leq Z_1(X) \leq 54.5 \\ 0, & \text{if } Z_1(X) \geq 54.5 \end{cases}$$

$$\mu_2(Z_2(X)) = \begin{cases} 1, & \text{if } Z_2(X) \leq 5.7 \\ \dfrac{7.8 - Z_2(X)}{7.8 - 5.7}, & \text{if } 5.7 \leq Z_2(X) \leq 7.8 \\ 0, & \text{if } Z_2(X) \geq 7.8 \end{cases}$$

$$\mu_3(Z_3(X)) = \begin{cases} 1, & \text{if } Z_3(X) \leq 161.3 \\ \dfrac{366.7 - Z_3(X)}{366.7 - 161.3}, & \text{if } 161.3 \leq Z_3(X) \leq 366.7 \\ 0, & \text{if } Z_3(X) \geq 366.7 \end{cases}$$

Using the method defines in Section 3; we calculate the compromise solution for the model, which is given in table 3.

Table 3: Compromise solution

Objective Values	The optimal number of quantities of each Foodstuff
Z_1=33.0, Z_2=6.9, Z_3=251.9	x_1=4, x_2=0, x_3=2, x_4=3, x_5=0, x_6=2, x_7=0, x_8=1, x_9=0, x_{10}=0

This solution is accepted by the DM, which belongs to the preferred compromise solution of fuzzy acceptance rate 0.620488. The membership values with the percentile contribution of each objective are shown in Fig. 1.
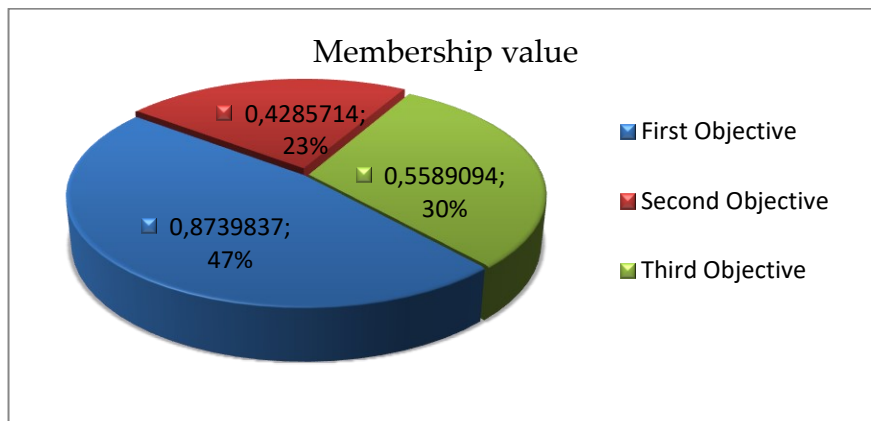
Fig. 1: Membership values of the objective with percentile contribution

Table 4: Comparison with weighted, pre-emptive and fuzzy gp

Method	Units of Foodstuff											Nutrition Quantity					Cost
	1	2	3	4	5	6	7	8	9	10	P	C_d	S_{Fl}	V_B	V_C	C_l	
Weighted GP	4	0	3	2	0	1	0	3	3	0	57.4	273.0	8.0	1.21	99	737	48.5
Pre-emptive GP	4	0	0	3	0	1	0	4	0	0	54.3	258.6	5.8	1.21	76	705	41.9
Fuzzy GP	4	0	2	3	0	2	0	1	0	0	59.0	251.9	6.9	1.21	99	707	33.0

The optimal compromise values of each foodstuffs with Weighted, Pre-emptive and Fuzzy GP are shown in Fig. 2.

Compromise optimal units of each foodstuff

	Food 1	Food 2	Food 3	Food 4	Food 5	Food 6	Food 7	Food 8	Food 9	Food 10
WGP	4	0	3	2	0	1	0	3	3	0
PGP	4	0	0	3	0	1	0	4	0	0
FGP	4	0	2	3	0	2	0	1	0	0
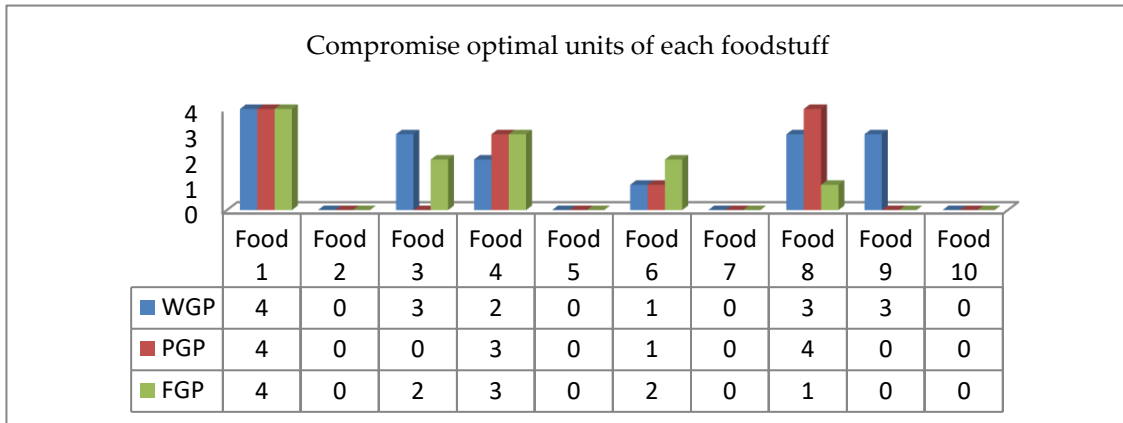
Fig 2: Compromise optimal unit for foodstuff

The comparison of membership values of each objective solved by Pre-emptive and Fuzzy GP are shown in Fig. 3.

Membership Values

	Carbohydrate	Saturated Fat	Total Cost
PGP	0,5121951	0,952381	0,5262902
FGP	0,8739837	0,4285714	0,5589094
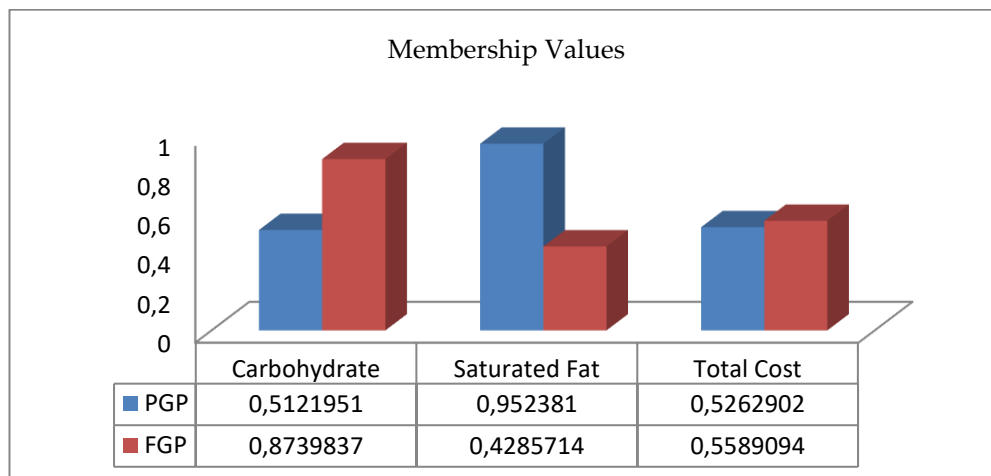
Fig 3: Graphical representation of membership values

V. Conclusion

The human body needs foods with a low content of Saturated Fat and Carbohydrate, although high in Protein, Vitamin B_6, Vitamin C, and Calcium. The multi-objective daily diet model is solved by using pre-emptive and fuzzy GP to satisfy daily nutrients through an example. We have designed the objective function as minimizing the total cost of the diet, Saturated Fat and carbohydrate. We use this approach to select diets and meet precise nutritional requirements. The comparison for the daily diet plan with weighted GP, pre-empty GP and fuzzy GP is also shown. The finding obtained in the fuzzy programming approach has been contrasted with the weighted GP approach and the pre-emptive GP approach, and it demonstrates that the fuzzy GP approach gives a more precise and accurate solution and is a useful technique.

References

[1] Smith, V. E. (1959). Linear programming models for the determination of palatable human diets. *Journal of Farm Economics*, *41*(2), 272-283.

[2] Anderson, A. M., & Earle, M. D. (1983). Diet planning in the third world by linear and goal programming. *Journal of the Operational Research Society*, *34*(1), 9-16.

[3] A. Charnes, & Cooper, W. W. (1961). *Management Models and Industrial Applications of linear programming*. J. Wiley.

[4] Ignizio, J. P. (1976). Goal Programming and Extensions Lexington Books. *Toronto: DC Health and Company*.

[5] Eghbali, H., Abdoos, E., Ashtiani, S., & Ahmadvand, M. (2013). Modelling the optimal diet problem for renal patients with fuzzy analysis of nutrients. *International Journal of Management and Fuzzy Systems*, *1*(1), 7-14.

[6] Nath, T., & Talukdar, A. (2014). Linear programming technique in fish feed formulation. *International Journal of Engineering Trends and Technology*, *11*(17), 132-135.

[7] Eghbali, H., Eghbali, M. A., & Kamyad, A. V. (2012). Optimizing human diet problem based on price and taste using multi-objective fuzzy linear programming approach. *An International Journal of Optimization and Control: Theories & Applications (IJOCTA)*, *2*(2), 139-151.

[8] Mamat, M., Zulkifli, N. F., Deraman, S. K., & Noor, N. M. M. (2012). Fuzzy linear programming approach in balance diet planning for eating disorder and disease-related lifestyle. *Applied Mathematical Sciences*, *6*(103), 5109-5118.

[9] Eghbali-Zarch, M., Tavakkoli-Moghaddam, R., Esfahanian, F., Azaron, A., & Sepehri, M. M. (2017). A New Multi-objective Optimization Model for Diet Planning of Diabetes Patients under Uncertainty. *Health Education and Health Promotion*, *5*(3), 37-55.

[10] Sheng, L. Z., & Sufahani, S. (2018, April). Optimal Diet Planning for Eczema Patient Using Integer Programming. In *Journal of Physics: Conference Series* (Vol. 995, No. 1, p. 012049). IOP Publishing.

[11] Ali, M., Sufahani, S., & Ismail, Z. (2016). A new diet scheduling model for Malaysian school children using zero-one optimization approach. *Global Journal of Pure and Applied Mathematics*, *12*(1), 413-419.

[12] Bhargava, A. K., Bansal, D., Chandramouli, A. B., & Kumar, A. (2011). Weighted Goal Programming Model Formulation and Calculation of Diet Planning. *International Transactions in Mathematical Sciences & Computer*, *4*(1).

[13] Decerle, J., Grunder, O., El Hassani, A. H., & Barakat, O. (2019). A memetic algorithm for multi-objective optimization of the home health care problem. *Swarm and evolutionary computation*, *44*, 712-727.

[14] Nguyen, T. V. L., & Montemanni, R. (2013). Scheduling and routing in-home health care service. In *Society 40th Anniversary Workshop–FORS40* (p. 52).

[15] En-nahli, L., Allaoui, H., & Nouaouri, I. (2015). Multi-objective modelling to human resource assignment and routing problem for home health care services. *IFAC-PapersOnLine*, *48*(3), 698-703.

[16] Mutingi, M., & Mbohwa, C. (2013, July). A home healthcare multi-agent system in a multi-objective environment. In *25th Annual Conf of the SAIIE* (pp. 1-10).

[17] Niakan, F., & Rahimi, M. (2015). A multi-objective healthcare inventory routing problem; a fuzzy possibilistic approach. *Transportation Research Part E: Logistics and Transportation Review*, *80*, 74-94.

[18] Othman, S. B., Hammadi, S., & Quilliot, A. (2015). Multi-objective evolutionary for multi-skill health care tasks scheduling. *IFAC-PapersOnLine*, *48*(3), 704-709.

[19] Turgay, S., & Taşkın, H. (2015). Fuzzy goal programming for health-care organization. *Computers & Industrial Engineering*, *86*, 14-21.

[20] Zhang, W., Cao, K., Liu, S., & Huang, B. (2016). A multi-objective optimization approach for health-care facility location-allocation problems in highly developed cities such as Hong Kong. *Computers, Environment and Urban Systems*, *59*, 220-230.

Inverse Ishita Distribution: Properties and Applications

Kamlesh Kumar Shukla

•

Department of Community Medicine, NIIMS, Noida
International University, Greater Noida, India
Email: kkshukla22@gmail.com

Abstract

In this paper, new lifetime distribution has been proposed which is an inverse of Ishita distribution Shanker and Shukla (2017). Its statistical and mathematical properties including Reneyi entropy and Stress-strength reliability measure have been discussed. Maximum likelihood estimation method has been used to estimate its parameter. Simulation study has also been carried out to check the behavior of maximum likelihood estimator. Finally, proposed distribution has been applied on lifetime datasets and compares its superiority over other inverse lifetime distributions.

Keywords: Inverse distribution, Stress-strength Reliability, Maximum likelihood estimation

I. Introduction

Shanker and Shukla (2017) proposed a one parameter lifetime distribution with the following probability density function (pdf) and cumulative distribution function (cdf) respectively:

$$f_1(y;\theta) = \frac{\theta^3}{\theta^3+2}\left(\theta+y^2\right)e^{-\theta x} \quad ; y > 0,\ \theta > 0 \tag{1.1}$$

$$F_1(y;\theta) = 1 - \left[1 + \frac{\theta y(\theta y + 2)}{(\theta^3+2)}\right]e^{-\theta y} \quad ; y > 0, \theta > 0 \tag{1.2}$$

This distribution is known as the Ishita distribution. The mathematical and statistical properties including its parameter estimation can be shown in Shanker and Shukla (2017). It's important applications from biological and engineering data have been described in their paper, and its superiority have been discussed over other one parameter life time classical distributions such as Lindley, Exponential distribution. Shukla (2019) has discussed and compared specially one parameter lifetime distribution including Lindley and Ishita distribution from Biological, Engineering, Agricultural and demographic data[2]. Lindley distribution proposed by Lindley (1958) and its pdf and cdf are defined respectively by

$$f_2(y;\theta) = \frac{\theta^2}{\theta+1}\left(1+y\right)e^{-\theta y} \quad ; y > 0,\ \theta > 0 \tag{1.3}$$

$$F_2(y;\theta) = 1 - \left[1 + \frac{\theta y}{(\theta+1)}\right]e^{-\theta y} \quad ; y > 0, \theta > 0 \tag{1.4}$$

Detailed about its mathematical and statistical properties including hazard rate and application from lifetime data have been discussed by Gitany et al (2008). The inverse Lindley distribution has been proposed by Sharma et al (2015) which is an inverse of Lindley distribution (ILD). It can be shown its important statistical properties, stress and strength reliability measure including its stress and strength parameter estimation method on real lifetime data in their paper. Its pdf and cdf are given respectively by

$$f_3(x;\theta) = \frac{\theta^2}{(\theta+1)x^3}(1+x)e^{-x/\theta} \quad ; x > 0, \ \theta > 0 \tag{1.5}$$

$$F_3(x;\theta) = 1 + \frac{\theta/x}{(\theta+1)}e^{-x/\theta} \quad ; x > 0, \theta > 0 \tag{1.6}$$

In another study, Keller and Kamath (1982) introduced Inverse exponential distribution (IED) and it has been studied and discussed as a lifetime model. Its pdf and cdf are given respectively by

$$f_4(x;\theta) = \frac{\theta}{x^2}e^{-x/\theta} \quad ; x > 0, \ \theta > 0 \tag{1.7}$$

$$F_4(x;\theta) = e^{-x/\theta} \quad ; x > 0, \theta > 0 \tag{1.8}$$

The main motivation of this paper is to introduce a new life time distribution are:

(i) It is observed that Ishita distribution is more flexible distribution than Lindley and exponential distribution especially for biological data.

(ii) Inverse of Ishita distribution would also be more flexible and gives good fit over Inverse Lindley distribution as well as exponential distribution.

The study has been divided into twelve sections, introduction of proposed study are discussed in the first section. Inverse Ishita distribution has been defined in the second section. Survival and hazards rate function are discussed in third section. Moment has been derived in fourth section. In the fifth section, stochastic ordering has been discussed. Reneyi Entropy measure has been discussed in sixth section. Order statistics of proposed distribution has been discussed in seventh section. Stress-Strength reliability measure has been derived in the eighth section. Maximum likelihood estimation method has been derived for estimation parameter of proposed distribution in ninth section. Simulation study for proposed distribution has been carried out in the tenth section. In the eleventh section, application of proposed distribution on real lifetime data has been presented. Conclusions have been given in the last section.

II. Inverse Ishita distribution

If a random variable Y has an Ishita distribution, the variable $X = \dfrac{1}{Y}$ will have an Inverse Ishita distribution (IID) of equation (1.1). A random variable X is said to have an Inverse Ishita distribution with scale parameter θ and its pdf and cdf are defined respectively by;

$$f_5(x;\theta) = \frac{\theta^3}{(\theta^3+2)x^4}(1+\theta x^2)e^{-\theta/x} \quad ; x > 0, \ \theta > 0 \tag{2.1}$$

$$F_5\left(x;\theta\right)=1+\frac{\dfrac{\theta}{x}\left(\dfrac{\theta}{x}+2\right)}{\left(\theta^3+2\right)}e^{-\theta/x}\ ;x>0,\theta>0 \tag{2.2}$$

The behavior of proposed distribution for varying value of θ has been presented in figure1. It is observed from figure1 that pdf of IID is decreasing as increased value of parameter θ
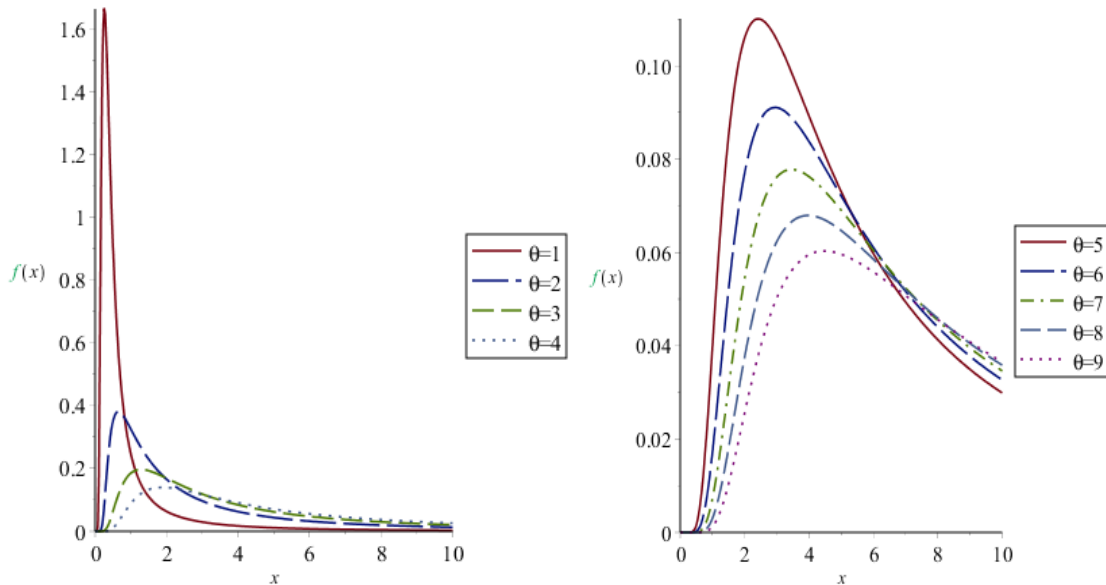
Figure1. *pdf of IID for varying value of* θ

III. Survival and Hazards function

Survival function $S\left(x;\theta\right)$ of IID can be defined as

$$S\left(y;\theta\right)=1-F_5(y;\theta)$$

$$S\left(x;\theta\right)=1-\left(1+\frac{\dfrac{\theta}{x}\left(\dfrac{\theta}{x}+2\right)}{\left(\theta^3+2\right)}\right)e^{-\theta/x}\ ;x>0,\theta>0$$

And hazard function $h\left(x;\theta\right)$ of IID can be defined as

$$h\left(x;\theta\right)=\frac{f_5(x;\theta)}{S(x;\theta)}$$

$$h\left(x;\theta\right)=\frac{\theta^3\left(1+\theta x^2\right)e^{-\theta/x}}{\left[x^2(\theta^3+2)-\left(x^2(\theta^3+2)+2\theta x+\theta^2\right)e^{-\theta/x}\right]}$$

The nature of survival and hazard function of IID for varying value of parameter θ are presented in figure2&3 respectively. Hazard function of IID distribution is also uni-model in x, and achieves its maxi-mum value at x_0. The turning point (x_0) of hazard function can be obtained as the solution of the following equation.

$$x_0(\theta^3+2)e^{\frac{\theta}{x_0}}\left(\frac{x_0^2\theta^2}{2}-\theta x_0^3+\frac{\theta}{2}-2x_0\right)+\theta x_0^4(\theta^3+2)+\theta^2 x_0^3$$

$$+2x_0^2(\theta^3+2)+3x_0\theta+\theta^2=0$$
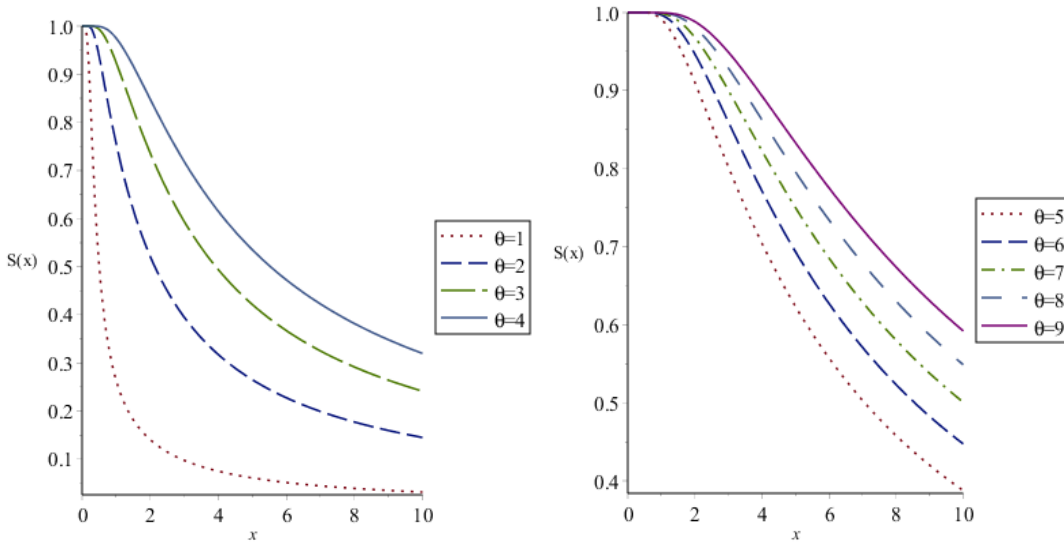
Figure2. *Survival function of IID for varying value of* θ
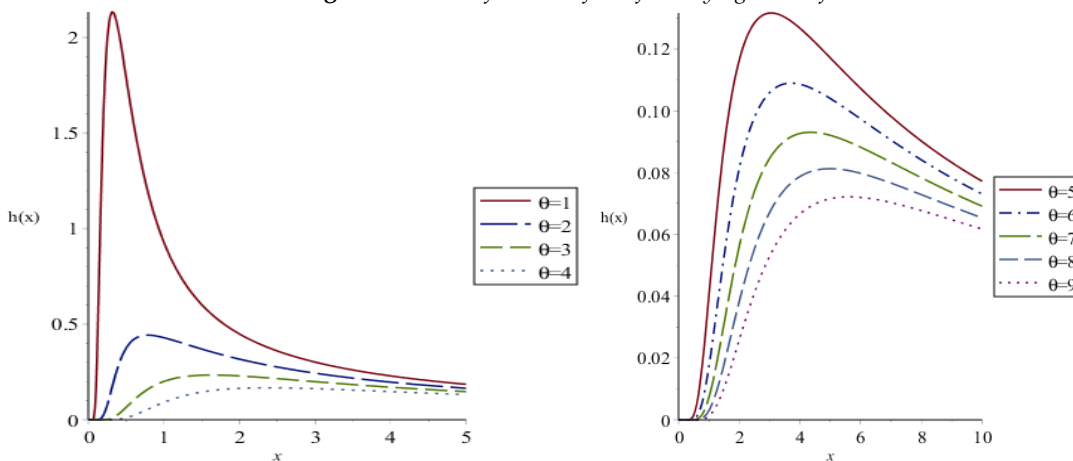
Figure3. *Hazard function of IID for varying value of* θ

IV. Moments

Moments of a distribution are used to study the most important characteristics of the distribution including mean, variance, skewness, kurtosis, etc. The r th moment about origin μ_r' of IID can be expressed in explicit expression in terms of complete gamma functions.

Theorem1: Suppose Y_i follows IID (θ). Then the r th moment about origin μ_r' of IID is

$$\mu_r' = \frac{\gamma(3-r)}{\theta^{-r}\left[(\theta^3+2)\right]} ; r \leq 2 \tag{4.1}$$

Considering (2.1), we have

$$\mu_r' = \int_0^\infty x^r \cdot \frac{\theta^3}{(\theta^3+2)x^4}(\theta x^2+1)e^{-\theta/x}dx$$

$$= \frac{\theta^3}{(\theta^3+2)}\left[\theta\int_0^\infty x^{r-2}e^{-\theta/x}dx + \int_0^\infty x^{r-4}e^{-\theta/x}dx\right]$$

$$= \frac{\theta^3}{(\theta^3+2)}\left[\theta\int_0^\infty x^{r-1-1}e^{-\theta/x}dx + \int_0^\infty x^{r-3-1}e^{-\theta/x}dx\right] \qquad (4.2)$$

Using inverse gamma function $\int_0^\infty y^{n-\alpha-1}e^{-\theta/y}dy = \frac{\gamma(\alpha-n)}{\theta^{\alpha-n}}$, (4.2) can be written as

$$\mu_r' = \frac{\gamma(3-r)}{\theta^{-r}\left[(\theta^3+2)\right]} \qquad (4.3)$$

It will exist if $r \le 2$, therefor only mean and Variance can be calculated substituting $r = 1,2$ in (4.3)

Mean and Variance are $\dfrac{\theta}{(\theta^3+2)}$, $\dfrac{\theta^2(\theta^3+1)}{(\theta^3+2)^2}$

Moments (4.3) does not exist at $r > 2$, therefore only coefficient of variance and Index of dispersion can be calculated of IID, which are $\sqrt{(\theta^3+1)}$ and (θ^3+1) respectively. Natures of mean and variance of IID are presented in figure5:
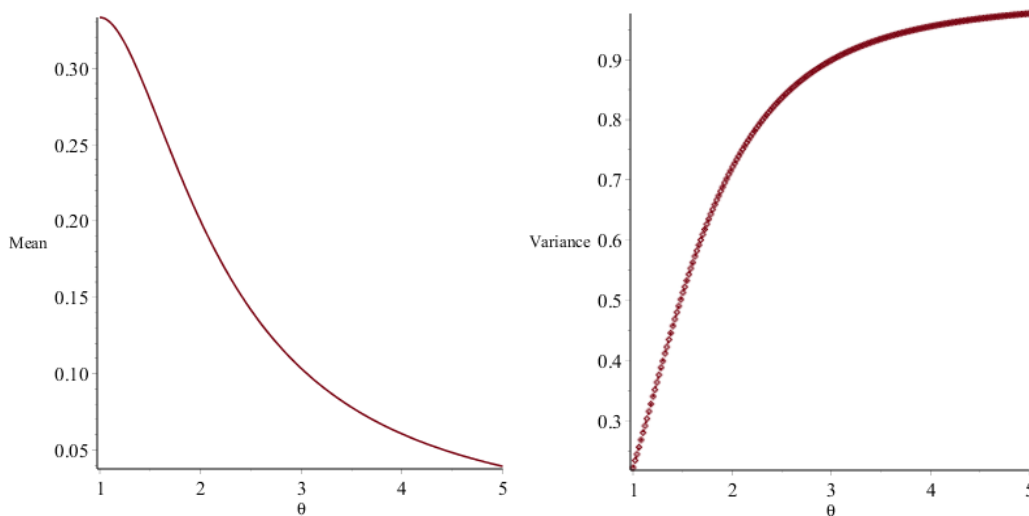
Figure4. *Mean Variance of IID for varying value of* θ

V. Stochastic Ordering

Stochastic ordering of positive continuous random variables is an important tool for judging their comparative behavior. A random variable X is said to be smaller than a random variable Y in the

(i)   stochastic order $(X \le_{st} Y)$ if $F_X(x) \ge F_Y(x)$ for all x

(ii)   hazard rate order $(X \le_{hr} Y)$ if $h_X(x) \ge h_Y(x)$ for all x

(iii)   mean residual life order $\left(X \leq_{mrl} Y \right)$ if $m_X \left(x \right) \leq m_Y \left(x \right)$ for all x

(iv)   likelihood ratio order $\left(X \leq_{lr} Y \right)$ if $\dfrac{f_X \left(x \right)}{f_Y \left(x \right)}$ decreases in x.

The following results due to Shaked and Shanthikumar(1994) are well known for establishing stochastic ordering of distributions

$$X \leq_{lr} Y \Rightarrow X \leq_{hr} Y \Rightarrow X \leq_{mrl} Y \tag{5.1}$$

$$\underset{X \leq_{st} Y}{\Downarrow}$$

The IID is ordered with respect to the strongest 'likelihood ratio ordering' as shown in the following theorem:

Theorem2: Let X and $Y \sim \text{IID}\left(\theta_1 \right)$ and $\left(\theta_2 \right)$ respectively. If $\theta_1 > \theta_2$ then $X \leq_{lr} Y$ and hence $X \leq_{hr} Y$, $X \leq_{mrl} Y$ and $X \leq_{st} Y$.

Proof: We have

$$\frac{f_X(x)}{f_Y(x)} = \frac{\theta_1^3 \left(\theta_2^3 + 2 \right)}{\theta_2^3 \left(\theta_1^3 + 2 \right)} \left(\frac{\theta_1 x^2 + 1}{\theta_2 x^2 + 1} \right) e^{-(\theta_1 - \theta_2)/x} \quad ; \ x > 0$$

Now

$$\log \frac{f_X(x)}{f_Y(x)} = \log \left| \frac{\theta_1^3 \left(\theta_2^3 + 2 \right)}{\theta_2^3 \left(\theta_1^3 + 2 \right)} \right| + \log \left(\frac{\theta_1 x^2 + 1}{\theta_2 x^2 + 1} \right) - \left(\theta_1 - \theta_2 \right) / x.$$

.

This gives $$\frac{d}{dx} \log \frac{f_X(x)}{f_Y(x)} = \frac{2x(\theta_1 - \theta_2)}{(\theta_2 x^2 + 1)^2} + \frac{(\theta_1 - \theta_2)}{x^2}$$

$$\frac{d}{dx} \log \frac{f_X(x)}{f_Y(x)} = \frac{(2x+1)(\theta_1 - \theta_2)}{x^2 (\theta_2 x^2 + 1)^2} > 0, \ for \theta_1 > \theta_2$$

Thus if $\theta_1 > \theta_2$, $\dfrac{d}{dx} \log \dfrac{f_X(x)}{f_Y(x)} > 0$. This means that $X \leq_{lr} Y$ and hence $X \leq_{hr} Y$, $X \leq_{mrl} Y$ and $X \leq_{st} Y$.

VI.   Order Statistics

Let $X_1, X_2, ..., X_n$ be a random sample of size n from IID (2.1). Let $X_{(1)} < X_{(2)} < ... < X_{(n)}$ denote the corresponding order statistics. The p.d.f. and the c.d.f. of the k th order statistic, say $Y = X_{(k)}$ are given by

$$f_Y \left(y \right) = \frac{n!}{(k-1)!(n-k)!} F^{k-1} \left(y \right) \left\{ 1 - F \left(y \right) \right\}^{n-k} f \left(y \right)$$

$$= \frac{n!}{(k-1)!(n-k)!} \sum_{l=0}^{n-k} \binom{n-k}{l} (-1)^l F^{k+l-1} \left(y \right) f \left(y \right)$$

and

$$F_Y(y) = \sum_{j=k}^{n} \binom{n}{j} F^j(y) \{1 - F(y)\}^{n-j}$$

$$= \sum_{j=k}^{n} \sum_{l=0}^{n-j} \binom{n}{j} \binom{n-j}{l} (-1)^l F^{j+l}(y),$$

respectively, for $k = 1, 2, 3, ..., n$.

Thus, the pdf and the cdf of k th order statistics of IID are obtained as

$$f_Y(y) = \frac{n!\theta^3 (1 + \theta x^2) e^{-\theta/x}}{(\theta^3 + 2)(k-1)!(n-k)!} \sum_{l=0}^{n-k} \binom{n-k}{l} (-1)^l \times \left[1 + \frac{\theta/x(\theta/x+2)}{\theta^3 + 2} e^{-\theta/x}\right]^{k+l-1}$$

and

$$F_Y(y) = \sum_{j=k}^{n} \sum_{l=0}^{n-j} \binom{n}{j} \binom{n-j}{l} (-1)^l \left[1 + \frac{\theta/x(\theta/x+2)}{\theta^3 + 2} e^{-\theta/x}\right]^{j+l}$$

VII.   Renyi Entropy

An entropy of a random variable X is a measure of variation of uncertainty. A popular entropy measure is Renyi (1961). If X is a continuous random variable having probability density function $f(.)$, then Renyi entropy is defined as

$$T_R(\gamma) = \frac{1}{1-\gamma} \log \left\{ \int f^\gamma(x) dx \right\}$$

where $\gamma > 0$ and $\gamma \neq 1$.

Thus, the Renyi entropy of IID(2.1) can be obtained as

$$T_R(\gamma) = \frac{1}{1-\gamma} \log \left[\int_0^\infty \frac{\theta^{3\gamma}}{(\theta^3 + 2)^\gamma} (1 + \theta x^2)^\gamma e^{-\theta\gamma/x} dx \right]$$

$$= \frac{1}{1-\gamma} \log \left[\int_0^\infty \frac{\theta^{3\gamma}}{(\theta^3 + 2)^\gamma} (1 + \theta x^2)^j e^{-\theta\gamma/x} dx \right]$$

$$= \frac{1}{1-\gamma} \log \left[\int_0^\infty \frac{\theta^{3\gamma}}{(\theta^3 + 2)^\gamma} \sum_{j=0}^\infty \binom{\gamma}{j} (\theta x^2)^j e^{-\theta\gamma/x} dx \right]$$

$$= \frac{1}{1-\gamma} \log \left[\sum_{j=0}^\infty \binom{\gamma}{j} \frac{\theta^{3\gamma+j}}{(\theta^3 + 2)^j} \int_0^\infty e^{-\theta\gamma/x} x^{2j+2-1-1} dx \right]$$

$$= \frac{1}{1-\gamma} \log \left[\sum_{j=0}^{\infty} \binom{\gamma}{j} \frac{\theta^{3\gamma+j}}{(\theta^3+2)^{\gamma}} \frac{\Gamma(-2j-1)}{(\theta\gamma)^{-2j-1}} \right]$$

VIII. Stress-strength Reliability

The stress- strength reliability describes the life of a component which has random strength X that is subjected to a random stress Y. When the stress applied to it exceeds the strength, the component fails instantly and the component will function satisfactorily till $X > Y$. Therefore, $R = P(Y < X)$ is a measure of component reliability and in statistical literature it is known as stress-strength parameter.

Let X and Y be independent strength and stress random variables having IID(2.1) with parameter (θ_1) and (θ_2) respectively. Then the stress-strength reliability R can be obtained as

$$R = P(Y < X) = \int_0^{\infty} P(Y < X \mid X = x) f_X(x) dx$$

$$= \int_0^{\infty} f(x;\theta_1) \, F(x;\theta_2) dx$$

$$= \int_0^{\infty} \frac{\theta_1^3}{(\theta_1^3+2)x^4} (1+\theta_1 x^2) e^{-\theta_1/x} \left(1 + \frac{\frac{\theta_2}{x}\left(\frac{\theta_2}{x}+2\right)}{(\theta_2^3+2)} \right) e^{-\theta_2/x} dx$$

Using inverse gamma function, it can be written as

$$R = \frac{\theta_1^3 \left[\begin{matrix} 2\theta_1\theta_2 (\theta_1+\theta_2)^3 + 2\theta_1 (\theta_1+\theta_2)^2 (\theta_2^3+\theta_2^2+2) \\ 12\theta_2(\theta_1+\theta_2) + 24(\theta_2^3+\theta_2^2+2) \end{matrix} \right]}{(\theta_1^3+2)(\theta_2^3+2)(\theta_1+\theta_2)^5}.$$

IX. Maximum Likelihood Estimation Method

Let $(x_1, x_2, x_3, \dots, x_n)$ be a random sample of size n from (2.1). The likelihood function, L of IID is given by

$$L = \left(\frac{\theta^3}{(\theta^3+2)} \right)^n \prod_{i=1}^n \frac{(\theta x_i^2+1)}{x^4} e^{-\sum_i \theta/x}$$

The log likelihood function is thus obtained as

$$\ln L = n \ln \left(\frac{\theta^3}{(\theta^3+2)} \right) + \sum_{i=1}^n \ln(\theta x_i^2+1) - \sum_{i=1}^n \ln(x_i^4) - \theta \sum_{i=1}^n (1/x_i)$$

the maximum likelihood estimate $\hat{\theta}$ of parameter θ is the solution of the log-likelihood equation $\frac{\partial \log L}{\partial \theta} = 0$. It is obvious that $\frac{\partial \log L}{\partial \theta} = 0$ will not be in closed form and hence some numerical optimization technique can be used e the equation for θ. In this paper the nonlinear method available in R software has been used to find the MLE of the parameter θ.

X. Simulation Study

 In this section, simulation study of proposed distribution has been carried out using acceptance and rejection method. To conduct simulation study, following steps have been follows: generate 1000 samples of size n = 20, 40, 60, 80 from the IID (2, 3, 4, and 5) compute the Bias and MSE using MLE (θ) and proposed value of parameter (θ)

Table1. *Average bias error (ABE) and Mean square error (MSE)of parameter*

n	Parameter (θ)	$\theta=2$		$\theta=3$		$\theta=4$		$\theta=5$	
		Bias	MSE	ABE	MSE	ABE	MSE	ABE	MSE
20	2	-0.02383	0.011362	-0.00135	3.63E-05	0.01573	0.00495	0.024822	0.01232
	3	-0.07383	0.109032	-0.05135	0.052731	-0.0342	0.02347	-0.02518	0.01267
	4	-0.12383	0.306701	-0.10135	0.205427	-0.0842	0.14200	-0.07518	0.11303
	5	-0.17383	0.604371	-0.15135	0.458122	-0.1342	0.36052	-0.12518	0.31339
40	2	-0.01157	0.005358	0.000535	1.15E-05	0.00947	0.00358	0.015616	0.00975
	3	-0.03657	0.053506	-0.02446	0.023940	-0.0155	0.00964	-0.00938	0.00352
	4	-0.06157	0.151654	-0.04946	0.097869	-0.0405	0.06570	-0.03438	0.04728
	5	-0.08657	0.299802	-0.07446	0.22179	-0.0655	0.17176	-0.05938	0.14105
60	2	-0.00932	0.005216	0.000379	8.62E-06	0.00682	0.00279	0.01061	0.0067
	3	-0.02599	0.04053	-0.01628	0.015917	-0.0098	0.00581	-0.00604	0.00219
	4	-0.04266	0.109177	-0.03295	0.06515	-0.0265	0.04216	-0.02271	0.03095
	5	-0.05932	0.211157	-0.04965	0.147734	-0.0431	0.11185	-0.03938	0.09305
80	2	0.007964	0.005074	0.000437	1.53E-05	0.00585	0.00274	0.008270	0.00547
	3	-0.00454	0.001646	-0.01206	0.011639	-0.0066	0.00353	-0.00422	0.00143
	4	-0.01704	0.023218	-0.02456	0.048264	-0.0191	0.02932	-0.01672	0.02238
	5	-0.02954	0.06979	-0.03706	0.109888	-0.0316	0.08012	-0.02922	0.06834

From the above table it is observed that most average bias errors are negative and it is decreasing as increased value of sample size.

XI. Application on real data

In this section, proposed distribution has been applied on two real datasets and compares with one parameter Inverse Lindley distribution (ILD) and Inverse Exponential distribution (IED).
 Goodness of fit has been decided using Akaike information criteria (AIC), Bayesian Information and criteria (BIC) values respectively, which are calculated for each distribution and also compared. As we know that best goodness of fit of the distribution can be decided on the basis of minimum value of AIC and BIC. Comparison of distributions is shown in table 2 as well as their fitted plots are presented in figure5&6. Table 2 shows that AIC & BIC of IID, ILD and IED (three distributions) have been calculated and compared, and it is observed that IID has minimum value of AIC and BIC in comparison   to ILD and IED. It can be say that it is good model and can be considered for life time data. From the figure 5&6, it can be seen that expected value of IID is much closed to probability of observed value on both the data sets in comparison to ILD and IED.
Data set 1: This data set represents remission times (in months) of a random sample of 128 bladder cancer patients reported in Lee and Wang (2003)
0.08,2.09,3.48,4.87,6.94,8.66,13.11,23.63,0.20,2.23,3.52,4.98,6.97,9.02,13.29,0.40,2.26,3.57,5.06,7.09,9.22,
13.80,25.74,0.50,2.46,3.64,5.09,7.26,9.47,14.24,25.82,0.51,2.54,3.70,5.17,7.28,9.74,14.76,6.1,0.81,2.62,3.82
,5.32,7.32,10.06,14.77,32.15,2.64,3.88,5.32,7.39,10.34,14.83,34.26,0.90,2.69,4.18,5.34,7.59
10.66,15.96,36.66,1.05,2.69,4.23,5.41,7.62,10.75,16.62,43.01,1.19,2.75,4.26,

5.41,7.63,17.12,46.12,1.26,2.83,4.33,5.49,7.66,11.25,17.14,79.05,1.35,2.87,5.62,7.87,11.64,17.36,1.40,3.02,
4.34,5.71,7.93,11.79,18.10,1.46,4.40,5.85,8.26

11.98,19.13,1.76,3.25,4.50,6.25,8.37,12.02,2.02,3.31,4.51,6.54,8.53,12.03,20.28,2.02,3.36,6.76,12.07,21.73,
2.07,3.36,6.93,8.65,12.63,22.69

Data Set 2: This data set is given by Linhart and Zucchini (1986)which represents the failure times of the air conditioning system of an airplane:

23, 261 ,87 ,7, 120, 14 ,62, 47 ,225, 71 ,246 ,21, 42 ,20, 5, 12, 120 ,11, 3, 14, 71 ,11, 14, 11, 16, 90, 1, 16 ,52, 95

Table 2: *MLE's, Standard Errors, - 2ln L, AIC and BIC of the fitted distributions for data set*

Data	Distribution	Parameter	$-2\ln L$	AIC	BIC
1	**IID**	$\theta = 2.9017$	**913.28**	**915.28**	**916.72**
	ILD	$\theta = 3.0857$	931.72	933.72	935.15
	IED	$\theta = 2.4799$	915.65	917.65	919.08
2	**IID**	$\theta = 11.1891$	**317.99**	**319.99**	**321.33**
	ILD	$\theta = 12.0387$	318.53	320.53	921.96
	IED	$\theta = 11.1798$	918.12	320.12	321.56
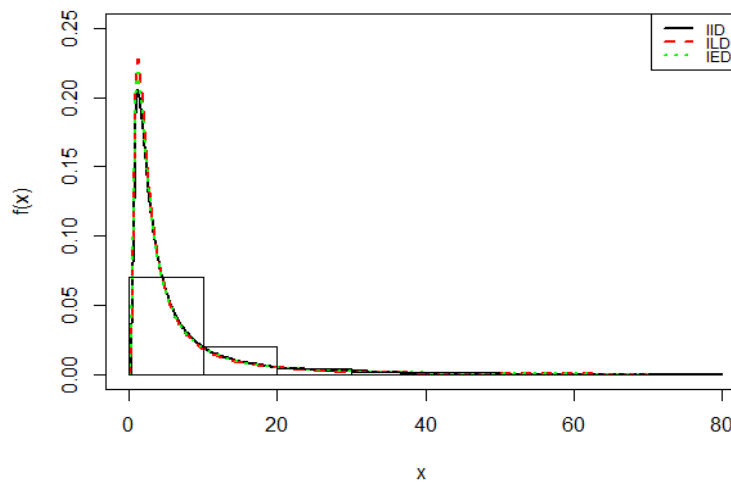
Figure 5. *Fitted plot of distributions for dataset-1*
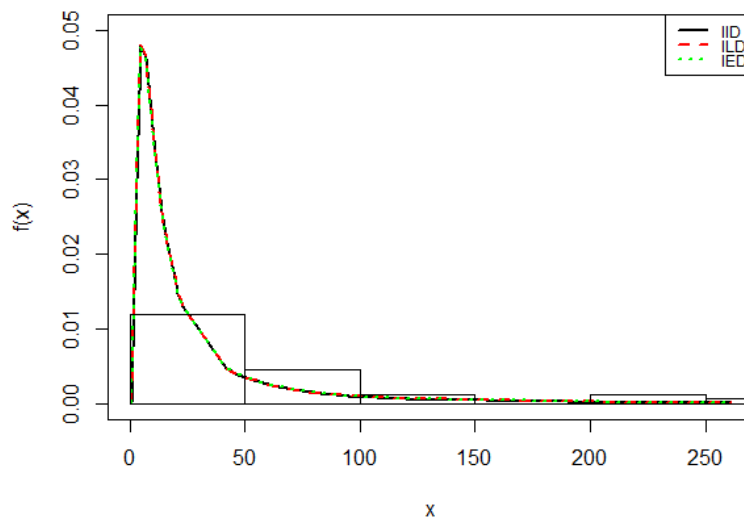
Figure6. *Fitted plot of distributions for dataset-2*

XII. Conclusions

A new lifetime distribution has been proposed. Statistical and mathematical properties including Renyi Entropy and Stress-Strength reliability have been derived. Simulation study of proposed distribution has been carried out to know the behavior of MLE estimate of parameter. Maximum Likelihood Estimation (MLE) Method has been used to estimate its parameter. The Proposed distribution has been applied on two real data sets and compare with two one parameter ILD and IED. It is observed from the table2 that IID gives better fit over both distributions on both the data sets.

Acknowledgement

References

[1] Ghitany, M.E., Atieh, B. and Nadarajah, S. (2008): Lidley distribution and its Application, Mathematics Computing and Simulation, 78, 493 – 506.

[2] Keller, A. Z., & Kamath, A. R. (1982). Reliability analysis of CNC machine tools. *Reliability Engineering*, 3, 449–473. doi:10.1016/0143-8174(82)90036-1

[3] Lee , ET and Wang JW. Statistical methods for survival data analysis, 3rd edition, John Wiley and Sons, New York, NY, USA, 2003.

[4] Lindley, D. V. (1958), Fiducial distributions and Bayes' theorem, Journal of the Royal Statistical Society, Series B, 20, 102- 107.

[5] Linhart, H. and Zucchini, W. Model Selection, John Wiley, New York, 1986.

[6] Renyi, A. (1961): On measures of entropy and information, in proceedings of the 4th Berkeley symposium on Mathematical Statistics and Probability, 1, 547 – 561, Berkeley, university of California press.

[7] Shaked, M. and Shanthikumar, J.G.(1994): Stochastic Orders and Their Applications, Academic Press, New York.

[8] Sharma, V. K., Singh, S. K., Singh, U., and Agiwal, V. (2015), The inverse Lindley distribution: a Stress-strength reliability model with application to head and neck cancer data, Journal of Industrial and Production Engineering, 2015 Vol. 32, No. 3, 162–173, ttp://dx.doi.org/10.1080/21681015.2015.1025901

[9] Shukla, K. K. (2019), A comparative study of one parameter distribution Biom & Biostats International J. 8(3),111-123.

[10] Shanker, R. and Shukla, K. K. (2017), "Ishita Distribution and its application to model lifetime data", Biometrics & Biostatistics International Journal,5(2),1-9

Identification of Failure Rate Behaviour of Increasing Convex (Concave) Transformations

[1]Deepthi K. S &[2]Chacko V. M

●

Department of Statistics,
St. Thomas' College (Autonomous), Thrissur, Kerala - 680 001 (India)
[1]dipthiks@gmail.com and [2]chackovm@gmail.com

Abstract

In this paper, increasing convex (concave) Total Time on Test (TTT) transform of a lifetime random variable is considered. In order to identify the failure rate model of functions of random variables, the TTT of transformed data can be used. Some properties of the transforms are derived. Some examples are given.

Keywords: Ageing patterns, Total Time on Test Transform, Increasing convex (concave) Total Time on Test transform

I. Introduction

The concept of the Total Time on Test (TTT) plots was first defined by Barlow and Campo (1975). The plots provide information about the identification of failure rate model. Incomplete type 2 censored data can be analysed using TTT transform. Aarset (1985) derived the exact distribution of TTT under the null hypothesis of exponentiality. Gupta and Michalek (1985) developed an explicit method to determine the reliability function by the TTT transform. Vera and Lynch (2005) introduced higher-order TTT transforms by applying definition of TTT recursively to the transformed distributions. Nair et. al (2008) studied the properties of TTT transform of order n and examined their applications in reliability analysis. Nair and Sankaran (2013) listed some known characterizations of common aging notions in terms of the total time on test transform (TTT) function. Franco-Pereira and Shaked (2013) derived two characterizations of the decreasing percentile residual life of order (DPRL(α)) aging notion in terms of the TTT function, and in terms of the observed TTT when X is observed. TTT statistic provide the central value of type 2 data. In order to get the dispersion values, we need the distributions of transformed variables.

The problem of identification of failure rate behavior of increasing convex (concave) transformation of random variable based on distributional properties of the variable is an unexplored one.

In this paper, we consider increasing convex (concave) Total Time on Test (ICXTTT (ICVTTT)) transform of a lifetime random variable. In section II, we provided TTT transform of increasing convex (concave) transformation of the random variable. Some general results about the ageing patterns are given in section III. In section IV, illustrative example is given.

II. Increasing Convex (Concave) TTT transform

In this section, we define ICXTTT (ICVTTT) transform. Given a sample of size n from the non-negative random variable (r.v.) X with distribution F, let $X_1 \leq X_2 \leq \ldots \leq X_k \leq \ldots \leq X_n$ be the order statistics corresponding to the sample. Total time test to the rth failure from distribution F is,

$$T(X_{(r)}) = nX_{(1)} + (n-1)(X_{(2)} - X_{(1)}) + \ldots + (n-r+1)(X_{(r)} - X_{(r-1)})$$

$$= \sum_{i=1}^{r} X_{(i)} + (n-r)X_{(r)}.$$

Let $H_n^{-1}\left(\frac{r}{n}\right) = \frac{1}{n}T(X_{(r)})$

$$H_n^{-1}\left(\frac{r}{n}\right) = \int_0^{F_n^{-1}\left(\frac{r}{n}\right)} (1 - F_n(u)) du.$$

The empirical distribution function defined in terms of the order statistics is

$$F_n(u) = \begin{cases} 0, & u < X_{(i)} \\ \frac{i}{n}, & X_{(i)} \leq u < X_{(i+1)} \\ 1 & X_{(n)} > u \end{cases}$$

If there exist an inverse function $F_n^{-1}(x) = \inf\{x : F_n(x) \geq u\}$. The fact that $F_n(u) \xrightarrow{a.s} F(u)$ almost surely (a.s.) implies, by Glivenko Cantelli Theorem,

$$\lim_{\substack{\frac{r}{n} \to t \\ n \to \infty}} \int_0^{F_0^{-1}\left(\frac{r}{n}\right)} (1 - F_n(u)) du = \int_0^{F^{-1}(t)} (1 - F(u)) du$$

uniformly in $t \in [0,1]$. Barlow and Campo (1975) defined TTT transform of F as

$$H_F^{-1}(t) = \int_0^{F^{-1}(t)} (1 - F(u)) du \qquad (1)$$

Let $g(x)$ be an increasing convex (concave) function. Let $G(x)$ be the distribution function of $g(x)$. Total observed values of transformed variables $g(X)$ under type 2 censored scheme is

$$Tg(X_{(r)}) = ng(X_{(1)}) + (n-1)(g(X_{(2)}) - g(X_{(1)})) + \ldots + (n-r+1)(g(X_{(r)}) - g(X_{(r-1)}))$$

$$= \sum_{i=1}^{r} g(X_{(i)}) + (n-r)g(X_{(r)}).$$

For $g(x)$, define

$$\left(H_n^{-1}\right)g\left(\frac{r}{n}\right) = \int_0^{H_n^{-1}\left(\frac{r}{n}\right)} (1 - H_n(w)) dw = \int_0^{g\left(F_n^{-1}\left(\frac{r}{n}\right)\right)} (1 - F_n(u)) du$$

where

$$H_n(u) = \begin{cases} 0, & g(u) < g(X_{(i)}) \\ \frac{i}{n}, & g(X_{(i)}) \leq g(u) < g(X_{(i+1)}) \\ 1 & g(X_{(n)}) > g(u) \end{cases}$$

$H_n^{-1}(x) = \inf\{x : H_n(x) \geq g(u)\}$ and the fact that $F_n(u) \xrightarrow{a.s} F(u)$ implies, $g(F_n(u)) \xrightarrow{a.s} g(F(u))$, then by Glivenko Cantelli Theorem,

$$\lim_{\substack{\frac{r}{n}\to t \\ n\to\infty}} \int_0^{g\left(F^{-1}\left(\frac{r}{n}\right)\right)} (1-F_n(u))du = \int_0^{g(F^{-1}(t))} (1-F(u))du$$

We define TTT of $g(x)$ as

$$\left(H_F^{-1}\right)g(t) = \int_0^{g\left(F^{-1}(t)\right)} (1-F(u))du \quad t\in[0,1]\tag{2}$$

Then,

$$\frac{d}{dt}\left(H_F^{-1}\right)g(t) = \frac{d}{dt}\int_0^{g\left(F^{-1}(t)\right)} (1-F(u))du$$

$$= \left[1-\int_0^{g\left(F^{-1}(t)\right)} f(u)du\right]g'\left(F^{-1}(t)\right)\frac{d}{dt}F^{-1}(t)$$

$$= \left[1-\int_0^{g\left(F^{-1}(t)\right)} f(u)du\right]g'\left(F^{-1}(t)\right)\frac{\dfrac{d}{dt}H_F^{-1}(t)}{1-t}$$

$$\frac{d}{dt}\left(H_F^{-1}\right)g(t)\Big|_{t=F(x)} = \left[1-\int_0^{g(x)} f(u)du\right]\frac{g'(x)}{\overline{F}(x)r(x)}.$$

That is,

$$\frac{d}{dt}\left(H_F^{-1}\right)g(t)\Big|_{t=F(x)} = \frac{\overline{F}(g(x))}{\overline{F}(x)}\cdot\frac{g'(x)}{r(x)}\tag{3}$$

Note that $H_F g(\cdot)$ (the inverse of $H_F^{-1}g(\cdot)$) is a distribution with support on $[0,\mu]$,

$$\left(H_F^{-1}\right)g(1) = \int_0^{g\left(F^{-1}(1)\right)} (1-F(u))du = \mu.$$

It is easy to verify that the scaled TTT transform $\dfrac{\left(H_F^{-1}\right)g(t)}{\left(H_F^{-1}\right)g(1)}$ is continuous increasing function on

$[0,1]$. Let $g(x)=x^2$, then

$$\left(H_F^{-1}\right)^2(t) = \int_0^{\left(F^{-1}(t)\right)^2} (1-F(u))du \qquad t\in[0,1]\tag{4}$$

$$\frac{d}{dt}\left(H_F^{-1}\right)^2(t) = \frac{d}{dt}\int_0^{\left(F^{-1}(t)\right)^2} (1-F(u))du$$

$$= \left[1-\int_0^{\left(F^{-1}(t)\right)^2} f(u)du\right]2F^{-1}(t)\frac{\dfrac{d}{dt}H_F^{-1}(t)}{1-t}$$

$$\frac{d}{dt}\left(H_F^{-1}\right)^2(t)\Big|_{t=F(x)} = \left[1-\int_0^{x^2} f(u)du\right]\frac{2x}{\overline{F}(x)r(x)}.$$

That is,

$$\frac{d}{dt}\left(H_F^{-1}\right)^2(t)\Big|_{t=F(x)} = \frac{\overline{F}(x^2)}{\overline{F}(x)}\cdot\frac{2x}{r(x)}\tag{5}$$

Clearly $\dfrac{\overline{F}(x^2)}{\overline{F}(x)}$ and x are increasing functions. So that, if $r(x)$ is decreasing, then

$\dfrac{d}{dt}\left(H_F^{-1}\right)^2(t)\Big|_{t=F(x)}$ is increasing. On the other hand, if $r(x)$ is increasing, then $\dfrac{d}{dt}\left(H_F^{-1}\right)^2(t)\Big|_{t=F(x)}$ is

decreasing if rate of increase of $x\dfrac{\overline{F}(x^2)}{\overline{F}(x)}$ is smaller than the rate of increase of $r(x)$. Note that

$\left(H_F^2\right)$ (the inverse of $\left(H_F^{-1}\right)^2$) is a distribution with support on $[0, \mu]$.

$$\left(H_F^{-1}\right)^2(1) = \int_0^{\left(F^{-1}(1)\right)^2} \left(1 - F(u)\right)du = \mu.$$

It is easy to verify that the scaled TTT transform $\dfrac{\left(H_F^{-1}\right)^2(t)}{\left(H_F^{-1}\right)^2(1)}$ is continuous increasing function on

$[0,1]$.

Example:- Let $F(x) = 1 - e^{-\frac{x}{\theta}}, x > 0, \theta > 0$ be the distribution function of Exponential distribution with mean θ. Then

$$\left(H_F^{-1}\right)^2(t) = \int_0^{\left(F^{-1}(t)\right)^2} \left(1 - F(x)\right)dx$$

$$= \int_0^{\left(F^{-1}(t)\right)^2} e^{-\frac{x}{\theta}} dx$$

$$= \int_0^{\left(F^{-1}(t)\right)^2} \theta dF(x)$$

$$\left(H_F^{-1}\right)^2(t)\Big|_{t=F(x)} = \theta F\left(\left(F^{-1}(t)\right)^2\right)$$

$\left(H_F^{-1}\right)^2(1)$ is the mean of exponential distribution. Therefore, $\dfrac{\left(H_F^{-1}\right)^2(t)}{\left(H_F^{-1}\right)^2(1)} = F\left(\left(F^{-1}(t)\right)^2\right)$.
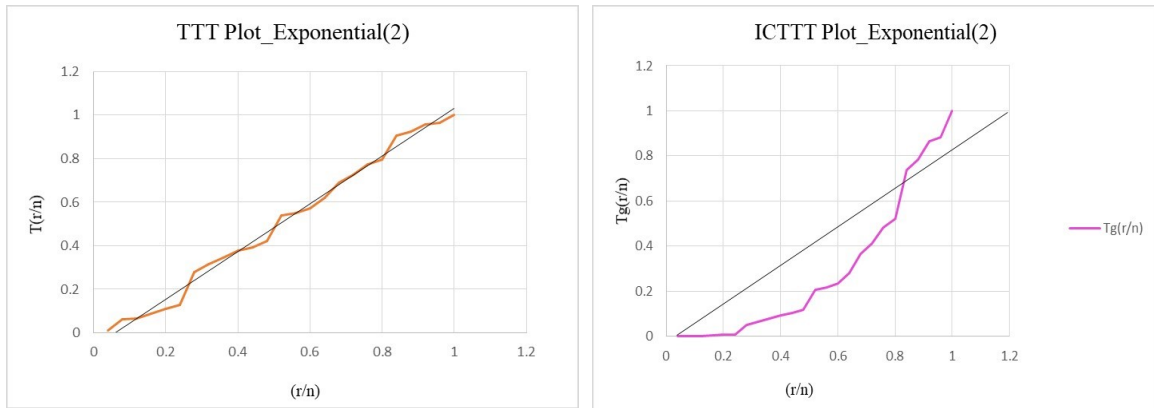
Figure 1: *TTT plot (top) and ICXTTT plot (bottom) for the Exponential Simulated data with parameter $\theta = 2$.*

In this Figure 1, it shows that the TTT-plot of Exponential data set indicates constant failure rate, but ICXTTT-plot for Exponential data set indicates that transformed data follows the bathtub shape failure rate pattern. It is clear that, square of exponential random variable follows some decreasing failure rate model.

III. Ageing Properties

We prove some general results about the ageing patterns of function $g(X)$ using $\dfrac{\left(H_F^{-1}\right)g(t)}{\left(H_F^{-1}\right)g(1)}$,

which is based on the failure rate function $r(x)$ of X .

Proposition 1. G is IFR $\Rightarrow \dfrac{\left(H_F^{-1}\right)g(t)}{\left(H_F^{-1}\right)g(1)}$ is concave in $t \in [0,1]$ if rate of increase of

$g'(x)\dfrac{\overline{F}(g(x))}{\overline{F}(x)}$ is smaller than the rate of increase of $r(x)$. G is DFR $\Rightarrow \dfrac{\left(H_F^{-1}\right)g(t)}{\left(H_F^{-1}\right)g(1)}$ is

convex in $t \in [0,1]$.

Proof. G is IFR implies $\dfrac{d}{dt}\left(H_F^{-1}\right)g(t)$ is decreasing in $t \in [0,1]$, if rate of increase of

$g'(x)\dfrac{\overline{F}(g(x))}{\overline{F}(x)}$ is smaller than the rate of increase of $r(x)$. $\Rightarrow \dfrac{\left(H_F^{-1}\right)g(t)}{\left(H_F^{-1}\right)g(1)}$ is concave in

$t \in [0,1]$. Similarly, G is DFR implies $\dfrac{d}{dt}\left(H_F^{-1}\right)g(t)$ is increasing in $t \in [0,1]$, $r(x)$ is

decreasing in $x \geq 0$.

$\Rightarrow \dfrac{\left(H_F^{-1}\right)g(t)}{\left(H_F^{-1}\right)g(1)}$ is convex in $t \in [0,1]$, if $r(x)$ is decreasing in $x \geq 0$.

Proposition 2. Let X has distribution F and $Y = g(X)$ has distribution $G(y)$. G is IFRA

(DFRA) $\Rightarrow \dfrac{\left(H_F^{-1}\right)g(t)}{F\left(g\left(F^{-1}(t)\right)\right)\left(H_F^{-1}\right)g(1)}$ is decreasing (increasing) in $t \in [0,1]$.

Proof. Let $Y = g(X)$ and $G(y)$ be the distribution function of Y. G is IFRA

$\Rightarrow \dfrac{1}{y}\int_0^y r(u)du$ is increasing in $y \geq 0$.

Let $T(y) = \int_0^y \overline{G}(u)du$. $\dfrac{T(y)}{y}$ is decreasing in $y \geq 0$, since it is an average of the decreasing

function $\overline{G}(y)$.

Then, $\dfrac{\int_0^y r(u)dT(u)}{T(y)}$ is increasing in $y \geq 0$.

Hence $\dfrac{G(y)}{\int_0^y \overline{G}(u)du}$ is increasing in $y \geq 0$ and $\dfrac{\int_0^y \overline{G}(u)du}{G(y)}$ is decreasing in, $y \geq 0$.

Then,

$\dfrac{\int_0^y \overline{G}(u)du}{G(y)} = \dfrac{\int_0^{g(x)} \overline{F}(w)dw}{F(g(x))}$ is decreasing in $x \geq 0$,

since $\overline{G}(u) = P(g(X) > u) = P(X > w) = \overline{F}(w)$ or some w corresponding to u.

$$\dfrac{\int_0^{g(x)} \overline{F}(w)dw}{F(g(x))}$$ is decreasing in $x \geq 0$.

Now make the change of variables $t = F(x)$ and $x = F^{-1}(t)$ and finally we have

$$\frac{\int_0^{g(F^{-1}(t))} \overline{F}(w)dw}{F(g(F^{-1}(t)))} = \frac{(H_F^{-1})g(t)}{F(g(F^{-1}(t)))} \text{ is decreasing in } t \in [0,1].$$

$$\Rightarrow \frac{(H_F^{-1})g(t)}{F(g(F^{-1}(t)))(H_F^{-1})g(1)} \text{ is decreasing in } t \in [0,1].$$

Similarly, for G is DFRA,

$$\frac{(H_F^{-1})g(t)}{F(g(F^{-1}(t)))} \text{ is increasing in } t \in [0,1].$$

$$\Rightarrow \frac{(H_F^{-1})g(t)}{F(g(F^{-1}(t)))(H_F^{-1})g(1)} \text{ is increasing in } t \in [0,1].$$

IV. Increasing Convex (Concave) TTT transform order

Let X and Y be two non-negative random variables with distributions F and H respectively. Clearly $X \leq_{ttt} Y$ if and only if

$$\int_0^{F^{-1}(t)}(1-F(u))du \leq \int_0^{H^{-1}(t)}(1-H(u))du \quad t \in [0,1]. \tag{6}$$

A sufficient condition for the order $\leq_{ttt}$ is the usual stochastic order:

$$X \leq_{st} Y \Rightarrow X \leq_{ttt} Y$$

where $X \leq_{st} Y$ means that $\overline{F}(x) \leq \overline{H}(x), \forall x \in R$ (see, Shaked and Shanthikumar (2007)).

Let X and Y be two random variables such that $Tg(X_{(n)}) \leq Tg(Y_{(n)})$ for all convex functions $g : R \to R$ and all samples of size n. Then X is smaller than Y in some stochastic sense, since $\frac{1}{n}Tg(X_{(n)})$ is average of total observed convex (concave) transformed time of a test.

Let X and Y be two non-negative random variables with absolutely continuous distribution functions F and H respectively. If

$$(H_F^{-1})g(t) \leq (H_H^{-1})g(t), \forall t \in [0,1]$$

where g is an increasing convex function, then X is smaller than Y in increasing convex TTT order (denoted as $X \leq_{icxttt} Y$).

Now we prove the relationship of ICXTTT (ICVTTT) transform orders to stochastic orders.

Theorem 1. Let X and Y be two non-negative random variables having absolutely continuous distribution functions F and G respectively. Then $X \leq_{st} Y \Rightarrow X \leq_{icxttt} Y$.

Proof. Let g be the convex (concave) function $g : R \to R$. Since,

$$X \leq_{st} Y, \quad g(F^{-1}(t)) \leq g(G^{-1}(t)) \text{ for all } t \in [0,1].$$

Hence,

$$\int_0^{g(F^{-1}(t))}(1-F(u))du \leq \int_0^{g(G^{-1}(t))}(1-G(u))du \text{ for all } t \in [0,1]$$

Then, $X \leq_{st} Y \Rightarrow X \leq_{icxttt} Y$.

V. Examples

Usually the TTT plot is drawn by plotting $T\left(\dfrac{r}{n}\right) = \dfrac{\sum\limits_{i=1}^{r} X_{(i)} + (n-r)X_{(r)}}{\sum\limits_{i=1}^{r} X_{(i)}}$ against $\dfrac{r}{n}$, where

$i = 1, 2, \ldots, r$ and $r = 1, 2, \ldots, n$. A TTT curve may be concave (convex) if corresponding distribution is IFR (DFR) distribution. A concave (convex) and then convex (concave) shape for TTT curve occurs, if the distribution is a bathtub (upside down bathtub) failure rate model. Finally, a TTT curve is straight line if the distribution is exponential.

Then the ICXTTT plot is drawn by plotting $Tg\left(\dfrac{r}{n}\right) = \dfrac{\sum\limits_{i=1}^{r} g(X_{(i)}) + (n-r)g(X_{(r)})}{\sum\limits_{i=1}^{r} g(X_{(i)})}$ against $\dfrac{r}{n}$,

where $i = 1, 2, \ldots, r$ and $r = 1, 2, \ldots, n$.

The scaled TTT-transform, which is independent of scale, is defined for values of t with $0 \le t \le 1$ and hence the transformed values are in $[0,1]$. Figure 2 and 3 shows scaled TTT-transforms and scaled ICXTTT-transforms of Aarset bathtub shaped failure rate data and Weibul simulated data.
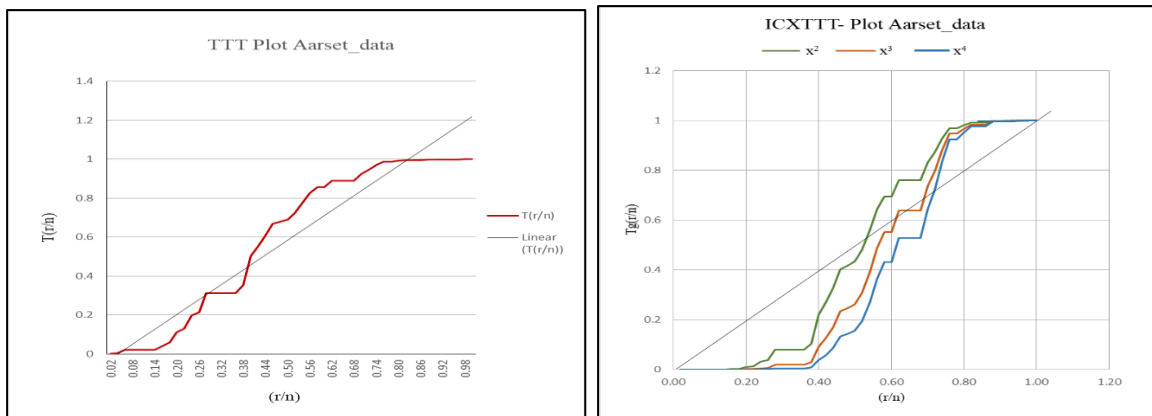
Figure 2. *TTT plot (top) and ICXTTT plot (bottom) for the Aarset data.*

In Figure 2, it shows that the data are known to have a bathtub-shaped failure rate as depicted in TTT plot and ICXTTT-plot.
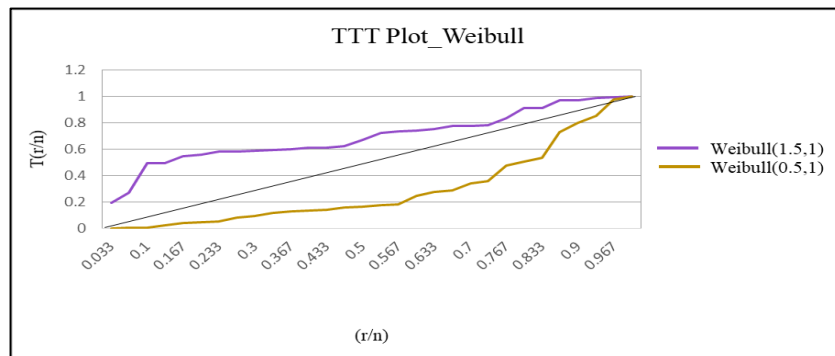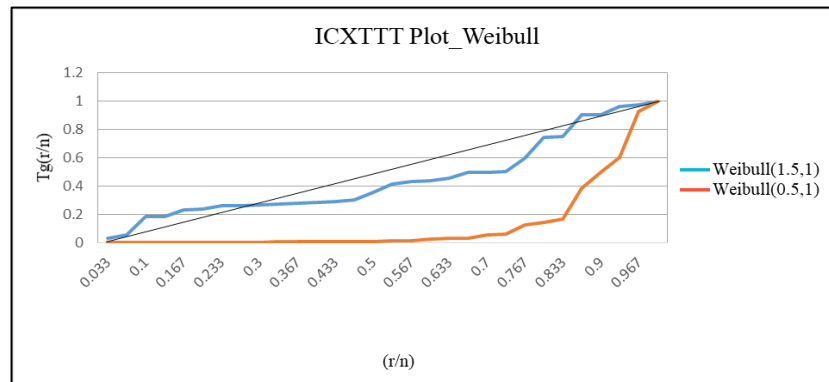
Figure 3._TTT plot (top) and ICXTTT plot (bottom) for the Weibull Simulated data with parameter $\alpha = 1.5, 0.5$ and $\lambda = 1$ respectively._

In Figure 3, it shows that the TTT-plot of $W(\alpha = 1.5, \lambda = 1)$ data set indicate IFR distribution, since it is concave, but ICXTTT-plot for $W(\alpha = 1.5, \lambda = 1)$ data set indicate an inverse bathtub shaped failure rate pattern for the failure rate. The TTT-plot of $W(\alpha = 0.5, \lambda = 1)$ shows $F(t)$ has DFR, since the plot is convex (see Barlow and Campo, 1975) and ICXTTT-plot based on a $W(\alpha = 0.5, \lambda = 1)$ is convex, which indicate a DFR distribution for the transformed data.

VI. Conclusion

This paper considered increasing convex (concave) TTT transform. Identification of the failure rate model of functions of random variables is discussed. Some properties of the transforms are derived with examples.

References

[1]   Aarset, M. V. (1985). How to Identify a Bathtub Hazard Rate, _IEEE Transactions on Reliability_, 36(1): 106-108.

[2]   Barlow, R. E. and Campo, R. A. (1975). Total time on test processes and applications to failure data analysis, _Reliability and Fault Tree Analysis_ (Eds: Barlow, R. E., Fussel, R., and Singpurwalla, N. D.), SIAM, Philadelphia, 451–481.

[3]   Chacko, V. M. (2010). On Total Time on Test Transform Order, _Reliability Theory and Applications_, 19(4): 50-55.

[4]   Franco-Pereira, A. M. and Shaked, M. (2013). The total time on test transform and the decreasing percentile residual life aging notion, _Statistical Methodology_, http://dx.doi.org/10.1016/j.stamet.2013.09.003.

[5]   Gupta, R. C. and Michalek, J. E. (1985). Determination of Reliability Functions by the TTT Transform, _IEEE Transactions on Reliability_, 34(2): 175-176.

[6]   Nair, N. U., Sankaran, P. G. and Vinesh Kumar, B. (2008). TTT transforms of order n and their implications in reliability analysis, _Journal of Applied Probability_, 46: 1127-1139.

[7]   Nair, N. U. and Sankaran, P. G. (2013). Some new applications of the total time on test transforms. _Statistical Methodology_, 10: 93-102.

[8]   Shaked, M. and Shanthikumar, J. G. Stochastic Orders, Springer, New York, 2007.

[9]   Vera, F. and Lynch, J. (2005). K-mart stochastic modeling using iterated total time on test transforms. _Modern Statistical and Mathematical Methods in Reliability_, World Scientific, Singapore, 395-409.

Designing of Special Type Double Sampling Plan for Life Tests Based on Percentiles Using Exponentiated Frechet Distribution

Neena Krishna P K

•

Research Scholar, Department of   Statistics, Bharathiar University
Coimbatore-46, Tamil Nadu, India
email: neenakrishnapk94@gmail.com

Dr S Jayalakshmi

•

Assistant Professor, Department of
Statistics , Bharathiar University
Coimbatore-46, Tamil Nadu, India
email: laxmij701@gmail.com

Abstract

Acceptance Sampling performs a major role in industry for monitoring process and assessing complains for reducing the cost and inspection time. A truncated life test may be conducted to determine the smallest sample size to ensure certain percentile life time of an items. The operating characteristic function values are obtained according to different quality levels and the minimum ratios of the true average life to the specified average life at the specified producer's risk are derived. Useful tables are provided for the proposed sampling plan.

Keywords: Special Type Double Sampling Plan, Exponentiated Frechet Distribution, Percentile

I. Introduction

In numerous statistical quality control (SQC) and reliability studies, acceptance sampling plans are executed to achieve the satisfactory inferential idea about a product. The acceptance sampling plans assosciated with accepting or rejecting a large-sized lot of products or items on the basis of the quality of products in a sample which are taken from lot. An acceptance sampling is a specified plan that determines the smallest sample size to be used for testing. If the quality characteristics of product follows a lifetime of an item, then it is termed as acceptance sampling technique for life test experiments or Reliability Sampling Plan. A common process in life testing is to terminate the life test by a predetermined time t_0 and mention the number of failures. One of the mission of these experiments is to set a lower confidence limit on the mean life. It is then to establish a specified mean life with a given probability of at least p* which provides protection to consumers. Many studies has been carried out for the designing of single sampling plan and double sampling plans for truncated life tests under different statistical distributions for life time. Truncated life tests in the exponential distribution was first evaluated by Epstein (1954). Further, various authors developed truncated life test sampling plan using various distributions, such as Goode and Kao

Neena Krishna P K, Dr S Jayalakshmi
DESIGNING OF SPECIAL TYPE DOUBLE SAMPLING PLAN...

RT&A, No 1 (61)
Volume 16, March 2021

(1961) using Weibull distribution, Gupta and Groll (1961) using gamma distribution, Kantam and Rosaiah (1998) using half logistic distribution, Kantam et al., (2001) using log-logistic distribution, Rosaiah and Kantam (2005) using inverse Rayleigh distribution, Balakrishnan et al., (2007) using generalized Birnbaum-Saunders distribution, Rosaiah et al., (2006) using exponentited log-logistic distribution etc.

Furthermore Lio et al (2009) have studied acceptance sampling plans from truncated life tests based on the assumptions of Brinbaum-Saunders distribution for percentiles and they also proposed that the acceptance sampling plan based on mean may not satisfy the demand of engineering on specific percentile of strength or the breaking stress. This describes the material strength of the products is declined significantly and may not meet consumer's satisfactory level. Percentiles gives more knowledge regarding the life time distribution than the mean life does. When the life time distribution is symmetric, the 50th percentile or the median is similar to the mean life. Hence, developing acceptance sampling plans based on percentiles of life time distributions can be used as a generalization of the developing acceptance sampling plans based on the mean life of items or products.

Rao and Kantam (2010) developed Acceptance Sampling plans for truncated life tests based on the log-logistic distribution for percentiles. Rao *et al.* (2012) also developed the Acceptance Sampling plans for percentiles based on the Inverse Rayleigh Distribution. Rao *et al.*(2014) further proposed the Acceptance Sampling plans based on the percentiles of Exponentiated half log logistic distribution. The exponentiated Fréchet distribution has been used in various fields of research applications. Acceptance sampling plan based on truncated life tests for the exponentiated Fréchet distribution (EFD) using average life was discussed by Al-Nassar and Al-Omari (2013). Gui and Aslam (2015) discussed acceptance sampling plans based on truncated life tests for weighted exponential distribution. Govindaraju (1984) has developed the Special Type Double Sampling Plan. The main aim of this paper is to develop the Special Type Double Sampling Plan for percentiles the lifetime distribution follows Exponentiated Frechet Distribution.

II. Exponentiated Frechet Distribution (EFD)

The Exponentiated Frechet Distribution was introduced and studied quite extensively by Nadarajah and Kotz .The EFD is mentioned as the inverse of exponentiated Weibull distribution. The probability density function (pdf) and cumulative distribution function (cdf) of EFD are given as

$$f(t;\sigma,\lambda,\theta) = \sigma^\lambda \lambda \theta \, t^{-(1+\lambda)} [1 - e^{-(\sigma/t)^\lambda}]^{\theta-1}; \; t>0, \sigma, \lambda > 0, \theta > 0 \tag{1}$$

$$F(t:\sigma,\lambda,\theta) = 1 - [1 - e^{-(\sigma/t)^\lambda}]^\theta; \quad t>0, \sigma, \lambda > 0, \theta > 0 \tag{2}$$

where $\sigma > 0$ is a scale parameter, $\lambda > 0$ and $\theta > 0$ are the parameters. When $\theta = 1$ it is the particular case for standard Frechet Distribution.

The moment generating function of the Exponentiated Frechet Distribution is given by

$$M_x(t) = \sigma^r \theta \Gamma(\theta+1) \sum_{i=0}^{\infty} \sum_{j=0}^{\infty} \sum_{r=0}^{\infty} (-1)^{\theta-i-1} \frac{t^r (\theta-i-j)^{\frac{r}{\lambda}-1} \Gamma[(1-\frac{r}{\lambda}), x(\theta-i-j)]}{\Gamma(i+1)\Gamma(\theta-i+1)\Gamma(r+1)} \tag{3}$$

Hazard Function

The hazard function for any distribution is given by

$$h(t) = \frac{f(t)}{1-F(t)} \tag{4}$$

Thus the hazard function for Exponentiated Frechet Distribution is given by

$$h(t) = \frac{\sigma^\lambda \lambda \theta\, t^{-(1+\lambda)}[1 - e^{-(\sigma/t)^\lambda}]^{\theta-1}}{[1 - e^{-(\sigma/t)^\lambda}]^\theta}$$

(5)

Percentile Estimator

The percentile estimator of any distribution is given by

$$P(t \le t_q) = q$$

(6)

The 100 q-th percentile of the EFD is as follows

$$t_q = \sigma \eta_q$$

(7)

t_q and q are directly proportional. Let

$$\eta_q = (-\ln(1 - (1-q)^{1/\alpha}))^{-(1/\lambda)}$$

(8)

Replacing the scale parameter $\sigma = t_q / \eta_q$

Hence, for fixed values $\lambda = \lambda_0$ and $\theta = \theta_0$, the quantile t_q is a function of the scale parameter σ, that is, $t_q \ge t_q^0 \Leftrightarrow \sigma \ge \sigma_0$

Where

$$\sigma_0 = \frac{t_q^0}{(-\ln(1-(1-q)^{1/\alpha_0}))^{-(1/\lambda_0)}}$$

σ_0 also depends on α_0 and λ_0, to build up acceptance sampling plans for the EFD ascertain $t_q \ge t_q^0$, equivalently that σ exceeds σ_0.

Replacing the scale parameter by $\sigma_0 = t_q^0 / \eta_q$, one can obtain the cumulative distribution function of Exponentiated Frechet Distribution is

$$F(t) = 1 - [1 - e^{-(t\eta_q / t_q)^{-\lambda}}]^\theta$$

(9)

Let $\delta = t/t_q$

$$F(t) = 1 - [1 - e^{-(\eta_q \delta_q^0 / (t_q / t_q^0))^{-\lambda}}]^\theta$$

(10)

Taking partial derivative with respect to δ

$$\partial F(t) / \partial \delta = \theta \lambda \eta_q (t_q^0 / t_q)[1 - e^{-(\eta_q \delta_q^0 / (t_q / t_q^0))^{-\lambda}}]^{\theta-1} e^{-(\eta_q \delta_q^0 / (t_q / t_q^0))^{-\lambda}}$$

III. Designing of the Special Type Double Sampling under Life Time Distributions

Assume that a life test is conducted and will be terminated at time t_0. A probability P^* to reject a bad lot is used to protect consumers. A bad lot means that the true *100qth* percentile is below the supposed 100qth percentile that is, $t_q < t_q^0$. The lot is confirmed as a good one if the lifetime data hold the null hypothesis $H_0 : t_q \ge t_q^0$ against the alternative

$H1: t_q < t_q^0$. The consumer's risk $1 - p^*$ is used as the significance level for this hypothesis testing and p^* is the consumer's confidence level.

I. Operating Procedure

The operating procedure of special type double sampling plan for the truncated life test has the following steps:

* Take a random sample of size n_1 from the lot and put on the test for pre-assigned experimental time t_0 and observe the number of defectives d_1.

   If $d_1 > 1$ reject the lot.

* If $d_1 = 0$, draw a second random sample of size n_2 and put them on the test for time t_0 and observe the number of defectives d_2.

   If $d_2 \leq 1$ accept the lot, Otherwise reject the lot.

   In a special Type Double Sampling Plan the decision of acceptance is made only after inspecting the second sample. This aspect differs from usual double sampling plan in which decision of acceptance can be made even before the inspection of the second sample.

   In Special Type Double Sampling Plan $n_1 and n_2$ denotes the sample size. For the proposed sampling plan the probability of acceptance is given by

$$p_a(p) = (1-p)^{n_1+n_2} + n_2 p(1-p)^{n-1}$$

The minimum sample size $n_1 and n_2$ can be calculated using the equation.

$$(1-p)^{n_1+n_2} + n_2 p(1-p)^{n-1} \leq 1 - p^*$$

where, p is the probability that an item fails before t0, which is given by

$$F(t) = 1 - [1 - e^{-(\eta_q \delta_q^0 / (t_q / t_q^0))^{-\lambda}}]^\theta$$

Determination of the minimum sample sizes for special type double sampling plan reduces to

   Minimize $\qquad\qquad ASN = n_1 + n_2(1-p)^n$

   Subject to

$$(1-p)^{n_1+n_2} + n_2 p(1-p)^{n-1} \leq 1 - p^*$$

where n_1 and n_2 are integers. The minimum sample sizes satisfying the condition can be obtained by search procedure
.

II. Construction of Tables

Step 1: Find the value of η for θ=2 and q=0.25.

Step 2: Set the evaluated η, $\lambda = 1,2$ and t/t_q =0.09, 0.11, 0.13, 0.15, 0.17, 0.19

Step 3: Find the smallest value for $n_1 and n_2$ satisfying $p_a(p) \leq 1 - p^*$, where, p^* is probability of rejecting the bad lots.

Step 4: For the $n_1 and n_2$ value obtained find the ratio $d_{0.25}$ such that $p_a(p) \geq 1 - \alpha$, where $\alpha = 0.05$, p= $F(\frac{t}{t_q^0}, \frac{1}{d_q})$ and $d_q = t_q / t_q^0$.

Example

Consider the life time distribution as Exponentiated Frechet Distribution if the experimenter is interested in showing that the true unknown 25th percentile life. Let the consumer risk be $1 - p^* = 0.05$. Suppose $\lambda = 2$, $\theta = 2$, $\alpha = 0.05$, $\beta = 0.10$, $t_q/t_q^0 = 3$, $\delta_q^0 = 0.13$ and η can be calculated as 2.713, then the minimum sample size n_1 and n_2 can be obtained from table 1. The values of n_1 and n_2 can be obtained as 10 and 6 respectively. The operating characteristics values for the proposed sampling plan is obtained and tabulated in table 2. For $n_1 = 10$, $n_2 = 5$, $t_q/t_q^0 = 5$, $t/t_q^0 = 0.11$ and $\lambda = 2$ then the operating characteristic function obtained from table 2 is 0.914607. In table 3, the respective ratio $d_{0.25}$ values is estimated by fixing the producer's risk, $\alpha = 0.05$.

Table 1: *Minimum Sample Size values of n_1 and n_2 for the 25th percentile of Special Type Double Sampling Plan under the assumption of Exponentiated Frechet Distribution.*

p^*	λ	t_q/t_q^0	t/t_q^0					
			0.09	0.11	0.13	0.15	0.17	0.19
0.99	1	2	12,11	9,6	7,4	6,4	6,2	5,1
		3	6,5	5,3	4,3	3,3	3,2	4,1
		5	4,1	3,2	3,1	3,1	3,1	3,1
	2	2	798,698	430,384	100,59	40,16	21,8	14,1
		3	420,376	69,55	26,15	12,9	10,1	7,1
		5	50,32	16,11	7,7	6,5	4,3	4,1
0.95	1	2	9,5	7,4	5,4	5,3	4,3	3,2
		3	8,7	6,4	4,3	3,3	3,2	2,2
		5	6,5	5,4	4,4	4,3	3,2	3,1
	2	2	227,196	57,32	22,12	13,4	8,3	3,2
		3	41,26	16,8	10,6	6,6	5,4	4,1
		5	10,5	6,4	4,3	3,2	2,2	2,1
0.90	1	2	11,9	7,5	5,5	5,4	4,4	3,2
		3	10,9	9,9	9,6	8,5	5,4	4,3
		5	9,9	8,6	5,4	4,3	2,2	2,1
	2	2	169,156	47,21	18,8	10,3	7,1	5,1
		3	31,21	13,5	6,4	4,3	3,2	3,1
		5	23,11	8,4	5,1	4,1	3,1	2,2
0.75	1	2	99,97	24,18	11,5	5,4	4,3	3,3
		3	4,4	4,4	4,3	3,3	3,2	2,2
		5	5,4	4,4	4,3	3,2	3,1	2,1
	2	2	102,94	25,17	11,5	5,4	4,1	3,1
		3	105,83	20,11	8,3	4,2	3,1	2,1
		5	5,3	3,1	2,2	2,1	2,1	2,1

Table 2: *Operating Characteristic value for the* 25th *percentile of Special Type Double Sampling Plan under the assumption of Exponentiated Frechet Distribution.*

p^*	λ	n_1	n_2	t_q / t_q^0	t / t_q^0					
					0.09	0.11	0.13	0.15	0.17	0.19
0.99	1	12	11	2	0.605243	0.772442	0.945587	0.978034	0.993716	0.995808
		6	5	3	0.764119	0.873191	0.979135	0.982082	0.982126	0.98509
		4	1	5	0.858265	0.965345	0.97215	0.979003	0.979099	0.972293
	2	40	16	2	0.662366	0.893797	0.976779	0.989225	0.991036	0.993717
		26	15	3	0.784096	0.988032	0.988048	0.988048	0.988048	0.988048
		16	11	5	0.855601	0.985653	0.993700	0.994604	0.996402	0.996405
0.95	1	9	5	2	0.691921	0.993712	0.995503	0.995506	0.996402	0.997302
		8	7	3	0.779626	0.994879	0.980334	0.988358	0.99282	0.997302
		6	5	5	0.792806	0.994607	0.996402	0.997300	0.997302	0.9982
	2	22	12	2	0.563506	0.685675	0.891024	0.994600	0.995503	0.994604
		16	8	3	0.695503	0.859640	0.996402	0.997302	0.998200	0.994604
		10	5	5	0.791028	0.914607	0.996402	0.997302	0.9982	0.998201
0.90	1	11	9	2	0.491008	0.699190	0.791917	0.992815	0.995503	0.996402
		9	6	3	0.607231	0.790231	0.880355	0.994607	0.996402	0.997302
		8	6	5	0.889190	0.912811	0.995503	0.996402	0.998200	0.998201
	2	47	21	2	0.487946	0.692818	0.995508	0.996405	0.997302	0.998200
		31	21	3	0.611458	0.778502	0.950136	0.975503	0.996402	0.997300
		23	11	5	0.790827	0.877635	0.972136	0.985503	0.996405	0.997302
0.75	1	24	18	2	0.411092	0.678502	0.790136	0.995503	0.996402	0.997300
		4	4	3	0.590827	0.777635	0.890136	0.995503	0.996405	0.997302
		5	4	5	0.696400	0.896400	0.946402	0.997300	0.997302	0.998200
	2	25	17	2	0.407400	0.582110	0.769282	0.996404	0.997302	0.998201
		20	11	3	0.595503	0.696400	0.896402	0.997302	0.997302	0.998201
		5	3	5	0.695506	0.797302	0.940982	0.998201	0.998201	0.998201

Table 3: *The ratio* $d_{0.25}$ *for accepting the lot with the producer's risk of 0.05 when*

$$\theta = 2$$

p^*	λ	t / t_q^0					
		0.09	0.11	0.13	0.15	0.17	0.19
0.99	2	2.344003	2.029148	1.027736	1.203372	1.251749	1.814854
	1	0.409894	0.396737	0.617704	0.464991	0.470858	0.486277
	0.75	0.379255	0.366778	0.326859	0.391388	0.295660	0.310311
	0.50	0.291685	0.270410	0.287141	0.312855	0.265462	0.262976
	0.25	0.217611	0.213765	0.228062	0.251749	0.258777	0.235822
0.95	2	3.628452	2.422327	1.74862	1.311969	1.02182	1.015266
	1	0.893549	0.670501	0.617704	0.535661	0.471674	0.501266
	0.75	0.628414	0.539050	0.475576	0.427177	0.387902	0.343006
	0.50	0.440772	0.400338	0.306644	0.340266	0.319427	0.253812
	0.25	0.258447	0.294061	0.228302	0.272212	0.238937	0.232853
0.90	2	2.422327	1.74862	1.311969	1.021820	1.501266	3.030129
	1	0.670501	0.617704	0.535661	0.471674	0.536410	0.697645
	0.75	0.539050	0.475576	0.427177	0.387902	0.253812	0.522105
	0.50	0.400338	0.306644	0.340266	0.319427	0.232853	0.383096
	0.25	0.294061	0.228302	0.272212	0.210886	0.207543	0.308925
0.75	2	1.679687	1.456120	1.835661	1.02182	1.190118	1.118228
	1	0.438826	0.514024	0.535661	0.470858	0.421973	0.553591
	0.75	0.398042	0.413224	0.316928	0.324011	0.359442	0.264479
	0.50	0.320421	0.335890	0.275242	0.319427	0.224150	0.238487
	0.25	0.245847	0.283336	0.238053	0.265462	0.206561	0.214106

IV. Conclusion

This paper indicates the Special Type Double Sampling Plan based on the percentiles of Exponentiated Frechet Distribution (EFD), when the life test is truncated for a pre-specified time. Special Type Double Sampling plan requires less Average Sample Number than the Single Sampling Plan results in the reduction of inspection cost. For these plans, the smallest sample sizes, which assured the median life time, is examined under the given consumer's risk and producer's risk. The industrial practitioner and the experimenter has to adopt the proposed plan to save the cost and time of the experiment. Extensive tables have been provided for the industrial use according to various parameters and percentile values.

References

[1] Al-Nassar, A.D. and Al-Omari, A.I. (2013). Acceptance sampling plan based on truncated life tests for exponentiated Fréchet distribution. *Journal of Statistics and Management Systems*, 16(1):13-24.

[2] Balakrishnan, N., Leiva, V. and Lopez, J. (2007). Acceptance sampling plans from truncated life tests based on the generalized Birnbaum-Saunders distribution. *Communications in statistics – Simulation and Computation*, 36:643-656.

[3] Epstein, B. (1954). Truncated life tests in the exponential case. *Annals of Mathematical Statistics*, 25:555–564.

[4] Goode, H. P. and Kao, J. H. K. (1961). Sampling plans based on the Weibull distribution. *Proceedings of the 7th National Syposium on Reliability and Qualilty Control*,24–40.

[5] Govindaraju, K. (1984). Contributions to the Study of Certain Special Purpose Plans, Ph.D. Thesis, Bharathiar University, Coimbatore, India.

[6] Gupta, S. S and Groll, P. A, (1961). Gamma distribution in acceptance sampling based on life tests, *Journal of the American Statistical Association*, 56:942–970.

[7] Jayalakshmi, S. (2007). Designing of Quick Switching System with Special Type Double Sampling plans Specified Quality levels. *ImpactJournal of Science and Technology*, 1(2):41-49.

[8] Kantam, R. R. L. and Rosaiah, K. (1998). Half Logistic distribution in acceptance sampling based on life tests, *IAPQR Transactions*, 23(2):117–125.

[9] Kantam, R.R.L. and Rosaiah, K. and Rao, G.S. (2001) Acceptance sampling based on life tests: Log-Logistic model. *Journal of Applied Statistics,* 28:121-128.

[10] Kotz, S. and Nadarajah, S. Extreme Value Distributions Theory and Applications, Imperial College Press, London,2000.

[11] Rao, G.S., Kantam, R.R.L., Rosaiah, K. and Reddy, J.P. (2012). Acceptance sampling plans for percentiles based on the Inverse Rayleigh Distribution. *Electronic Journal of Applied Statistical Analysis.* 5(2):164-177.

[12] Rao, G. S, and Naidu, Ch. R. (2014). Acceptance Sampling Plans for Percentiles based on the Exponentiated half log logistic distribution. *Applications and Applied Mathematics: An International Journal* 9(1):39-53.[

13] Rosaiah, K. and Kantam, R. R. L. (2005). Acceptance sampling based on the inverse Rayleigh distribution. *Economic Quality Control* 20:277-286.

M. L. Soujanya, P. Vijaya Laxmi, E. Sirisha
IMPACT OF NEGATIVE ARRIVALS AND MULTIPLE WORKING
VACATION ON DUAL SUPPLIER INVENTORY MODEL…

RT&A, No 1 (61)
Volume 16, March 2021

Impact of Negative Arrivals and Multiple Working Vacation on Dual Supplier Inventory Model with Finite Lifetimes

M. L. Soujanya [a,*], P. Vijaya Laxmi [b], E. Sirisha [c]

•

[a]Department of Mathematics,
Vignan's Institute of Information Technology (Autonomous),
Visakhapatnam, India.
mailto:drmlsoujanya@gmail.comdrmlsoujanya@gmail.com
[b]Department of Applied Mathematics,
Andhra University, Visakhapatnam, India.
mailto:drmlsoujanya@gmail.comvijayalaxmiau@gmail.com
[c]Department of Computer Science and Engineering,
Gayatri Vidya Parishad College of Engineering (Autonomous),
Visakhapatnam, India.
mailto:drmlsoujanya@gmail.com, sirisha@gvpce.ac.in

Abstract

In this paper we analyzed an inventory model with two-suppliers, finite life times, multiple working vacations and customers who arrive according to RCE process. Perishable and replenishment rates of two-suppliers are exponentially distributed. The server takes exponential working vacations when the queue is empty. Arrival process follows Poisson distribution and the probability for an ordinary customer is p and for negative customer is q. Limiting distribution of the assumed model is obtained. Numerical results are presented for cost function and various system performance parameters. The impact of two-suppliers on the optimal reorder points will be useful in developing strategies for handling various perishable inventory problems with replenishment rates.

Keywords: (s, S) policy, Two-supply inventory, Lead time, RCE process, Multiple working vacations, Matrix analytic method.

1 Introduction

In an (s, S) inventory policy, the quantity $Q(= S - s)$ is placed if inventory falls to s, so that the maximum inventory level is S. This policy has been widely discussed for almost a century. However in inventory models with more than one supplier we can improve the quality of service, develop strong relationship with the customers, reduce loss of sales due to stock shortages, enhanced profits, etc. In two-supply (s, S) inventory policy, two orders of quantities Q_1 and Q_2 are placed whenever inventory level drops to r and s respectively. For literature on inventory models with two supplies one can refer Yang and Wei-Chung [12] and Vijayashree and Uthaykumar [8].

The life time of inventory items is indefinitely long in many classic inventory models like, vegetables, food items, medical products, etc., which become unusable after a certain period. That means there exists a real - life inventory system which consists of products having a finite lifetime.

M. L. Soujanya, P. Vijaya Laxmi, E. Sirisha
IMPACT OF NEGATIVE ARRIVALS AND MULTIPLE WORKING
VACATION ON DUAL SUPPLIER INVENTORY MODEL…

RT&A, No 1 (61)
Volume 16, March 2021

These type of products are called as perishable products and the corresponding inventory system can be considered as a perishable inventory system. Yonguri et. al. [13] studied an inventory models for perishable items with and without backlogging. "A deterministic perishable inventory model with time dependent demands is developed by Sushil and Ravendra [7]. Dinesh and Roberto [1] discussed a perishable inventory model with style goals."

"Sivakumar and Arivarignan [6] introduced negative customers in inventories with finite queues". "For more literature on this concept, one may refer Manual et al. [3, 4]."

In the working vacation (WV) model, the server without stopping the service completely, he continuous with lower service rate. "A continuous review inventory system with a single and multiple server vacations is given by Jayaraman et al. [2]. Periyasamy [5] discussed an inventory system with finite life times, retrial demands and multiple server vacations." For more literature on working vacations on may refer the papers by Vijaya Laxmi and Soujanya, [9, 10] and [11].

In the present paper, an inventory policy with two supply chains for replacement in which one having a lesser lead time is considered. Demands occur according to Poisson distribution. The arriving person may join the system with possibility p or remove one customer from the queue with probability q. The perishable, service rates in busy and WV are exponentially distributed. Limiting distributions are found. Several system performance parameters of the assumed model are presented. Also the analysis of the cost function is also carried out using direct search method.

2 Description of the model

In two supply inventory model, when inventory shrinks to $r(> \frac{S}{2})$, a quantity $Q_1(= S - r)$ is placed from the first supplier and is replenished with an exponential rate η_1. If it falls to $s(< Q_1)$ a quantity $Q_2(= S - s > s + 1)$ is placed from another supplier and is replenished with an exponential rate $\eta_2(\eta_2 > \eta_1)$. Arrival process follows Poisson distribution with rate λ. The arrived customer joins the queue with probability p and removes an existing customer from the end with probability $q(= 1 - p)$. Consider exponential Vacation time, service times during regular period and WV with rates β, μ_b and μ_v, respectively. We assume that, the server stays idle in any period at zero inventory level. Perishable rate follows exponential distribution with rate γ.

Let $N(t)$ be the length of the queue, $L(t)$ be the quantity of inventory and $\zeta(t)$ be the state of the server, which is defined as

$$\zeta(t) = \begin{cases} 0, & server\ is\ active; \\ 1, & server\ is\ in\ WV. \end{cases}$$

It is clear that the Markov process $\{(N(t), \zeta(t), L(t) | t \geq 0\}$ is a state space model with

$$E = \{\{(i, j, k) | i \geq 0, j = 1,2, 0 \leq k \leq S\}$$

Describe the order sets as

$$< i, j > = \begin{cases} ((< i, j, k >))_{j=1, k=1,2,\dots,S} \\ ((< i, j, k >))_{j=2, k=0,1,\dots,S}. \end{cases}$$

$$< i > = ((< i, j >))_{j=1,2.}$$

Then E can be denoted as $(< 0 >, < 1 >, \dots)$. Therefore, the transition rate matrix P is

$$P = < 0 > < 1 > < 2 > < 3 > \cdots$$
$$< 0 > A_0 C 0 0 \dots$$
$$< 1 > B A C 0 \dots$$
$$< 2 > 0 B A C \dots$$
$$< 3 > 0 0 B A \dots$$
$$\vdots \vdots \vdots \vdots \vdots \ddots$$

where

$$A_0 = 1 2 1 [A_0]^{11} [A_0]^{12} 2 [A_0]^{21} [A_0]^{22},$$

M. L. Soujanya, P. Vijaya Laxmi, E. Sirisha
IMPACT OF NEGATIVE ARRIVALS AND MULTIPLE WORKING
VACATION ON DUAL SUPPLIER INVENTORY MODEL…

RT&A, No 1 (61)
Volume 16, March 2021

$$[A_0]^{11} = \begin{cases} -(p\lambda + \eta_1 + \eta_2 + l\gamma), & m = l , l = 1,2,\dots,s; \\ -(p\lambda + \eta_1 + l\gamma), & m = l, l = s+1, \dots, r; \\ -(p\lambda + l\gamma), & m = l, l = r+1, \dots, S; \\ l\gamma, & m = l-1, \; l = 2, \dots, S; \\ \eta_1, & m = l+Q_1, \; l = 1, \dots, r; \\ \eta_2, & m = l+Q_2, \; l = 1,\dots,s; \\ 0, & otherwise. \end{cases}$$

$$[A_0]^{12} = \begin{cases} \gamma, & m = l-1 , l = 1; \\ 0, & otherwise. \end{cases} , [A_0]^{21} = \begin{cases} \beta, & m = l , l = 1,2,\dots,S; \\ 0, & otherwise. \end{cases} ,$$

$$[A_0]^{22} = \begin{cases} -(p\lambda + \eta_1 + \eta_2), & m = l, l = 0; \\ -(p\lambda + \eta_1 + \eta_2 + \beta + l\gamma), & m = l , l = 1,2,\dots,s; \\ -(p\lambda + \eta_1 + \beta + l\gamma), & m = l, l = s+1, \dots, r; \\ -(p\lambda + \beta + l\gamma), & m = l, l = r+1, \dots, S; \\ l\gamma, & m = l-1, \; l = 1, \dots, S; \\ \eta_1, & m = l+Q_1, \; l = 0, \dots, r; \\ \eta_2, & m = l+Q_2, \; l = 0,\dots,s; \\ 0, & otherwise. \end{cases}$$

$$C = 121[C_0]^{11}[C_0]^{12}2[C_0]^{21}[C_0]^{22}, [C_0]^{12} = [C_0]^{21} = 0$$

$$[C_0]^{11} = \begin{cases} p\lambda, & m = l , l = 1,\dots,S; \\ 0, & otherwise. \end{cases} , [C_0]^{22} = \begin{cases} p\lambda, & m = l , l = 0,\dots,S; \\ 0, & otherwise. \end{cases} ,$$

$$B = 121[B]^{11}[B]^{12}2[B]^{21}[B]^{22}, [B]^{21} = 0, [B]^{12} = \begin{cases} \mu_b, & m = l-1, l = 1; \\ 0, & otherwise. \end{cases} ,$$

$$[B]^{11} = \begin{cases} \mu_b, & m = l-1, l = 2, \dots, S; \\ q\lambda, & m = l , l = 1,\dots,S; \\ 0, & otherwise. \end{cases} , [B]^{22} = \begin{cases} \mu_v, & m = l-1, l = 1,\dots S; \\ q\lambda, & m = l, l = 0,\dots,S; \\ 0, & otherwise. \end{cases} ,$$

$$A = 121[A_1]^{11}[A_1]^{12}2[A_1]^{21}[A_1]^{22},$$

$$[A]^{11} = \begin{cases} -(p\lambda + q\lambda + \eta_1 + \eta_2 + l\gamma + \mu_b), & m = l , l = 1,2,\dots,s; \\ -(p\lambda + +q\lambda + \eta_1 + l\gamma + \mu_b), & m = l, l = s+1, \dots, r; \\ -(p\lambda + q\lambda + l\gamma + \mu_b), & m = l, l = r+1, \dots, S; \\ l\gamma, & m = l-1, \; l = 2, \dots, S; \\ \eta_1, & m = l+Q_1, \; l = 1, \dots, r; \\ \eta_2, & m = l+Q_2, \; l = 1,\dots,s; \\ 0, & otherwise. \end{cases}$$

$$[A]^{12} = \begin{cases} \gamma, & m = l-1 , l = 1; \\ 0, & otherwise. \end{cases} , [A]^{21} = \begin{cases} \beta, & m = l , l = 1,2,\dots,S; \\ 0, & otherwise. \end{cases} ,$$

$$[A]^{22} = \begin{cases} -(p\lambda + q\lambda + \eta_1 + \eta_2 + \mu_v), & m = l, l = 0; \\ -(p\lambda + q\lambda + \eta_1 + \eta_2 + \mu_v + \beta + l\gamma), & m = l , l = 1,2,\dots,s; \\ -(p\lambda + q\lambda + \eta_1 + \beta + l\gamma + \mu_v), & m = l, l = s+1, \dots, r; \\ -(p\lambda + q\lambda + \beta + l\gamma + \mu_v), & m = l, l = r+1, \dots, S; \\ l\gamma, & m = l-1, \; l = 1, \dots, S; \\ \eta_1, & m = l+Q_1, \; l = 0, \dots, r; \\ \eta_2, & m = l+Q_2, \; l = 0,\dots,s; \\ 0, & otherwise. \end{cases}$$

M. L. Soujanya, P. Vijaya Laxmi, E. Sirisha
IMPACT OF NEGATIVE ARRIVALS AND MULTIPLE WORKING
VACATION ON DUAL SUPPLIER INVENTORY MODEL…

RT&A, No 1 (61)
Volume 16, March 2021

3 Analysis of the Model

Initially the stability condition of the defined model is determined and then the limiting probabilities are derived in this section.

3.1 Stability condition

For the stability condition, consider the matrix $G = A + B + C$ as
$$G = \begin{matrix} & 1 & 2 \\ 1 & [G]^{11} & [G]^{12} \\ 2 & [G]^{21} & [G]^{22} \end{matrix},$$

$$[G]^{11} = \begin{cases} -(\eta_1 + \eta_2 + \mu_b + l\gamma), & m = l, l = 1; \\ -(\eta_1 + \eta_2 + l\gamma), & m = l, l = 2, \dots, s; \\ -(\eta_1 + l\gamma), & m = l, l = s + 1, \dots, r; \\ -l\gamma, & m = l, l = r + 1, \dots, S; \\ l\gamma, & m = l - 1, l = 2, \dots, S; \\ \eta_1, & m = l + Q_1, l = 1, \dots, r; \\ \eta_2, & m = l + Q_2, l = 1, \dots, s; \\ 0, & otherwise. \end{cases}$$

$$[G]^{12} = \begin{cases} \gamma, & m = l - 1, l = 1; \\ 0, & otherwise. \end{cases} , [G]^{21} = \begin{cases} \beta, & m = l, l = 1,2, \dots, S; \\ 0, & otherwise. \end{cases} ,$$

$$[G]^{22} = \begin{cases} -(p\lambda + q\lambda + \eta_1 + \eta_2 + \mu_v), & m = l, l = 0; \\ -(p\lambda + q\lambda + \eta_1 + \eta_2 + \mu_v + \beta + l\gamma), & m = l, l = 1,2, \dots, s; \\ -(p\lambda + q\lambda + \eta_1 + \beta + l\gamma + \mu_v), & m = l, l = s + 1, \dots, r; \\ -(p\lambda + q\lambda + \beta + l\gamma + \mu_v), & m = l, l = r + 1, \dots, S; \\ l\gamma, & m = l - 1, l = 1, \dots, S; \\ \eta_1, & m = l + Q_1, l = 0, \dots, r; \\ \eta_2, & m = l + Q_2, l = 0, \dots, s; \\ 0, & otherwise. \end{cases}$$

Let Π be the limiting distribution of G, i.e., $\Pi G = 0$ and $\Pi e = 1$, where $\Pi = (\Pi_1, \Pi_2)$. From $\Pi G = 0$, we get

$$\Pi_1[G]^{11} + \Pi_2[G]^{21} = 0$$
$$\Pi_1[G]^{12} + \Pi_2[G]^{22} = 0$$

On solving the above two equations, one can get $\Pi_2 = -\Pi_1[G]^{12}[G]^{22^{-1}}$. Using Π_2 value is $\Pi e = 1$, we get

$$\Pi_1 = [1 - [G]^{12}[G]^{22^{-1}}]^{-1}$$
$$\Pi_2 = -[1 - [G]^{12}[G]^{22^{-1}}]^{-1}[G]^{12}[G]^{22^{-1}}$$

3.2 Computation of Steady State Vectors

The limiting distribution for the defined model is
$$\pi_i^{(j,k)} = \lim_{t \to \infty} Pr[N(t) = i, \zeta(t) = j, L(t) = k | N(0), \zeta(0), L(0)]$$

where $\pi_i^{(j,k)}$ is the probability of ith demand at j^{th} state with k inventories. These probabilities are shortly represented as π_i. "The limiting distribution is given by $\pi_i = \pi_0 R^i, i \geq 1$, where R is the minimal non-negative solution of the matrix-quadratic equation $R^2 B + RA + C = 0$."

For finding π_0 and π_1, we have from $\pi P = 0$,
$$\pi_1 = -\pi_0 C(A + RB)^{-1} = \pi_0 w,$$

where
$$w = -C(A + RB)^{-1}.$$

Further, $\pi_0 A_0 + \pi_1 B = 0, i.e., \pi_0(A_0 + wB) = 0$.

First take π_0 as the limiting distribution of $A_0 + wB$. Then π_i, for $i \geq 1$ can be found using

M. L. Soujanya, P. Vijaya Laxmi, E. Sirisha
IMPACT OF NEGATIVE ARRIVALS AND MULTIPLE WORKING
VACATION ON DUAL SUPPLIER INVENTORY MODEL…

RT&A, No 1 (61)
Volume 16, March 2021

$\pi_1 = \pi_0 w, \pi_i = \pi_1 R^{i-1}, i \geq 2$. Therefore the limiting distribution of the system is obtained as follows.

$$(\pi_0 + \pi_1 + \pi_2 + \cdots)e = \pi_0(1 + w(I - R)^{-1})e.$$

4 System performance measures

1. Percentage of server busy period is
$$P_b = \sum_{i=1}^{\infty} \sum_{k=1}^{S} \pi_i^{(1,k)} * 100.$$

2. Percentage of server working vacation period is
$$P_v = \sum_{i=1}^{\infty} \sum_{k=0}^{S} i\pi_i^{(2,k)} * 100.$$

3. **Average inventory level:** The average inventory level (E_{IL}) is defined as
$$E_{IL} = \sum_{i=0}^{\infty} \sum_{k=1}^{S} k\pi_i^{(1,k)} + \sum_{i=1}^{\infty} \sum_{k=0}^{S} \pi_i^{(2,k)}.$$

4. **Average service rate:** The average service rate is defined as
$$E_{SR} = \sum_{i=0}^{\infty} \sum_{k=1}^{S} [\mu_b \pi_i^{(1,k)} + \mu_v \pi_i^{(2,k)}].$$

5. **Average server vacation period:** Average server vacation period (E_{SV}) is
$$E_{SV} = \sum_{i=0}^{\infty} \sum_{k=0}^{S} \beta \pi_i^{(2,k)}.$$

6. **Average negative arrivals:** Average negative arrivals (E_{NA}) is defined as
$$E_{NA} = \sum_{i=0}^{\infty} \sum_{k=1}^{S} q\lambda[\pi_i^{(1,k)} + \pi_i^{(2,k)}].$$

7. **Average arrival rate:** The average arrival rate (E_{AR}) is defined as
$$E_{AR} = \sum_{i=1}^{\infty} \sum_{k=1}^{S} p\lambda[\pi_i^{(1,k)} + \pi_i^{(2,k)}].$$

8. **Average replenishment rate from 1st supplier:** The average replenishment rate from 1st supplier (E_{RR_1}) is
$$E_{RR_1} = \sum_{i=0}^{\infty} \sum_{k=1}^{r} \eta_1 \pi_i^{(1,k)} + \sum_{i=0}^{\infty} \sum_{k=0}^{r} \eta_1 \pi_i^{(2,k)}.$$

9. **Average replenishment rate from 2nd supplier:** The average replenishment rate from 2nd supplier (E_{RR_2}) is
$$E_{RR_2} = \sum_{i=0}^{\infty} \sum_{k=1}^{s} \eta_2 \pi_i^{(1,k)} + \sum_{i=0}^{\infty} \sum_{k=0}^{s} \eta_2 \pi_i^{(2,k)}$$

10. **Average lifetime:** The average lifetime (E_{FR}) is defined as
$$E_{FR} = \sum_{i=0}^{\infty} \sum_{k=1}^{S} k\gamma[\pi_i^{(1,k)} + \pi_i^{(2,k)}].$$

4.1 Cost analysis

Let

C_{S_1} = Setup cost from the 1st supplier,

C_{S_2} = Setup cost from the 2nd supplier,

C_H = Holding cost,

C_F = Failure cost,

C_N = Loss due to negative arrivals,

C_V = Fixed cost when the server is on vacation,

C_A = Fixed cost for arrivals,

C_{ST} = service cost.

Therefore, the total average cost is defined as

M. L. Soujanya, P. Vijaya Laxmi, E. Sirisha
IMPACT OF NEGATIVE ARRIVALS AND MULTIPLE WORKING
VACATION ON DUAL SUPPLIER INVENTORY MODEL…

RT&A, No 1 (61)
Volume 16, March 2021

$$TC(s,r) = \begin{cases} C_{S_1}E_{RR_1} + C_{S_2}E_{RR_2} + C_H E_{IL} + C_F E_{PR} + \\ C_N E_{NA} + C_V E_{SV} + C_A E_{AR} + C_{ST} E_{ST}. \end{cases}$$

5 Numerical analysis

For this section, let us fix the parameters as $S = 14, p = 0.6, q = 0.4, \lambda = 2.3, \mu_b = 1.2, \mu_v = 0.8, \eta_1 = 0.4, \eta_2 = 4.7\gamma = 0.2, \beta = 1.2$.
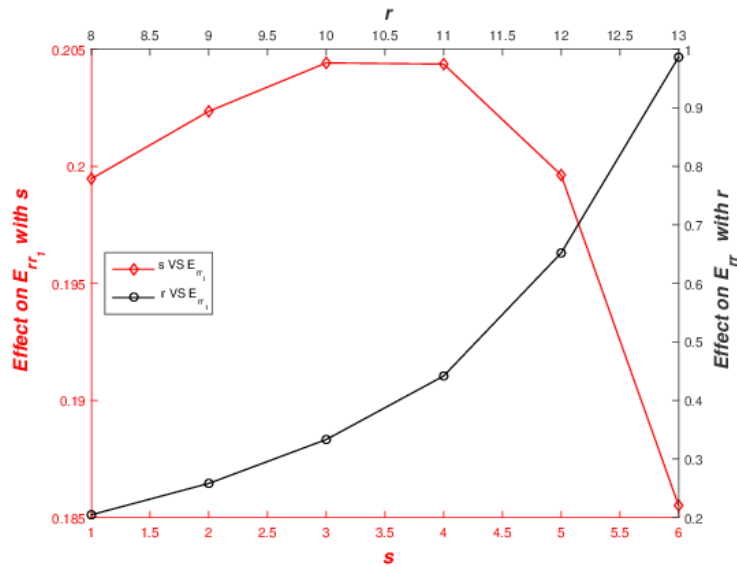
Figure 1: Effect of (s,r) on E_{RR_1}

Figure 1 presents the effect of reordering points (s,r) on the Average replenishment rate of the first supplier (E_{RR_1}). Since E_{RR_1} is effected with r, it rises as r rises and drops as s rises.
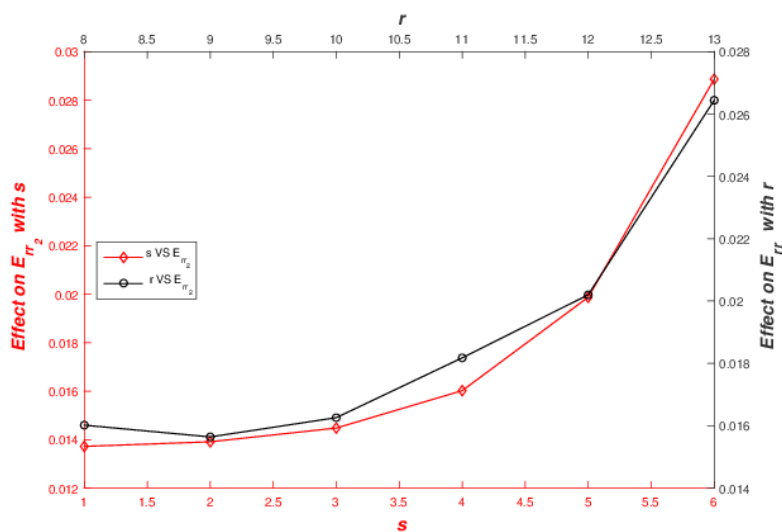
Figure 2: Effect of (s,r) on E_{RR_2}

M. L. Soujanya, P. Vijaya Laxmi, E. Sirisha
IMPACT OF NEGATIVE ARRIVALS AND MULTIPLE WORKING
VACATION ON DUAL SUPPLIER INVENTORY MODEL…

RT&A, No 1 (61)
Volume 16, March 2021

Figure 2 presents the effect of reordering points (s, r) on the Average replenishment rate of the second supplier (E_{RR_2}). Even though E_{RR_2} is effected with s, the second replenishment order is placed after the first replenishment order is done. Due to this E_{RR_2} increases with the increase in both s and r as show in Figure 2
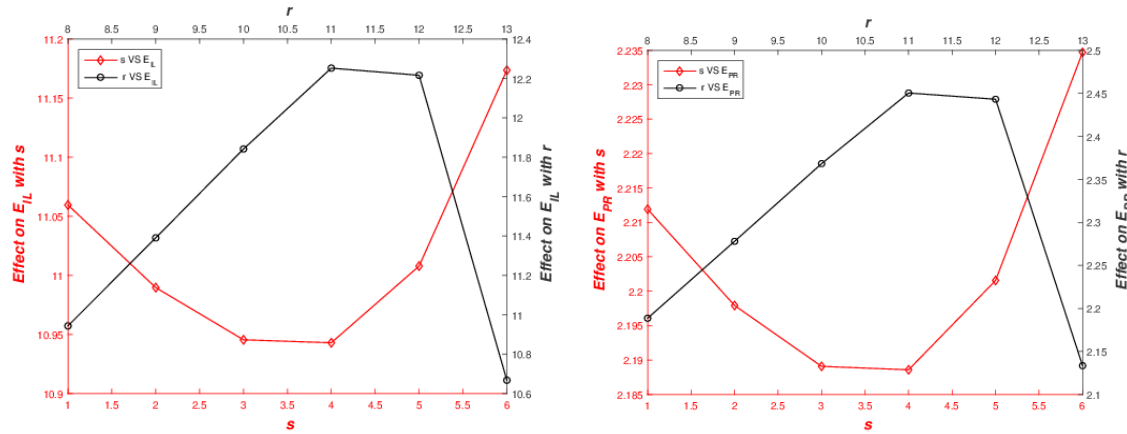
Figure 3: Effect of (s, r) on the E_{IL} Figure 4: Effect of (s, r) on the E_{PR}

The effect (s, r) on E_{IL} and E_{PR} are shown in Figure 3 and Figure 4 respectively. According to our assumption $s < S - r$, first order is placed if inventory falls to r. Also $\eta_2 > \eta_1$, replenishment time of the first supplier is greater than that of the second supplier. Due to this E_{IL} and E_{PR} increases up to $r = 11(rvsE_{IL}$ and $rvsE_{PR})$ and from $s = 4(svsE_{IL}$ and $svsE_{PR})$ which is evident from figures 3 and 4.

Table 1: Values of s^*, r^* and $TC(s^*, r^*)$

Case 1	(s^*, r^*)	(4,8)	(3,9)	(3,10)	(5,11)	(4,12)
	$TC(s^*, r^*)$	684.852	690.974	696.967	703.395	705.422
Case 2	(s^*, r^*)	(4,8)	(3,9)	(3,10)	(5,11)	(4,12)
	$TC(s^*, r^*)$	686.896	693.546	700.301	707.848	711.938
Case 3	(s^*, r^*)	(4,8)	(3,9)	(3,10)	(5,11)	(4,12)
	$TC(s^*, r^*)$	684.948	691.060	697.054	703.518	705.543
Case 4	(s^*, r^*)	(4,8)	(3,9)	(3,10)	(5,11)	(4,12)
	$TC(s^*, r^*)$	903.71	918.745	933.036	947.758	949.734
Case 5	(s^*, r^*)	(4,8)	(3,9)	(3,10)	(5,11)	(4,12)
	$TC(s^*, r^*)$	700.172	706.918	713.492	720.500	722.524
Case 6	(s^*, r^*)	(4,8)	(3,9)	(3,10)	(5,11)	(4,12)
	$TC(s^*, r^*)$	586.104	592.269	598.219	604.647	606.674
Case 7	(s^*, r^*)	(4,8)	(3,9)	(3,10)	(5,11)	(4,12)
	$TC(s^*, r^*)$	684.575	690.697	696.690	703.118	705.114
Case 8	(s^*, r^*)	(4,8)	(3,9)	(3,10)	(5,11)	(4,12)
	$TC(s^*, r^*)$	388.608	394.730	400.723	407.151	409.178
Case 9	(s^*, r^*)	(4,8)	(3,9)	(3,10)	(5,11)	(4,12)
	$TC(s^*, r^*)$	678.421	684.543	690.536	696.964	698.991

Table 1 gives s^* and r^* that minimize $TC(s, r)$, for different numerical examples which are defined as the following cases.

1. $C_{S_1} = 10, C_{S_2} = 14, C_H = 10, C_F = 13, C_N = 150, C_V = 100, C_A = 250, C_{ST} = 20$
2. $C_{S_1} = 20, C_{S_2} = 14, C_H = 10, C_F = 13, C_N = 150, C_V = 100, C_A = 250, C_{ST} = 20$

M. L. Soujanya, P. Vijaya Laxmi, E. Sirisha
IMPACT OF NEGATIVE ARRIVALS AND MULTIPLE WORKING
VACATION ON DUAL SUPPLIER INVENTORY MODEL...

RT&A, No 1 (61)
Volume 16, March 2021

3. $C_{S_1} = 10, C_{S_2} = 20, C_H = 10, C_F = 13, C_N = 150, C_V = 100, C_A = 250, C_{ST} = 20$

4. $C_{S_1} = 10, C_{S_2} = 14, C_H = 30, C_F = 13, C_N = 150, C_V = 100, C_A = 250, C_{ST} = 20$

5. $C_{S_1} = 10, C_{S_2} = 14, C_H = 10, C_F = 20, C_N = 150, C_V = 100, C_A = 250, C_{ST} = 20$

6. $C_{S_1} = 10, C_{S_2} = 14, C_H = 10, C_F = 13, C_N = 50, C_V = 100, C_A = 250, C_{ST} = 20$

7. $C_{S_1} = 10, C_{S_2} = 14, C_H = 10, C_F = 13, C_N = 150, C_V = 50, C_A = 250, C_{ST} = 20$

8. $C_{S_1} = 10, C_{S_2} = 14, C_H = 10, C_F = 13, C_N = 150, C_V = 100, C_A = 50, C_{ST} = 20$

9. $C_{S_1} = 10, C_{S_2} = 14, C_H = 10, C_F = 13, C_N = 150, C_V = 100, C_A = 250, C_{ST} = 15$

Table 1 gives s^* and r^* that minimize $TC(s, r)$. One can observe that the optimum reorder points in all the cases is $r = 8$ for the first supplier and $s = 3$ for the second supplier. We know that the average inventory level is more when compared to other performance measures discussed in Section 4. However the total cost function increases with increase in holding cost which is evident form Case 4. Cost values are minimum in Case 8 due to decrease in the fixed cost per unit arrival. Also, cost value rises with the increase in the reordering point of the first supplier.

Conclusion

In this paper, some investigations are done on the impact of two suppliers on an inventory model having negative arrivals, finite lifetimes and multiple working vacations. The main motive of this paper is to place an order for inventory using two suppliers instead of a single supplier. The limiting distribution of the assumed model is derived. Various system performance parameters are discussed and analyzed assumed cost function to obtain s^* and r^*. Later, one can extend this paper with multi supply inventory models.

Funding

Declaration of Conflicting Interests

The Authors declare that there is no conflict of interest.

References

[1] Dinesh S. and Roberts R. (2017). Inventory models for perishable items and style goods. *Problems & Solutions in Inventory Management*, 233–250.

[2] Jayaraman R., Sivakumar B. and Arivarignan G. (2012). A perishable inventory system with postponed demands and multiple server vacations, *Modelling and Simulation in Engineering*, **2012**, Article ID 620960, 17 pages. 2012.

[3] Manual P., Sivakumar B. and Arivarignan G. (2007). A perishable inventory system with service facilities, MAP arrivals and PH-service time. *Journal of Systems Science and Systems Engineering*, 16, 62–73.

[4] Manual P., Sivakumar B. and Arivarignan G.(2007). Perishable inventory systems with postponed demands and negative customers. *Journal of Applied Mathematics and Decision Science*, 1–12.

[5] Periyasamy C.(2013). A finite source perishable inventory system with retrial demands and multiple server vacations, *International Journal of Engineering Research & Techology*, 2(10), 3802–3815.

[6] Sivakumar B. and Arivarignan G.(2005). A perishable inventory system with service facilities and negative customers, *Advance Modelling Optimization, 7, 193–210.*

[7] Sushil Kumar and Ravendra Kumar. (2015). A deterministic inventory model for perishable items with time dependent demand and shortages. *International Journal of Mathematics And its Applications*, 3(4-F), 105–111.

M. L. Soujanya, P. Vijaya Laxmi, E. Sirisha
IMPACT OF NEGATIVE ARRIVALS AND MULTIPLE WORKING
VACATION ON DUAL SUPPLIER INVENTORY MODEL…

RT&A, No 1 (61)
Volume 16, March 2021

[8]   Vijayashree M. and Uthaykumar R. (2016). Two-Echelon supply chain inventory model with controllable lead time, *International Journal of System Assurance Engineering and Management*, 7, 112–125.

[9]   Vijaya Laxmi P. and Soujanya M. L. (2017). Perishable inventory model with retrial demands, negative customers and multiple working vacations, *International Journal of Mathematical Modelling and Computations*, 7(4), 239–254.

[10]   Vijaya Laxmi P. and Soujanya M. L. (2017). Retrial inventory model with negative customers and multiple working vacations, *International Journal of Management Sciences and Engineering Management*, 12(4), 237–244.

[11]   Vijaya Laxmi P. and Soujanya M. L. (2018). Perishable inventory model with *MAP* arrivals, retrial demands and multiple working vacations, *International Journal of Inventory Research*,5(2).

[12]   Yang M. F. and Wei-Chung, Three-Echelon inventory model with permissible delay in payments under controllable lead time and backorder consideration, *Mathematical Problems in Engineering*, 2014, Artical ID: 809149, 16 Pages.

[13]   Yonguri Duan, Guiping Li, James M. (2012). Tien and Jiazhen Huo, Inventory models for perishable items with inventory level dependent demand rate, *Applied Mathematicall Modelling*, 36(10), 5015–2028.

Accuracy and Precision Requirements in Probability Models

Zinovi Krougly

•

Department of Applied Mathematics,
Western University, London, Ontario, Canada N6A5B7
e-mail: zkrougly@uwo.ca

Abstract

Numerical Laplace transform and inverse Laplace transform is a challenging task in queueing theory and others probability models. A double transformation approach is used to find stable, accurate, and computationally efficient methods for performing the numerical Laplace and inverse Laplace transform. To validate and improve the inversion solution obtained, direct Laplace transforms are taken of the numerically inverted transforms to compare with the original function. Algorithms provide increasing accuracy as precision level increases. The most promising methods were applied to computational probability models, when there are no closed-form solutions of the Laplace transform inversion.The computational efficiency compared to precision levels is demonstrated for different service models in $M/G/1$ queuing systems.

Keywords: Numerical Laplace Transform, Numerical Laplace Transform Inversion, High Precision Computation, Applications in Probability Models

1 Introduction

Numerical inverting of Laplace transform to get various performance measures is an important techniques in queueing theory and related stochastic models [1], [6], [16]. Laplace transform techniques may simplify the task of solving systems of differential equations [5], and can be considered in terms of typical applications [4], [8].

Inverting the Laplace transform is a challenging task. This challenge faced in many application areas including the finding of various performance measures in queueing and related probability models [1], [6], [16].

Several algorithms have been proposed for numerical Laplace transforms inversion, see for instance the surveys in [4] and [13]. The Gaver-Stehfest algorithm [18] is one of the most powerful algorithms for this purpose. The convergence of this algorithm has been examined in [14]. Unfortunately despite its theoretical advantages, in many practical applications, numerical approximation often encounters numerical accuracy problems [1], [9], [11], [12], [13], [15]. As such, small rounding errors in computation in standard double arithmetic may significantly corrupt the results, rendering these algorithms impractical to apply. With extended precision, we are able to add additional significant figures, and produce results that converge to the solution.

We used C++ and Matlab numerical class library [10], [12] and applied ARPREC, Arbitrary precision computation package [3], for numerical implementation of Laplace transform and inversions.

In [9] has been introduced double transformation approach which perform computationally efficient methods for inverse Laplace transform. Challenging numerical examples involving periodic and oscillatory functions, are investigated. It was found that the number of

expansion terms and precision level selected must be in a harmonious balance in order for correct and stable results to be obtained. In this paper we examine the stability and accuracy of the Laplace transform inversion by the Gaver-Stehfest algorithm [18]. The numerical results were first compared to known analytical solutions. The most interesting methods were then applied to computational probability models, where the solution requires numerical Laplace transform inversion. For computation efficiency a composite Simpson's rule is implemented for the numerical direct Laplace transform [9]. The numerical examples illustrate the computational accuracy and efficiency of the direct Laplace transform and its inverse due to increasing precision level (N) and the number of terms (L) included in the expansion. The remainder paper is organized as follows. In general, we use lowercase letters to denote the function $f(t)$ to be transformed, and the uppercase letter $C(s)$ to denote its Laplace transform, for example $\mathcal{L}\{f(t)\} = C(s)$. If the closed form of $C(s)$ inversion is unknown, we compare the original $C(s)$ and numerical solution $\tilde{\tilde{C}}(s)$ after double transformation. The results are illustrated in the plots and error estimations.

In Section 2, a brief description and notation of the underlying theory is given. In section 3 introduced numerical computation of the direct Laplace transform by composite Simpson's rule. In section 4 defined numerical Laplace double transformation technique. Section 5, 6 and 7 illustrated challenges numerical examples and the role of high precision arithmetic in application for probability models. Numerical Laplace transform and their inverses, particular for applications in M/D/1 and M/G/1 queue, are given in sections 8, 9 and 10. We examine the stability and accuracy of the Laplace transform inversion and the role that the number of expansion terms and precision level play in the numerical approximation. We discuss the numerical double transformation technique to confirm agreement of the numerical inversion results. Section 11 demonstrates double transformation technique and precision requirement for approximation of waiting time distribution in M/D/1 queue.

2 Numerical Laplace transforms and their inverses

Let $f(t)$ be a function defined for $t \geq 0$. Then the integral

$$\mathcal{L}\{f(t)\} = \int_0^\infty e^{-st} f(t) dt. \tag{2.1}$$

is said to be the Laplace transform of $f(t)$, provided the integral converges. The symbol $\mathcal{L}$ is the Laplace transformation operator, which act on the function $f(t)$ and generates a new function, $C(s) = \mathcal{L}\{f(t)\}$.

If $C(s)$ represents the Laplace transform of a function $f(t)$, that is, $\mathcal{L}\{f(t)\} = C(s)$, then $f(t)$ is the inverse Laplace transform of $C(s)$ and $f(t) = \mathcal{L}^{-1}\{C(s)\}$. The inverse Laplace transform $\mathcal{L}^{-1}\{C(s)\}$ is uniquely determined in the sense that if $C(s) = G(s)$ and $f(t)$ and $g(t)$ are continuous functions, then $f(t) = g(t)$.

The Laplace transform can be inverted either algebraically or numerically. The notation $\tilde{f}(t)$ used for the numerical approximation to $f(t)$ (numerical inversion of the Laplace transform $C(s)$), and $\tilde{C}(s)$ for the numerical Laplace transform of $f(t)$.

If t is the random variable with the probability density function f and the cumulative distribution function F, this gives

$$C(0) = \int_0^\infty e^{-st} dF(t) = \int_0^\infty e^{-st} f(t) dt = 1 \tag{2.2}$$

3 Numerical computation of the direct Laplace transform

To validate and improve the inversion solution obtained by Gaver-Stehfest algorithm, the numerical direct Laplace transform are used for this inversion, to compare it with the original Laplace transform. To insure high accuracy of approximation, numerical direct Laplace transform are implemented [9] by the composite Simpson's Rule [2]. We used a composite Simpson's Rule calculation with large number of subintervals to ensure high accuracy.

The Laplace transform of a function $f(t)$ is defined by (2.1) on the interval $[0, \infty]$. The problem of an infinite upper limit of integration may be removed by the substitution $t = -\ln(u), dt = u^{-1}du$ which replaces infinite by finite limits.

When $t = 0$, $u = 1$ and when $t \to \infty$, $u \to 0$. Then

$$\int_0^\infty e^{-st}f(t)dt = \int_0^1 e^{\ln(u^s)}f(-\ln(u))u^{-1}du = \int_0^1 u^{s-1}f(-\ln(u))du \qquad (3.1)$$

The behaviour of the function to be transformed, needs to be considered at the new limits, and the exponential function inside the integral requires special examination in terms of high accuracy.

3.1 Compute the direct Laplace transform by composite Simpson's rule

For integration over the interval $[a, b]$, an even n is chosen such that the function is adequately smooth over each subinterval $[x_j, x_{j+1}]$ where $x_j = a + jh$ for all $j \in \{0,1,2,\dots,n\}$ with $h = \frac{b-a}{n}$. In particular, $x_0 = a$ and $x_n = b$. Then, the composite Simpson's Rule is given by [2]:

$$\int_a^b f(x)dx \approx \frac{h}{3}\left[f(x_0) + 2\sum_{j=1}^{n/2-1} f(x_{2j}) + 4\sum_{j=1}^{n/2} f(x_{2j-1}) + f(x_n)\right] \qquad (3.2)$$

Applying this to the transformed integrand from the equation (3.1) we get $u_j = jh$ for all $j \in \{0,1,2,\dots,n\}$ with $h = \frac{1}{n}$. Therefore,

$$C(s) \approx \frac{1}{3n}\left[0^{s-1}f(-\ln(0)) + 2\sum_{j=1}^{n/2-1} u_{2j}^{s-1}f(-\ln(u_{2j})) + 4\sum_{j=1}^{n/2} u_{2j-1}^{s-1}f(-\ln(u_{2j-1})) + 1^{s-1}f(-\ln(1))\right]$$
$$(3.3)$$

The basic Simpson's rule formula divides the interval $[a, b]$ of integration into two pieces. To apply the composite Simpson's rule, the interval $[a, b]$ must be divided into an even number of subintervals $n = 2m$. Then $h = \frac{b-a}{n} = \frac{b-a}{2m}$.

4 Numerical Laplace double transformation technique

We define the following double transformation technique for the Laplace transform of the inversion [9]:

$$\tilde{\tilde{C}}(s) = \mathcal{L}\{\mathcal{L}^{-1}\{C(s)\}\} \qquad (4.1)$$

This definition will be used to estimate the accuracy of the Laplace transform inversion, when its closed-form is unknown.

After applying the Laplace transform, the problem is said to be in the Laplace domain and it is denoted as a function of s not t. While calculations might be easier in the Laplace domain, leaving the solution in the Laplace domain is typically not useful. To transform the result back into the time-domain, inverse Laplace transforms are used.

When the analytical answer is unknown, it is difficult to know whether or not the numerical inversion results are accurate. Moreover, it is hard to judge whether or not changes to the method improve or degrade the inversion estimate.

The following steps are used:

1. Begin with the Laplace domain function $C(s)$.

2. Compute the numerical inversion using some set of parameters. In this case, we will control precision level and the number of terms in the approximation. Setting precision level to N_1, we get

$$\hat{f}_{N_1}(t) = \mathcal{L}_{N_1}^{-1}\{C(s)\} \tag{4.2}$$

3. Take the Numerical Laplace Transform of $\hat{f}_{N_1}(t)$, resulting in

$$\mathcal{L}\{\hat{f}_{N_1}(t)\} = \tilde{\hat{C}}_{N_1}(s) \tag{4.3}$$

4. Compare the functions $C(s)$ and $\tilde{\hat{C}}_{N_1}(s)$, and define the error-function as:

$$\varepsilon_{N_1}(s) = |C(s) - \tilde{\hat{C}}_{N_1}(s)| \tag{4.4}$$

5. Repeat the process with some other precision level N_2.

6. Compare $\varepsilon_{N_1}(s)$ and $\varepsilon_{N_2}(s)$. Precision level that provides lower errors is superior, and the difference between the error functions can provide a way of quantifying the accuracy improvement gained from increasing precision level.

To validate and improve the inversion solution obtained by Gaver-Stehfest algorithm, the numerical direct Laplace transform are used for this inversion, to compare it with the original Laplace transform. To insure high accuracy of approximation, numerical direct Laplace transform are implemented [9] by the composite Simpson's Rule [2]. We used a composite Simpson's Rule calculation with large number of subintervals to ensure high accuracy.

5 Testing numerical inversion algorithms in arbitrary precision

This demonstration applies the inverse Laplace transforms of the test functions (Table 1) to various type numerical accuracy.

Given $C(s)$ we want to find $f(t)$ such that the following must hold:

$$C(s) = \int_0^\infty e^{-st} f(t) dt. \tag{5.1}$$

Table 1: Laplace and inverse transforms for test functions used in the numerical calculations

No	$C(s)$	$f(t)$	Function type	Transformation algorithm
1.	$\frac{1}{(1+s/\beta)^\alpha}$	$\frac{\beta^\alpha}{\Gamma(\alpha)}t^{\alpha-1}e^{-t\beta}$	Gamma distribution	$\mathcal{L}^{-1}\{C(s)\}, \mathcal{L}\{\mathcal{L}^{-1}\{C(s)\}\}$
2.	$\frac{1}{\Gamma(\alpha)}\int_0^s t^{\alpha-1}e^{-t}dt$	Closed-form unknown	Incomplete gamma function	$\mathcal{L}^{-1}\{C(s)\}, \mathcal{L}\{\mathcal{L}^{-1}\{C(s)\}\}$
3.	$\exp(-as^\alpha)$	$\delta(t-a)$, if $\alpha = 1$	Shifted Dirac delta function	$\mathcal{L}^{-1}\{C(s)\}, \mathcal{L}\{\mathcal{L}^{-1}\{C(s)\}\}$
4.	$\sum_{i=1}^2 \frac{p_i\mu_i}{\mu_i+s}$	$\sum_{i=1}^2 p_i\mu_i e^{-\mu_i t}$	Hyperexponential distribution	$\mathcal{L}^{-1}\{C(s)\}, \mathcal{L}\{\mathcal{L}^{-1}\{C(s)\}\}$
5.	$\frac{(1-\rho)s}{s-\lambda[1-B^*(s)]}$	Closed-form unknown	$W_q(t)$ in $M/G/1$ models	$\mathcal{L}^{-1}\{C(s)\}, \mathcal{L}\{\mathcal{L}^{-1}\{C(s)\}\}$

Example 1. Find $\tilde{f}_{01} = \mathcal{L}^{-1}\{C_{01}(s)\}$, where

$$C_{01}(s) = 1(1 + s/\beta)^{\alpha} \quad (\beta > 0 \text{ and } \alpha > 0) \tag{5.2}$$

then we know that

$$f_{01}(t) = \beta^{\alpha}\Gamma(\alpha)t^{\alpha-1}e^{-t\beta} \tag{5.3}$$

where $\Gamma(\alpha)$ is the gamma function.

We are reached higher accuracy for the numerical inverting of the function $C_{01}(s) = 1(1 + s/\beta)^{\alpha}$ by multiple precision calculations. The exact inversion is $f_{01}(t) = \beta^{\alpha}\Gamma(\alpha)t^{\alpha-1}e^{-t\beta}$. The results shown in Fig.1 correspond to the parameters $\beta = 1$ and $\alpha = 20$. Fig. 1 illustrate a poor approximation for double precision level (N = 16). The numerical inversion evaluated also with precision level and the number of terms $(N, L) = (32, 32)$. Two screenshots are presented in Fig. 2 for the same function, as in Fig. 1. We see significant improvements in accuracy as precision level increased to 256, at order at least roughly 10^{-73}.
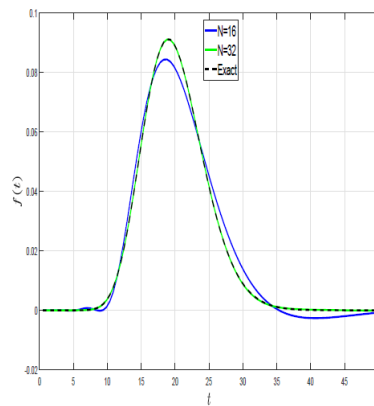
Figure 1: Inverse Laplace transform of the function $C_{01}(s) = 1/(1 + s/\beta)^{\alpha}$ evaluated in double and multiple precision. The exact and numerical solution with precision level N = 32 are indistinguishable to the eye
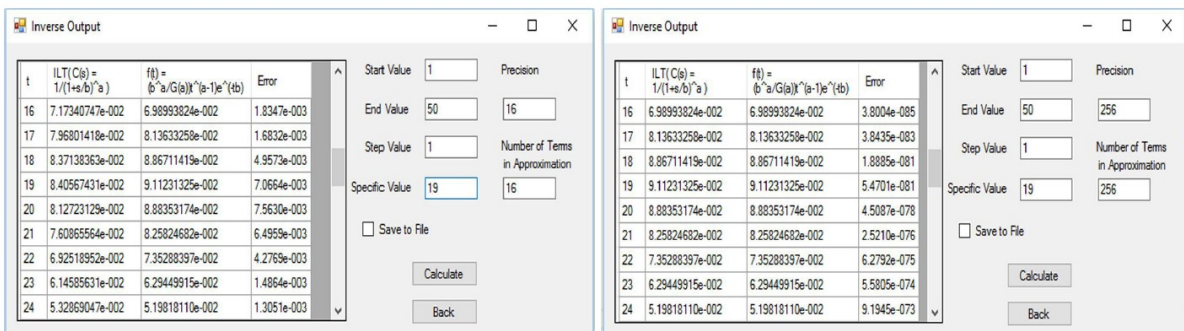
Figure 2: Two screenshots for inverse Laplace transform of the function $C_{01}(s) = 1/(1 + s/\beta)^{\alpha}$ evaluated in double and multiple precision

Numerous examples exists where there are no closed-form solution of the Laplace transform inversion. For such problems we compare numerical solution $\tilde{\tilde{C}}$ (s) after double transformation technique (4.1) with the original Laplace transform $C(s)$.

First we illustrate that double transformation technique in Fig. 3 for the gamma distribution with $\alpha = 1$ (exponential distribution) and $\alpha = 2.5$. Both Laplace transform and inverting worked extremely well. The errors E are the following: 2.5×10^{-5} and 7.45×10^{-4} corresponding to the plots on the left and the right sides.
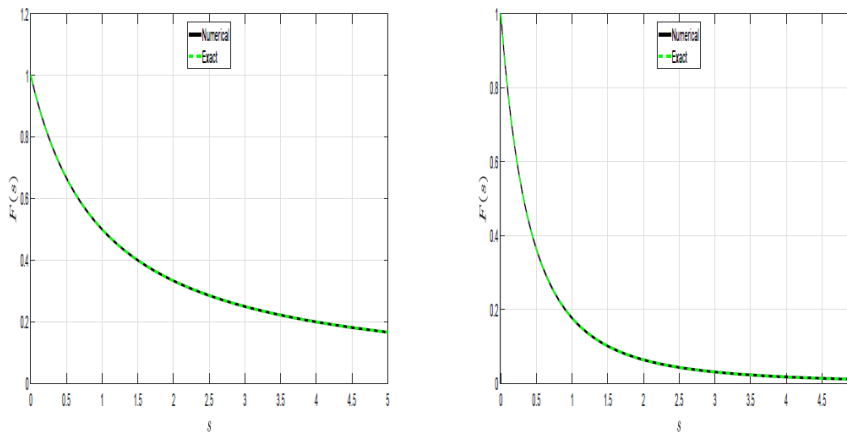
Figure 3: Given the original Laplace transform $C_{01}(s) = 1/(1 + s/\beta)^{\alpha}$. Compute its numerical approximation $\tilde{\tilde{C}}_{01}(s) = \mathcal{L}\{\mathcal{L}^{-1}\{1/(1 + s/\beta)^{\alpha}\}\}$ evaluated for $\beta = 1.0$ and $\alpha = 1.0$ (left plot) and $\alpha = 2.5$ (right plot). The original and numerical solution are indistinguishable to the eye

6 Numerical inverse Laplace transform of the incomplete Gamma function

The following example is quite different from the previous as we cannot express the inverse Laplace transform analytically. The lower incomplete gamma function P and the upper incomplete gamma function Q are defined by

$$P(\alpha, x) = \frac{1}{\Gamma(\alpha)} \int_0^x t^{\alpha-1} e^{-t} dt \qquad (6.1)$$

$$Q(\alpha, x) = \frac{1}{\Gamma(\alpha)} \int_0^\infty t^{\alpha-1} e^{-t} dt \qquad (6.2)$$

We used the normalized definition of the incomplete gamma function, where $P(\alpha, x) + Q(\alpha, x) = 1$

Example 2. We determine $\tilde{f}_{02}(t) = \mathcal{L}^{-1}\{C_{02}(s)\}$ and $\tilde{C}_{02}(s) = \mathcal{L}\{\mathcal{L}^{-1}\{C_{02}(s)\}\}$, where

$$C_{02}(s) = P(\alpha, s) = \frac{1}{\Gamma(\alpha)} \int_0^s t^{\alpha-1} e^{-t} dt, \qquad (6.3)$$

We obtained the approximation (Fig. 4) for the inverting of the function (6.3) with the parameters $\alpha = 1.0$. As easy to prove, the exact solution of inverse Laplace transform is $-\delta(t - 1)$, where $\delta(t)$ is the Dirac delta function (7.1).

Improvements can be effected with increasing the number of precision N from double precision (left plot) to precision level 32 and 64 (right plot). We use the number of terms in approximation equals to precision level, $L = N$. To obtain a more accurate estimate precision levels 500 and 1000 used as displayed in (Fig. 5).
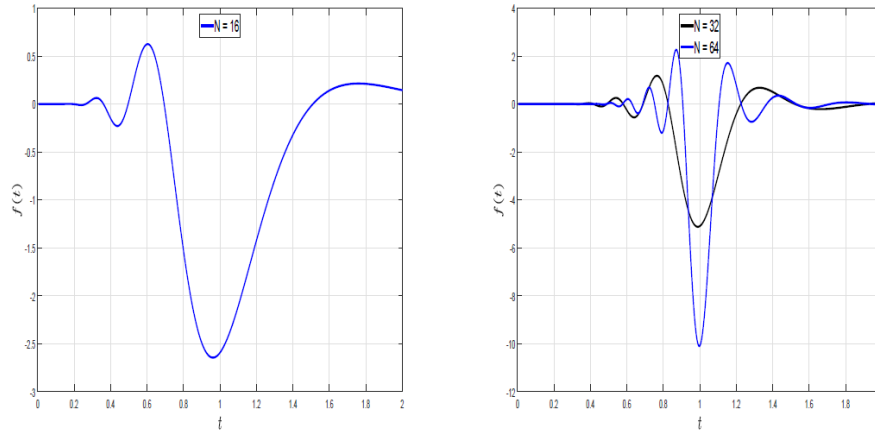
Figure 4: Inverse Laplace transform of the function $C_{02}(s) = \frac{1}{\Gamma(\alpha)} \int_0^s t^{\alpha-1} e^{-t} dt$ in double precision (left plot) and precision level 32 and 64 (right plot). Note that two plots use different scale
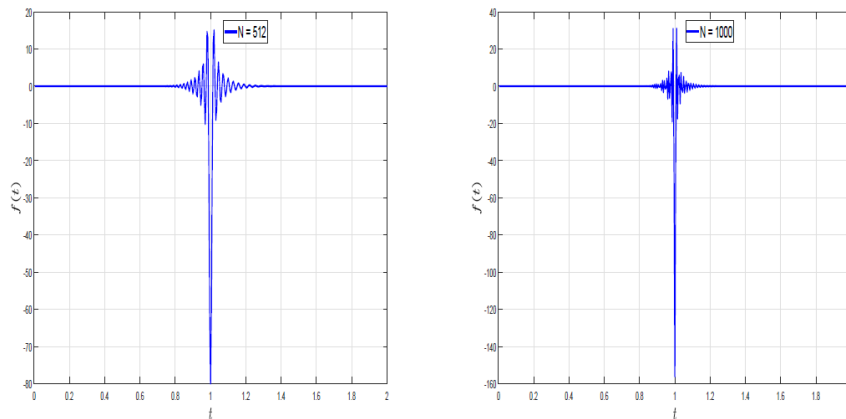
Figure 5: Inverse Laplace transform of the function $C_{02}(s) = \frac{1}{\Gamma(\alpha)} \int_0^s t^{\alpha-1} e^{-t} dt$ in precision level 512 (left plot) and 1000 (right plot). Note that two plots use different scale

The original $C_{02}(s)$ compares with numerical solution $\tilde{\tilde{C}}_{02}(s) = \mathcal{L}\{\mathcal{L}^{-1}\{C_{02}(s)\}\}$ evaluated after double transformation. So, $\tilde{f}_{02}(t)$ computed as numerical inversion of $C_{02}(s)$. Then Laplace transform $\tilde{\tilde{C}}_{02}(s)$ of $\tilde{f}_{02}(t)$ compares with the original function $C_{02}(s)$. The original Laplace transform $C_{02}(s)$ (Exact) and numerical approximation (Numerical) of this double transformation seen in Fig. 6. The following parameters used: α = 0.5, 1, 3 and 5.
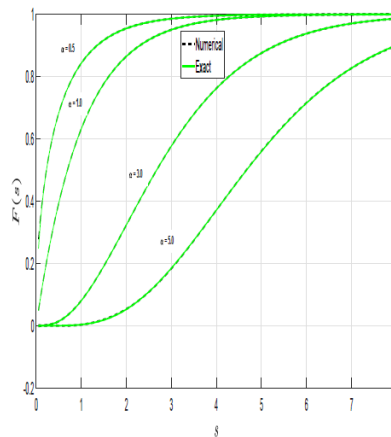
Figure 6: Given the incomplete gamma function $C_{02}(s) = \frac{1}{\Gamma(\alpha)}\int_0^s t^{\alpha-1}e^{-t}dt$. Compute its numerical approximation $\tilde{\tilde{C}}_{02}(s) = \mathcal{L}\{\mathcal{L}^{-1}\{\frac{1}{\Gamma(\alpha)}\int_0^s t^{\alpha-1}e^{-t}dt\}\}$ for values α = 0.5, 1, 3 and 5.

7 Approximation of the Dirac delta function

The Dirac delta function [5] can be loosely thought of as a function on the real line which is zero everywhere except at the origin, where it is infinite,

$$\delta(t) = \begin{pmatrix} +\infty & (t = 0) \\ 0 & (t \neq 0) \end{pmatrix} \qquad (7.1)$$

and which is also constrained to satisfy the identity

$$\int_{-\infty}^{\infty} \delta(t)dt = 1 \qquad (7.2)$$

This is merely a heuristic characterization. The Dirac delta is not a function in the traditional sense as no function defined on the real numbers has these properties. This function can be rigorously defined either as a distribution or as a measure.

Noting that the Dirac delta function can be defined as the limit (in the sense of distributions) of the sequence of zero-centered normal distributions,

$$\delta_a(t) = \frac{1}{a\sqrt{\pi}}e^{-t^2/a^2}, \qquad (7.3)$$

as $a \to 0$.

By analytic continuation of the Fourier transform, the Laplace transform of the delta function is found to be [5],

$$\int_0^\infty e^{-st}\delta(t-a)dt = e^{-as}, \qquad (7.4)$$

consistent with the definition of the Laplace transform of $\delta(t-a)$ as e^{-as}.

Example 3. Find $\tilde{f}_{03}(t) = \mathcal{L}^{-1}\{C_{03}(s)\}$ and $\tilde{C}_{03}(s) = \mathcal{L}\{\mathcal{L}^{-1}\{C_{03}(s)\}\}$, where

$$C_{03}(s) = \exp(-as^\alpha) \quad (a > 0 \text{ and } \alpha \in (0,1]) \qquad (7.5)$$

The expression of the inverse Laplace transform, in terms of standard mathematical functions, is unknown. We can handle the inverse Laplace transform and double transformation technique, including Dirac delta function and its shifted form.

So, if $\alpha = 1$, then $f(t) = \delta(t - a)$, where $\delta(t)$ is the Dirac delta function [5].

Mathematica gives for $a = 0.5$ and $\alpha = 0.5$

$$\mathcal{L}^{-1}\{\exp(-as^\alpha)\} = \frac{0.14104739588693907\exp(-0.0625/t)}{t^{3/2}}. \tag{7.6}$$

Numerical inversion of Laplace transform $C_{03}(s) = e^{-as}$ is known to be equivalent to the approximation of the Dirac delta function. Fig. 7 illustrates the approximation of the Dirac delta function with parameter $a = 1$ evaluated in double precision. On the left plot used equal number of terms and precision level $L = N$. This approximation take negative values while the delta function is strictly positive. On the right plot $N = 16$ and $L = 64$. When looking at numerical inversion, it is important to note the accuracy with a varying number of expasion terms and precision level. We compare the inverses using Gaver-Stehfest implementation and observe the accuracy of the inversions as we increase the number of the expansion terms and precision level. However, there exists a limit to adding additional terms [12]. As we increase the number of expansion terms using $L = 64$ we quickly discover that the numerical inversion becomes unstable and our function is dominated by numerical error (right plot).
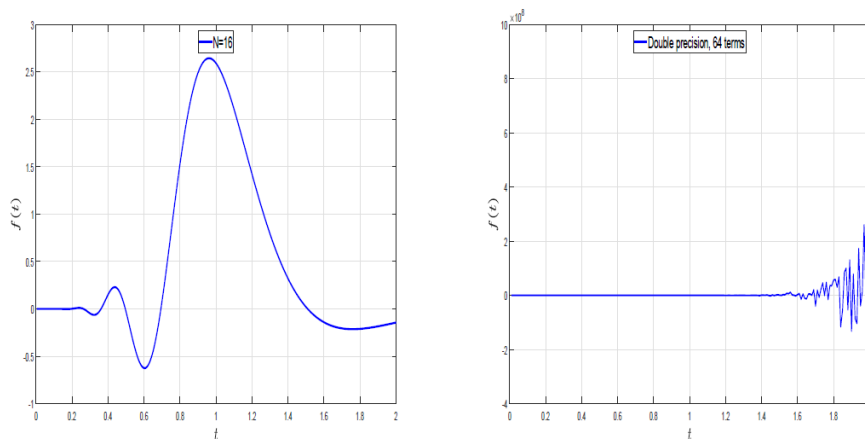
Figure 7: Approximation of the Dirac delta function, $a = 1$, in double precision. Precision level N and the number of expansion terms N are (16, 16) (left plot) and (16, 64) (right plot)

Extended precisions (Fig. 8) allow to combat the numerical limitation that we experience when dealing with double precision. Thus, we can use a larger number of terms. These examples use equal number of terms and precision level $L = N$. To improve the accuracy of the approximation we extended precision level to 32, 64, 128, 512 and 1000.
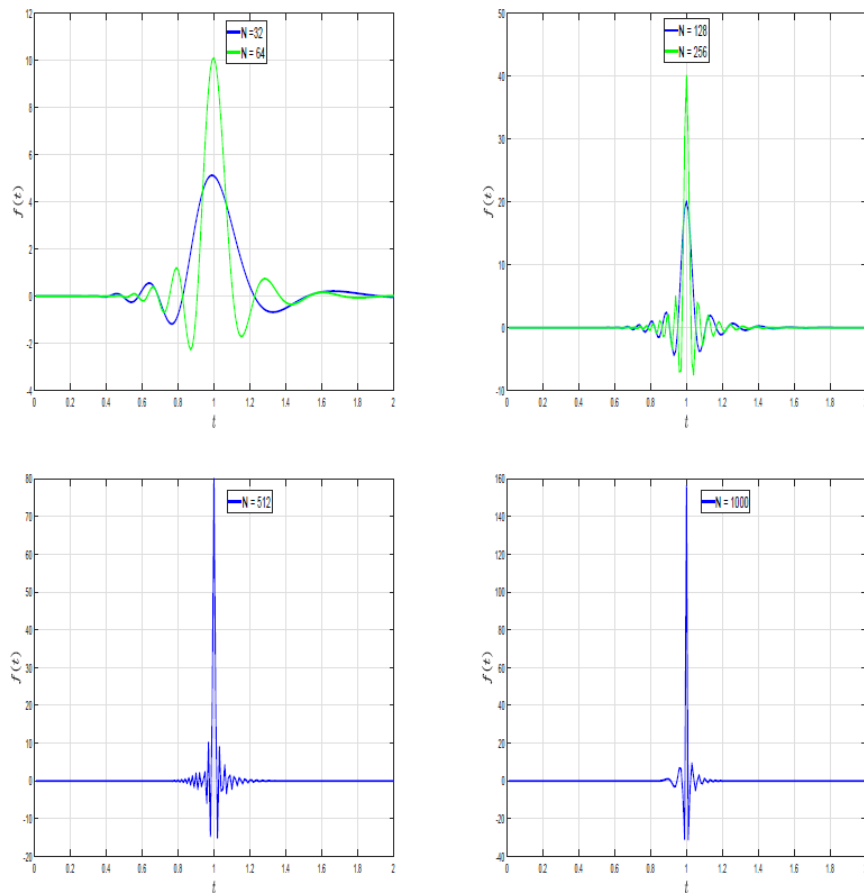
Figure 8: Approximation of the Dirac delta function, a = 1. Precision level N and number of terms L are equal, $N = L$: 32, 64, 128, 256, 512 and 1000. Note the difference in scales seen in four plots

In Fig. 9 are shown Inverse Laplace transform (left plot) and Numerical Laplace double transformation (right plot) of $C_{03}(s) = \exp(-as^\alpha)$ evaluated for a = 0.5 and α = 0.5. The analytical solution of the inverse Laplace transform are given by (7.6). The approximation are given in double precision, and the errors are: $E = 6.6 \times 10^{-4}$ and 1.3×10^{-2} corresponding to the left and to the right plot. In Fig. 10 presented the screenshot for Laplace transform inversion of $C_{03}(s) = \exp(-as^\alpha)$ evaluated for the same a and α with precision level 64. Note the accuracy of approximation improved at the order of at least 10^{-18}.
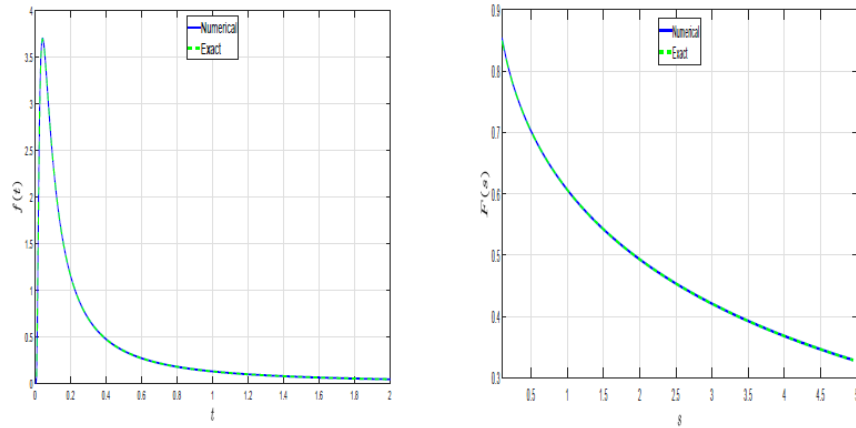
Figure 9: Given the original Laplace transform $C_{03}(s) = \exp(-as^{\alpha})$. Compute its inverse Laplace transform (left plot) and numerical approximation $\tilde{\tilde{C}}_{03}(s) = \mathcal{L}\{\mathcal{L}^{-1}\{\exp(-as^{\alpha})\}\}$ (right plot)
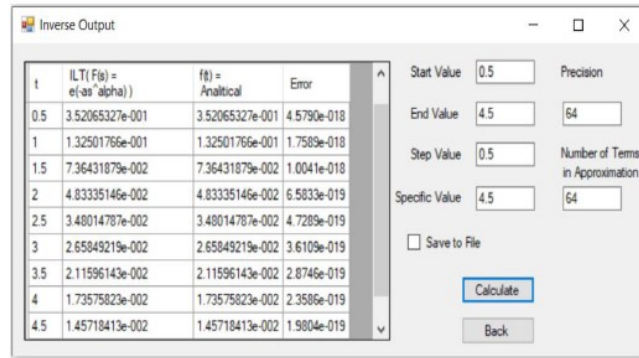
Figure 10: The screenshot for inverse Laplace transform of the function $C_{03} = \exp(-as^{\alpha})$, evaluated for $a = 0.5$ and $\alpha = 0.5$ with precision level 64

Tab. 2 displays numerical error $\varepsilon_{03}(s) = |C_{03}(s) - \tilde{\tilde{C}}_{03}(s)|$ for the numerical approximation $\tilde{\tilde{C}}_{03}(s) = \mathcal{L}\{\mathcal{L}^{-1}\{\exp(-as^{\alpha})\}\}$, evaluated for $a = 0.5$ and $\alpha = 0.5$, in varying precision levels of 16 and 64.

Table 2: Numerical error $\varepsilon_{03}(s) = |C_{03}(s) - \tilde{\tilde{C}}_{03}(s)|$ for the numerical approximation $\tilde{\tilde{C}}_{03}(s) = \mathcal{L}\{\mathcal{L}^{-1}\{\exp(-as^{\alpha})\}\}$, evaluated for $a = 0.5$ and $\alpha = 0.5$, in varying precision levels of 16 and 64. Values 9.23e-6 $\equiv 9.23 \times 10^{-6}$

s	Numerical	Error	Error
	Solution	L = 16	L = 64
0.5	0.7022	9.23e-6	2.76e-6
1	0.6065	4.03e-7	9.13e-10
2	0.4931	6.81e-7	3.51e-17
3	0.4206	4.38e-7	3.69e-23
4	0.3679	7.82e-8	1.97e-24
5	0.3269	2.25e-7	3.94e-25

8 Waiting times distribution in $M/G/1$ queue

The $M/G/1$ model assumes Poisson arrival at rate λ to a single server with generally distributed service time S. The coefficient of variation c_S of S defined by $c_S = \sigma/b$, where $b = E[S]$ and σ are the expectation and the standard deviation of S.

If $c_S = 1$, we have M/M/1 model with $B^*(s) = \mu/(\mu + s)$.

The PDF and CDF of waiting time simplified to [17]

$$w_q(t) = \mu(1 - \rho)e^{-\mu(1-\rho)t}, t \geq 0, \quad PDF, \quad M/M/1 \tag{8.1}$$

$$W_q(t) = 1 - \rho e^{-\mu(1-\rho)t}, t \geq 0, \quad CDF, \quad M/M/1 \tag{8.2}$$

If the coefficient $c_S > 1$ an approximation can be effective provided by hyperexponential distribution using for it the definition by parallel stages.

Let the service time S follows a hyperexponential H_2 distribution whose PDF is given by (9.2), and the CDF is defined by (9.3).

The Laplace transform of the PDF is given by (9.1). This gives the Laplace transform of the CDF

$$F(s) = C(s)/s = \frac{1}{s}\sum_{i=1}^{2} \frac{p_i\mu_i}{\mu_i+s} \tag{8.3}$$

First and second derivatives of $C(s)$ are:

$$\frac{dC(s)}{ds} = -\sum_{i=1}^{2} \frac{p_i\mu_i}{(\mu_i+s)^2} \tag{8.4}$$

$$\frac{d^2C(s)}{ds^2} = 2\sum_{i=1}^{2} \frac{p_i\mu_i}{(\mu_i+s)^3} \tag{8.5}$$

The expectation $E[S] = -\frac{dC(s)}{ds}\big|_{s=0}$ and the variance $Var[S] = E[S^2] - (E[S])^2$ of the random variable S are the following:

$$E[S] = \frac{p_1}{\mu_1} + \frac{p_2}{\mu_2} \tag{8.6}$$

$$Var[S] = \frac{p_1(2-p_1)}{\mu_1^2} + \frac{p_2(2-p_2)}{\mu_2^2} - \frac{2p_1p_2}{\mu_1\mu_2} \tag{8.7}$$

$$E[S^2] = \frac{d^2C(s)}{ds^2}\big|_{s=0} = \frac{2p_1}{\mu_1^2} + \frac{2p_2}{\mu_2^2} \tag{8.8}$$

To satisfy the condition (8.6), let

$$\mu_1 = 2p_1 E[S], \quad \mu_2 = 2p_2 E[S] \tag{8.9}$$

Substituting (8.6), (8.8) and (8.9) in $c_S^2 = \frac{(\sigma[S])^2}{(E[S])^2} = \frac{E[S^2]-(E[S])^2}{(E[S])^2}$, this gives the unique H_2 PDF [6]:

$$p_1 = \frac{1}{2}\left(1 + \sqrt{\frac{c_S^2-1}{c_S^2+1}}\right), p_2 = 1 - p_1, \mu_1 = \frac{2p_1}{E[S]}, \mu_2 = \frac{2p_2}{E[S]} \tag{8.10}$$

9 Solving performance measures in $M/H_2/1$ queue

Example 4. Two cases consider for this $M/G/1$ queue example.

Case 1. Laplace transform are given for PDF of the service time distribution.

Find $\tilde{f}_{04}(t) = \mathcal{L}^{-1}\{C_{04}(s)\}$ and $\tilde{C}_{04}(s) = \mathcal{L}\{\mathcal{L}^{-1}\{C_{04}(s)\}\}$, where

$$C_{04}(s) = \sum_{i=1}^{2} \frac{p_i \mu_i}{\mu_i + s}, \quad (0 \le p_1 \le 1, 0 \le p_2 \le 1, p_1 + p_2 = 1), \tag{9.1}$$

$$f_{04}(t) = \sum_{i=1}^{2} p_i \mu_i e^{-\mu_i t} \quad (t > 0). \tag{9.2}$$

Case 2. Identical to case 1, but now for CDF.

Find $\tilde{F}_{04}(t) = \mathcal{L}^{-1}\{F_{04}(s)\}$ and $\tilde{F}_{04}(s) = \mathcal{L}\{\mathcal{L}^{-1}\{F_{04}(s)\}\}$, where

$$F_{04}(s) = C_{04}(s)/s = \frac{1}{s}\sum_{i=1}^{2} \frac{p_i \mu_i}{\mu_i + s} \tag{9.3}$$

$$F_{04}(t) = 1 - \sum_{i=1}^{2} p_i e^{-\mu_i t}, \quad (t > 0). \tag{9.4}$$

Several cases were considered for $M/G/1$ queue example. First is for Laplace transform of the PDF for service time distribution. Second is identical but for CDF. The $M/G/1$ queue describes with $\lambda = 0.8$, the expectation $E[S] = 1$, and the coefficient of variation c_s = 1.5, 2.5 and 4.5. In Fig. 11 are shown inverse Laplace transform of the function $C_{04}(s)$, evaluated for the PDF (left plot), and inverse Laplace transform $C_{04}(s)/s$ evaluated for the CDF (right plot). The errors are: $E = 3.52 \times 10^{-5}$ (left plot) and $E = 1.2 \times 10^{-5}$ (right plot).
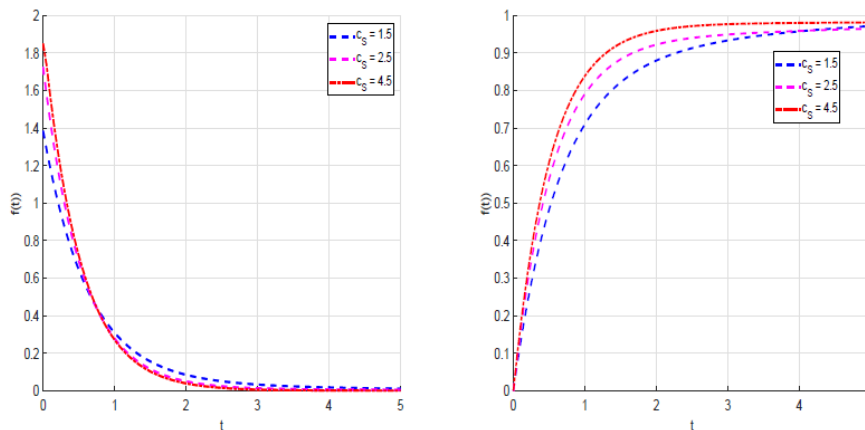
Figure 11: Inverse Laplace transform of the functions $C_{04}(s)$, evaluated for the PDF (left plot), and for $C_{04}(s)/s$ evaluated for the CDF (right plot). The $M/G/1$ queue has $\lambda = 0.8$, the expectation $E[S] = 1.0$, and the coefficients of variation c_s = 1.5, 2.5 and 4.5.

10 Waiting time distribution in M/D/1 queues

Let service times has E_k density with mean $1/\mu$ and PDF

$$f(t) = \frac{(\mu k)^k t^{k-1} e^{-k\mu t}}{(k-1)!} \quad (0 < t < \infty) \tag{10.1}$$

and LST

$$B^*(s) = \left(\frac{\mu k}{s+\mu k}\right)^k \tag{10.2}$$

The model M/D/1 can be considered as a limited case of $M/E_k/1$. As $k \to \infty$ and $\mu \to \infty$ in such a way that $k\mu^{-1} \to b$ $(0 < b < \infty)$ then E_k service times are deterministic with the constant b. The traffic intensity $\lambda b < 1$. Now $B^* \to e^{-bs}$ as $k \to \infty$. PDF of waiting time has the Laplace transform [17].

$$W_q(s) = \frac{(1-\rho)s}{s-\lambda[1-e^{-bs}]} \tag{10.3}$$

Example 5. Numerically estimate waiting time distribution $W_q(t)$ for different service models in M/G/1 queue. The Laplace transform of $W_q(t)$ is given by Pollaczek-Khinchine (P-K) transform equation [17]

$$W_q(s) = \frac{w_q(s)}{s} = \frac{(1-\rho)}{s-\lambda[1-B^*(s)]}, \text{where} \tag{10.4}$$

$$B^*(s) = \int_0^\infty dF(t) = \int_0^\infty e^{-st} f(t)dt, \tag{10.5}$$

$B^*(s)$ is the Laplace-Stieltjes transform (LST) of $F(t)$, $F(t)$ is the CDF of the service time distribution, λ and b are the averages of arrival rate and service tine distribution, and $\rho = \lambda b$ is the traffic intensity.

As with $M/G/1$ queue the following service models considered:

$$M/M/1 \quad B^*(s) = \frac{\mu}{s+\mu} \tag{10.6}$$

$$M/E_k/1 \quad B^*(s) = \left(\frac{\mu}{s+\mu}\right)^k \tag{10.7}$$

$$M/D/1 \quad B^*(s) = e^{-bs} \tag{10.8}$$

$$M/H_2/1 \quad B^*(s) = \sum_{i=1}^2 \frac{p_i \mu_i}{\mu_i+s} \tag{10.9}$$

Consider $M/G/1$ model for calculating waiting time distributions. For the system $M/H_2/1$ the arrival rate $\lambda = 5.0$. The service time distribution is H_2 evaluated for $\mu = 6$, $b = 1/\mu$ and $c_S = 1.5$. For this $M/H_2/1$ system the traffic intensity $\rho = \lambda/\mu$, and the CDF at the time 0 is $F(0) = 1 - \rho$.

Gaver-Sthefest algorithm used for inverting Laplace transform for variety $B^*(s)$ in (10.4). The CDF distribution of the waiting time in queue distribution CDF for $M/D/1, M/H_2/1$ and $M/M/1$ are shown in Fig. 12.
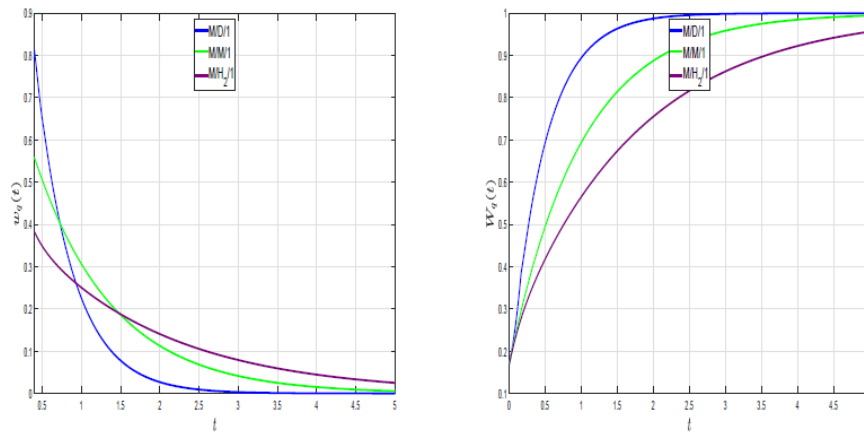
Figure 12: PDF and CDF waiting time distributions for $M/M/1$, $M/D/1$ and $M/H_2/1$

For $M/D/1$ queue service times are deterministic and equal to the value b. For deterministic service $B * (s)$ are given by (10.8). We compare $W_q(t)$ calculated by inverting of (10.4) with $W_q(t)$ also known and analytically given by [17]:

$$W_q(t) = (1 - \rho) \sum_{i=0}^{[t/b]} e^{-\lambda(ib-t)} \frac{(ib-t)^i}{i!} \lambda^i, \qquad (10.10)$$

where $[x]$ is the greatest integer less than or equal to x.

Figure 13 shows results for this queue with $\lambda = 5.0$, $\mu = 6.0$ ($b = 1/\mu$ and $\rho = \lambda/\mu = 0.8$). The figure shows errors, by analytical estimate, in logarithmic scale $\text{Log} W_q(t)$ (left plot). The estimate for $W_q(t)$ is then obtained by Gaver-Stehfest algorithm. We failed to get the numerical analytical solution for precision level: $N = 16$ if $t > 10$; $N = 64$ if $t > 26$; $N = 256$ if $t > 90$. Only for $N = 512$ and $N = 1000$ we get the correct result for all range $0 < t \leq 100$. Gaver-Stehfest inversion $W_q(t)$ are shown in the right plot, even for double precision we have accurate solution, and can not distinguish by eyes the curves with different precision $N = 16, 64, 256$ and 512.
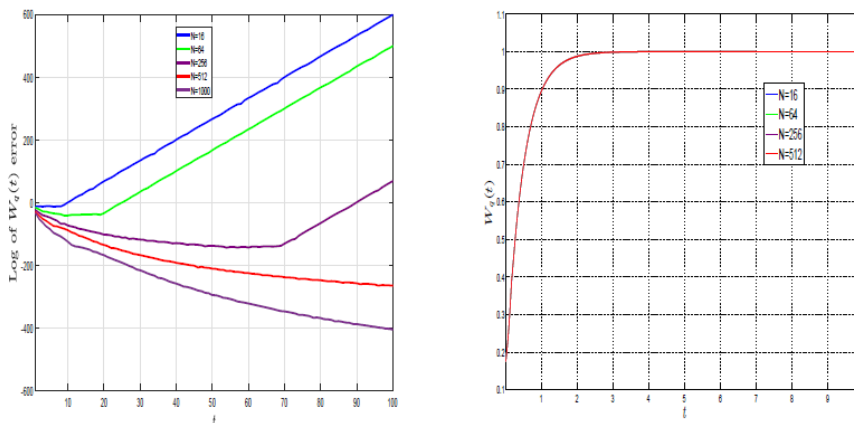
Figure 13: $M/D/1$ outputs: Log of $W_q(t)$ error (left plot) and $W_q(t)$
by Gaver-Stehfest inversion (right plot)

Fig. 14 shows numerical results in double precision (N = 16) for $M/D/1$ waiting time distribution $W_q(t)$ by analytical solution (10.10) and Gaver-Stehfest inversion. The analytical solution is dominated by noise after $t > 9$.
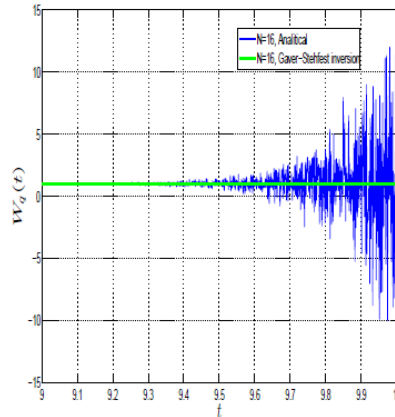
Figure 14: $W_q(t)$ for $M/D/1$,CDF waiting time distribution
by analytical solution and Gaver-Stehfest inversion

The most common service time distribution is the exponential, in which case the waiting time distribution are available in closed-form. For more general cases, closed-form solutions of (P-K) $M/G/1$ transform equation are mathematically intractable. The following specific example used to compare analytical solution and Gaver-Stehfest inversion. Consider the system $M/H_2/1$ with pdf for service time distribution [7]

$$B(t) = \frac{1}{4}\lambda e^{-\lambda t} + \frac{3}{4}(2\lambda)e^{-2\lambda t}, \tag{10.11}$$

where λ is the arrival rate, $b = 5/(8\lambda)$, and $rho = \lambda b = 5/8$. For numerical solutions we used $\lambda = 5$. The corresponding laplace transform $B^*(s)$ is

$$B^*(s) = \left(\frac{1}{4}\right)\frac{\lambda}{\lambda+s} + \left(\frac{3}{4}\right)\frac{2\lambda}{2\lambda+s} \tag{10.12}$$

Using $B^*(s)$ and (P-K) transform equation (10.4) $W_q(s)$ and $W_q(t)$ for the waiting time density [7]:

$$w_q^*(s) = (1-\rho)\left[1 + \frac{\lambda/4}{(3/2)\lambda+s} + \frac{3\lambda/4}{(1/2)\lambda+s}\right] \tag{10.13}$$

$$w_q^((t) = \frac{3}{8}u_0(t) + \frac{3\lambda}{32}e^{-(3/2)\lambda t} + \frac{9\lambda}{32}e^{-(1/2)\lambda t} \quad t \geq 0, \tag{10.14}$$

where $u_0(t)$ is unit impulse function.

The analytical solution for CDF of waiting time distribution can be easily found as:

$$W_q^*(s) = (1-\rho)\left[\frac{1}{s} + \frac{\lambda/4}{((3/2)\lambda+s)s} + \frac{3\lambda/4}{((1/2)\lambda+s)s}\right] \tag{10.15}$$

$$W_q^((t) = (1-\rho)\left[\frac{8}{3} - \frac{1}{6}e^{-(3/2)\lambda t} - \frac{3}{2}e^{-(1/2)\lambda t}\right] \quad t \geq 0 \tag{10.16}$$

Fig. 15 shows numerical results in double precision (N = 16) for $M/H2/1$ waiting time distribution for PDF (on the left) and CDF (on the right). To recognize by eyes the distinguish an analytical and Gaver-Stehfest inversion outputs is almost impossible.
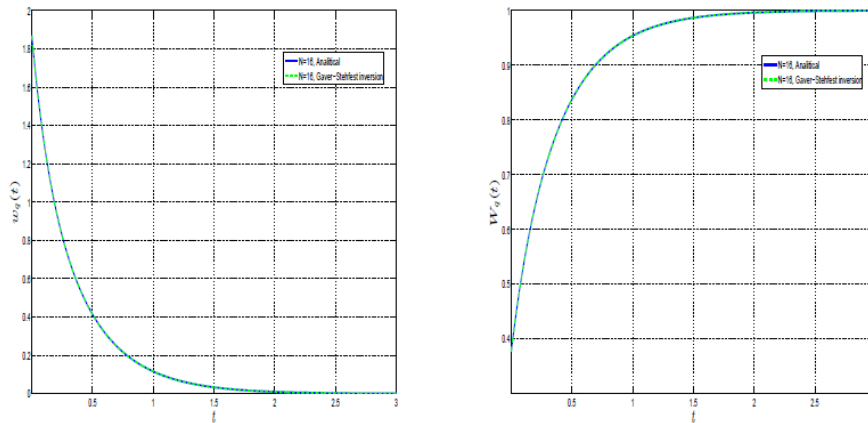
Figure 15: Waiting time distribution for $M/H_2/1$ by analytical solution and Gaver-Stehfest inversion for PDF (left plot) and CDF (right plot)

11 Accuracy and precision requirements of the $M/D/1$ large t analysis

The results of double transformation approximation for waiting time distribution $W_q(s)$ in $M/D/1$ are shown in Figs. 16 and 17.

The following double transformation technique used for the Laplace transform of the inversion:

$$\widetilde{\widetilde{W}}_q(s) = \mathcal{L}\{\mathcal{L}^{-1}\{W_q(s)\}\} \tag{11.1}$$

The exact solution is original $W_q(s)$ which compares with $\widetilde{\widetilde{W}}_q(s)$ after double transformation technique. Laplace transform inversion implemented by the Gaver-Stehfest algorithm, and a composite Simpson's rule is performed for the numerical direct Laplace transform. Approximation for the waiting time distribution in $M/G/1$ queue is convenient for light traffic intensity and small t, providing suitable approximation in double precision. The Figures fit the wide-range small Laplace transform parameter s, corresponding to large number t.
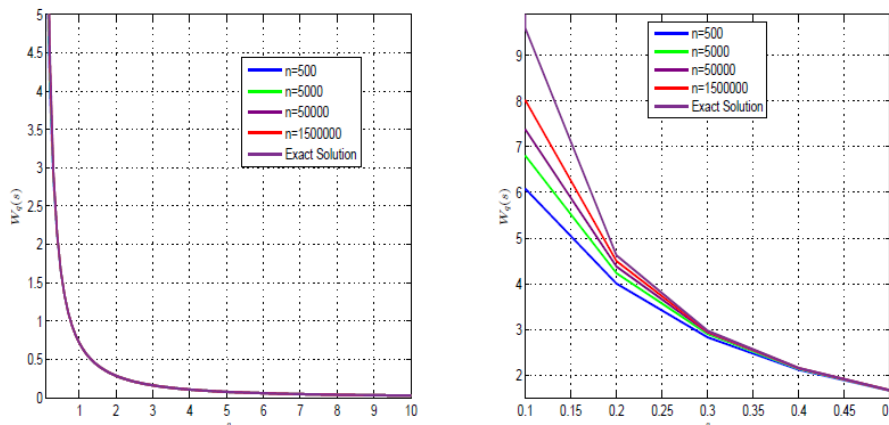
Figure 16: Double transformation approximation for waiting time distribution $W_q(s)$ of the $M/D/1$: double precision (N = 16) with different number of subinterval n = 500, 5000, 50000, 150000 and ranges [0.1, 10] (left plot), and [0.1, 5] (right plot)
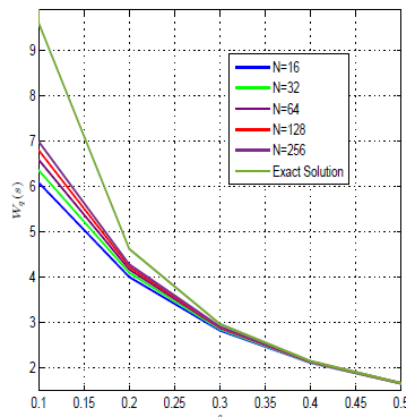
Figure 17: Double transformation approximation for waiting time distribution $W_q(s)$ of the $M/D/1$ with multiple precision calculation with the number of subintervals $n = 500$

On the Fig. 16 all curves are given for double precision level (N = 16) with different number of subinterval n = 500, 5000, 50000 and 150000 in numerical direct Laplace calculation. It looks like the is no effect of n increased for s on the interval [0.1, 10] (left plot), but curve are different for s on the smaller interval [0.1, 0.5] (right plot).

The Fig.17 demonstrate the impact of precision level N. The number of subintervals n = 500. In double precision the method does not work well, and significant improvements in accuracy illustrated as precision level increased up to 256.

12 Conclusions

Accuracy and stability of numerical Laplace transform and inversion are crucial for many applications in computation probability models. In this work, we proposed and evaluated different numerical implementations of the Laplace transform and inversion in multiple precision arithmetic systems. We are concerned with transformation that can occur in two ways.

If the examples cover functions with known inverses, accuracy of multiple precision models can be asserted by comparison to the exact solution.

The most realistic and challenging problems cover functions with analytically unknown inverses. So double transformation approach proposed to find computationally efficient methods for performing the numerical Laplace transform and inversion. In this approach numerical Laplace transform inversion used directly as input into numerical Laplace transform. The accuracy can be asserted by comparison to the original Laplace planform. We observe the accuracy of the inversions as we increase the number of the expansion terms and precision, which lead to stable solutions. The computational efficiency compared to precision levels is demonstrated for waiting times distribution in $M/G/1$ queuing systems.

References

[1] J. Abate, P. Valko, Multi-precision Laplace transform inversion, International Journal for Numerical Methods in Engineering 60 (2004) 979-993.
[2] K. E. Atkinson, An Introduction to Numerical Analysis, second ed., John Wiley & Sons, 1989.
[3] D. H. Bailey, Y. Hida, X. S. Li, B. Thompson, ARPREC: An Arbitrary Precision Computation Package, Tech. Rep. LBNL-53651, Lawrence Berkley National Lab., 2002.
[4] A. M. Cohen, Numerical Methods for Laplace Transform Inversion, Springer, 2007.

[5] C. Edwards, C. Penney, Differential Equations and Boundary Value Problems: Computing and Modeling, 5th ed., 2015.

[6] E. Kao, An Introduction to Stochastic Processes, Duxbury Press, 1997.

[7] L. Kleinrock, Queueing Systems, Volume I, Hardcover, 1975

[8] E. Kreyszig, Advanced Engineering Mathematics, 10th ed., 2011.

[9] Z. Krougly, M. Davison, S. Aiyar, The role of high precision arithmetic in calculating numerical Laplace and inverse Laplace transforms, Applied Mathematics 8 (2017) 562-589.

[10] Z. L. Krougly, D. J. Jeffrey, Implementation and application of extended precision in Matlab, in: N. Mastorakis et al (Eds.), Proc. of the Applied Computing Conference ACC'09, WSEAS Press (2009) 103-108.

[11] Z. L. Krougly, D. A. Stanford, Iterative algorithms for performance evaluation of closed network models, Performance Evaluation 61 (2005), 41-64.

[12] Z. L. Krougly, D. J. Jeffrey, D. Tsarapkina, Software implementation of numerical algorithms in arbitrary precision, in: 15th International Symposium on Symbolic and Numeric Algorithms for Scientific Computing (SYNASC 2013), N. Bjorner et al. (Eds.), IEEE Computer Society (2014) 132-138.

[13] K. L. Kuhlman, Review of inverse Laplace transform algorithms for Laplace-space numerical approaches, Numerical Algorithms 63 (2013) 339-355.

[14] A. Kuznetsov, On the convergence of the Gaver–Stehfest algorithm, SIAM J. Numer. Anal. 51 (2013) 2984-2998.

[15] A. Murli, M. Rizzardi, Algorithm 682 Talbot's method for the Laplace inversion problem, ACM Transactions on Mathematical Software 16 (1990) 158-168.

[16] S. Nadarajah, S. Kotz, On the Laplace transform of the Pareto distribution, Queueing System 54 (2006) 243-244.

[17] J.F. Shortle, J.F. Thompson, D. Gross, C. M. Harris. Fundamentals of Queueing Theory, 5th ed., Wiley, New York, 2018.

[18] H. Stehfest, *Algorithm 368: Numerical Inversion of Laplace Transform*, Communications of the ACM, 13(1), 1970: 47-49.

Yogesh Pal, Santosh Kumar, Madhulika Singh
ANALYSIS AND DESIGNING A DNA FINGERPRINTING BASED
IDENTIFICATIONS (DNAFIDS) MODEL …

RT&A, No 1 (61)
Volume 16, March 2021

Analysis and Designing A DNA Fingerprinting Based Identifications (DNAFIDs) Model and Database Management System

Yogesh Pal

•

Research Scholar, Department of Computer Science & Engineering,
Maharishi University of Information Technology, Lucknow
Er.yogeshpal15@gmail.com

Santosh Kumar

•

Associate Professor, Department of Computer Science & Engineering,
Maharishi University of Information Technology, Lucknow
Sant7783@hotmail.com

Madhulika Singh

•

Professor, School of Science, Maharishi University
of Information Technology, Lucknow
Madhulika.anil@gmail.com

Abstract

The revolutionary discovery in forensic investigation in DNA fingerprinting that helps to identify individuals it is an important tool for molecular research that support the human breeding. DNA fingerprinting model played an important role in identifying an individual in millions of people by looking in unique patterns in their DNA. DNA fingerprinting is a technique that simultaneously detects lots of minisatellites in genome to produce a pattern unique to an individual. In this research work, we analyzed DNA fingerprinting based identification and designed a DNA fingerprinting based identification model along with DNA database management system for 360 degree interlinking i.e. all services and progresses will be progressed by DNAFIDs and database.

Keywords: DNA Fingerprint, DNA Database Management System, Algorithm.

1. Introduction

The individual-explicit DNA designs give an incredible technique to singular recognizable proof and paternity testing. At that point, it was imagined that the execution of these applications would be extended, and that major lawful issues would be experienced as DNA proof continued from the exploration lab to the court. Ensuing history demonstrated that this forecast was unduly negative. After agreeably settled the migration question by DNA fingerprinting, the DNA proof is utilized in

Yogesh Pal, Santosh Kumar, Madhulika Singh
ANALYSIS AND DESIGNING A DNA FINGERPRINTING BASED
IDENTIFICATIONS (DNAFIDS) MODEL …

RT&A, No 1 (61)
Volume 16, March 2021

different cases everywhere on the world. Thusly, the DNA fingerprinting based model is planned here for ID and confirmations of people.

DNA fingerprinting is otherwise called DNA profiling, it is a method applied by the analysts/researcher to discover the genunity of the person's personality. As practically 100% of the genomes are indistinguishable all through the human populace yet there are still a little sum level of genomes fluctuates which don't have such a great amount of effect on the distinguishing proof of people. The variable DNA Sequences named polymorphic producers can be utilized to both separate and relate people. In spite of the fact that it is another innovation, it had an extraordinary effect nearly on each field like criminal equity, paternity tests and legacy matters to set up recognize in criminal cases.

An article data set is an information base administration framework in which data is spoken to as items as utilized in object-situated programming. Item information bases are not the same as social information bases which are table-arranged. Item social information bases are a half breed of the two methodologies. Subsequently, a DNA unique mark information base is planned here that includes the creation of a lot of heterogeneous information for which stockpiling, examination, and recovery are time and asset expending. To handle the a lot of information produced by research centres and lead quality control, an information base administration framework is direly expected to follow tests and investigate information.

DNA fingerprints can be overseen methodically by a PC, and can be sorted out in DNA unique mark information bases. DNA unique mark data sets are fundamental and significant apparatuses for plant sub-atomic examination since they give amazing specialized and data uphold for crop reproducing, assortment quality control, assortment right assurance, and sub-atomic marker-helped rearing. Building a DNA unique mark information base includes the creation of a lot of heterogeneous information for which stockpiling, examination, and recovery are time and asset devouring. Some organic information the executives programming has been created. For instance, SLIMS can arrange, store, and access test data; AutoLabDB gives information base pattern to help mechanized labs.

In this paper, we portray the DNA-Fingerprinting based recognizable proof framework (DNAFIDs) that is created for tackle the issues identified with research the legitimacy of the people. DNAFIDs has programmed assortment, stockpiling, and productive administration capacities dependent on combining and correlation calculations to deal with gigantic measures of unique mark information, and the framework can likewise perform hereditary investigations.

2. Background

There are a few analysts have done parcel of exploration to improve the presentation and time inertness. Let us first quickly examined some exploration works identified with DNA Fingerprinting database.

Receptacle et al [1] have built up the plant global DNA-fingerprinting framework (PIDS) utilizing an open source web worker and free programming that has programmed assortment, stockpiling, and productive administration capacities dependent on combining and examination calculations to deal with enormous microsatellite DNA unique mark information. Wilton, R. et al [2] have assembled a smaller, effectively recorded information base that contains the crude read information for more than 250 human genomes, including trillions of bases of DNA, and that permits clients to look through these information progressively. The Terabase Search Engine empowers recovery from this information base of the apparent multitude of peruses for any genomic area surprisingly fast. Jasrotia et al [3] have introduced VigSatDB the world's first extensive microsatellite information base of sort Vigna, containing >875 K putative microsatellite markers with 772 354 basic and 103 865 compound markers mined from six genome gatherings of three Vigna species, specifically, Vigna radiata (Mung bean), Vigna angularis (Adzuki bean) and

Yogesh Pal, Santosh Kumar, Madhulika Singh
ANALYSIS AND DESIGNING A DNA FINGERPRINTING BASED
IDENTIFICATIONS (DNAFIDS) MODEL …

RT&A, No 1 (61)
Volume 16, March 2021

Vigna unguiculata(Cowpea). Backiyarani et al [4] have given data on in silico polymorphic SSRs (2830 SSRs) between the differentiating cultivars for each pressure and inside pressure. Data on in silico polymorphic SSRs explicit to differentially communicated qualities under tested condition for each pressure can likewise be gotten to. This information base encourages the recovery of results by exploring the tabs for cultivars, stress and polymorphism. Struyf et al [5] have grouped the investigations by purposes: (I) identification and leeway; (ii) discouragement; and (iii) criminological logical information. Every classification utilizes various estimations to assess viability. Mantelatto et al [6] have planned to get successions of the mitochondrial markers (COI and 16S) for decapod scavangers appropriated at the São Paulo coastline and to test the precision of these markers for species ID from this district by contrasting our groupings with those effectively present in the GenBank information base. Zhou et al [7] have chosen 23 sets of SSR groundworks to distinguish and break down 73 assortments of head lettuce. The outcomes recognized a sum of 117 transformed alleles identified in 23 loci, with the quantity of every loci going from 2 to 11, with a normal of 5.1 changed alleles per locus. Sochorová, et al [8] have set up the animal rDNA data set containing cytogenetic data about these loci in 1343 animal species (264 families) gathered from 542 distributions. Bengtsson-Palme et al [9] have introduced an update to Metaxa2 that empowers the utilization of any hereditary marker for ordered characterization of metagenome and amplicon succession information. Li et al [10] have built up a novel strategy for SSR genotyping, named as AmpSeq-SSR, which joins multiplexing polymerase chain response (PCR), directed profound sequencing and far reaching examination. Yu et al [11] have built up an information base, PMDBase, which coordinates a lot of microsatellite DNAs from genome sequenced plants species and incorporate a web administration for microsatellite DNAs ID. Benschop et al. [12] analyzed for blended DNA profiles of variable intricacy whether the genuine benefactors are recovered, what the quantity of bogus positives over a LR limit is and the positioning situation of the genuine contributors. Carew et al [13] have inspected the utilization of DNA scanner tags for species recognizable proof and think about DNA barcoding endeavors of macroinvertebrates from Australia with those internationally. We consider the function of high-throughput sequencing of DNA scanner tags in freshwater bioassessment and its likely use in biosurveillance. Saja et al [14] have fabricated a DNA profile information base framework dependent on fifteen autosomal STR loci, which are (D3S1358, VWA, FGA, D8S1179, D21S11, D18S51, D5S818, D13S317, D7S820, TH01, TPOX, CSF1PO, D19S433, D2S1338, D16S539) in addition to Amelogenin (AMEL) to decide sex.

3. Methodologies and Experiments

3.1.   Fingerprinting Database Implementation

Unique mark information bases are organized assortments of unique mark information mostly utilized for either assessment or operational acknowledgment purposes. The fingerprints in information bases for assessment are generally separated from the character of the relating people, are freely accessible for research purposes, and typically comprise of crude unique mark pictures obtained with live-examine sensors or digitized from inked unique mark impacts on paper. These information bases are the reason for research in programmed unique mark acknowledgment, and along with explicit trial conventions, are the reason for various innovation assessments and benchmarks.

The unique mark information are put away in various unique mark data sets as indicated by their various purposes and capacities as follows. Trial Fingerprint Database (TFD): An experimenter can transfer an Excel document, Gene Mapper yield record, and task record into the EFD. Unique finger impression data is recorded and can be questioned and followed. Each bit of unique mark information in the TFD must be inspected through the Fingerprint Merging

Yogesh Pal, Santosh Kumar, Madhulika Singh
ANALYSIS AND DESIGNING A DNA FINGERPRINTING BASED
IDENTIFICATIONS (DNAFIDS) MODEL …

RT&A, No 1 (61)
Volume 16, March 2021

Algorithm by the experimenter before the unique mark information are submit consequently to the Sample Fingerprint Database (SFD). This combining calculation can tackle the issue of unique mark duplication in numerous tests of a solitary experimenter and diminish trial blunders. This plan additionally guarantees the respectability of information and keeps away from the nonappearance of loci information. Test Fingerprint Database (SFD): An experimenter can review the example unique mark information (in the SIT) from the TFD. After the information are inspected and affirmed by the experimenter, a lot of test fingerprints are created and submitted consequently to the Local Fingerprint Database (LFD) utilizing the Fingerprint Merging Algorithm. By consolidating the examined information, any counterfeit mistakes brought about by various experimenters can be diminished. The two layers of information review and union (TFD–SFD and SFD–LFD) accomplish adequate quality confirmation of the trial results information. Neighborhood Fingerprint Database (LFD): The LFD can be utilized for unique mark information correlations and reports. A locking capacity is given and, once bolted, the information can't be changed. DNA Fingerprinting Database can track DNA samples through workflows, which allows users to trace back to GE and CE files (CE image on each primer locus). Users can also query the sample sources.

The entire DNA unique mark information base contains fundamental data, exploratory data, and unique mark information data. These information are referred to one another by IDs or scanner tag numbers. To tackle the difficult that unique mark information are viable with various harvest groundworks, DNA Fingerprinting Database stores unique finger impression information and unique mark picture data in autonomous records. The unique mark information record is related with the capacity way data of the unique finger impression picture, and afterward the finger impression information document way data is put away in the fundamental data table of unique mark information. When stacking and refreshing unique mark information and unique mark pictures, just new data should be composed into the unique finger impression information document. This methodology keeps away from the issue of moderate tasks, for example, questions that utilization an information base to store a lot of double information. Further, the unique mark information and finger impression picture data are put away with more noteworthy opportunity, and the DNA unique finger impression data set can be sponsored up and reestablished all the more rapidly.

Figure 3.1.1. Class diagram for DNA Fingerprinting Database

Yogesh Pal, Santosh Kumar, Madhulika Singh
ANALYSIS AND DESIGNING A DNA FINGERPRINTING BASED
IDENTIFICATIONS (DNAFIDS) MODEL …

RT&A, No 1 (61)
Volume 16, March 2021
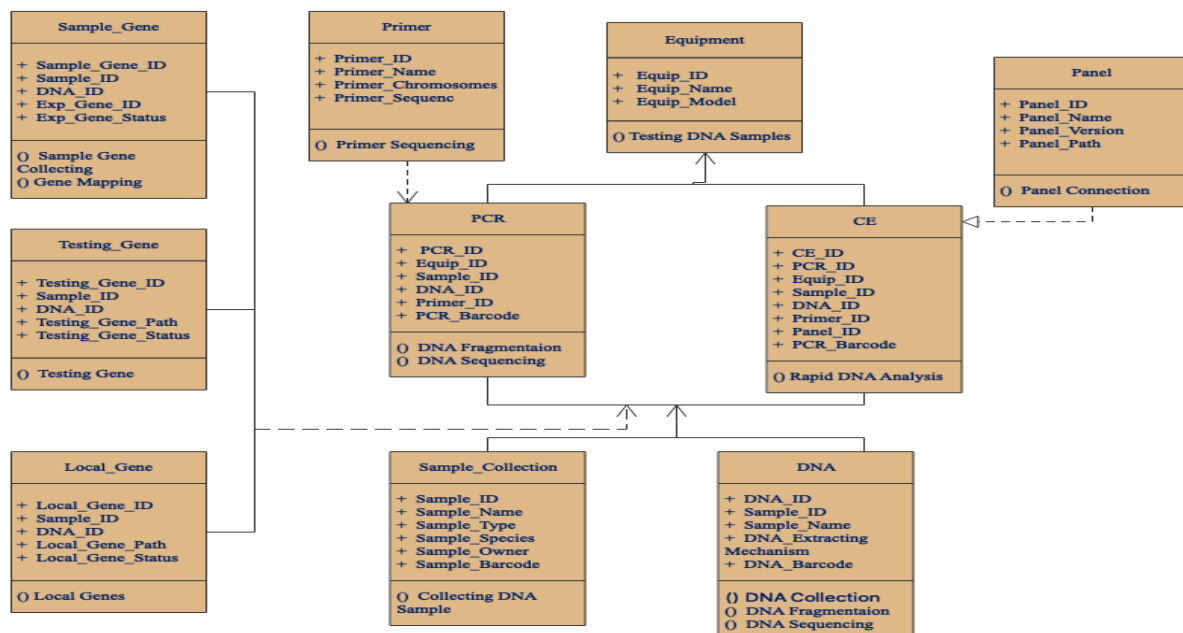
3.2.   DNA Fingerprinting Model

In spite of the fact that the larger part of the human genome is indistinguishable over all people, there are locales of variety. This variety can happen any place in the genome, including territories that are not known to code for proteins. Examination concerning these noncoding districts uncovers rehashed units of DNA that shift long among people. Researchers have discovered that one specific sort of rehash, known as a short couple rehash (STR), is moderately handily estimated and analyzed between various people. Truth be told, the Federal Bureau of Investigation (FBI) has recognized 13 center STR loci that are currently regularly utilized in the distinguishing proof of people in the United States, and Interpol has distinguished 10 standard loci for the United Kingdom and Europe. Nine STR loci have likewise been distinguished for Indian populaces. As its name infers, a STR contains rehashing units of a short (commonly three-to four-nucleotide) DNA succession. The quantity of rehashes inside a STR is alluded to as an allele. For example, the STR known as D7S820, found on chromosome 7, contains somewhere in the range of 5 and 16 rehashes of GATA. Accordingly, there are 12 distinct alleles feasible for the D7S820 STR. A person with D7S820 alleles 10 and 15, for instance, would have acquired a duplicate of D7S820 with 10 GATA rehashes from one parent, and a duplicate of D7S820 with 15 GATA rehashes from their other parent. Since there 12 unique alleles for this STR, there are hence 78 various potential genotypes, or sets of alleles. In particular, there are 12 homozygotes, in which a similar allele is gotten from each parent, just as 66 heterozygotes, in which the two alleles are unique.

3.2.1.   Class Diagram for DNA Fingerprinting Identification Database

The core functions of DNA fingerprinting database (DNAFDs) include data generation, data storage, data audit, and data analysis. By providing automatic data generation, storage, audit, and rapid comparison functions, it can replace the previous methods of manually entering data into the database and manually comparing and merging data. Only a small amount of data needs to be corrected manually, namely data that the algorithm cannot automatically determine, to achieve the target of rapid processing of DNA fingerprint data. The data generation function in DNAFIDs is divided into two parts, Test information processing and fingerprint data analysis processing. These two parts correspond to the phases before and after a complete Testing, namely the experimental phase and the data analysis phase. Thus, DNAFIDs provides comprehensive data analysis auxiliary functions for the experimenter, simplifies the often difficult data analysis phase, improves the quality of data analysis, and provides the basis for the analysis of mass fingerprint data. The modular structure of DNAFID is shown in Figure 3.2.1.1.
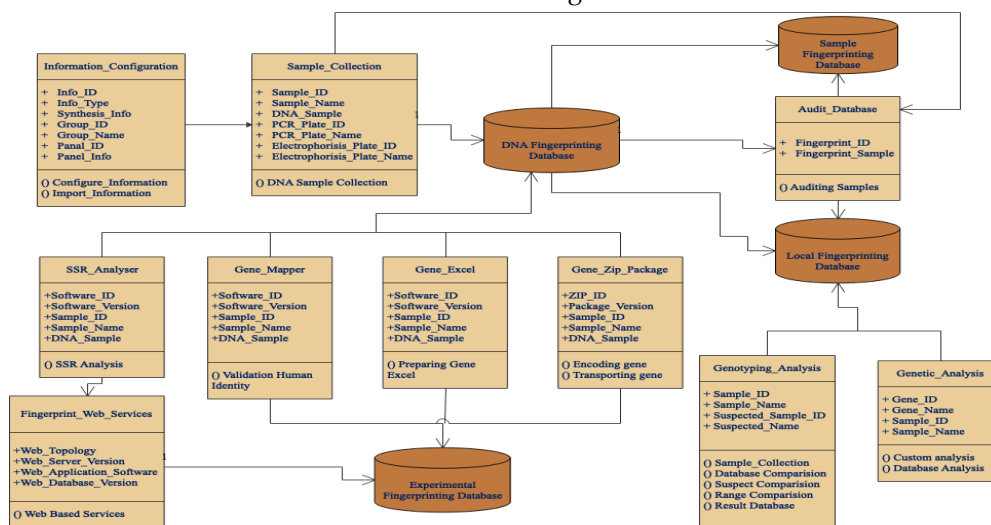
Figure 3.2.1.1. Class Diagram for DNA Fingerprint Identification System

Yogesh Pal, Santosh Kumar, Madhulika Singh
ANALYSIS AND DESIGNING A DNA FINGERPRINTING BASED
IDENTIFICATIONS (DNAFIDS) MODEL ...

RT&A, No 1 (61)
Volume 16, March 2021

3.3.   DNA Fingerprinting Algorithm

The DNA fingerprinting or DNA profiling is the technique to applied on the criminal check and wrongdoing scene examination. In any case, it is likewise pertinent to building up a connection between two people and to know somebody's character. The testing strategy is drilled for people as well as for any living beings present on earth. DNA is our outline, premise of life, encodes proteins, and directs quality articulation. It is comprised of sugar, phosphate, and nitrogenous bases. DNAs are situated on chromosomes. The entire arrangement of DNA or chromosomes is known as the genome. Strangely, there are a few districts in our genome that are exceptional and hypervariable.

As the DNA Profiling or DNA fingerprinting ID is broadly utilized in criminal confirmation, wrongdoing scene examination and paternity check yet restricted utilized continuously and moment individual ID since it required additional time and research centres to play out the DNA fingerprinting test. We attempting to plan and build up a model for DNA profiling or DNA fingerprinting to distinguish an individual immediately. The Fingerprint Comparison Algorithm is applied to finish the correlation between the source and target fingerprints, which can uncover contrasts, missing, or no contrasts between fingerprints. DNA Fingerprinting Database centres around the canter recognizable proof capacity, including valid ID, virtue ID, and paternity testing. It additionally has a hereditary examination work that permits clients to perform hereditary bunching and heterosis bunch investigations of their transferred information.

3.3.1.   Process for DNA Comparison

There are two steps first one is producing or extracting DNA and other one is comparing or merging the DNA. Therefore, the first part containing several steps for extracting DNA these are:

3.3.1.1. DNA Extraction

DNA can be extracted from human material like blood, hair, skin etc. therefore, several steps for it such as:
1. Cut the DNA into thousands of pieces in various length through restriction enzymes.
2. Separate DNA according their size through gel electrophoresis.
3. Producing a single stands of DNA by unzipping DNA after blotted out of the triagile gel on to a robust piece of nylon membrane.
4. Incubated the nylon membrane with radioactive probes which are attached to minisatellites in genome.
5. The minisatellites visualised by exposing the nylon membrane to x-ray film. A radioactive pattern of 30 dark brands appeared on film known DNA Fingerprint.

3.3.1.2. DNA Comparison

DNA Comparison or DNA profiling also known as Short Tendom Repeats (STRs) analysis relies on microsatellites rather than minisatellites. An algorithm is designed here for it:
Step 1: Set result = 1 if sample matched, Set result = 0 if sample not matched

Yogesh Pal, Santosh Kumar, Madhulika Singh
ANALYSIS AND DESIGNING A DNA FINGERPRINTING BASED
IDENTIFICATIONS (DNAFIDS) MODEL ...

RT&A, No 1 (61)
Volume 16, March 2021

Step 2: Insert Loci 1 and Loci 2
Step 3: Compare the values of Loci 1 and Loci 2
       If Loci 1 == Loci 2 or Loci 1 <= Loci 2
       Return 1
       Else
       Return 0
       Endif
Step 4: Return result
Step 5: Exit

4. Modelling and their Functionalities

DNA fingerprinting Database system was constructed using a relational database. The database is implemented based on the current mainstream open source software SQL Server. Figure 4.1 shows the entity relationship model (ERD). Using Chen's ERD notation to represent the ERD, we first identified 10 entities and four relationships. A table-like model is constructed based on the ERD. The "PCR" and "CE" entities shown in Figure 4.1. are each split into two tables, "PCR" and "PCR_well", and "CE" and "CE_well". These tables are used to include additional information to describe the wells in the plate and to accurately locate them. All the entities are related by the source of the sample and associated with basic information such as primers, panels, and detection equipment to build a complete fingerprint data information system.
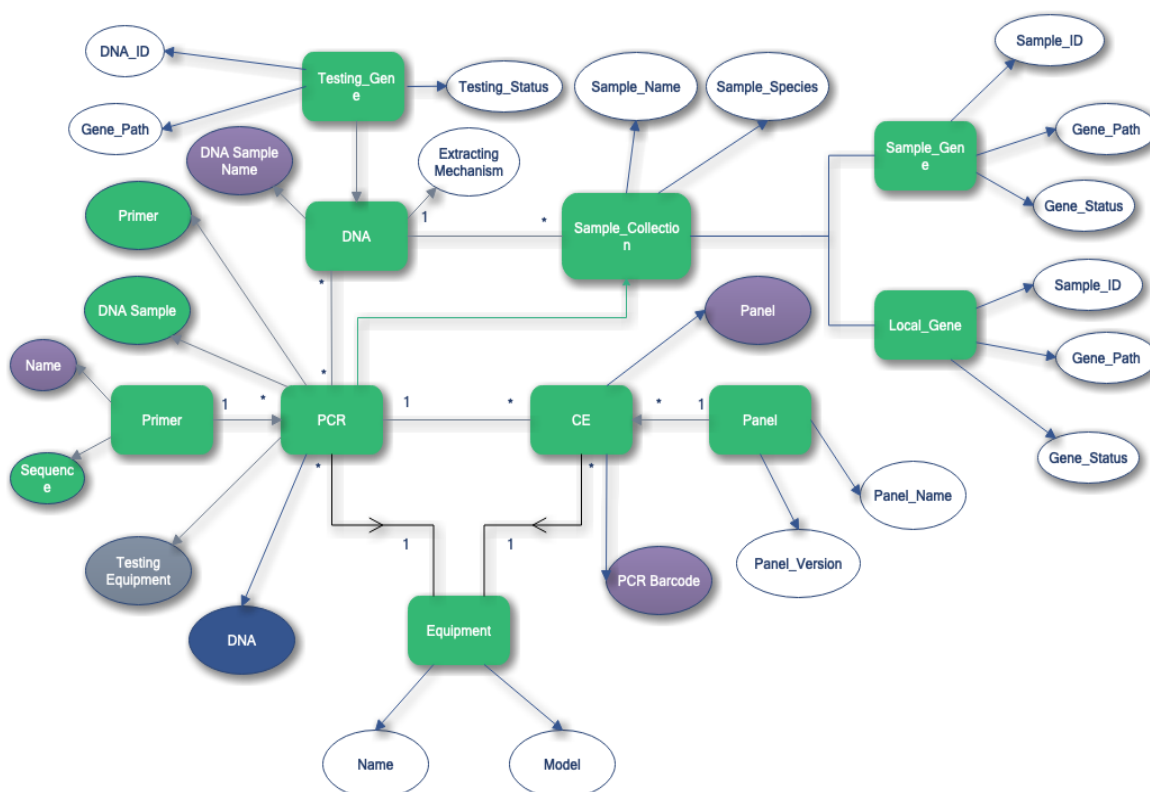
Figure 4.1. E-R Diagram for DNA Fingerprinting Database System

The whole DNA fingerprint database contains basic information, Testing information, and fingerprint data information. These data are referenced to each other by IDs or bar code numbers. To solve the problem that fingerprint data are compatible with different person primers, DNA

Yogesh Pal, Santosh Kumar, Madhulika Singh
ANALYSIS AND DESIGNING A DNA FINGERPRINTING BASED
IDENTIFICATIONS (DNAFIDS) MODEL …

RT&A, No 1 (61)
Volume 16, March 2021

Fingerprinting Database System stores fingerprint data and fingerprint image information in independent files. The fingerprint data file is associated with the storage path information of the fingerprint image, and then the fingerprint data file path information is stored in the basic information table of fingerprint data. When loading and updating fingerprint data and fingerprint images, only new information needs to be written into the fingerprint data file. This approach avoids the problem of slow operations such as queries that use a database to store a large amount of binary data. Further, the fingerprint data and fingerprint image information are stored with greater freedom, and the DNA fingerprint database can be backed up and restored more quickly.

Conclusion

DNA Fingerprinting is a fundamental apparatus in our research center. It helps with computerizing DNA unique mark analyzes and diminishes human mistake. It can finish test following and perform normal hereditary investigation, in this manner improving work proficiency and quality. PIDS can uphold every single diploid plant and can be reached out to help polyploid species. We can furnish clients with free customization and expansion of back-end capacities to meet the necessities of their labs, for example, those associated with human and microorganism research. PIDS can screen the test cycle and guarantee the normalization of DNA unique mark information. It very well may be utilized to direct between information base discussions, and trade unique mark information between unique mark information bases, with complete unique mark information handling administrations. PIDS incorporates area measurements, unique mark combining, finger impression correlation, and hereditary examination works, and is viable with single and blended DNA test preparing strategies. PIDS has a total loci insights work that can address the issues of a research center's inward unique mark information base development. PIDS can likewise satisfy the prerequisites for guideline unique mark information base development and sharing, and supports the extension of different identification innovations and various unique mark information administrations.

Acknowledgements

References

[1]   Bin J., Yikun Z., Hongmei Y., Yongxue H., Haotian W., Jie R., Jianrong G., Jiuran Z. and Fengge W., "PIDS: A User-Friendly Plant DNA Fingerprint Database Management System", genes MDPI, 11, 373, 1-15, 2020.

[2]   Wilton, R.; Wheelan, S.J.; Szalay, A.S.; Salzberg, S.L. The Terabase Search Engine: A large-scale relational database of short-read sequences. *Bioinformatics* **2019**, *35*, 665–670. [CrossRef] [PubMed]

[3]   Jasrotia, R.S.; Yadav, P.K.; Angadi, U.B.; Tomar, R.S.; Jaiswal, S.; Rai, A.; Kumar, D. VigSatDB: Genome-wide microsatellite DNA marker database of three species of Vigna for germplasm characterization and improvement, Database, Vol. **2019**, pp. 1-3, *2019*.

[4]   Backiyarani, S.; Chandrasekar, A.; Uma, S.; Saraswathi, M.S., "MusatransSSRDB (a transcriptome derived SSR database)—An advanced tool for banana improvement". *J. Biosci*, **2019**, Vol. *44*, *Issue 3*, pp. 110–116.

[5]   Struyf, P.; De, M.S.; Vandeviver, C.; Renard, B.; Vander, B.T., "The effectiveness of DNA databases in relation to their purpose and content: A systematic review", *Forensic Sci. Int.* **2019**, *301*, 371–381.

Yogesh Pal, Santosh Kumar, Madhulika Singh
ANALYSIS AND DESIGNING A DNA FINGERPRINTING BASED
IDENTIFICATIONS (DNAFIDS) MODEL …

RT&A, No 1 (61)
Volume 16, March 2021

[6]   Mantelatto, F.L.; Terossi, M.; Negri, M.; Buranelli, R.C.; Robles, R.; Magalhaes, T.; Tamburus, A.F.; Rossi, N.; Miyazaki, M.J. DNA sequence database as a tool to identify decapod crustaceans on the Sao Paulo coastline. *Mitochondrial DNA Part A* **2018**, *29*, 805–815.

[7]   Zhou, H.Y.; Zhang, P.H.; Luo, J.; Liu, X.Y.; Fan, S.X.; Liu, C.J.; Han, Y.Y. The establishment of a DNA fngerprinting database for 73 varieties of Lactuca sativa capitate L. using SSR molecular markers. *Hortic. Environ. Biotechnol.* **2018**, *60*, 95–103.

[8]   Sochorová, J.; Garcia, S.; Gálvez, F.; Symonová, R.; Kovarˇík, A. Evolutionary trends in animal ribosomal DNA loci: Introduction to a new online database. *Chromosoma* **2018**, *127*, 141–150.

[9]   Bengtsson-Palme, J.; Richardson, R.T.; Meola, M.; Wurzbacher, C.; Tremblay, E.D.; Thorell, K.; Kanger, K.; Eriksson, K.M.; Bilodeau, G.J.; Johnson, R.M.; et al. Metaxa2 Database Builder: Enabling taxonomic identification from metagenomic or metabarcoding data using any genetic marker. *Bioinformatics* **2018**, *34*, 4027–4033.[PubMed]

[10]   Li, L.; Fang, Z.W.; Zhou, J.F.; Chen, H.; Hu, Z.F.; Gao, L.F.; Chen, L.H.; Ren, S.; Ma, H.Y.; Lu, L.; et al. An accurate and efficient method for large-scale SSR genotyping and applications. *Nucleic Acids Res.* **2017**, *10*, e88.

[11]   Yu, J.Y.; Dossa, K.; Wang, L.H.; Zhang, Y.X.; Wei, X.; Liao, B.S.; Zhang, X.R. PMDBase: A database for studying microsatellite DNA and marker development in plants. *Nucleic Acids Res.* **2017**, *45*, 1046–1053.[PubMed]

[12]   Benschop, C.C.G.; Van, D.M.L.; De, J.J.; Vanvooren, V.; Kempenaers, M.; Van, D.B.C.; Barni, F.; Reyes, E.L.; Moulin, L.; Pene, L.; et al. Validation of SmartRank: A likelihood ratio software for searching national DNA databases with complex DNA profiles. *Forensic Sci. Int. Genet.* **2017**, *29*, 145–153.

[13]   Carew, M.E.; Nichols, S.J.; Batovska, J.; St, C.R.; Murphy, N.P.; Blacket, M.J.; Shackleton, M.E. A DNA barcode database of Australia's freshwater macroinvertebrate fauna. *Mar. Freshw. Res.* **2017**, *68*, 1788–1802.

[14]   Saja D. K., Muayad S. C., Mohammed Mahdi A. Z., "DNA-Profile Database Building Using STR DNA Marker For Diyala Province Population", International Journal of Advanced Research in Computer Engineering & Technology, Vol. 5, Issue 3, pp. 614-619, March 2016.

Rakesh Kumar, Bhavneet Singh Soodan, Sapana Sharma
MODELLING HEALTH CARE QUEUE MANAGEMENT SYSTEM
FACING PATIENTS' IMPATIENCE USING QUEUING THEORY

RT&A, No 1 (61)
Volume 16, March 2021

Modelling Health Care Queue Management System Facing Patients' Impatience using Queuing Theory

Rakesh Kumar [1], Bhavneet Singh Soodan [1] and Sapana Sharma [2]

•

[1]School of Mathematics
Shri Mata Vaishno Devi University, Katra, J&K (India), Pin Code -182320
bhavneet5678@gmail.com and rakesh.kumar@smvdu.ac.in
[2] Department of Mathematics,
Cluster University of Jammu, J&K (India), Pin Code-180004
sapanasharma736@gmail.com

Abstract

In this paper, we study a finite capacity single server queuing model with balking and correlated reneging and discuss its application in queues at health care facilities. The reneging considered so far in the queuing literature is a function of system-state. In many practical situations, reneging may depend on factors other than the system-state. For instance, in health care systems the reneging of patients at two consecutive time marks may be correlated in a sense that if a patient reneges at a time mark then there is a probability that a patient may renege at the next time mark due to the factors like improper check-up, sluggish management, unnecessary costly prescription by doctors, etc. The steady-state solution of the model is derived by using matrix-decomposition method. Finally, the transient performance analysis of the model is performed using Runge-Kutta method.

Keywords: Queuing model, Correlated reneging, Balking, Health care queue management, Transient performance analysis

1 Introduction

Queues are the common sight of any service providing system. Consistent long queues, delay in services, and low service quality drastically affect the business and perception of any institution providing any sort of service. Customers in queues may tend to leave if they are subjected to wait longer than their patience level. This phenomenon is known as reneging in queuing terminology. This impacts the business entity to lose potential customers and profits. Thus, foreseeing long term benefits it becomes a matter of high importance for a business institution to avoid any such aversive situation even if it requires capital investment.

In critical systems like health care queue management systems, in order to improve the standard of service it is very important to assign sufficient resources to handle the patient behavior during long waiting times in queues [42]. Fomundam and Herrmann [10] work on the design of health care systems using queuing theory. Lakshmi and Shivakumar [35] review the practical use of queuing theory in health care management. Jeffery and James[16] propose a queuing theory-based method to estimate the ratio of patients leaving a hospital Emergency Department (ED) without treatment by considering them as balked or reneged patients. Obulor and Eke [40] use queuing model to analyse the appointment scheduling process to have reduced waiting times for patients and reduced idle times for health staff. The authors in [2] use queuing theory to discuss latest mathematical modelling techniques in the planning of health care systems.

Rakesh Kumar, Bhavneet Singh Soodan, Sapana Sharma
MODELLING HEALTH CARE QUEUE MANAGEMENT SYSTEM
FACING PATIENTS' IMPATIENCE USING QUEUING THEORY

RT&A, No 1 (61)
Volume 16, March 2021

Queuing systems with customers' impatience are used to model and analyse a number of real life systems like hospitals handing critical patients, modelling computer-communication systems with packet loss, impatient telephone switch board customers, and perishable inventory systems. The study of queuing models with impatience starts in late 1950s. Haight [11] first uses the concept of balking in a single server queuing model. Haight [12] then studies a single server queuing system with reneging. The steady-state analysis of the model is performed. Ancker and Gafarian [3] investigate an M/M/1/N queuing model with balking and reneging where reneging of customers was in accordance with exponential distribution and the balking probability for an arriving customers is n/N, where n is number of customers in the system and N is the system capacity. Anker and Gafarian [4] examine an infinite capacity single server Markovian queuing model with balking and reneging. For the arriving customers probability of balking is $1 - (\beta/n)$; n=1,2,3,... where n is the number of customers present in the system and β is a measure of customer's desire to join the queue. Subba Rao [43] analyse an M/G/1/N queuing system with balking, reneging and interruptions. She uses supplementary variable technique and discrete transforms to obtain the solution of the model. Since then, a lot of research are written on queuing models with reneging and balking. Kumar et al. [18] consider a single server infinite capacity Markovian queuing system with balking and analysed its transient solution. Kumar and Sharma [20] bring the new concept of retention of reneging customers in queuing theory. They study an M/M/1/N queuing system with reneging and retention of reneging customers and obtained the steady-state solution of the model. Kumar and Sharma [29] obtain the transient solution of a single server queuing model with reneging and retention of reneging customers. Kumar and Sharma [30] study an M/M/c queuing model with balking, reneging and retention of reneging customers and derive its transient solution. Yang and Wu [45] include the concept of retention of reneging customers in a finite capacity queuing system with working breakdowns. They use the matrix-decomposition method for the steady-state solutions. Kumar and Soodan [32] consider a single server queuing model with correlated arrivals and reneging and analysed its transient behavior. For more insights on queuing models with reneging and retention of reneging customers one can refer [19, 21, 22, 23, 24, 25, 26, 27, 28, 31, 44]

The majority of work done so far in the literature considers reneging as a function of system-state (such as queue length or time in the queue). But, in many real life scenarios the reneging of customers may depend on other factors also. Kumar and Soodan [33, 34] introduce the concept of correlated reneging in queuing theory. In the scenarios like health care systems, launching of quality branded product, movie of a famous actor, etc. the length of the queue does not demoralize the customers in the queue. In such high-end products and services, customers wish to stay in the queue. But, for these services and products to survive in market they have to maintain the perception in the masses. The perception impacts the decision-making of customers where the similar customers appear in conjunction (physically or virtually). If the perception about the product or service goes negative the word-of mouth publicity critically influences the customers to renege.

For example, consider a health care system that analogs to a queuing system in which the arrival of patients in the medical facility is similar to the arriving customers, the diagnosing of patients by a doctor is similar to the servicing customers, and the abandoning of the patient from the health care system before the consultation of doctor as reneging customers. At times the reneging of patients could be bursty due to many reasons like improper check-up, sluggish management, unnecessary costly prescription by doctors, etc. which may prevail a bad perception among masses. That is, for a patient reneging at any time instant, there would be a probability of a patient to renege at the next time instant influenced by the decision of earlier patient. Thus, the probability of reneging is dependent on a recently reneged customer where the similar customers appear in conjunction to share their views and experiences. So, influenced by the decision of earlier patient, other patients may also decide to renege.

Rakesh Kumar, Bhavneet Singh Soodan, Sapana Sharma
MODELLING HEALTH CARE QUEUE MANAGEMENT SYSTEM
FACING PATIENTS' IMPATIENCE USING QUEUING THEORY

RT&A, No 1 (61)
Volume 16, March 2021

We referred this form of reneging as correlated reneging. Sometimes, it happens that the arriving patient leaves the system before joining it. This situation is known as balking in queuing theory.

Mohan [37] first introduces the concept of correlation in gambler's ruin problem. Murari [38] studies a queuing system with correlated arrivals and general service time distribution. Mohan and Murari [39] obtain the transient solution of a queuing model with correlated arrivals and variable service capacity. Conolly [7] considers a queuing system having services depending on inter-arrival times. Conolly and Hadidi [8] consider a model having arrival pattern impacting the service pattern. They examine the initial busy period, state and output processes. Cidon et al. [5] consider a queue in which service time is correlated to inter-arrival time. They study this correlation in case of communication systems and showed the impact through numerical results by comparing with less reliable models. Patuwo et al. [41] work on serial correlation in the arrivals. They study the consequences of correlation on mean queuing performances. They found that positive serial correlations may have vital influence on mean queue length. Drezner [9] performs the performance analysis of $M^c/G/1$ queues. Adan and Kulkarni [1] study a single server queue in which both the inter-arrival times and service times rely on same discrete-time Markov chain, a generalisation of $MAP/G/1$ queuing model. They also obtain the waiting time, steady-state and queue length distribution along with moments for this model. Iravani and Luangkesorn [15] study a model of parallel queues with correlated arrivals and bulk services. To obtain the performance measures they use the matrix geometric method. Hwang and Sohraby [14] consider a correlated queue of packets moving in transmission line with finite capacity. Numerical examples are illustrated to exhibit the importance of correlation on system performances. Hunter [13] studies the consequences of correlated arrivals on the steady-state queue length process for single server queuing model. He extends the concept to four different models and compared their condition for stability and queuing behavior. Kamoun and ali [17] consider a single server queuing model with finite capacity and correlated arrival in which the packets are submitted to random interruptions. The approximations for the queue length distributions of products in machine repair problem are obtained. Claeys et al. [6] study a discrete-time $D - BMAP/G^{l,c}/1$ queue and obtain various performance measures associated with buffer content. They illustrate that the correlated in arrivals cannot be neglected for the evaluation of performance measures and buffer management. Lambert et al. [36] study a discrete time $D - MAP/PH/1$ queuing model and develop an algorithm to deliberate the queue length and delay distribution of customers. They also give some advice to design optical buffers.

In this paper, we study a finite capacity single server queuing model with balking and correlated reneging and discuss their application in queues at health care facilities. Rest of the paper is as follows: In section 2, the stochastic queuing model is described. In section 3, the mathematical model is presented. In section 4, steady-state analysis of the model is done. Section 5 deals with the transient performance analysis of the model. Finally, the paper is concluded in section 6.

2 Stochastic queuing model

We consider a finite capacity single server Markovian queuing model with balking and correlated reneging. The state-transition diagram of the queuing model is shown in figure 1. Patients arrive at a health care facility one by one in accordance with Poisson process with parameter λ. There is a single queue and a single server. The service-times are independently, identically and exponentially distributed with parameter μ. On arrival, the incoming patient may decide to not join the queue (i.e. balk) with certain probability (say, $1 - \beta$). This means the arriving patient may join the queue with probability β. The capacity of the system is finite (say, K), and K=N+1, where N is the capacity of the queue. After joining the queue and waiting for some time, a

Rakesh Kumar, Bhavneet Singh Soodan, Sapana Sharma
MODELLING HEALTH CARE QUEUE MANAGEMENT SYSTEM
FACING PATIENTS' IMPATIENCE USING QUEUING THEORY

RT&A, No 1 (61)
Volume 16, March 2021

patient may leave the queue (renege) without the check-up. The reneging of the patients can take place only at the transition marks $t_0, t_1, t_2, ...$ where $\theta_r = t_r - t_{r-1}, r = 1,2,3...,$ are random variables with $P[\theta_r \leq x] = 1 - exp(-\xi x); \xi \geq 0, r = 1,2,3, ...$ That is, the distribution of inter-transition marks is negative exponential with parameter ξ. The reneging at two consecutive transition marks is governed by the following transition probability matrix:

$$
\begin{array}{cc}
 & \text{to } t_r \\
 & \begin{array}{cc} 0 & \quad\quad 1 \end{array} \\
\text{from } t_{r-1} \quad
\begin{array}{c} 0 \\ 1 \end{array}
\left\|
\begin{array}{cc}
p_{00} & p_{01} \\
p_{10} & p_{11}
\end{array}
\right\|
\end{array}
$$

where, 0 refers to no reneging and 1 refers to the occurrence of reneging. Thus, the notation p_{ij} (i and j can either be 0 or 1) represents the probability of transitioning from present state to next possible state due to the reneging between the two consecutive transition marks.

Also, $p_{00} + p_{01} = 1$ and $p_{10} + p_{11} = 1$. Thus, the reneging in two consecutive transition marks is correlated. In case of no correlation: $p_{00} = p_{10}$ and $p_{01} = p_{11}$.
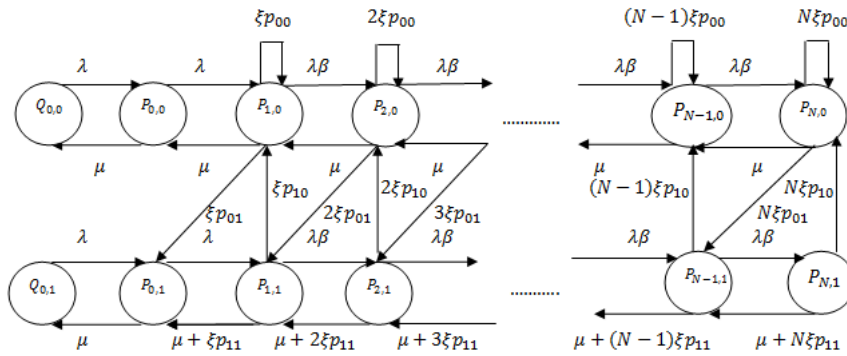
Figure 1: State-transition diagram of the model

3 Mathematical model

Defining the probabilities:

$Q_{0,r}(t)$ is the probability that at time t queue length is zero, the server is idle, and r is an indicator whether a patient has reneged or not at the previous transition mark (r=0 refers that a patient has not reneged and r=1 refers that a patient has reneged at previous transition mark).

$P_{0,r}(t)$ is the probability that at time t queue length is zero, the server is not idle, and r is an indicator whether a patient has reneged or not at the previous transition mark (r=0 refers that a patient has not reneged and r=1 refers that a patient has reneged at previous transition mark).

$P_{n,r}(t)$ is the probability that at time t queue length is $1 \leq n \leq N$, the server is not idle, and r is an indicator whether a patient has reneged or not at the previous transition mark (r=0 refers that a patient has not reneged and r=1 refers that a patient has reneged at previous transition mark).

$p_{i,j}$ = the probability of transitioning from present state to next possible state due to the reneging between the two consecutive transition marks, where both i and j can either be 0 or 1. 0 refers to no reneging and 1 refers to the occurrence of reneging at the considered transition mark.

The differential equations of the model are:

$$\frac{d}{dt}Q_{0,0}(t) = -\lambda Q_{0,0}(t) + \mu P_{0,0}(t) \tag{1}$$

$$\frac{d}{dt}P_{0,0}(t) = -(\lambda + \mu)P_{0,0}(t) + \mu P_{1,0} + \lambda Q_{0,0}(t) \tag{2}$$

Rakesh Kumar, Bhavneet Singh Soodan, Sapana Sharma
MODELLING HEALTH CARE QUEUE MANAGEMENT SYSTEM
FACING PATIENTS' IMPATIENCE USING QUEUING THEORY

RT&A, No 1 (61)
Volume 16, March 2021

$$\frac{d}{dt}P_{1,0}(t) = -(\lambda\beta + \mu + n\xi)P_{1,0}(t) + \mu P_{2,0}(t) + \lambda P_{0,0}(t)$$
$$+\xi[p_{00}P_{1,0}(t) + p_{10}P_{1,1}(t)] \tag{3}$$

$$\frac{d}{dt}P_{n,0}(t) = -(\lambda\beta + \mu + n\xi)P_{n,0}(t) + \mu P_{n+1,0}(t) + \lambda\beta P_{n-1,0}(t)$$
$$+n\xi[p_{00}P_{n,0}(t) + p_{10}P_{n,1}(t)], 1 < n < N \tag{4}$$

$$\frac{d}{dt}P_{N,0}(t) = -(\mu + N\xi)P_{N,0}(t) + \lambda\beta P_{N-1,0}(t)$$
$$+N\xi[p_{00}P_{N,0}(t) + p_{10}P_{N,1}(t)] \tag{5}$$

$$\frac{d}{dt}Q_{0,1}(t) = -\lambda Q_{0,1}(t) + \mu P_{0,1}(t) \tag{6}$$

$$\frac{d}{dt}P_{0,1}(t) = -(\lambda + \mu)P_{0,1}(t) + \mu P_{1,1} + \lambda Q_{0,1}(t) + \xi[p_{11}P_{1,1}(t)$$
$$+p_{01}P_{1,0}(t)] \tag{7}$$

$$\frac{d}{dt}P_{1,1}(t) = -(\lambda\beta + \mu + n\xi)P_{1,1}(t) + \mu P_{2,1}(t) + \lambda P_{0,1}(t)$$
$$+2\xi[p_{01}P_{2,0}(t) + p_{11}P_{2,1}(t)] \tag{8}$$

$$\frac{d}{dt}P_{n,1}(t) = -(\lambda\beta + \mu + n\xi)P_{n,1}(t) + \mu P_{n+1,1}(t) + \lambda\beta P_{n-1,1}(t)$$
$$+(n + 1)\xi[p_{01}P_{n+1,0}(t) + p_{11}P_{n+1,1}(t)], 1 < n < N \tag{9}$$

$$\frac{d}{dt}P_{N,1}(t) = -(\mu + N\xi)P_{N,1}(t) + \lambda\beta P_{N-1,1}(t) \tag{10}$$

4 Steady-state analysis of the model

In this section, we derive the steady state solution of the model using matrix-decomposition method.

4.1 Steady-state equations

Let us define the steady-state probabilities as follows: $Q_{0,i} = \lim_{t\to\infty}Q_{0,i}(t)$, i= 0,1 and $P_{n,i} = \lim_{t\to\infty}P_{n,i}(t)$, n=0,1,2,... and i= 0,1

From the equations (1)-(10) we have the steady-state equations as follows:

$$0 = -\lambda Q_{0,0} + \mu P_{0,0} \tag{11}$$
$$0 = -(\lambda + \mu)P_{0,0} + \mu P_{1,0} + \lambda Q_{0,0} \tag{12}$$
$$0 = -(\lambda\beta + \mu + n\xi)P_{1,0} + \mu P_{2,0} + \lambda P_{0,0} + \xi[p_{00}P_{1,0} + p_{10}P_{1,1}] \tag{13}$$
$$0 = -(\lambda\beta + \mu + n\xi)P_{n,0} + \mu P_{n+1,0} + \lambda\beta P_{n-1,0}$$
$$+n\xi[p_{00}P_{n,0} + p_{10}P_{n,1}], \quad 1 < n < N \tag{14}$$
$$0 = -(\mu + N\xi)P_{N,0} + \lambda\beta P_{N-1,0} + N\xi[p_{00}P_{N,0} + p_{10}P_{N,1}] \tag{15}$$
$$0 = -\lambda Q_{0,1} + \mu P_{0,1} \tag{16}$$
$$0 = -(\lambda + \mu)P_{0,1} + \mu P_{1,1} + \lambda Q_{0,1} + \xi[p_{11}P_{1,1} + p_{01}P_{1,0}] \tag{17}$$
$$0 = -(\lambda\beta + \mu + n\xi)P_{1,1} + \mu P_{2,1} + \lambda P_{0,1} + 2\xi[p_{01}P_{2,0} + p_{11}P_{2,1}] \tag{18}$$
$$0 = -(\lambda\beta + \mu + n\xi)P_{n,1} + \mu P_{n+1,1} + \lambda\beta P_{n-1,1}$$
$$+(n + 1)\xi[p_{01}P_{n+1,0} + p_{11}P_{n+1,1}], \quad 1 < n < N \tag{19}$$
$$0 = -(\mu + N\xi)P_{N,1} + \lambda\beta P_{N-1,1} \tag{20}$$

4.2 Steady-state solution

We use a matrix-decomposition method to get the steady-state probabilities in a recursive manner. Let $P = (P_{0,0}, P_0, P_{0,1}, P_1)$ be the vectors of the steady-state probabilities, where $P_0 = (P_{1,0}, P_{2,0}, \ldots\ldots P_{N,0})$ and $P_1 = (P_{1,1}, P_{2,1}, \ldots\ldots P_{N,1})$. Also, from equations (11) and (16) we can express $Q_{0,0}$ and $Q_{0,0}$ as

$$Q_{0,0} = \frac{\mu}{\lambda}P_{0,0} \tag{21}$$
$$Q_{0,1} = \frac{\mu}{\lambda}P_{0,1} \tag{22}$$

respectively. Substituting the values of $Q_{0,0}$ and $Q_{0,1}$ in equations (11) and (16), we can re-write the set of steady-state differential equations as:

Rakesh Kumar, Bhavneet Singh Soodan, Sapana Sharma
MODELLING HEALTH CARE QUEUE MANAGEMENT SYSTEM
FACING PATIENTS' IMPATIENCE USING QUEUING THEORY

RT&A, No 1 (61)
Volume 16, March 2021

$$0 = -\lambda P_{0,0} + \mu P_{1,0} \tag{23}$$

$$0 = -(\lambda\beta + \mu + n\xi)P_{1,0} + \mu P_{2,0} + \lambda P_{0,0} + \xi[p_{00}P_{1,0} + p_{10}P_{1,1}] \tag{24}$$

$$0 = -(\lambda\beta + \mu + n\xi)P_{n,0} + \mu P_{n+1,0} + \lambda\beta P_{n-1,0}$$
$$+n\xi[p_{00}P_{n,0} + p_{10}P_{n,1}], \quad 1 < n < N \tag{25}$$

$$0 = -(\mu + N\xi)P_{N,0} + \lambda\beta P_{N-1,0} + N\xi[p_{00}P_{N,0} + p_{10}P_{N,1}] \tag{26}$$

$$0 = -\lambda P_{0,1} + \mu P_{1,1} + \xi[p_{11}P_{1,1} + p_{01}P_{1,0}] \tag{27}$$

$$0 = -(\lambda\beta + \mu + n\xi)P_{1,1} + \mu P_{2,1} + \lambda P_{0,1} + 2\xi[p_{01}P_{2,0} + p_{11}P_{2,1}] \tag{28}$$

$$0 = -(\lambda\beta + \mu + n\xi)P_{n,1} + \mu P_{n+1,1} + \lambda\beta P_{n-1,1}$$
$$+(n+1)\xi[p_{01}P_{n+1,0} + p_{11}P_{n+1,1}], \quad 1 < n < N \tag{29}$$

$$0 = -(\mu + N\xi)P_{N,1} + \lambda\beta P_{N-1,1} \tag{30}$$

Thus, the steady-state equations from (23)-(30) can be expressed in matrix form as

$$PQ = 0 \tag{31}$$

Where 0 is the column vector of zeros, and

$$Q = \begin{pmatrix} -\lambda & A_{12} & 0 & A_{14} \\ A_{21} & A_{22} & A_{23} & A_{24} \\ 0 & A_{32} & -\lambda & A_{34} \\ A_{41} & A_{42} & A_{43} & A_{44} \end{pmatrix} \tag{32}$$

is a $(2N + 2) \times (2N + 2)$ square matrix.

Each entry of the matrix **Q** is given below:

$$\mathbf{A_{12}} = \begin{pmatrix} \lambda & 0 & . & . & .0 \end{pmatrix}_{1\times N}, \mathbf{A_{14}} = \begin{pmatrix} 0 & 0 & . & . & .0 \end{pmatrix}_{1\times N}, A_{21} = \begin{pmatrix} \mu \\ 0 \\ . \\ . \\ . \\ 0 \end{pmatrix}_{N\times 1},$$

$$A_{22} =$$
$$\begin{pmatrix} -(\lambda\beta + \mu + \xi - \xi p_{00}) & \lambda\beta & . & . & . & . & 0 \\ \mu & -(\lambda\beta + \mu + 2\xi - 2\xi p_{00}) & . & . & . & . & 0 \\ 0 & \mu & . & . & . & . & 0 \\ . & . & . & . & . & . & . \\ . & . & . & . & . & . & . \\ . & . & . & . & . & . & . \\ 0 & 0 & . & . & . & . & \lambda\beta \\ 0 & 0 & . & . & . & . & -(\mu + N\xi - N\xi p_{00}) \end{pmatrix}_{N\times N},$$

$$A_{23} = \begin{pmatrix} \xi p_{01} \\ 0 \\ . \\ . \\ . \\ 0 \end{pmatrix}_{N\times 1}, A_{24} = \begin{pmatrix} 0 & 0 & 0 & . & . & . & 0 & 0 \\ 2\xi p_{01} & 0 & 0 & . & . & . & 0 & 0 \\ 0 & 3\xi p_{01} & 0 & . & . & . & 0 & 0 \\ 0 & 0 & 0 & . & . & . & . & 0 \\ 0 & 0 & 0 & . & . & . & . & 0 \\ 0 & 0 & 0 & . & . & . & . & 0 \\ 0 & 0 & 0 & . & . & . & 0 & 0 \\ 0 & 0 & 0 & . & . & . & N\xi p_{01} & 0 \end{pmatrix}_{N\times N},$$

$$\mathbf{A_{32}} = \begin{pmatrix} 0 & 0 & . & . & .0 \end{pmatrix}_{1\times N}, \mathbf{A_{34}} = \begin{pmatrix} \lambda & 0 & . & . & .0 \end{pmatrix}_{1\times N}, A_{43} = \begin{pmatrix} \mu + \xi p_{11} \\ 0 \\ . \\ . \\ . \\ 0 \end{pmatrix}_{N\times 1},$$

Rakesh Kumar, Bhavneet Singh Soodan, Sapana Sharma
MODELLING HEALTH CARE QUEUE MANAGEMENT SYSTEM
FACING PATIENTS' IMPATIENCE USING QUEUING THEORY

RT&A, No 1 (61)
Volume 16, March 2021

$$A_{41} = \begin{pmatrix} 0 \\ 0 \\ . \\ . \\ . \\ 0 \end{pmatrix}_{N \times 1}, A_{42} = \begin{pmatrix} \xi p_{10} & 0 & 0 & . & . & . & 0 & 0 \\ & 0 & 2\xi p_{10} & . & . & . & 0 & 0 \\ 0 & 0 & 3\xi p_{01} & . & . & . & 0 & 0 \\ 0 & 0 & 0 & . & . & . & 0 & 0 \\ 0 & 0 & 0 & . & . & . & 0 & 0 \\ 0 & 0 & 0 & . & . & . & 0 & 0 \\ 0 & 0 & 0 & . & . & . & (N-1)\xi p_{10} & 0 \\ 0 & 0 & 0 & . & . & . & 0 & N\xi p_{10} \end{pmatrix}_{N \times N},$$

$$A_{44} = \begin{pmatrix} -(\lambda\beta + \mu + \xi) & \lambda\beta & 0 & . & . & . & 0 & 0 \\ (\mu + 2\xi p_{11}) & -(\lambda\beta + \mu + 2\xi) & \lambda\beta & . & . & . & 0 & 0 \\ 0 & (\mu + 3\xi p_{11}) & \lambda\beta & . & . & . & 0 & 0 \\ . & . & . & . & . & . & . & . \\ . & . & . & . & . & . & . & . \\ . & . & . & . & . & . & . & . \\ 0 & 0 & 0 & . & . & . & -(\lambda\beta + \mu + (N-1)\xi) & \lambda\beta \\ 0 & 0 & 0 & . & . & . & (\mu + N\xi p_{11}) & -(\mu + N\xi) \end{pmatrix}_{N \times N}$$

where A_{14} and A_{32} are row vectors having order N and all the elements are zero, A_{41} is a column vector of order N having all elements equal to zero. From equation (31) it follows that

$$-\lambda P_{0,0} + P_0 A_{21} = 0 \tag{33}$$

$$P_{0,0} A_{12} + P_0 A_{22} + P_1 A_{42} = 0 \tag{34}$$

$$P_0 A_{23} - \lambda P_{0,1} + P_1 A_{43} = 0 \tag{35}$$

$$P_0 A_{24} + P_{0,1} A_{34} + P_1 A_{44} = 0 \tag{36}$$

From equation (36), we get

$$P_1 = -(P_{0,1}\mathbf{A_{34}} + P_0\mathbf{A_{24}})\mathbf{A_{44}^{-1}} \tag{37}$$

Substitute (37) in (35), and solve we get

$$P_0 = \frac{(\lambda + \mathbf{A_{34}A_{44}^{-1}A_{43}})P_{0,1}}{\mathbf{A_{23} - A_{24}A_{44}^{-1}A_{43}}} = \mathbf{\Psi_1} P_{0,1} \tag{38}$$

where,

$$\mathbf{\Psi_1} = \frac{(\lambda + \mathbf{A_{34}A_{44}^{-1}A_{43}})}{\mathbf{A_{23} - A_{24}A_{44}^{-1}A_{43}}}$$

Now, substitute the value of P_0 from (38) to (33), and solve we get

$$P_{0,0} = \frac{\mathbf{\Psi_1 A_{21}}}{\lambda} P_{0,1}. \tag{39}$$

Substituting the value of $\mathbf{P_0}$ from 38) in (37), on solving we get,

$$\mathbf{P_1} = -(\mathbf{A_{34} + \Psi_1 A_{24}})\mathbf{A_{44}^{-1}} P_{0,1} \tag{40}$$

Substituting the value of $P_{0,0}$ from equation 39 to (21), we have

$$Q_{0,0} = \frac{\mu}{\lambda} P_{0,0} = \frac{\mu}{\lambda^2} \mathbf{\Psi_1 A_{21}} P_{0,1} \tag{41}$$

We can obtain the unknown constant $P_{0,1}$ by using normalization equation:

$$Q_{0,0} + Q_{0,1} + \sum_{n=0}^{N} \sum_{1=0}^{1} P_{n,i} = Q_{0,0} + Q_{0,1} + P_{0,0} + P_0 e + P_{0,1} + P_1 e = 1 \tag{42}$$

where **e** is the unit column vector of dimension N.

Substituting the values from equations (22), (38)-(41) to (42) we get the explicit expression for $P_{0,1}$ as:

$$P_{0,1} = \frac{1}{\frac{\mu}{\lambda^2}\mathbf{\Psi_1 A_{21}} + \frac{\mu}{\lambda} + \frac{\mathbf{\Psi_1}}{\lambda}\mathbf{A_{21}} + \mathbf{\Psi_1 e} + 1 - (\mathbf{A_{34} + \Psi_1 A_{24}})\mathbf{A_{44}^{-1}e}} \tag{43}$$

Thus, the steady-state probabilities $Q_{0,0}, Q_{0,1}, P_0, P_1$ and $P_{0,1}$ can be computed using equations (22), (38)-(41) respectively.

Rakesh Kumar, Bhavneet Singh Soodan, Sapana Sharma
MODELLING HEALTH CARE QUEUE MANAGEMENT SYSTEM
FACING PATIENTS' IMPATIENCE USING QUEUING THEORY

RT&A, No 1 (61)
Volume 16, March 2021

5 Transient performance analysis of the model

In this section, we perform the transient analysis of the model. To obtain the transient solution we use the Runge-Kutta method of fourth order. The $''ode45''$ function of MATLAB software is used to compute the transient numerical results.

5.1 Performance Measures

We study the following performance measures in the transient state:
1. Expected number of patients in queue $(L_q(t))$:
$$L_q(t) = \sum_{n=1}^{N} (n)[P_{n,0}(t) + P_{n,1}(t)] \tag{44}$$
2. Expected waiting time of patients in queue $(W_q(t))$:
$$W_q(t) = \frac{L_q(t)}{\mu[1 - Q_{0,0}(t) - Q_{0,1}(t) - P_{0,0}(t) - P_{0,1}(t)]} \tag{45}$$
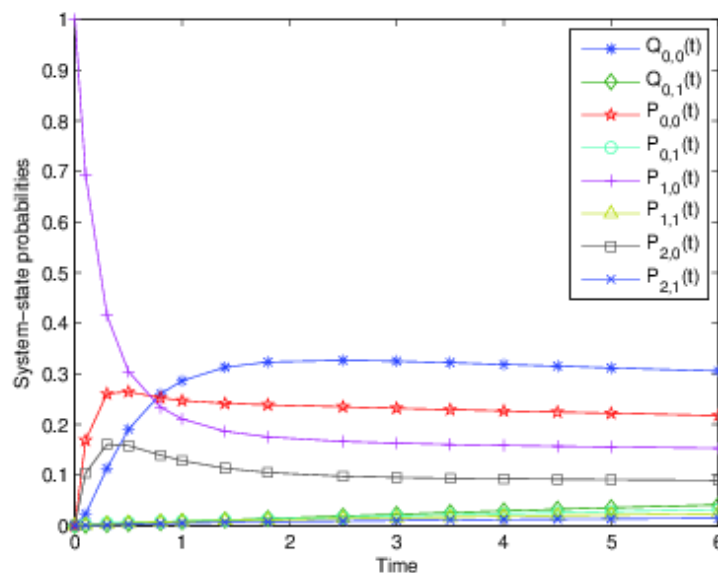
Figure 2: System-State probabilities vs Time
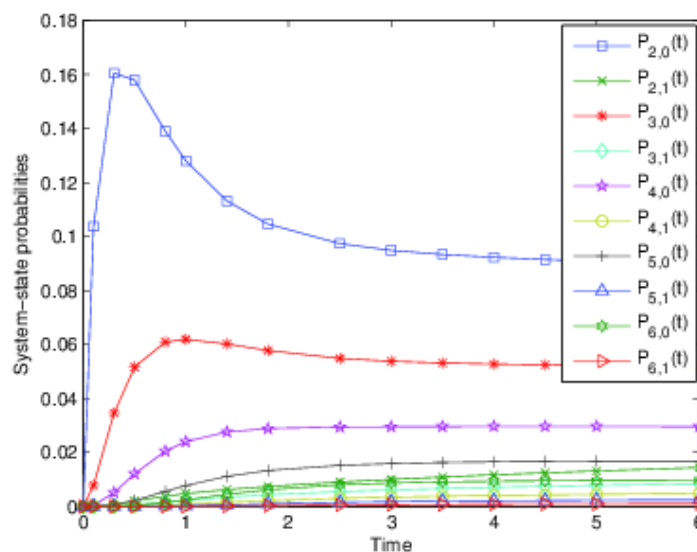
Figure 3: System-state probabilities vs Time (detail)

Rakesh Kumar, Bhavneet Singh Soodan, Sapana Sharma
MODELLING HEALTH CARE QUEUE MANAGEMENT SYSTEM
FACING PATIENTS' IMPATIENCE USING QUEUING THEORY

RT&A, No 1 (61)
Volume 16, March 2021

In figures 2 and 3, the variation in system-state probabilities of patients with respect to time is shown. It is seen that except the probability $P_{1,0}(t)$ all other probabilities initially starts from zero and asymptotically reach the steady-state. $P_{1,0}(t)$ initially starts from 1 due to the initial condition we considered i.e. $P_{1,0}(0) = 1$. The values of parameters are: $\lambda = 1.8, \mu = 2.5, \beta = 0.85, \xi = 0.2, N = 6, p_{00} = 0.8, p_{01} = 0.2, p_{10} = 0.7$ and $p_{11} = 0.3$.
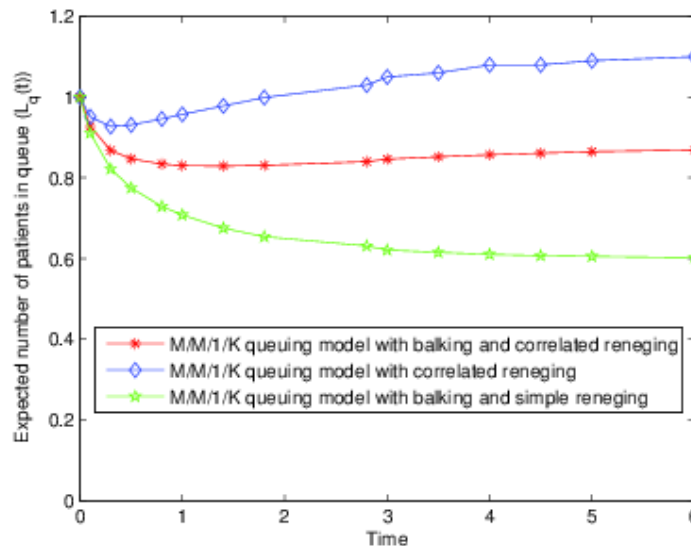
Figure 4: Expected number of patients in queue vs time
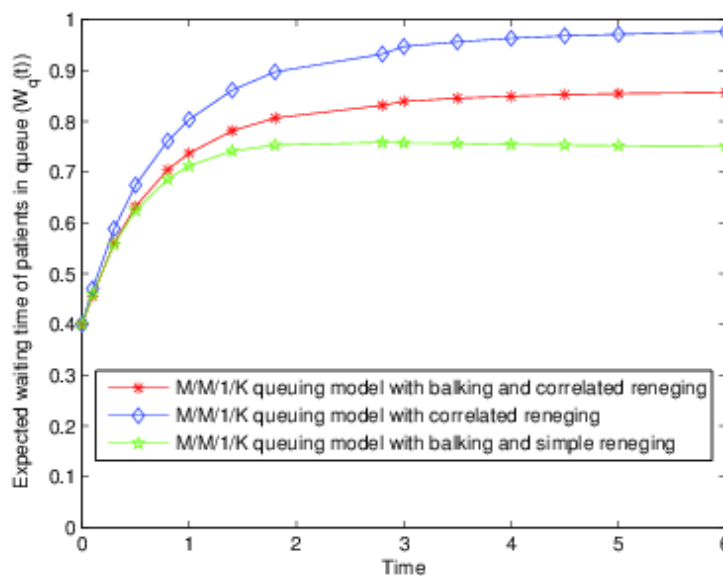
Figure 5: Expected waiting time of patients in queue vs time

Figures 4 and 5 show a comparative analysis of variation in expected number of patients in queue and expected waiting time of patients in queue respectively for the three queueing models. In figure 4 it is observed that the expected number of patients in queue for the M/M/1/K queuing model with balking and correlated reneging is higher than that of M/M/1/K queuing model with simple reneging and balking. This shows that in the cases of correlated reneging the expected number of patients in queue is actually higher than that of we considered so far.

Rakesh Kumar, Bhavneet Singh Soodan, Sapana Sharma
MODELLING HEALTH CARE QUEUE MANAGEMENT SYSTEM
FACING PATIENTS' IMPATIENCE USING QUEUING THEORY

RT&A, No 1 (61)
Volume 16, March 2021

Also, the expected number of patients in queue for M/M/1/K queuing model with correlated reneging is higher than that of M/M/1/K queuing model with balking and correlated reneging which shows the effect of balking. In figure 5 similar trend is observed for variation in expected waiting time of patients in queue. The values of the parameters are: $\lambda = 1.8, \mu = 2.5, \xi = 0.2, \beta = 0.85, N = 6, p_{0,0} = 0.8, p_{0,1} = 0.2, p_{1,0} = 0.7$, and $p_{1,1} = 0.3$ with initial condition $P_{1,0}(0) = 1$.
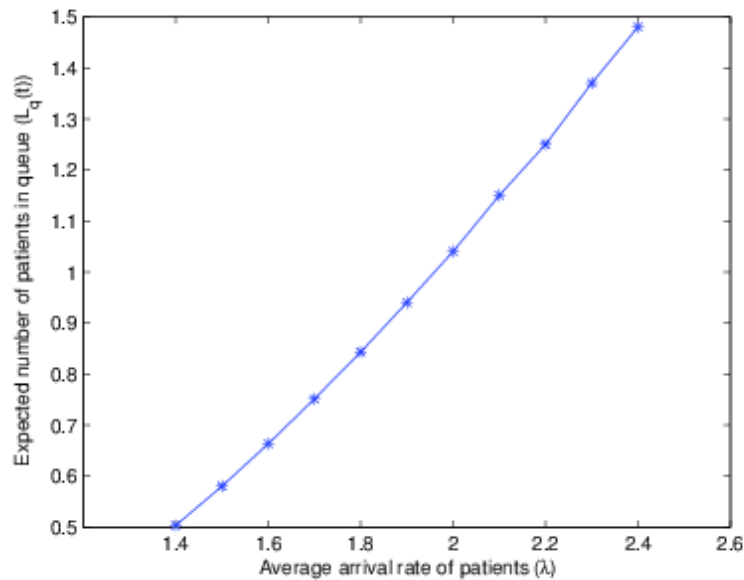
Figure 6: Variation in expected number of patients in queue with respect to average arrival rate of patients (λ)
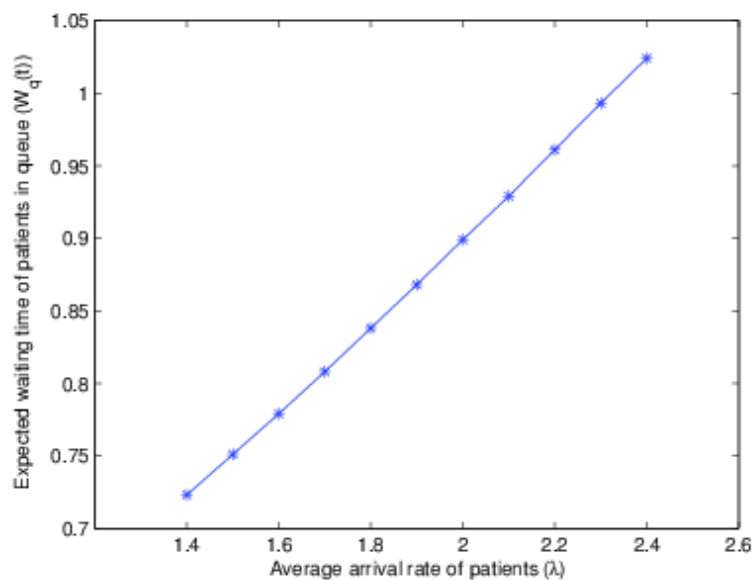
Figure 7: Variation in expected waiting time of patients in queue with respect to average arrival rate of patients (λ)

In figures 6 and 7 the effect of average arrival rate of patients on expected number of

Rakesh Kumar, Bhavneet Singh Soodan, Sapana Sharma
MODELLING HEALTH CARE QUEUE MANAGEMENT SYSTEM
FACING PATIENTS' IMPATIENCE USING QUEUING THEORY

RT&A, No 1 (61)
Volume 16, March 2021

patients in queue and expected waiting time of patients in queue is observed respectively. One can easily see that with the increase in average arrival both the expected number of patients in queue and expected waiting time of patients in queue increase. The values of the parameters are: $\mu = 2.5, \xi = 0.2, \beta = 0.85, N = 6, t = 3, p_{0,0} = 0.8, p_{0,1} = 0.2, p_{1,0} = 0.7$, and $p_{1,1} = 0.3$ with initial condition $P_{1,0}(0) = 1$.
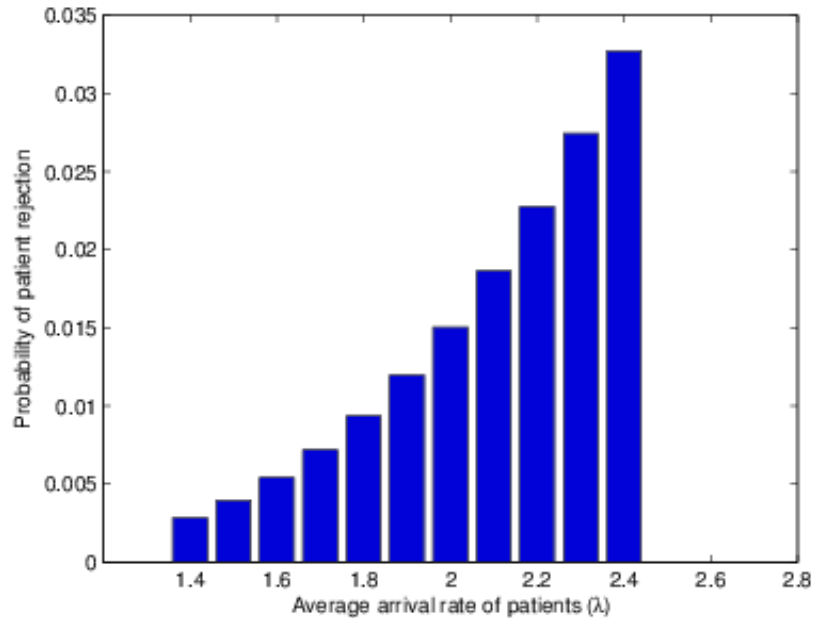

Figure 8: Probability of patient rejection vs Average arrival rate of patients (λ)
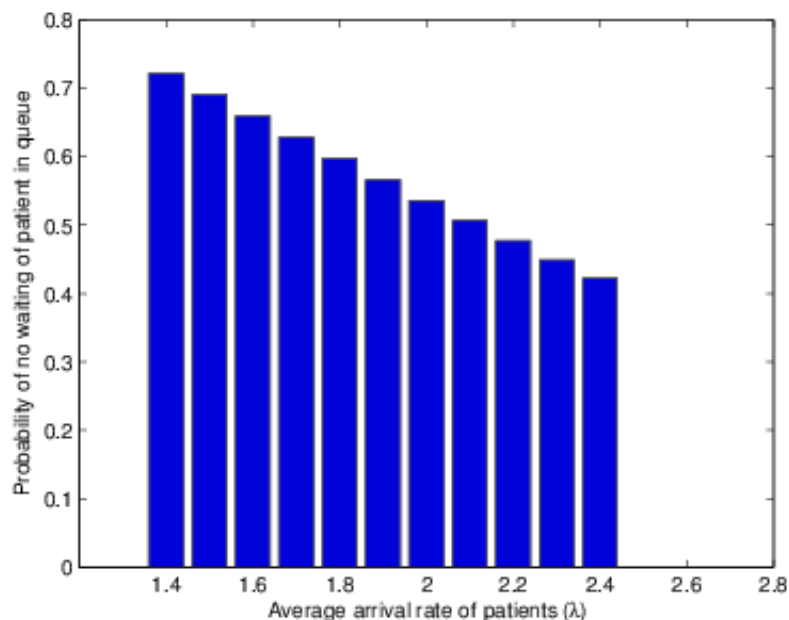
Figure 9: Probability of no waiting of pateint in queue vs Average arrival rate of patients (λ)

In figures 8 and 9 the effect of average arrival rate of patients on probability of patient rejection and probability of no waiting of patient in queue is observed respectively. One can easily see that with the increase in average arrival rate of patients, the probability of patient rejection

Rakesh Kumar, Bhavneet Singh Soodan, Sapana Sharma
MODELLING HEALTH CARE QUEUE MANAGEMENT SYSTEM
FACING PATIENTS' IMPATIENCE USING QUEUING THEORY

RT&A, No 1 (61)
Volume 16, March 2021

increases whereas the probability of no waiting of patient in queue decreases. The values of the parameters are: $\mu = 2.5, \xi = 0.2, \beta = 0.85, N = 6, t = 3, p_{0,0} = 0.8, p_{0,1} = 0.2, p_{1,0} = 0.7$, and $p_{1,1} = 0.3$ with initial condition $P_{1,0}(0) = 1$.
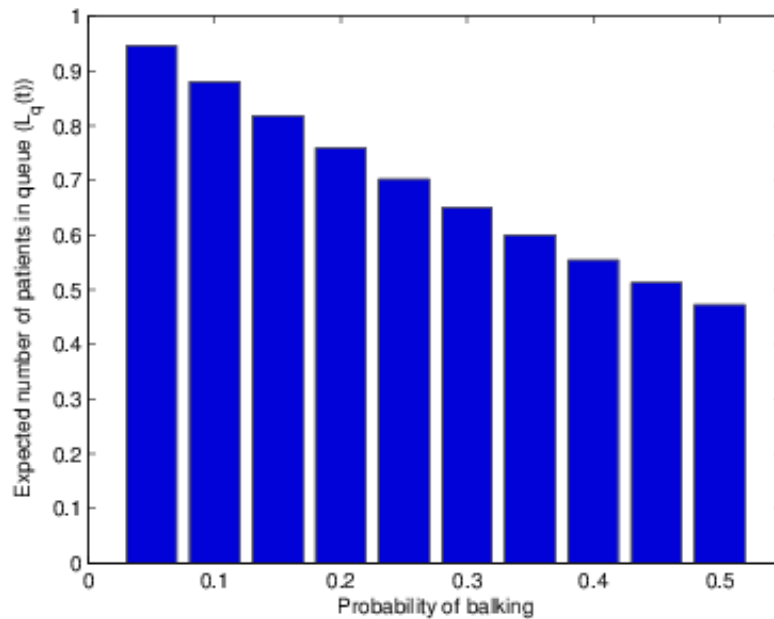
Figure 10: Variation in $L_q(t)$ w.r.t. Probability of balking
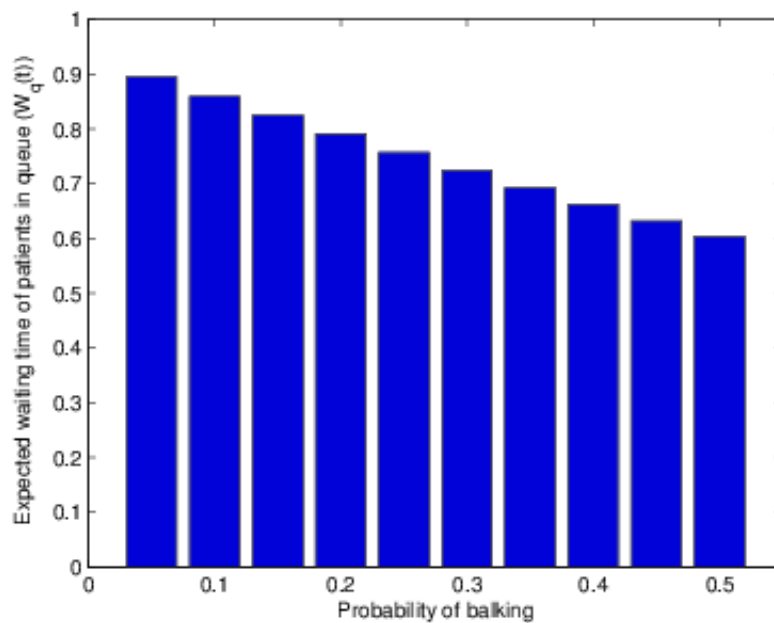
Figure 11: Variation in $W_q(t)$ w.r.t.Probability of balking

In figures 10 and 11 the effect of probability of balking on expected number of patients in queue and expected waiting time of patients in queue is observed respectively. It is seen that with the increase in probability of balking both the performance parameters decreases which is quite obvious. The values of the parameters are: $\lambda = 1.8, \mu = 2.5, \xi = 0.3, N = 6, p_{0,0} = 0.8, p_{0,1} = 0.2, p_{1,0} = 0.7$, and $p_{1,1} = 0.3$ with initial condition $P_{1,0}(0) = 1$ at t=3.

Rakesh Kumar, Bhavneet Singh Soodan, Sapana Sharma
MODELLING HEALTH CARE QUEUE MANAGEMENT SYSTEM
FACING PATIENTS' IMPATIENCE USING QUEUING THEORY

RT&A, No 1 (61)
Volume 16, March 2021

Figure 12: Variation in expected number of patients in queue
with respect to rate of transition marks
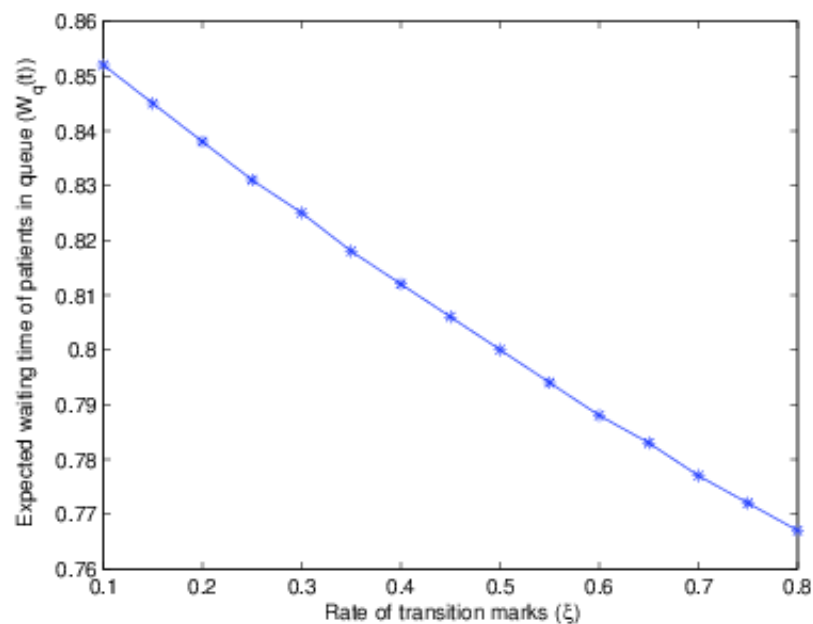
Figure 13: Variation in expected waiting time of patients in queue
with respect to rate of transition marks

In figures 12 and 13 the variation in expected number of patients in queue and expected waiting time of patients in queue with respect to change in rate of transition marks is observed respectively. It is seen that with the increase in rate of transition marks both the performance paramters decreases which is quite obvious. The values of the parameters are: $\lambda = 1.8, \mu = 2.5, \beta = 0.85, N = 6, p_{0,0} = 0.8, p_{0,1} = 0.2, p_{1,0} = 0.7$, and $p_{1,1} = 0.3$ with initial condition $P_{1,0}(0) = 1$ at t=3.

Rakesh Kumar, Bhavneet Singh Soodan, Sapana Sharma
MODELLING HEALTH CARE QUEUE MANAGEMENT SYSTEM
FACING PATIENTS' IMPATIENCE USING QUEUING THEORY

RT&A, No 1 (61)
Volume 16, March 2021

6 Conclusion

A queuing model with balking and correlated reneging is studied. The application of the model in health care queue management system is extensively explained and transient-state analysis is performed. The steady-state solution is obtained using matrix-decomposition method.

References

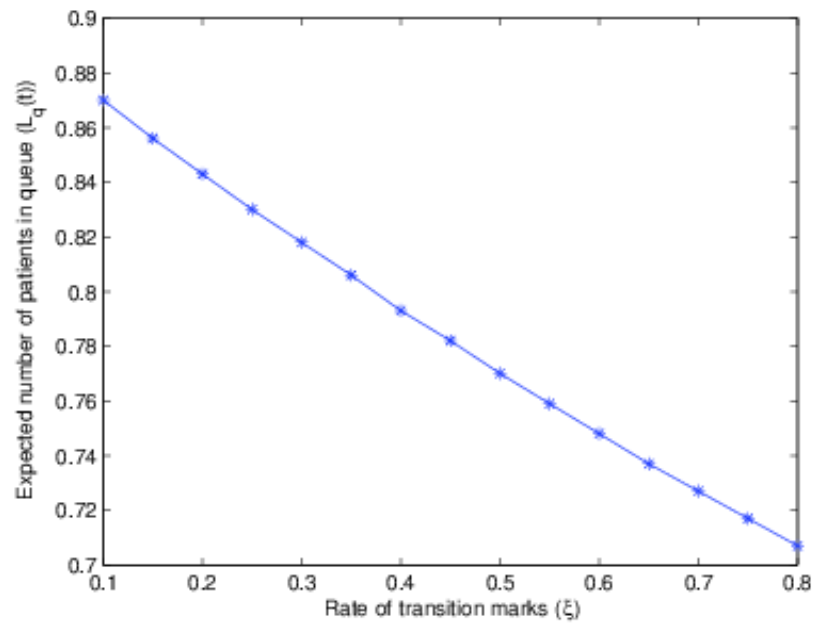[1]   Adan, I.J. and Kulkarni, V.G. (2003) Single-server queue with Markov-dependent inter-arrival and service times. *Queueing Systems*, 45:113–134.

[2]   Afolalu, A., Adelakun, O.J., Ongbali, S.O., Abioye, A.A. and Ajayi, O.O. (2019) Queueing Theory – A Tool for Production Planning in Health Care. *Proceedings of the World Congress on Engineering*.

[3]   Ancker, C.J. and Gafarian, A.V. (1963). Queuing problems with balking and reneging I. *Operations Research*, 11:88–100.

[4]   Ancker, C.J. and Gafarian, A.V. (1963) Queuing problems with balking and reneging II. *Operations Research*, 11:928–937.

[5]   Cidon, I., GuΓ©rin, R., Khamisy, A. and Sidi, M. (1993) Analysis of a correlated queue in a communication system. *IEEE Transactions on Information Theory*, 39:456–465.

[6]   Claeys, D., Steyaert, B., Walraevens, J., Laevens, K. and Bruneel, H. (2013) Analysis of a versatile batch-service queueing model with correlation in the arrival process. *Performance Evaluation*, 70:300–316.

[7]   Conolly, B. W. (1968) The waiting time process for a certain correlated queue. *Operations Research*, 16:1006–1015.

[8]   Conolly, B. W. and Hadidi, N. (1969) A correlated queue. *Journal of Applied Probability*, 6:122–136.

[9]   Drezner, Z. (1999) On a Queue with Correlated Arrivals. *Journal of Applied Mathematics and Decision Sciences*, 3:75–84.

[10] Fomundam, S. and Herrmann, J. (2007) A Survey of Queuing Theory Applications in Healthcare. *The Institute for Systems Research*, The Institute for Systems Research ISR Technical Report, 1–24.

[11] Haight, F.A. (1957) Queuing with Balking. *Biometrika*, 44:362–369.

[12] Haight, F.A. (1959) Queuing with Reneging. *Metrika*, 2:186–197.

[13] Hunter, J.J. (2007) Markovian queues with correlated arrival processes. *Asia-Pacific Journal of Operational Research*, 24:593–611.

[14] Hwang, G. U. and Sohraby, K. (2004) Performance of correlated queues: the impact of correlated service and inter-arrival times. *Performance Evaluation*, 55:129–145.

[15] Iravani, S. M., Luangkesorn, K. L. and Simchi-Levi, D. (2004) A general decomposition algorithm for parallel queues with correlated arrivals. *Queueing Systems*, 47:313–344.

[16] Jeffery, K. C. and James, R. B. (2010) Developing nonlinear queuing regressions to increase emergency department patient safety: Approximating reneging with balking. *Computers & Industrial Engineering*, 59:378–386.

[17] Kamoun, F. and Ali, M. M. (1995) Queuing Analysis of ATM Tandem Queues with Correlated Arrivals. *In Proceedings of INFOCOM'95, IEEE*, 2:709–716.

[18] Kumar, B.K., Parthasarathy P.R. and Sharafali, M. (1993) Transient solution of an M/M/1 queue with balking. *Queueing Systems*, 13:441-448.

[19] Kumar, R. and Sharma, S.K. (2012) An M/M/1/N queuing model with retention of reneged customers and balking. *American Journal of Operational Research*, 2:1-5.

[20] Kumar, R. and Sharma, S. K. (2012) $M/M/1/N$ queuing system with retention of reneged customers. *Pakistan Journal of Statistics and Operation Research*, 8:859–866.

[21] Kumar, R. and Sharma, S.K. (2012) A multi-server Markovian queueing system with discouraged arrivals and retention of reneged customers. *International Journal of Operations Research*, 9:173-184.

[22] Kumar, R. (2013) Economic analysis of an M/M/c/N queuing model with balking, reneging and retention of reneged customers. *Opsearch*, 50:383-403.

[23] Kumar, R. and Sharma, S.K. (2013) An M/M/c/N queuing system with reneging and retention of reneged customers. *International Journal of Operational Research*, 17:333-334.

Rakesh Kumar, Bhavneet Singh Soodan, Sapana Sharma
MODELLING HEALTH CARE QUEUE MANAGEMENT SYSTEM
FACING PATIENTS' IMPATIENCE USING QUEUING THEORY

RT&A, No 1 (61)
Volume 16, March 2021

[24] Kumar, R. and Sharma, S.K. (2014) Two Heterogeneous Server Markovian Queueing Model with Discouraged Arrivals, Reneging and Retention of Reneged Customers. *International Journal of Operations Research*, 11:64-68.

[25] Kumar, R. and Sharma, S.K. (2014) A multi-server Markovian feedback queue with balking, reneging and retention of reneged customers. *AMO-Advanced Modeling and Optimization*, 16:395-406.

[26] Kumar, R. and Sharma, S.K. (2014) A Markovian multi-server queuing model with retention of reneged customers and balking. *International Journal of Operational Research*, 20:427-438.

[27] Kumar, R. (2016) A single-server Markovian queuing system with discouraged arrivals and retention of reneged customers. *Yugoslav journal of operations research*, 24:119-126.

[28] Kumar, R. and Sharma, S. (2017) Transient Analysis of a Multi-server Queuing Model with Discouraged Arrivals and Retention of Reneging Customers. *International Conference on Analytical and Computational Methods in Probability Theory, Springer* (pp. 54-64).

[29] Kumar, R. and Sharma, S. (2018) Transient performance analysis of single-server queuing model with retention of reneging customers. *Yugoslav Journal of Operations Research*, 28:315–331.

[30] Kumar, R. and Sharma, S. (2018) Transient analysis of an M/M/c queuing system with balking and retention of reneging customers. *Communications in Statistics-Theory and Methods*, 47:1318-1327.

[31] Kumar, R. and Sharma, S. (2019) Transient solution of a two-heterogeneous serversв™ queuing system with retention of reneging customers. *Bulletin of the Malaysian Mathematical Sciences Society*, 42:223-240.

[32] Kumar, R. and Soodan, B.S. (2019) Transient Analysis of a Single-Server Queuing System with Correlated Inputs and Reneging. *Reliability: Theory & Applications*, 14:102–106.

[33] Kumar, R. and Soodan, B.S. (2019) Transient Numerical Analysis of a Queueing Model with Correlated Reneging, Balking and Feedback. *Reliability: Theory & Applications*, 14:46-54.

[34] Kumar, R. and Soodan, B.S. (2020) Transient Solution of a Single Server Queuing Model with Correlated Reneging Using Runge-Kutta Method. *International Journal of Mathematical, Engineering and Management Sciences*, 5:886-896.

[35] Lakshmi, C. and Sivakumar, A. (2013) Application of queueing theory in health care: A literature review. *Operations Research for Health Care*, 2:25–29.

[36] Lambert, J., Houdt, B.V. and Blondia, C. (2006) Queues with correlated service and inter-arrival times and their application to optical buffers. *Stochastic Models*, 22:233–251.

[37] Mohan, C. (1955) The gambler's ruin problem with correlation. *Biometrika*, 42:486–493.

[38] Murari, K. (1969) A Queueing Problem with Correlated Arrivals and General Service Time Distribution. *ZAMMвJournal of Applied Mathematics and Mechanics*, 49:151–156.

[39] Mohan, C. and Murari, K. (1972) Time dependent solution of correlated queuing problem with variable capacity. *Metrika*, 19:209–215.

[40] Obulor, R. and Eke, B.O. (2016) Outpatient Queueing Mdel Development for Hospital Appointment System. *International Journal of Scientific Engineering and Applied Science (IJSEAS)*, 2:15–22.

[41] Patuwo, B. E., Disney, R. L. and McNickle, D. C. (1993) The effect of correlated arrivals on queues. *IIE transactions*, 25:105–110.

[42] Peter, O. and Sivasamy, R. (2019) Queuing Theory Techniques and Its Real Applications to Health Care Systems – Outpatient Visits. *International Journal of Healthcare Management*, DOI: 10.1080/20479700.2019.1616890.

[43] Rao, S.S. (1965) Queuing models with balking, reneging, and interruptions. *Operations Research*, 13:596–608.

[44] Sharma, S.K. and Kumar, R. (2012) A Markovian feedback queue with retention of reneged customers. *AMO-Advanced Modeling and Optimization*, 14:673-680.

[45] Yang, D.Y. and Wu, Y.Y. (2017) Analysis of a finite-capacity system with working breakdowns and retention of impatient customers. *Journal of Manufacturing Systems*, 44:207–216.

Harris Generalized Linear Exponential Distribution and Its Applications

Albin Paul[a], K.K. Jose[b]

•

[a]St.Thomas College Palai, Kerala, India
albinpaul0333@gmail.com
[b]School of Mathematics and Statistics,
Mahatma Gandhi University,
Kottayam, Kerala, India.
kkj.smsda.mgu@gmail.com

Abstract

In this paper we consider an extension of the linear exponential distribution based on the Harris generalization method, which includes some of the life time distribution as sub models. Along with the four parameter generalization namely Harris generalized linear exponential distribution, we derive some of its properties such as moments, quantiles and moment generating function. A compound form expression of the density function is given. For the given model the Rényi entropy, mean residual life and the distribution of order statistics is derived. The problem of estimation of parameters is considered and validated with respect to two real data sets.

Keywords: Harris generalization, Linear exponential distribution, Order Statistics, Moment generating function, Entropy, Mean residual life, Data analysis

1 Introduction

Introduction of new parameters to the well established classical distributions may result in more flexible new families of distributions. Several extended forms of distributions have been studied by many researchers like Azzalini (1985), Marshall and olkin (1997), Ferreira and Steel (2007), Jose et al (2010), Krishna et al (2013), Jose and Sivdas (2015) etc. Recently Aly and Benkherouf (2011) introduced a method for developing new classes of distributions by adding two new parameters to an existing distribution, which includes the baseline distribution as a special case and gives more flexible models for various types of data. This method is based on probability generating function introduced by Harris (1948). Hence the resulting family of distributions is known as Harris Generalized (HG) family of distributions. This family of distributions can be considered as a generalization of Marshall Olkin family of distributions introduced by Marshall and olkin (1997). Some properties and applications of HG family of distributions are studied by Aly and Benkherouf (2011), Batsidis and lemonte (2014) and Cordeiro et al (2015) etc. Aly and Benkherouf (2011) derived the general structure of HG family of distributions as follows.

The survival function of HG family of distributions is given by

$$\bar{G}(x;\ \theta, r) = \left(\frac{\theta(\bar{F}(x))^r}{1 - \bar{\theta}(\bar{F}(x))^r} \right)^{\frac{1}{r}},\ 0 < \theta < \infty,\ r > 0,\ \bar{\theta} = 1 - \theta \tag{1.1}$$

where $\bar{F}(.)$ is the survival function of the baseline distribution. The corresponding density function is

$$g(x) = \frac{\theta^{\frac{1}{r}} f(x)}{\left(1 - \bar{\theta}(\bar{F}(x))^r \right)^{\left(\frac{r+1}{r} \right)}}\ ,\quad x > 0 \tag{1.2}$$

If r=1 in equations (1.1) and (1.2), reduces to the corresponding survival function and density function of Marshall-Olkin family of distributions. The density function of HG family of distributions can be expressed as a linear combination of exponentiated family of distributions as given in Batsidis and lemonte (2014) and Barreto-Souza et al (2013) as follows.

For $\theta \in (0, 1)$

$$g(x) = f(x) \sum_{i=0}^{\infty} w_i (\bar{F}(x))^{r_i} \tag{1.3}$$

where $w_i = w_i(\theta, r) = \theta^{\frac{1}{r}} \bar{\theta}^i \frac{\Gamma(r^{-1} + i + 1)}{\Gamma(r^{-1} + 1)i!}$

For $\theta > 1$

$$g(x) = f(x) \sum_{i=0}^{\infty} v_i (\bar{F}(x))^{r_i} \tag{1.4}$$

where $v_i = v_i(\theta, r) = (-1)^i \theta^{-1} \sum_{j=1}^{\infty} \binom{j}{i} \left(\frac{\theta - 1}{\theta} \right)^j \frac{\Gamma(r^{-1} + j + 1)}{\Gamma(r^{-1} + 1)j!}$

From (1.3) and (1.4) it is clear that the HG family of distributions can be expressed as the baseline distribution $f(x)$, multiplied by an infinite power series which differ only for the coefficients.

The aim of this paper is to study a new univariate family of distribution based on the Harris generalization method. The contents are organized as follows. In Section 2 we discuss the Linear exponential distribution. In Section 3 we introduce the Harris generalized linear exponential distribution. In Section 4 we represent the Harris generalized linear exponential distribution as a compound distribution with exponential density. In Section 5 and 6 we evaluate the Entropy and Mean residual life. Section 7 gives the distribution of order statistics. Section 8 and 9 discuss the maximum likelihood estimation of the parameters and an application to a real data set.

2 Linear Exponential Distribution

The Linear Exponential (LE) distribution is an important distribution that has rich variety of applications for modeling life time data. The LE distribution is also known as Linear Failure rate distribution. The LE distribution contains Rayleigh and Exponential distribution as special cases and they are well known in the literature for a variety of applications.

From Lai et al (2006) and Zang et al (2005), the LE distribution models phenomenon with increasing failure rate, the accuracy of the statistical procedures depends on the probability model or distributions which are considered for the analysis. Recently there has been a renewed interest in the study of extended versions of conventional classical distributions. Since the real data is affected by various factors, the statistical models derived using the extended form of distribution shows more significant applications in reliability, medical science, finance, economics etc. The LE distribution has many applications in applied statistics, reliability analysis, medical studies (See Carbone et al (1967), Broadbent (1958)). Recently many studies have been done on LE distribution and its generalizations by introducing additional parameters (See Mahmoud and Alam (2010), Cordeiro et al (2015), Nadarajah et al (2014) etc).

The LE distribution with the parameters β_1 and β_2, (LE(β_1, β_2)) has the following cumulative distribution function

$$F(x;\ \beta_1, \beta_2) = 1 - \exp\left(-\beta_1 x - \frac{\beta_2}{2} x^2 \right) \tag{2.1}$$

If we put β_2=0 in (2.1) we can obtain the exponential distribution with parameter β_1 and if we put β_1=0 in (2.1) we get the Rayleigh distribution with parameter β_2.

The probability density function (pdf) of LE(β_1, β_2) distribution is given by

$$f(x; \beta_1, \beta_2) = (\beta_1 + \beta_2 x)\exp\left(-\beta_1 x - \frac{\beta_2}{2}x^2\right), \quad x > 0, \quad \beta_1, \beta_2 > 0.$$

3 Harris Generalized Linear Exponential Distribution

By applying the method given in Aly and Benkherouf (2011) Harris Extended Linear exponential distribution is introduced by Batsidis and lemonte (2014). Here we call this family of distributions as Harris Generalized distribution. By taking LE distribution as the baseline distribution, we get the Harris generalized Linear exponential (HGLE) distribution. The application of this family of distribution in the context of reliability test plan were studied by JoseandPaul(2018).

The substitution of the survival function of LE(β_1, β_2) distribution in (1.1) gives the HGLE distribution with parameters $\theta, r, \beta_1, \beta_2$ and is denoted as HGLE($\theta, r, \beta_1, \beta_2$),

The survival function of the HGLE distribution is obtained as

$$\bar{G}(x) = \left(\frac{\theta\exp\left(-r\left(\beta_1 x + \frac{\beta_2}{2}x^2\right)\right)}{1-\bar{\theta}\exp\left(-r\left(\beta_1 x + \frac{\beta_2}{2}x^2\right)\right)}\right)^{\frac{1}{r}} \tag{3.1}$$

The pdf of HGLE distribution is given by

$$g(x) = \frac{\theta^{\frac{1}{r}}(\beta_1+\beta_2 x)\exp\left(-\left(\beta_1 x+\frac{\beta_2}{2}x^2\right)\right)}{\left(1-\bar{\theta}\exp\left(-r\left(\beta_1 x+\frac{\beta_2}{2}x^2\right)\right)\right)^{1+\frac{1}{r}}} \tag{3.2}$$

where $x > 0, \theta > 0, r > 0, \beta_1 > 0, \beta_2 > 0, \bar{\theta} = 1 - \theta$.

The corresponding hazard rate function is given by

$$h(x) = \frac{(\beta_1+\beta_2 x)}{1-\bar{\theta}\exp\left(-r\left(\beta_1 x+\frac{\beta_2}{2}x^2\right)\right)} \tag{3.3}$$

By taking r=1 in (3.2) we get the Marshall-Olkin Linear Exponential distribution (MOLE), and when r=1 and $\theta = 1$, (3.2) reduces to the LE distribution. When β_2=0, (3.2) gives the Harris Extended Exponential distribution as given in Pinho et al (2015). In the same way it will reduce to Marshall Olkin Exponential distribution and Exponential distribution when r=1 and r=1, $\theta = 1$ respectively. If $\beta_1 = 0$ this distribution reduces to the Harris extended form of Rayleigh distribution and it includes the Marshall-Olkin generalization of Rayleigh distribution (if r=1), Rayleigh distribution (if $\theta = 1$) as its special cases.

The quantile function of HGLE distribution can be obtained by inverting the cdf given in (2.1), and is obtained as

$$x_p = \frac{\beta_1}{\beta_2}\left[\sqrt{1 + \frac{2\beta_2}{r\beta_1^2}\log(\bar{\theta} + \theta(1 - p)^{-r})} - 1\right], \tag{3.4}$$

where $0 < p < 1$.

Some possible shapes of the pdf of HGLE distribution for different values of parameters are given in Fig. 1.

Some possible shapes of the hazard rate function of the distribution for different values of parameters are given in Fig. 2
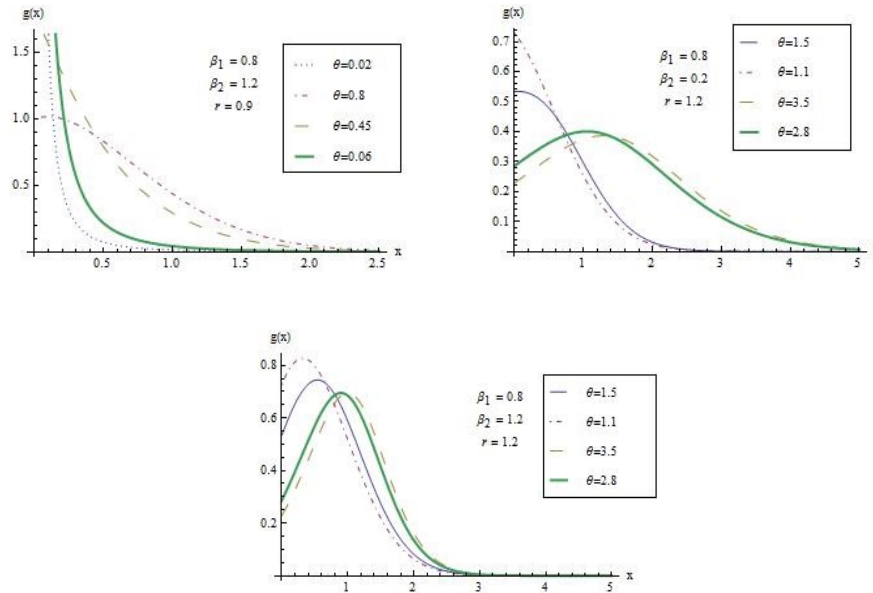
Figure 1: pdf of HGLE Distribution for different values of parameters.
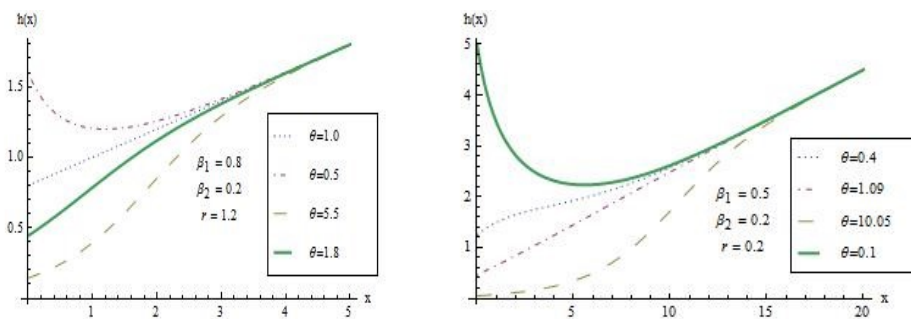
Figure 2: Hazard rate function of HGLE Distribution for different values of parameters.

Theorem: 1 *The pdf of HGLE distribution can be represented as a linear combination of Linear exponential density function as*

$$g(x) = \sum_{i=0}^{\infty} \eta_i f_{(\beta_1^*, \beta_2^*)}(x)$$

where $f_{(\beta_1^*, \beta_2^*)}(x)$ follows LE distribution with parameters $\beta_1^* = (ri+1)\beta_1$ and
$\beta_2^* = (ri+1)\beta_2$.

Proof: Consider the pdf of HGLE distribution given in (3.2),

For $\theta < 1$,

the expression given by (3.2) can be expanded using the negative binomial power series as follows,

$$g(x) = \theta^{\frac{1}{r}}(\beta_1 + \beta_2 x)\exp\left(-\left(\beta_1 x + \frac{\beta_2}{2}x^2\right)\right)\sum_{i=0}^{\infty}\binom{i+r^{-1}}{i}\bar{\theta}^i\exp\left(-\left(\beta_1 x + \frac{\beta_2}{2}x^2\right)ri\right)$$

$$= \sum_{i=0}^{\infty}\frac{\bar{\theta}^i\theta^{\frac{1}{r}}}{(ri+1)}\binom{i+r^{-1}}{i}\left((ri+1)(\beta_1 + \beta_2 x)\exp\left(-(ri+1)\left(\beta_1 x + \frac{\beta_2}{2}x^2\right)\right)\right)$$

$$= \sum_{i=0}^{\infty}\eta_i f_{(\beta_1^*, \beta_2^*)}(x)$$

Here for $\theta < 1$, $\quad \eta_i = \frac{\bar{\theta}^i \theta^{\frac{1}{r}}}{(ri+1)} \begin{pmatrix} i + r^{-1} \\ i \end{pmatrix}$ $\qquad\qquad$ (3.5)

and $\quad f_{(\beta_1^*, \beta_2^*)}(x) = \left((ri+1)(\beta_1 + \beta_2 x) \exp\left(-(ri+1)\left(\beta_1 x + \frac{\beta_2}{2} x^2 \right) \right) \right)$

where $f_{(\beta_1^*, \beta_2^*)}(x)$ follows LE distribution with parameters $\beta_1^* = (ri+1)\beta_1$ and $\beta_2^* = (ri+1)\beta_2$.

For $\theta > 1$, let us take $\theta = \theta_1^{-1}$ so that $0 < \theta_1 < 1$.

On simplification (3.2) reduces to

$$g(x) = \frac{\theta_1(\beta_1 + \beta_2 x)y}{\left(1 - \bar{\theta}_1(1 - y^r)\right)^{1 + \frac{1}{r}}}$$

where $y = \exp\left(-\left(\left(\beta_1 x + \frac{\beta_2}{2} x^2 \right) \right) \right)$ and $\bar{\theta}_1 = 1 - \theta_1$. Since the denominator lies in the interval (0, 1),

we can use the negative binomial power series expansion, then we have

$$g(x) = \theta_1(\beta_1 + \beta_2 x)y \sum_{j=0}^{\infty} \bar{\theta}_1{}^j (1 - y^r)^j \begin{pmatrix} j + r^{-1} \\ j \end{pmatrix}$$

$$= \theta_1(\beta_1 + \beta_2 x)y \sum_{j=0}^{\infty} \sum_{i=0}^{j} (-1)^i (\bar{\theta}_1)^j y^{ri} \begin{pmatrix} j + r^{-1} \\ j \end{pmatrix} \begin{pmatrix} j \\ i \end{pmatrix}$$

Interchanging the order of summation and substituting y we get

$$g(x) = \sum_{i=0}^{\infty} \frac{\theta_1(-1)^i}{(ri+1)} \left(\sum_{j=i}^{\infty} (\bar{\theta}_1)^j \begin{pmatrix} j + r^{-1} \\ j \end{pmatrix} \begin{pmatrix} j \\ i \end{pmatrix} \right)$$

$$\left\{ (ri+1)(\beta_1 + \beta_2 x) \exp\left(-(ri+1)\left(\beta_1 x + \frac{\beta_2}{2} x^2 \right) \right) \right\}$$

which leads to

$g(x) = \sum_{i=0}^{\infty} \eta_i f_{(\beta_1^*, \beta_2^*)}(x)$ where

$$\eta_i = \frac{\theta_1(-1)^i}{(ri+1)} \left(\sum_{j=i}^{\infty} (\bar{\theta}_1)^j \begin{pmatrix} j + r^{-1} \\ j \end{pmatrix} \begin{pmatrix} j \\ i \end{pmatrix} \right) \qquad\qquad (3.6)$$

and

$$f_{(\beta_1^*, \beta_2^*)}(x) = \left((ri+1)(\beta_1 + \beta_2 x) \exp\left(-(ri+1)\left(\beta_1 x + \frac{\beta_2}{2} x^2 \right) \right) \right)$$

which is the pdf of LE distribution with parameters $\beta_1^* = (ri+1)\beta_1$ and $\beta_2^* = (ri+1)\beta_2$.

Theorem: 2 *The moment generating function of HGLE distribution, denoted as M(t) is given by*

$M(t) = \sum_{i=0}^{\infty} \eta_i \omega_{s,ri}$ *and* $\omega_{s,ri}$ *can be expressed as*

$$\omega_{s,ri} = \int_0^{\infty} \exp(tx)(ri+1)(\beta_1 + \beta_2 x) \exp\left(-(ri+1)\left(\beta_1 x + \frac{\beta_2}{2} x^2 \right) \right) dx$$

$$For\ \theta < 1,\ \eta_i = \frac{\bar{\theta}^i \theta^{\frac{1}{r}}}{(ri+1)} \begin{pmatrix} i + r^{-1} \\ i \end{pmatrix}$$

For $\theta \geq 1$, $\qquad \eta_i = \frac{\theta_1(-1)^i}{(ri+1)} \sum_{j=0}^{\infty} \bar{\theta}_1^j \begin{pmatrix} j + r^{-1} \\ j \end{pmatrix} \begin{pmatrix} j \\ i \end{pmatrix}$, *where* $\theta_1 = \frac{1}{\theta}, 0 \leq \theta_1 \leq 1$.

Proof:

We have $M(t) = \int_0^{\infty} \exp(tx) f(x; \theta, r, \beta_1, \beta_2) dx$

$$= \int_0^{\infty} \exp(tx) \sum_{i=0}^{\infty} \eta_i (ri+1)(\beta_1 + \beta_2 x) \exp\left(-(ri+1)\left(\beta_1 x + \frac{\beta_2}{2} x^2 \right) \right) dx$$

(by using theorem 1)

$$= \sum_{i=0}^{\infty} \eta_i \int_0^{\infty} (ri+1)(\beta_1 + \beta_2 x) \exp\left(-\left((ri+1)\beta_1 - t \right)x \right) \exp\left(-(ri+1)\left(\frac{\beta_2}{2} x^2 \right) \right) dx$$

consider

$$\int_0^\infty (ri+1)\beta_1 x^{2s}\exp\big(-((ri+1)\beta_1-t)x\big)dx + \int_0^\infty (ri+1)\beta_2 x^{2s+1}\exp\big(-((ri+1)\beta_1-t)x\big)\,dx$$

$$= \frac{(ri+1)\beta_1\Gamma(2s+1)}{\big((ri+1)\beta_1-t\big)^{2s+1}} + \frac{(ri+1)\beta_2\Gamma(2s+2)}{\big((ri+1)\beta_1-t\big)^{2s+2}}; \quad t \leq \beta_1$$

Then

$$M(t) = \sum_{i=0}^\infty \eta_i \sum_{s=0}^\infty \frac{\left((ri+1)\frac{\beta_2}{2}\right)^s}{s!}(-1)^s\left(\frac{(ri+1)\beta_1\Gamma(2s+1)}{\big((ri+1)\beta_1-t\big)^{2s+1}} + \frac{(ri+1)\beta_2\Gamma(2s+2)}{\big((ri+1)\beta_1-t\big)^{2s+2}}\right); \quad t \leq \beta_1$$

where η_i can be chosen suitably for $\theta \leq 1$ and $\theta > 1$ as given in equation (3.5) and (3.6).

Theorem: 3

If X has $HGLE(r,\beta_1,\beta_2,\theta)$ distribution. The the kth moment of X denoted by μ_k is given by,

$$\mu_k = \sum_{i=0}^\infty \sum_{s=0}^\infty \theta^{\frac{1}{r}}\bar\theta^i \binom{1+r^{-1}}{i}\frac{\left(-(ri+1)\frac{\beta_2}{2}\right)^s}{s!}\left(\frac{\beta_1\Gamma(k+2s+1)}{\big((ri+1)\beta_1\big)^{(k+2s+1)}} + \frac{\beta_2\Gamma(k+2s+2)}{\big((ri+1)\beta_1\big)^{(k+2s+2)}}\right)$$

Proof:

We have,

$$\mu_k = \int_0^\infty x^k \frac{\theta^{\frac{1}{r}}(\beta_1+\beta_2 x)\exp\left(-\left(\beta_1+\frac{\beta_2}{2}x^2\right)\right)}{\left(1-\bar\theta\exp\left(-r\left(\beta_1+\frac{\beta_2}{2}x^2\right)\right)\right)^{1+\frac{1}{r}}}dx \qquad \int_0^\infty x^k g(x)dx$$

$$= \int_0^\infty x^k \theta^{\frac{1}{r}}(\beta_1+\beta_2 x)\sum_{i=0}^\infty \binom{1+r^{-1}}{i}\bar\theta^i\exp\left(-(ri+1)\left(\beta_1 x+\frac{\beta_2}{2}x^2\right)\right)dx$$

Interchanging the integration and summation we get

$$= \sum_{i=0}^\infty \binom{1+r^{-1}}{i}\theta^{\frac{1}{r}}\bar\theta^i\int_0^\infty x^k(\beta_1+\beta_2 x)\exp\left(-(ri+1)\left(\beta_1 x+\frac{\beta_2}{2}x^2\right)\right)dx$$

$$= \sum_{i=0}^\infty \binom{1+r^{-1}}{i}\theta^{\frac{1}{r}}\bar\theta^i\sum_{s=0}^\infty \frac{\left(-(ri+1)\frac{\beta_2}{2}\right)^s}{s!}\left(\int_0^\infty \beta_1 x^{k+2s}\exp\big(-(ri+1)(\beta_1 x)\big)dx + \right.$$

$$\left. \int_0^\infty \beta_2 x^{k+2s+1}\exp\big(-(ri+1)(\beta_1 x)\big)dx\right)$$

$$= \sum_{i=0}^\infty \sum_{s=0}^\infty \theta^{\frac{1}{r}}\bar\theta^i \binom{1+r^{-1}}{i}\frac{\left(-(ri+1)\frac{\beta_2}{2}\right)^s}{s!}\left(\frac{\beta_1\Gamma(k+2s+1)}{\big((ri+1)\beta_1\big)^{(k+2s+1)}} + \frac{\beta_2\Gamma(k+2s+2)}{\big((ri+1)\beta_1\big)^{(k+2s+2)}}\right)$$

This completes the proof of the theorem.

4 Compounding

Ghitany et al (2005), Ghitany and Kotz (2007) and Krishna et al (2013) expressed Marshall Olkin extended forms of distributions Marshall and olkin (1997) as compound distributions with exponential as mixing density. This gives a new parametric family of distributions in terms of existing ones.

Let $\bar F(x/\alpha), x \in \Re, \alpha \in \Re$, be the conditional survival function of a continuous random variable X given . Let follows a distribution with probability density function $m(\alpha)$. A distribution with survival function

$$\bar F(x) = \int_{-\infty}^\infty \bar F(x/\alpha)m(\alpha)\,d\alpha, \; x \in \Re$$

is called a compound distribution with mixing density $m(\alpha)$.

The following theorem shows that under suitable conditions the HGLE distribution can be obtained as a compound distribution.

Theorem: 4 *Let X be a continuous random variable with conditional pdf given by $\bar F(x/\alpha) =$*

$$exp\left(\left(exp\left(-r\left(\beta_1 x + \frac{\beta_2}{2}x^2\right)\right)\right)^{-1} - 1\right)\alpha, \qquad x, r, \beta_1, \beta_2, \alpha > 0.$$

Let α follows an exponential distribution with with pdf given by $m(\alpha) = \theta e^{-\theta\alpha}$, θ, $\alpha > 0$. Then the proportional failure rate model of the compound distribution of X becomes the HGLE (r, θ, β_1, β_2) distribution.

Proof: For all $x > 0$, β_1, β_2, $\theta > 0$, the unconditional survival function of x is given by

$$\bar{F}(x) = \int_0^\infty \bar{F}(x/\alpha)m(\alpha)d\alpha$$

$$= \alpha \int_0^\infty exp\left(\left(exp\left(-r\left(\beta_1 x + \frac{\beta_2}{2}x^2\right)\right)\right)^{-1} - 1\right)\alpha \; exp(-\alpha\theta) \; d\alpha$$

$$\bar{F}(x) = \frac{\alpha}{exp\left(-r\left(\beta_1 x + \frac{\beta_2}{2}x^2\right)\right)^{-1} - \bar{\alpha}}$$

$$\bar{F}(x) = \frac{\alpha exp\left(-r\left(\beta_1 x + \frac{\beta_2}{2}x^2\right)\right)}{1 - \bar{\alpha}exp\left(-r\left(\beta_1 x + \frac{\beta_2}{2}x^2\right)\right)}$$

Let us take the proportional failure rate model of $\bar{F}(x)$, Then

$$\bar{G}(x) = \bar{F}(x)^{\frac{1}{r}}$$

$$\bar{G}(x) = \left(\frac{\alpha exp\left(-r\left(\beta_1 x + \frac{\beta_2}{2}x^2\right)\right)}{1 - \bar{\alpha}exp\left(-r\left(\beta_1 x + \frac{\beta_2}{2}x^2\right)\right)}\right)^{\frac{1}{r}}$$

which is the survival function of a random variable with HGLE distribution with parameter $(r, \theta, \beta_1, \beta_2)$.

5 Renyi Entropy

Numerous measures of entropy are discussed and studied by many researchers and these Entropy measures has been used in various situations of science and technology especially in communications engineering and information technology. The entropy of a random variable X with density function $g(x)$ is a measure of uncertainty. The Rényi entropy is defined by

$$I_g(\delta) = (1 - \delta)^{-1}\log \int_{-\infty}^\infty g^\delta(x)dx$$

where $\delta > 0$ and $\delta \neq 1$

$$I_g(\delta) = (1 - \delta)^{-1}\log\left(\begin{array}{c} \sum_{k=0}^\infty \sum_{s=0}^\infty \sum_{i=0}^\delta \theta^{\frac{\delta}{r}}(1-\theta)^k \frac{\Gamma\delta\left(1+\frac{1}{r}\right)+k}{\Gamma\delta\left(1+\frac{1}{r}\right)k!}\binom{\delta}{i}\beta_1^i\beta_2^{\delta-i} \\ \\ (-1)^s \frac{\left((\delta+rk)\frac{\beta_2}{2}\right)^s}{s!} \frac{\Gamma(\delta+2s-i+1)}{((\delta+rk)\beta_1)^{(\delta+2s-i+1)}} \end{array}\right)$$

Table 1 displays the Renyi entropy for HGLE distribution at $\delta = 2.0, 2.5, 3.0$, $\beta_1 = 0.5$, $\beta_2 = 0.9$, $r = 1.2$ and for different choices of $\theta > 1$.

θ	$I_g(\delta) \; \delta = 2.0$	$I_g(\delta) \; \delta = 2.5$	$I_g(\delta) \; \delta = 3.0$
1.5	0.8290	0.7549	0.7336
2.0	0.8530	0.8003	0.7783
2.5	0.8661	0.8228	0.7995
3.0	0.8731	0.8342	0.8094
3.5	0.8765	0.8396	0.8134
4.0	0.8777	0.8415	0.8141

Table 1: Renyi Entropy of HGLE Distribution at $\delta = 2.0, 2.5, 3.0$, $r = 1.2$, $\beta_1 = 0.5$, $\beta_2 = 0.9$

6 Mean Residual Life

The expected additional life time given that a component has survived until time t is called mean residual life (MRL). The importance of MRL function in reliability and survival analysis is that it describes the aging process. Also MRL function uniquely determines its distribution function.

The MRL of a random variable X representing life of a component is given as follows.

$$M_R(t) = \frac{1}{\bar{G}(t)} \int_t^\infty \bar{G}(x)dx, \ \ t > 0$$

The MRL function of a lifetime random variable X with HGLE distribution is given by

$$M_R(t) = \left(\frac{1 - \bar{\theta}\exp\left(-r\left(\beta_1 x + \frac{\beta_2}{2}t^2\right)\right)}{\theta\exp\left(-r\left(\beta_1 x + \frac{\beta_2}{2}t^2\right)\right)} \right)^{\frac{1}{r}} \int_t^\infty \left(\frac{\theta\exp\left(-r\left(\beta_1 x + \frac{\beta_2}{2}x^2\right)\right)}{1 - \bar{\theta}\exp\left(-r\left(\beta_1 x + \frac{\beta_2}{2}x^2\right)\right)} \right)^{\frac{1}{r}} dx$$

Table 2 displays MRL function for HGLE distribution at point t=0.2, 0.5, 0.9, $r = 1.2, \beta_1 = 0.5, \beta_2 = 0.9$ and for different choices of parameter θ.

θ	MRL,t=0.2	MRL,t=0.5	MRL,t=0.9
1.0	0.8087	0.6906	0.5735
1.5	0.9191	0.7676	0.6143
2.0	1.0034	0.8302	0.6502
2.5	1.0716	0.8829	0.6823
3.0	1.1288	0.9284	0.7114
3.5	1.1781	0.9685	0.7379

Table 2: Mean residual life of HGLE Distribution at $r = 1.2$, $\beta_1 = 0.5$, $\beta_2 = 0.9$

7 Order Statistics

Let $X_1, X_2, \ldots, X_n$ be a random sample taken from HGLE distribution and $X_{1:n}, X_{2:n}, \ldots, X_{n:n}$ be the corresponding order statistics. We derive the pdf of ith order statistics $X_{i:n}$ which is denoted as $g_{i:n}(x)$, and express it as a linear combination of HGLE density function. We have the general formula for the pdf of the ith order statistics as follows

$$g_{i:n}(x) = \frac{n!}{(i-1)!(n-i)!} g(x) \left(\bar{G}(x)\right)^{n-i} \left(1 - \bar{G}(x)\right)^{i-1}$$

By using Binomial expansion, we get

$$g_{i:n}(x) = \frac{n!}{(i-1)!(n-i)!} g(x) \sum_{j=0}^{i-1} (-1)^j \binom{i-1}{j} \left(\bar{G}(x)\right)^{n+j-i}$$

On simplification $g_{i:n}(x)$ reduces to

$$g_{i:n}(x) = \frac{n!}{(i-1)!(n-i)!} \sum_{j=0}^{i-1} \binom{i-1}{j} \frac{(-1)^j}{(n+j-i+1)} \theta^{\left(\frac{n+j-i+1}{r}\right)}$$

$$(n+j-i+1)(\beta_1 + \beta_2 x) \frac{\exp\left(-(n+j-i+1)\left(\beta_1 x + \frac{\beta_2}{2}x^2\right)r\right)}{\left(1 - \bar{\theta}\exp\left(-\left(\beta_1 x + \frac{\beta_2}{2}x^2\right)r\right)\right)^{1+\frac{(n+j-i+1)}{r}}}$$

$$= \frac{n!}{(i-1)!(n-i)!} \sum_{j=0}^{i-1} \binom{i-1}{j} \frac{(-1)^j}{(n+j-i+1)} g_{n,j,i}(x)$$

where $g_{n,j,i}(x)$ is the density function of HGLE distribution with parameters $r(n+j-i+1)^{-1}$, θ, $(n+j-i+1)\beta_1$, $(n+j-i+1)\beta_2$.

The kth moment of ith order statistic of HGLE distribution can be derived by using Theorem 3 as the distribution of order statistics can be expressed as the linear combination of HGLE density function. Consider the asymptotic distribution of the first order statistic $X_{1:n}$ and n^{th} order statistic $X_{n:n}$. y using the asymptotic results for $X_{1:n}$ and $X_{n:n}$ (Arnold et al (1992), Kotz and Nadarajah (2001)),

we can find the limiting distribution of extreme order statistics. We have

$$\lim_{n\to\infty} P(X_{1:n} \leq a_n^* + b_n^* t) = 1 - \exp(-t^{-\alpha}), \quad t > 0, \ \alpha > 0, \tag{7.1}$$

of Weibull type, where $a_n^* = G^{-1}(0)$ and $b_n^* = G^{-1}\left(\frac{1}{n}\right) - G^{-1}(0)$ if and only if $G^{-1}(0)$ is finite and, for all $t > 0$ and $c > 0$,

$$\lim_{\epsilon\to 0^+} \frac{G(G^{-1}(0)+\epsilon t)}{G(G^{-1}(0)+\epsilon)} = t^{\alpha}. \tag{7.2}$$

For the maximal order statistics $X_{n:n}$, we have

$$\lim_{n\to\infty} P(X_{n:n} \leq a_n + b_n t) = \exp(-e^{-t}), \quad -\infty < t < \infty \tag{7.3}$$

of extreme value type, where $a_n = G^{-1}\left(1 - \frac{1}{n}\right)$ and $b_n = \frac{1}{ng(a_n)}$ if

$$\lim_{x\to\infty} \frac{d}{dx}\left(\frac{1}{h(x)}\right) = 0. \tag{7.4}$$

The selection of the norming constants a_n and b_n are not unique but depend on G. In general we use the result given in (Arnold et al (1992)) and the same used in (Ghitany and Kotz (2007)). The following theorem gives the limiting distributions of the smallest and largest order statistics from the HGLE distribution.

Theorem: 5

Let $X_{1:n}$ and $X_{n:n}$ be, respectively, the smallest and largest order statistics from $HGLE(\theta, r, \beta_1, \beta_2)$ distribution. Then

(i). $\lim\limits_{n\to\infty} P\{X_{1:n} \leq b_n^* t\} = 1 - \exp(-t), \ t > 0$, where $b_n^* = G^{-1}\left(\frac{1}{n}\right)$ and $G^{-1}(.)$ is given by (3.4).

(ii). $\lim\limits_{n\to\infty} P\{X_{n:n} \leq a_n + b_n t\} = \exp(-e^{-t}), \ -\infty < t < \infty$, where $a_n = G^{-1}\left(1 - \frac{1}{n}\right), \ b_n = \frac{1}{ng(a_n)}$, and $g(.)$ and $G^{-1}(.)$, respectively are given by (3.2) and (3.4).

Proof:

(i). For HGLE distribution $G^{-1}(0) = 0$ which is finite and by using L Hospitals rule

$$\lim_{\epsilon\to 0^+} \frac{G(G^{-1}(0)+\epsilon t)}{G(F^{-1}(0)+\epsilon)} = t \lim_{\epsilon\to 0^+} \frac{g(\epsilon t)}{g(t)} = t.$$

From (7.2) we have $\alpha=1$ and the asymptotic distribution of $X_{1:n}$ is of Weibull type, where

$$b_n^* = G^{-1}\left(\frac{1}{n}\right) = \frac{\beta_1}{\beta_2}\left[\sqrt{1 + \frac{2\beta_2}{r\beta_1^2}\log\left(\bar{\theta} + \theta\left(1 - \frac{1}{n}\right)^{-r}\right)} - 1\right]$$

Hence (i) follows from (7.1) and (7.2).

(ii). For HGLE distribution, by using Von Mises sufficient condition for the weak convergence and the properties given in ([?]), we get,

$$\lim_{x\to G^{-1}(1)} \frac{d}{dx}\left(\frac{1}{h(x)}\right) = \lim_{x\to\infty} \left(\frac{r(1-\theta)\exp\left(-r\left(\beta_1 x + \frac{\beta_2}{2}x^2\right)\right)}{-\frac{\left(1-(1-\theta)\exp\left(-r\left(\beta_1 x + \frac{\beta_2}{2}x^2\right)\right)\beta_2\right)}{(\beta_1+\beta_2 x)^2}} \right) = 0$$

where $a_n = G^{-1}(1 - n^{-1})$, $G^{-1}(.)$ given in (3.4) and $b_n = \frac{1}{ng(a_n)}$, where b_n can be obtained by using a_n and (3.2). Hence, statement (ii) follows from (7.3) and (7.4).

8 Estimation

In this section we consider maximum likelihood estimation for a given sample $X_1, X_2, \ldots, X_n$. Then the log likelihood function is given by

$$\log L = \frac{n}{r}\log\theta + \sum_{i=0}^{n}\log(\beta_1 + \beta_2 x_i) - \sum_{i=0}^{n}\left(\beta_1 x_i + \frac{\beta_2}{2}x_i^2\right)$$

$$- \left(1 + \frac{1}{r}\right)\sum_{i=0}^{n}\log\left(1 - \bar{\theta}\exp\left(-r\left(\beta_1 x_i + \frac{\beta_2}{2}x_i^2\right)\right)\right)$$

The maximum likelihood estimates can be obtained by solving the equations $\frac{\partial logL}{\partial r} = 0, \frac{\partial logL}{\partial \beta_1} = 0, \frac{\partial logL}{\partial \beta_2} = 0, \ \frac{\partial logL}{\partial \theta} = 0$. These equations are non-linear and can be solved iteratively using nlm program in R software.

9 Data Analysis

Example 1

Consider the data set which gives the survival times for 121 breast cancer patients treated over the period 1929-1938 (Boag (1984), Lawless (2003)). We compare the HGLE distribution with two other distributions LE distribution with cdf given in (2.1) and MOLE distribution. The survival function of MOLE distribution can be derived by setting r=1 in (3.1). For the given data set, we estimate the unknown parameter of each distribution by the maximum likelihood method, with these obtained estimates we obtain the values of Kolmogrov Smirnov (K-S) statistics and p value. From the values given in Table 3, we observe that HGLE distribution is a competitive distribution compared with other two distributions.

Model	Parameters	Estimates	Log likelihood	K-S Statistics	p value
LE	β_1	0.0155	579.72	0.0826	0.3816
	β_2	0.000186			
MOLE	β_1	0.0029963			
	β_2	0.0000612	579.456	0.0563	0.8354
	θ	2.360			
HGLE	r	3.800			
	β_1	0.0199	578.780	0.0542	0.8698
	β_2	0.000135			
	θ	2.099			

Table 3: Fitting for the LE, MOLE and HGLE Distribution

Example 2

Consider the data set given in Chhikara and Folks (1989) and Lawless (2003), the data on repair times (in hours) for 46 failures of an airbone communications receiver and here we compare the HGLE distribution with MOLE distribution. Table 4 gives the MLE's of the fitted models to the current data with the K-S statistics and p- value. From the given table we can conclude that the HGlE distribution better fits the given data than the MOLE distribution.

Model	Parameters	Estimates	Log likelihood	K-S Statistics	p value
MOLE	β_1	0.00535			
	β_2	0.00324	103.5308	0.0955	0.785
	θ	0.0163			
HGLE	r	2.1513			
	β_1	0.000401	102.176	0.0676	0.9827
	β_2	0.00721			
	θ	0.00687			

Table 4: Fitting for the MOLE and HGLE Distribution
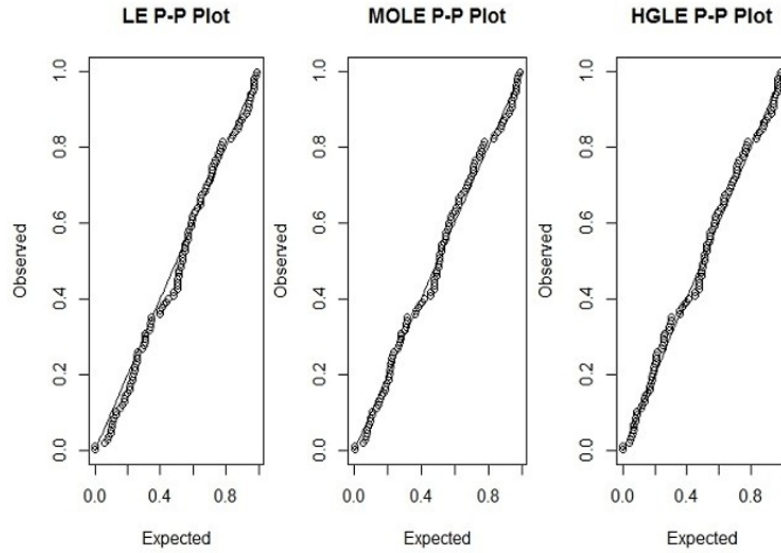
Figure 3: P P Plot for LE distribution, MOLE distribution and HGLE
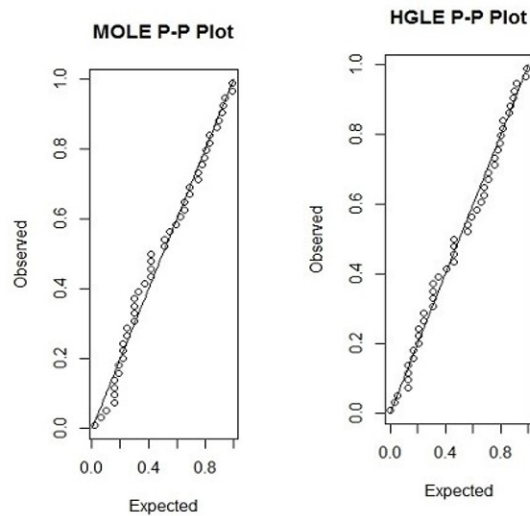
Figure 4: P P Plot for MOLE distribution and HGLE distribution

10 Conclusion

In this paper we have shown a generalization of LE distribution namely HGLE distribution. We have studied some of the statistical properties of the distribution such as probability density function, hazard rate function, moment generating function, distribution of order statistics, asymptotic distribution of extreme order statistics, Renyi entropy etc. The method of maximum likelihood estimation is also derived and also described two cases of real data application to show how HGLE distribution performs better than its baseline distributions.

References

[1] Aly and Benkherouf (2011) Aly and Benkherouf. L., A new family of distribution based on probability generating functions, *Sankhya B-Applied and Interdisciplinary Statistics*, **73**(1), 70-80, (2011).

[2] Arnold et al (1992) Arnold, B.C., Balakrishnan, N., and Nagaraja, H.N., A first course in order statistics. New York: Wiley, (1992).

[3] Azzalini (1985) Azzalini, A., A class of distributions which includes the normal ones, *Scandinavian Journal of Statistics*, **12**, 171-178, (1985).

[4] Barreto-Souza et al 2013 Barreto-Souza, W., Lemonte, A.J. and Cordeiro, G.M., General results for the Marshall-Olkin's family of distributions, *Annals of the Brazilian Academy of Sciences*, **85**, 3-21, (2013).

[5] Batsidis and lemonte (2014) Batsidis, A. and Lemonte, A.J., On the Harris extended family of distributions, *Statistics, A Journal of Theoretical and Applied Statistics*, **49**, 1400-1421, (2014).

[6] Boag (1984) Boag, J. W., Maximum likelihood estimates of the proportion of patients cured by Cancer therapy, *Journal of Royal Statistical Society B,* **11**, 15-53, (1984).

[7] Broadbent (1958) Broadbent, S., Simple mortality rates, *Journal of Applied Statistics*, **7**, 86, (1958).

[8] Carbone et al (1967) Carbone, P., Kellerthouse, L. and Gehan, E., Plasmacytic Myeloma: A Study of the relationship of survival to various clinical manifestations and anomalous protein type in112 patients, *American Journal of medicine*, **42** 937-948, (1967).

[9] Embrechts et al (2013) Embrechts P., Klüppelberg, C., and Mikosch T. *Modelling Extremal Events for Insurance and Finance*, Springer, (2013).

[10] Chhikara and Folks (1989) Chhikara, R. S. and Folks, J. L., The Inverse Gaussian Distribution; Theory, Methodology and Applications, Marcel Dekker, New York, (1989).

[11] Cordeiro et al (2015)Cordeiro, G. M., Ortega, E. M. M., and Lemonte, A. J., The Poisson generalized linear failure rate model. *Communications in Statistics-Theory and Methods*, **44**(10), 2037-2058, (2015).

[12] Ferreira and Steel (2007) Ferreira, J.T.A.S. and Steel, M.F.J., A new class of skewed multivariate distributions with applications to regression analysis, *Statistica Sinica*, **17**, 505-529, (2007).

[13] Ghitany et al (2005) Ghitany, M.E., AL-Hussaini, E.K. and Al-Jarallah, R.A., Marshall-Olkin extended Weibull distribution and its application to censored data. *Journal of Applied Statistics,* **32**, 1025-1034, (2005).

[14] Ghitany and Kotz (2007) Ghitany, M.E. and Kotz, S., Reliability properties of Extended linear failure rate distributions. *Probability in the Engineering and Informational Sciences,* **21**, 441-450, (2007).

[15] Harris (1948) Harris, T.E., Branching processes . *The Annals of Mathematical Statistics*, **19**(4), 474-494, (1948).

[16] Jose et al (2010) Jose, K.K., Naik, S.R. and Ristic, M.M., Marshall- Olkin *q*- Weibull distribution and max-min process, *Statistical papers*, **51**, 837-851, (2010).

[17] JoseandPaul(2018), Jose, K.K. and Paul, A., Reliability Test Plans for Percentiles Based on the Harris Generalized Linear Exponential Distribution, *Stochastics and Quality Control*, 33(1), 61-70, (2018).

[18] Jose and Sivdas (2015) Jose, K. K. and Sivadas, R., Marshall-Olkin Exponentiated Generalized Fréchet Distribution and Its Applications, *Journal of Probability and Statistical Science*, **13** (2), 167-178, (2015).

[19] Kotz and Nadarajah (2001) Kotz, S. and Nadarajah, S., *Extreme Value Theory, Theory and Applications*. Singapore: World Scientific, (2001).

[20] Krishna et al (2013) Krishna, E., Jose, K. K., Alice, T. and Ristic, M.M., Marshall−Olkin Fréchet distribution, *Communications in Statistics - Theory and Methods*, **42**, 4091-4107, (2013).

[21] Lai et al (2006) Lai, Diew, C. and Xie, M., Bathtub Shaped Failure Rate life Distributions, Stochastic ageing and dependence for reliability. Springer, New York, (2006).

[22] Lawless (2003) Lawless, Statistical Models and Methods for Lifetime Data, Second Edition, John Wiley & Sons Inc., NewYork, (2003).

[23] Marshall and olkin (1997) Marshall, A. and Olkin, I., A new method for adding a parameter to a family of distributions with applications to the exponential and Weibull families, *Biometrika*, **84**, 641-652, (1997).

[24] Mahmoud and Alam (2010) Mahmoud, M.A.W. and Alam, F.M.A., The generalized linear exponential distribution, *Statistics and Probability Letters*, **80** 1005-1014, (2010).

[25] Nadarajah et al (2014) Nadarajah, S., Shahsanaei, F., and Rezaei, S., A new four-parameter lifetime distribution. *Journal of Statistical Computation and Simulation*, **84** 2, 248-263, (2014).

[26] Pinho et al (2015) Pinho, L.G.B., Cordeiro, G.M. and Nobre, J.S., The Harris extended exponential distribution, *Communications in Statistics- Theory and Methods*, **44** (16), 3486-3502, (2015).

[27] Zang et al (2005) Zhang, T., Xie, M., Tang, L.C., and Ng, S.H., Reliability and modeling of systems integrated with firmware and hard ware, *International Journal of Reliability, Quality and safety Engineering*, **12**(3), 227-239, (2005).

Neelesh Gupta, A. R. Nigwal, U. K. Khedlekar
AN IMPERFECT PRODUCTION SYSTEM WITH REWORK AND
DISRUPTION FOR DELAYING ITEMS CONSIDERING SHORTAGE

RT&A, No 1 (61)
Volume 16, March 2021

An Imperfect Production System with Rework and Disruption for Delaying items Considering Shortage

Neelesh Gupta [1]   A. R. Nigwal [2]. and U. K. Khedlekar [3]

•

Department of Mathematics and Statistics
[1,3]Dr. Harisingh Gour Vishwavidyalaya, Sagar M.P. India
(A Central University)
[2]Govt. Ujjain Engineering College Ujjain M. P. India
mailto:john@smith.comuvkkcm@yahoo.co.in

Abstract

In this article, we have developed an imperfect production system under the following four different cases. The first one is imperfect production with rework, and without disruption, second one is imperfect production with rework and disruption, third one is imperfect production with rework, disruption,and without backlogging, fourth one is imperfect production with rework, disruption and backlogging. For these all cases, we have optimized the regular production time, rework production time, backlog time and backlog quantity. In this article we have considered the demand rate, production rate defective item's production rate and deteriorating rate are all constant. We have also considered the production rate is always grater than the demand rate. The model is illustrated by numerically and analyzed by graphically.

Keywords: Imperfect production, Disruption, Deterioration, Backlogging, rework.
AMS Subject Classification: 90B05, 90B30, 90B50

1 Introduction

Serving advanced quality products and to make availability service can attract to customers and keep them coming back. However in real situation production process are not always perfect. Due to economic and environmental issues imperfect quality items are reworked to become serviceable again. Moreover shortages of an item are one of the crucial occurrence for any business organization which affects their profit seriously. Shortages may be divided into two categories one is natural shortages and other one is artificial shortages. The natural shortages of items may occur due to the following reasons: (1) the lack of coordination between various team members of production management, (2) The production of items is less than the demand, (3) Disruption like labor strike, political issues, and machines breakdown situation, etc. The artificial shortages of items are made by business organizations through advertising before the launching of new items or overstocking of popular items.

In this article we have developed a mathematical model for four various cases, first one is imperfect production with rework, and without disruption, second one is imperfect production with rework and disruption, third one is imperfect production with rework, disruption,and without backlogging, fourth one is imperfect production with rework, disruption and backlogging considering production and demand rate of product are constant.

Ghare *et al.* (1963) presented the classical inventory model for deteriorating items in which

Neelesh Gupta, A. R. Nigwal, U. K. Khedlekar
AN IMPERFECT PRODUCTION SYSTEM WITH REWORK AND
DISRUPTION FOR DELAYING ITEMS CONSIDERING SHORTAGE

RT&A, No 1 (61)
Volume 16, March 2021

they consider the deterioration and demand rate are constant without shortages. Chakarbarti *et al.* (1997) introduced an EOQ model with linearly increasing demand allowing shortages in all cycle, and they found both the recorder number and time interval between two successive reorders. Furthermore all the shortage interval are determined in an optimal manner so as minimized the average total system cost. Mandel *et al.* (2017) investigated an inventory model for seasonal products using preservation technology investment to reduce the deterioration rate by considering stock dependent demand rate and allowing with shortage. Dye (2007) analyzed a pricing and ordering policy for deteriorating items allowing with time dependent backlogging rate in demand. He *et al.* (2010) suggested a production inventory model for a deteriorating items considering with disruption in production. In this study they considered a fact that some products may deteriorate during their shortage period. Khedlekar *et al.* (2014) presented a disrupted production inventory model by considering constant production rate and variable demand rate. A flexible optimal decisions have been developed by authors but due to disruption shortage is not considered by them. Furthermore in 2018 Khedlekar *et al.* (2018) developed a production inventory model by considering disruption during the production period allowing with shortage. For this, they considered, time dependent demand rate, incorporating shortages at the end of each production cycle but they have not considered the imperfect production.

In general, it is found that items always deteriorate continuously concerning time. Wee (1997), formulated a replenishment policy for time varying deteriorating rate of items by considering price dependent linear function of price allowing with shortages. After this in 2003, Papchristos and Skouri (2003), extended the model of wee (1997) by incorporating demand rate is a convex function of price and backlogging rate is a time dependent function. Dye (2013) studied the effect of preservation technology investment on a non instantaneous inventory system but he did not consider the shortages of items. Bhunia *et al.* (2009) developed a economical production model by using the application of TGA for deteriorating items. In this study they considered the price dependent demand function allowing with partial backlogging but they did not studied by considering imperfect production and production disruption. Dave *et al.* (1981) presented an EOQ model for deteriorating items, in which the demand rate is taken as linear function of time with constant deterioration rate of on hand inventory.

Goyal *et al.* (2001) and Baker *et al.* (2012) depicted a detailed review over the last 20 years. Rosenblatt *et al.* (1986) studied the effect of an imperfect production process on the optimal production time by assuming that the production system may be deteriorate during the production process and may be produce some defective items but they did not incorporate the rework of defective items. Shah *et al.* (2013) developed an inventory model for non instantaneous time-varying deteriorating items in which they considered demand rate is a function of retail price and advertisement cost of items. Due to increased competition, growth in population and globalisation. Recently there are two facts arise about production management, the first one is due to the pressure, the production of items run continuously, and the second one is the involvement of various stages in production system. Therefore the probability of defective item's production rate increases and consequently, the production management has to motivated for the rework process.

Hayak *et al.* (2001) studied the effect of imperfect quality items on finite production inventory model, when regular production stops and imperfect quality items are assumed to be rewoked at a stationary rate. Further they also incorporated the shortage and and backordered but they did not consider the production disruption in their inventory system. Chiu(2011) minimized the total production cost, delivery cost for their EMQ inventory model and they also incorporated rework process of defective items and multiple shipments. Samanta *et al.* (2004) developed a continuous production control inventory model for deteriorating items with shortages. They formulated the optimal average system cost, stock level, backlog level, when the deterioration rate is very small. He *et al.* (2010) developed a production inventory model for deteriorating items considering multiple market demand, where each market has constant demand rate with different selling cycles. They also provided a method to find the solution of optimal production plan and

Neelesh Gupta, A. R. Nigwal, U. K. Khedlekar
AN IMPERFECT PRODUCTION SYSTEM WITH REWORK AND
DISRUPTION FOR DELAYING ITEMS CONSIDERING SHORTAGE

RT&A, No 1 (61)
Volume 16, March 2021

replenishment time. Khedlekar and Shukla *et al.* (2013) developed an inventory model for deteriorating items, considering the demand as a parametric dependent linear function of time and price both. Further they also examined the coefficient of time-parameter and coefficient of price-parameter, simultaneously and proved that time is dominating variable over price in terms of earning more profit. They also introduced the concept for logarithm demand.

Recently, Pervin *et al.* (2018) introduced an integrated EPQ inventory model with time and price dependent demand. They also considered a production rate is a linear function of time and based on customers demand. To reduce the deterioration rate, they applied the preservation technology and optimized the investment cost. In real life, due to the imperfect production, many production systems have encountered considerable losses in their production. Our model is associated with the EPQ model with disruption articulated by Parlor *et al.* (1991) In this paper, we develops a deteriorated imperfect production inventory model with and without disruption. We considere rework on defective items at the end of the regular production. We also provided some useful results to find the optimal regular production rate, production time and rework time. In this paper, we incorporated the shortage at the end of planning horizon because after the planning horizon there is a possibility of some disruption before starting the next production run. For development of model we assumed that at the beginning of each cycle, the manufacturer decide the optimal production rate, production time and rework time with and without disruption so that the production quantity may meets both demand and deterioration. Furthermore, we also assumed that all units of product sold out at the end of each cycle and inventory level decreases to zero.

The development of this paper is organized as follows. In section 2 the notation and assumption are given which are used throughout in this study. In section 3 we have given development of mathematical EPQ model for imperfect production system with rework in four various cases. Case I develops a simple EPQ model which optimizes the regular and rework production time. Case 2 develops two situations which are, first one is when the system gets disrupted but not backlog and second one is a system is disrupted allowing with backlogging. Case 3 develops the deteriorated imperfect production and disrupted system with rework. Case 4 develops the deteriorated imperfect production and disrupted system with rework, allowing with shortage. We optimize the regular production time and rework production time and we also optimize the time of placing the order and order quantity for placing the order when a shortage occurs. In section 4 we have given a three numerical examples and managerial implications which illustrated the proposed model. In section 5 we have concluded the study.

2 Model Notations and Assumptions

2.1 Notations:

The following notations are used to develop the model.
1. The finite planning time interval is H,
2. The finite production rate per unit time is P,
3. The demand per unit time is d,
4. Te rate of deterioration per unit time is θ, which is constant,
5. The production time without disruption is T_P,
6. The production time with disruption is T_d,
7. New production time after system get disrupted T_d^P,
8. The production rate per unit time of defective items is v,
9. Rework rate per unit time of defective items is P_r,
10. At a t on hand inventory level of defective items is $I_d(t)$,
11. The time of placing the order for replenishment, when shortages occur is T_r,
12. The Economical order quantity is Q_r for placing the order when shortages occurs.

Neelesh Gupta, A. R. Nigwal, U. K. Khedlekar
AN IMPERFECT PRODUCTION SYSTEM WITH REWORK AND
DISRUPTION FOR DELAYING ITEMS CONSIDERING SHORTAGE

RT&A, No 1 (61)
Volume 16, March 2021

2.2 Assumptions

The following assumption are used to develop the proposed model.
- Shortages are allowed and backlogged,
- Recovered imperfect quality items are considered as good quality items.
- It is assumed that defective items are fully reworkable into good items and there is no scrap items,
- The production rate, demand rate, defective item's production rate, rework rate is same in every cycle,
- The demand rate per unit time is deterministic and finite,
- The imperfect items' production rate is always grater than the sum of demand rate and defective items' production rate.

3 The Mathematical Model

In this section, the mathematical model is developed for four various cases, which are sequentially as follows:

3.1 Imperfect Production and Rework without Disruption

The as per assumption imperfect production rate is P, which is always grater then the sum of demand rate d and the defective items' production rate v. Let $I_1(t)$ be a regular production inventory level till the time T_P. After that the regular production is stopped and rework process starts at a rate P_r per unit time. Let $I_2(t)$ be the inventory level of perfect items till the time t_1. After the time t_1, rework process is also stopped. During the time interval $[t_1, H]$ inventory level decreases due to demand and deterioration and at $t = H$ inventory level become zero.

The inventory level of the items' at time t over the interval [0, H], is governed by the following differential equations.
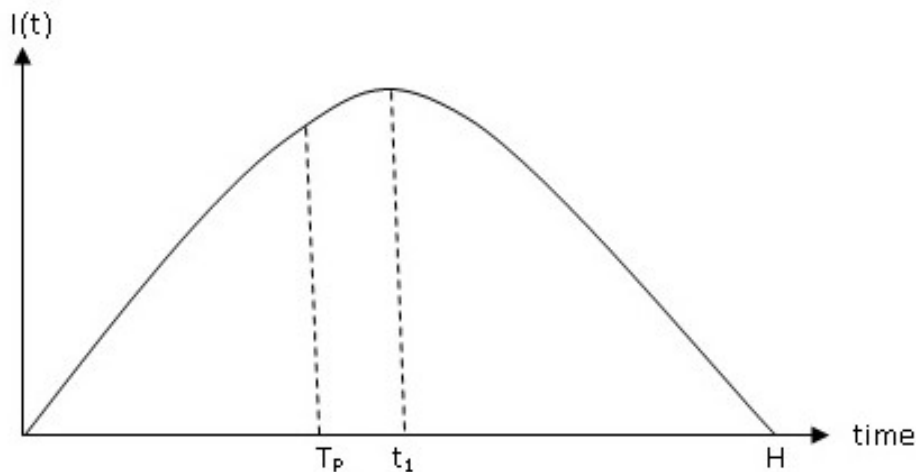

Figure 1: Production system without disruption

$$\frac{dI_1(t)}{dt} + \theta I_1(t) = P - v - d, 0 \leq t \leq T_P, I_1(0) = 0, \tag{1}$$

$$\frac{dI_2(t)}{dt} + \theta I_2(t) = P_r - d, T_P \leq t \leq t_1, I_1(T_P) = I_2(T_P), \tag{2}$$

$$\frac{dI_3(t)}{dt} + \theta I_3(t) = -d, t_1 \leq t \leq H, I_3(H) = 0 \tag{3}$$

Neelesh Gupta, A. R. Nigwal, U. K. Khedlekar
AN IMPERFECT PRODUCTION SYSTEM WITH REWORK AND
DISRUPTION FOR DELAYING ITEMS CONSIDERING SHORTAGE

RT&A, No 1 (61)
Volume 16, March 2021

Using the boundary conditions, the solution of above differential equations are

$$I_1(t) = \left(\frac{P-D-v}{\theta}\right)(1 - e^{-\theta T}), 0 \leq t \leq T_P \tag{4}$$

$$I_2(t) = \frac{P_r-d}{\theta}(1 - e^{\theta(T_P-t)}) + \frac{P-d-v}{\theta}(e^{\theta(T_P-t)} - 1), T_P \leq t \leq t_1 \tag{5}$$

$$I_3(t) = \frac{d}{\theta}(e^{(\theta(H-t))} - 1), t_1 \leq t \leq H. \tag{6}$$

Proposition 4.1 *If v is the defective item rate per unit time, P_r is the rework rate per unit time and T_P is the regular production rate per time, then the rework time ie t_1, where*

$$t_1 = \left(\frac{v+P_r}{P_r}\right)T_P \tag{7}$$

Proof. Let v be the defective items' production rate in time interval $[0,T_P]$, so the total defective items are vT_P and let P_r be the rework rate, so that the total reworkable items are $P_r(t_1 - T_P)$. In this model we assume that all defective items are reworkable, i e.

$$vT_P = P_r(t_1 - T_P) \tag{8}$$

therefore, the rework time t_1 will be

$$t_1 = \left(\frac{v+P_r}{P_r}\right)T_P. \tag{9}$$

Theorem 4.2 *If T_P is the regular production time without disruption, then*

$$T_P = \frac{\frac{d}{\theta}(e^{\theta H}-1)}{P-d\frac{v+P_r}{P_r}+de^{\theta H\frac{v+P_r}{P_r}}} \tag{10}$$

Proof. Let T_P be the regular production time and $(t_1 - T_P)$ be the rework time. We know that the graph inventory is continuous at time t_1 shown in Fig.1

$$I_3(t_1) = I_1(T_P) + vT_P - d(t_1 - T_P),$$

by using this conditions given in the equations 4 and 6, we have

$$\frac{d}{\theta}(e^{\theta(H-t_1)} - 1) = \left(\frac{P-D-v}{\theta}\right)(1 - e^{-\theta T_P}) + vT_P - d(t_1 - T_P), \tag{11}$$

with the help of proposition 3.1 the above equation reduces into the following

$$\frac{d}{\theta}\left((e^{\theta H} - 1) - \frac{v+P_r}{P_r}\theta e^{\theta H}T_P\right) = \left(\frac{P-d-v}{\theta}\right)\theta T_P + (v - d\left(\frac{v+P_r}{P_r}\right) + d)T_P. \tag{12}$$

so, the regular production time without disruption is

$$T_P = \frac{\frac{d}{\theta}(e^{\theta H}-1)}{P-d\frac{v+P_r}{P_r}+de^{\theta H\frac{v+P_r}{P_r}}} \tag{13}$$

From proposition 3.1 the rework time is t_1

$$t_1 = \left(\frac{v+P_r}{P_r}\right)\frac{\frac{d}{\theta}(e^{\theta H}-1)}{P-d\frac{v+P_r}{P_r}+de^{\theta H\frac{v+P_r}{P_r}}}T_P \tag{14}$$

Differentiating the equations 13 and 14 with respect to disruption rate θ, respectively, we have

$$\frac{dT_P}{d\theta} = \frac{(d\log\theta(e^{\theta H}-1)+de^{\theta H})}{\left(P-d\left(\frac{v+P_r}{P_r}\right)+de^{\theta H}\left(\frac{v+P_r}{P_r}\right)\right)} - \frac{\left(\frac{d}{\theta}\right)^2 e^{\theta H}(e^{\theta H}-1)\left(\frac{v+P_r}{P_r}\right)}{\left(P-d\left(\frac{v+P_r}{P_r}\right)+de^{\theta H}\left(\frac{v+P_r}{P_r}\right)\right)^2} \tag{15}$$

$$\frac{dt_1}{d\theta} = \left(\frac{v+P_r}{P_r}\right)\left[\frac{(d\log\theta(e^{\theta H}-1)+de^{\theta H})}{\left(P-d\left(\frac{v+P_r}{P_r}\right)+de^{\theta H}\left(\frac{v+P_r}{P_r}\right)\right)} - \frac{\left(\frac{d}{\theta}\right)^2 e^{\theta H}(e^{\theta H}-1)\left(\frac{v+P_r}{P_r}\right)}{\left(P-d\left(\frac{v+P_r}{P_r}\right)+de^{\theta H}\left(\frac{v+P_r}{P_r}\right)\right)^2}\right] \tag{16}$$

Neelesh Gupta, A. R. Nigwal, U. K. Khedlekar
AN IMPERFECT PRODUCTION SYSTEM WITH REWORK AND
DISRUPTION FOR DELAYING ITEMS CONSIDERING SHORTAGE

RT&A, No 1 (61)
Volume 16, March 2021

The above equations 15 and 16 manifests that the manufacturer has to produce more products when deterioration rate increases. Hence, if the deterioration rate decreases then the planning time interval and production cost decrease accordingly. Thus, we have the following corollary.

Corollary 4.3 *Assuming $\theta << 1$, then T_P and t_1 are havels in θ.*

3.2 Imperfect Production and Rework with Disruption

In this case, we assumed that $I_1(t)$ be the regular production inventory level till the time T_d. After this time the system get disrupted. Let $I_2(t)$ be a disrupted production inventory level with new production rate $P + \delta P$ where $\delta P < 0$. At time t= H-t_1 the production is stopped. The regular production and disrupted production has produced a defective items at a rate v. Let $I_3(t)$ be a rework inventory level with rework rate P_r.

The inventory level of both (perfect and imperfect) items at time t over the interval [0, H], is governed by the following differential equations.
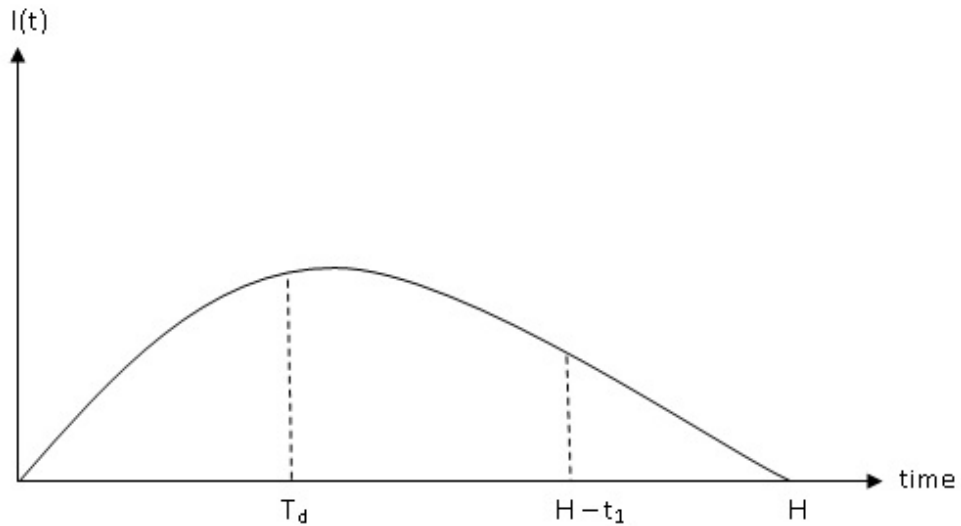
Figure 2: Inventory system with disruption

$$\frac{dI_1(t)}{dt} + \theta I_1(t) = P - v - d, 0 \le t \le T_d, I_1(0) = 0 \tag{17}$$

$$\frac{dI_2(t)}{dt} + \theta I_2(t) = P + \delta P - v - d, T_d < t < H - t_1 I_1(T_d) = I_2(T_d) \tag{18}$$

$$\frac{dI_3(t)}{dt} + \theta I_3(t) = P_r - d, H - t_1 < t < H, I_3(H) = 0 \tag{19}$$

Using the boundary conditions, the solutions of differential equations are

$$I_1(t) = \left(\frac{P-D-v}{\theta}\right)(1 - e^{-\theta t}) \tag{20}$$

$$I_2(t) = \frac{P+\delta P-v}{\theta}\left(1 - e^{\theta(T_d-t)}\right) + \frac{P-D-v}{\theta}\left(e^{\theta(t_d-t)} - e^{-\theta t}\right) \tag{21}$$

$$I_3(t) = is expressed by the following propositions \tag{22}$$

Proposition 4.4 *If v is the defective items' production rate, P_r is the rework rate and H is the total length of cycle, then the rework time is t_1, where*

$$t_1 = \frac{vH}{P_r+v}. \tag{23}$$

Proof. Let v be the defective items' production rate in the time interval $[0, H - t_1]$, so that the total defective items are $v(H - t_1)$ and let P_r be the rework rate in the time interval $[H - t_1, H]$, so

Neelesh Gupta, A. R. Nigwal, U. K. Khedlekar
AN IMPERFECT PRODUCTION SYSTEM WITH REWORK AND
DISRUPTION FOR DELAYING ITEMS CONSIDERING SHORTAGE

RT&A, No 1 (61)
Volume 16, March 2021

that the total reworkable items are $P_r t_1$. As over assumptions all defective items are reworkable, i.e.

$$P_r t_1 = v(H - t_1) \tag{24}$$

therefore, the rework time t_1 is

$$t_1 = \frac{vH}{P_r + v} \tag{25}$$

Since the inventory is continuous at $H - t_1$, which is shown in Fig 2., i.e. $I_3(H - t_1) = I_2(H - t_1) + v(H - t_1)$

by using this conditions given in the equations 18 and 19, we have

$$I_3(t) = v(H - t_1)e^{-\theta t} + \frac{P_r - d}{\theta}(1 - e^{-\theta t}) + \frac{P - d - v}{\theta}(e^{\theta(t_d - t)} - e^{-\theta t})$$
$$+ \frac{P + \delta P - d - v}{\theta}(e^{\theta(H - t - t_1)} - e^{\theta(t_d - t)}) \tag{26}$$

So, the inventory level $I_3(t)$ becomes

$$I_3(t) = v(H - \frac{vH}{P_r + v})e^{-\theta t} + \frac{P_r - d}{\theta}(1 - e^{-\theta t}) + \frac{P - d - v}{\theta}(e^{\theta(t_d - t)} - e^{-\theta t})$$
$$+ \frac{P + \delta P - d - v}{\theta}(e^{\theta(H - t - \frac{vH}{P_r + v})} - e^{\theta(t_d - t)}) \tag{27}$$

Hence the inventory level $I_3(t)$ at the time H will be

$$I_3(H) = v(H - \frac{vH}{P - r + v})e^{-\theta H} + \frac{P_r - d}{\theta}(1 - e^{-\theta H}) + \frac{P - d - v}{\theta}(e^{\theta(t_d - t)} - e^{-\theta H})$$
$$+ \frac{P + \delta p - d - v}{\theta}(e^{\theta(H - \frac{vH}{P_r + v} - H)} - e^{(t_d - H)}) \tag{28}$$

Proposition 4.5 *If $I_3(H) \geq 0$, then the disrupted production rate follows the following inequalities.*

$$\delta P \geq -(P - d - v)r - \frac{vH(1 - \frac{v}{P_r + v})e^{-\theta H} + \frac{P_r - v}{\theta}(1 - e^{-\theta H}) + \frac{P - d - v}{\theta}(e^{\theta(t_d - H)} - e^{-\theta H})}{e^{\theta(\frac{-nuH}{P_r + v})} - e^{t_d - H}} \tag{29}$$

Proof. If $I_3(H) \geq 0$. that is

$$\delta P \geq -(P - d - v)r - \frac{vH(1 - \frac{v}{P_r + v})e^{-\theta H} + \frac{P_r - v}{\theta}(1 - e^{-\theta H}) + \frac{P - d - v}{\theta}(e^{\theta(t_d - H)} - e^{-\theta H})}{e^{\theta(\frac{-nuH}{P_r + v})} - e^{t_d - H}} \tag{30}$$

this means that the manufacturer can still satisfy the demand after disrupted production.

And if $I_3(H - t_1) = v(H - t_1)$ then we found the $I_3(t)$

$$I_3(t) = \frac{P - r - d}{\theta}\left(1 - e^{\theta(H - \frac{vH}{P_r + v} - t)}\right) + vH\left(1 - \frac{v}{P_r + v}\right)e^{\theta(H - \frac{vH}{P_r + v} - t)} \tag{31}$$

And if $I_2(H) < 0$. that is

$$-P \leq \delta P \leq -(P - d - v)r - \frac{vH(1 - \frac{v}{P_r + v})e^{-\theta H} + \frac{P_r - v}{\theta}(1 - e^{-\theta H}) + \frac{P - d - v}{\theta}(e^{\theta(t_d - H)} - e^{-\theta H})}{e^{\theta(\frac{-nuH}{P_r + v})} - e^{(t_d - H)}}, \tag{32}$$

Then the manufacturer will face shortage.

3.3 The Imperfect Production and Rework and Disruption without Backlogging

In this case, we assume that $I_1(t)$ be the regular production inventory level till the time T_d, after that time the system get disrupted due to some appropriate problems. Let $I_2(t)$ be a disrupted production inventory level with disrupted production rate $P + \delta P$ ($\delta P < 0$) in the interval time $[T_d, T_d^P]$. Regular and disrupted production process have produced defective items at a rate v. Afterward rework process starts on defective items at a rate P_r during the time $[t_1, T_d^P]$. Let $I_3(t)$ be the inventory level during the time interval $[t_1, T_d^P]$ and finally production stopped. Again costumer $I_4(t)$ represents the inventory level during the time interval $[t_1, H]$. The inventory at a time t is governed by the following differential equations

$$\frac{dI_1(t)}{dt} + \theta I_1(t) = P - d - v, 0 \leq t \leq T_d, I_1(0) = 0. \tag{33}$$

$$\frac{dI_2(t)}{dt} + \theta I_2(t) = P + \delta P - d - v, T_d \leq t \leq T_d^P, I_1(T_d) = I_2(T_d). \tag{34}$$

$$\frac{dI_3(t)}{dt} + \theta I_3(t) = P_r - d, T_d^P \leq t \leq t_1, I_3(t_1) = I_4(t_1). \tag{35}$$

Neelesh Gupta, A. R. Nigwal, U. K. Khedlekar
AN IMPERFECT PRODUCTION SYSTEM WITH REWORK AND
DISRUPTION FOR DELAYING ITEMS CONSIDERING SHORTAGE

RT&A, No 1 (61)
Volume 16, March 2021

$$\frac{dI_4(t)}{dt} + \theta I_4(t) = -d, t_1 \leq t \leq H, I_4(H) = 0. \tag{36}$$
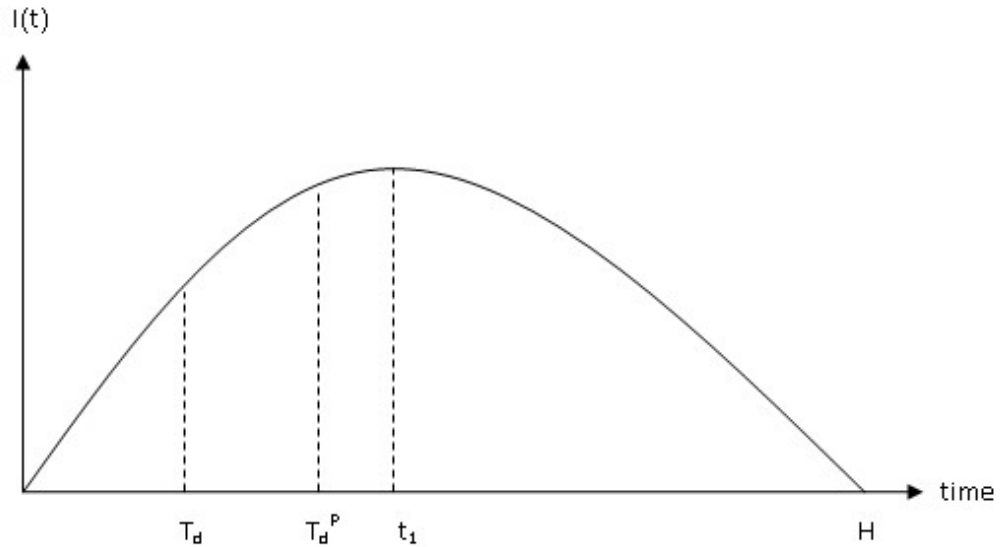
Figure 3:

Using the boundary conditions, the solution of above differential equations are

$$I_1(t) = \left(\frac{P-D-v}{\theta}\right)(1 - e^{-\theta t}), 0 \leq t \leq T_d \tag{37}$$

$$I_2(t) = \frac{P+\delta P-d-v}{\theta}\left(1 - e^{\theta(T_d-t)}\right) \tag{38}$$

$$+ \frac{P-d-v}{\theta}(e^{\theta(T_d-t)} - e^{-\theta t}), T_d \leq t \leq T_d^P \tag{39}$$

$$I_3(t) = \frac{P_r-d}{\theta}\left(1 - e^{\theta(T_d^P)}\right) + \frac{P+\delta P-d-v}{\theta}\left(e^{\theta(T_d^P)} - e^{\theta(T_d-t)}\right)$$

$$+ \frac{P-d-v}{\theta}\left(e^{\theta(T_d-t)} - e^{-\theta t}\right), T_d^P \leq t \leq t_1 \tag{40}$$

$$I_4(t) = \frac{d}{\theta}\left(e^{\theta(H-t)} - 1\right) t_1 \leq t \leq H \tag{41}$$

Proposition 4.6 *If v is the defective items' production rate, P_r is the rework rate and T_P is the production time under disruption, then the rework time is given by t_1, where*

$$t_1 = \left(\frac{v+P_r}{P_r}\right) T_d^P \tag{42}$$

Proof. Let v is the defective item production rate in the time interval $[0, T_d^P]$, so the total defective items are vT_d^P. Let P_r be the rework rate in the interval $[T_d^P, t_1]$, so the total reworkable items are $P_r(t_1 - T_d^P)$. In this case, all the defective items are reworkable, i.e.

$$vT_d^P = P_r(t_1 - T_d^P) \tag{43}$$

so, the rework time will be

$$t_1 = \left(\frac{v+P_r}{P_r}\right) t_d^P \tag{44}$$

Using equation 40 the total inventory after rework process

$$I_3(t) = \frac{P_r-d}{\theta} + \frac{d}{\theta}\left[e^{\theta(H-t)} - e^{\theta\left(\frac{v+P_r}{P_r}T_d^P - t\right)}\right] - \frac{P_r-d}{\theta}e^{\theta\left(\frac{v+P_r}{P_r}T_d^P - t\right)} \tag{45}$$

Theorem 4.7 *If T_d^P is the regular production time after disruption, then*

$$T_d^P = \frac{\frac{d}{\theta}(e^{\theta H}-1) + \delta P T_d}{\left(\frac{v+P_r}{P_r}(de^{\theta H}-1) + (P+\delta P - 2d)\right)} \tag{46}$$

Neelesh Gupta, A. R. Nigwal, U. K. Khedlekar
AN IMPERFECT PRODUCTION SYSTEM WITH REWORK AND
DISRUPTION FOR DELAYING ITEMS CONSIDERING SHORTAGE

RT&A, No 1 (61)
Volume 16, March 2021

Proof. Since the inventory is continuous on t_1, which is shown in Fig.2, i.e.

$$I_4(t_1) = I_3(T_d^P) + \nu T_d^P - d(t_1 - T_d^P)$$

by using this condition respectively in the equation 40 and equation 41, we have

$$\frac{d}{\theta}\left(e^{\theta(H-t_1)-1}\right) = \frac{P+\delta P-d-\nu}{\theta}\left(1 - e^{\theta(T_d-T_d^P)}\right) + \frac{P-d-\nu}{\theta}\left(e^{\theta(T_d-T_d^P)} - e^{-\theta T_d^P}\right)$$

$$+\nu T_d^P - d(t_1 - T_d^P) \tag{47}$$

with the help of above proposition above equation reduces into the following form,

$$\frac{\nu+P_r}{P_r}de^{\theta H}T_d^P + (P+\delta P-d-\nu)(T_d^P - T_d) + (P-d-\nu)T_d + \left(\nu - d\frac{\nu+P_r}{P_r} - d\right)T_d^P \tag{48}$$

$$\left(\frac{\nu+P_r}{P_r}de^{\theta H} + (P+\delta P-2d)-d\right) + dfrac\nu + P_rP_r\right)t_d^P = \frac{d}{\theta}(e^{\theta H}-1) + \delta PT_d \tag{49}$$

So, the regular production time during disruption

$$T_d^P = \frac{\frac{d}{\theta}(e^{\theta H}-1)+\delta PT_d}{\left(\frac{\nu+P_r}{P_r}(de^{\theta H}-1)+(P+\delta P-2d)\right)} \tag{50}$$

From proposition 3.6 the rework production time is

$$t_1 = \left(\frac{\nu+P_r}{P_r}\right)\frac{\frac{d}{\theta}(e^{\theta H}-1)+\delta PT_d}{\left(\frac{\nu+P_r}{P_r}(de^{\theta H}-1)+(P+\delta P-2d)\right)} \tag{51}$$

Differentiating equation 50 and equation 51 with respect to the the deterioration rate θ respectably, we have

$$\frac{dT_d^P}{d\theta} = \frac{K\left(\frac{d}{\theta}He^{\theta H}+\frac{d}{\theta^2}(1-e^{\theta H})\right)+M\left(d\left(\frac{\nu+P_r}{P_r}\right)He^{\theta H}\right)}{K^2} \tag{52}$$

$$\frac{dt_1}{d\theta} = \left(\frac{\nu+P_r}{P_r}\right)\frac{K\left(\frac{d}{\theta}He^{\theta H}+\frac{d}{\theta^2}(1-e^{\theta H})\right)+M\left(d\left(\frac{\nu+P_r}{P_r}\right)He^{\theta H}\right)}{K^2} \tag{53}$$

where

$$K = \frac{\nu+P_r}{P_r}(de^{\theta H}-1) + (P+\delta P-2d)) \tag{54}$$

$$M = \frac{d}{\theta}(e^{\theta H}-1) + \delta PT_d \tag{55}$$

the above equation 52 and equation 53 manifests that manufacturer has to produce more product when increases the deterioration rate. Thus, we have the following corollary.

Corollary 4.8 *Assuming $\theta << 1$. then the T_d^P and t_1 have positive growth with respect to θ.*

3.4 The Imperfect Production with Rework Disruption and Backlogging

In this case, We assumed $I_1(t)$ be a regular production inventory level till the time T_d, after that the production get disrupted consequently the regular production has been stopped and during the regular production defective items are produced at a rate ν. Let $I_2(t)$ be the inventory level during the rework time interval [T_d, t_1]. After stopping rework process, stored inventory fulfill the demand and at time Tr inventory reach to zero level. Let $I_4(t)$ be the inventory level when the production is restarted till the time $H - t_2$ at a disrupted production rate $P + \delta P$. During the interval $H - t_2$ production system also produced defective items at rate ν. Let $I_5(t)$ be the inventory level during the time interval $[H - t_2, H]$ when rework process is in progress at a rate P_r. At any time t, the inventory status is governed by the following equations

Neelesh Gupta, A. R. Nigwal, U. K. Khedlekar
AN IMPERFECT PRODUCTION SYSTEM WITH REWORK AND
DISRUPTION FOR DELAYING ITEMS CONSIDERING SHORTAGE

RT&A, No 1 (61)
Volume 16, March 2021
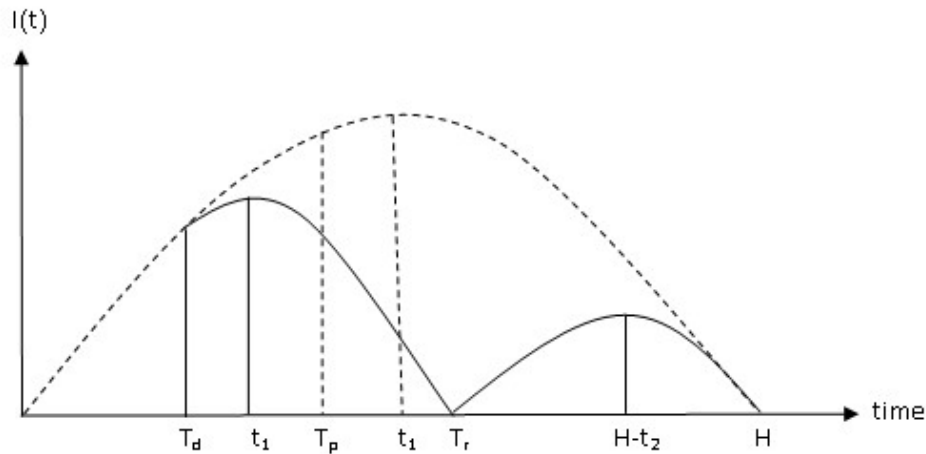
Figure 4:

$$\frac{dI_1(t)}{dt} + \theta I_1(t) = P - d - v, 0 \le t \le T_d, I_1(0) = 0 \tag{56}$$

$$\frac{dI_2(t)}{dt} + \theta I_2(t) = P_r - d, T_d \le t \le t_1, I_1(T_d) = I_2(T_d) \tag{57}$$

$$\frac{dI_3(t)}{dt} + \theta I_3(t) = -d, t_1 \le t \le T_r, I_2(t_1) = I_3(t_1) \tag{58}$$

$$\frac{dI_4(t)}{dt} + \theta I_4(t) = P + \delta P - d - v, 0 \le T_r \le H - t_2, I_4(T_r) = 0 \tag{59}$$

$$\frac{dI_5(t)}{dt} + \theta I_5(t) = P_r - d, H - t_2 \le t \le H, I_5(H) = 0. \tag{60}$$

Using the boundary conditions the solution of the above differential equations are

$$I_1(t) = \frac{P-d-v}{\theta}(1 - e^{-\theta t}), 0 \le t \le T_d \tag{61}$$

$$I_2(t) = \frac{P_r-d}{\theta}(1 - e^{\theta(T_d-t)}) + \frac{P-d-v}{\theta}(e^{\theta(t_d-t)} - e^{-\theta t}), T_d \le t \le t_1 \tag{62}$$

$$I_3(t) = \frac{d}{\theta}(e^{\theta(t_1-t)} - 1) + \frac{P_r-d}{\theta}(e^{\theta(t_1-t)} - e^{\theta(T_d-t)})$$

$$+ \frac{p-d-v}{\theta}(e^{\theta(T_d-t)} - e^{-\theta t}), t_1 \le t \le T_r \tag{63}$$

$$I_4(t) = \frac{P+\delta P-d-v}{\theta}(1 - e^{\theta(T_r-t)}), 0 \le T_r \le H - t_2, \tag{64}$$

$$I_5(t) = \frac{P_r-d}{\theta}(1 - e^{\theta(H-t)}), H - t_2 \le t \le H. \tag{65}$$

Proposition 4.9 *If v is the defective items' production rate, P_r is the rework rate, T_d is the disruption time on regular process, then the rework time after regular process is t_1, where*

$$t_1 = \frac{v+P_r}{P_r}T_d. \tag{66}$$

Proof. Let v is the defective item rate on time interval $[0, T_d]$, so the total defective items are vT_d and lat P_r is the rework production rate, so the total reworkable items are $P_r(t_1 - T_d$. In this model, all defective items are reworkable, i.e.

$$vt_d = P_r(t_1 - T_d), \tag{67}$$

so, the rework production time after regular process

$$t_1 = \frac{v+P_r}{P_r}T_d. \tag{68}$$

Proposition 4.10 *If v is the defective item rate, P_r is the rework production rate, T_r is the total backlog time and H is the total time cycle, then the rework production time under backlog process is*

Neelesh Gupta, A. R. Nigwal, U. K. Khedlekar
AN IMPERFECT PRODUCTION SYSTEM WITH REWORK AND
DISRUPTION FOR DELAYING ITEMS CONSIDERING SHORTAGE

RT&A, No 1 (61)
Volume 16, March 2021

$$t_2 = \frac{v(H-T_r)}{v+P_r}. \tag{69}$$

Proof. Let v is the defective item rate on time interval $[T_r, H-T_2]$, so, the total defective items are $v(H-t_2-T_r)$, and let P_r is the rework production rate, then the total reworkable items are $P_r t_2$. In this model, the total defective items are reworkable, i.e.

$$v(H-t_2-T_r) = P_r t_2 \tag{70}$$
$$v(H-T_r) = (v+p_r)t_2, \tag{71}$$

so, the rework production time under backlog process is

$$t_2 = \frac{v(H-T_r)}{v+P_r}. \tag{72}$$

Theorem 4.11 *If T_r is the time of placing when shortage occur, then*

$$T_r = \frac{1}{\theta}\log\left(\frac{P_r e^{\theta\left(\frac{v+P_r}{p_r}\right)T_d}+(P-P_r-v)e^{\theta T_d}-(P-d-v)}{d}\right) \tag{73}$$

Proof. Let T_r is the time of placing when shortage occur, and the inventory $I_3(t)$ fulfill the demand and reach to zero at the time T_r shown in Fig. 4. i.e. $I_3(T_r) = 0$.

using equation 63, we have

$$\frac{d}{\theta}(e^{\theta(t_1-T_r)}-1) + \frac{P_r-d}{\theta}(e^{\theta(t_1-T_r)}-e^{\theta(T_d-T_r)}) + \frac{P-d-v}{\theta}(e^{\theta(T_d-T_r)}-e^{-\theta T_r}) = 0. \tag{74}$$

$$\frac{d}{\theta}e^{\theta T_r} = \frac{P_r}{\theta}e^{\theta t_1} + \frac{P-P_r-v}{\theta}e^{\theta T_d} - \frac{P-d-v}{\theta} \tag{75}$$

$$T_r = \frac{1}{\theta}\log\left(\frac{P_r e^{\theta t_1}+(P-P_r-v)e^{\theta T_d}-(P-d-v)}{d}\right) \tag{76}$$

from proposition 3.9, the time of placing the order when shortage accrue is

$$T_r = \frac{1}{\theta}\log\left(\frac{P_r e^{\theta\left(\frac{v+P_r}{p_r}\right)T_d}+(P-P_r-v)e^{\theta T_d}-(P-d-v)}{d}\right) \tag{77}$$

from eq.3.9 on hand inventory is

$$I_4(t) = \frac{P+\delta P-d-v}{\theta}\left(1 - e^{\theta\left(\frac{1}{\theta}\log\frac{P_r e^{\theta\left(\frac{v+P_r}{p_r}\right)T_d}+(P-P_r-v)e^{\theta T_d}-(P-d-v)}{d}-t\right)}\right). \tag{78}$$

Theorem 4.12 *If Q_r is the order quantity for placing the order when shortages occurs, then*

$$Q_r = \frac{P+\delta P-d-v}{\theta}\left(1 - e^{\theta\left(T_r-v\frac{v(H-T_r)}{v+P_r}-H\right)}\right) + v\left(H-T_r-\frac{v(H-T_r)}{v+P_r}\right) \tag{79}$$

Proof. We know that the quantity

$$Q_r = I_4(H-t_2) + v(H-t_2-T_r), \tag{80}$$

from equation(10) and corollary(3.3), shortage quantity Q_r will be

$$Q_r = \frac{P+\delta P-d-v}{\theta}\left(1 - e^{\theta\left(T_r-v\frac{v(h-T_r)}{v+P_r}-H\right)}\right) + v\left(H-T_r-\frac{v(h-T_r)}{v+P_r}\right) \tag{81}$$

Neelesh Gupta, A. R. Nigwal, U. K. Khedlekar
AN IMPERFECT PRODUCTION SYSTEM WITH REWORK AND
DISRUPTION FOR DELAYING ITEMS CONSIDERING SHORTAGE

RT&A, No 1 (61)
Volume 16, March 2021

4 Numerical Examples of Various Cases

Example 5.1 *for case I: We use the following numbers as the base value of parameter P= 500, δP = -5, d= 50 θ = 0.01, H = 30, ν = 10%, P_r = 10, we obtained T_P = 3.37 and t_1 = 3.41.*

Example 5.2 *for case III:We used the following number as the based of parameter P= 500, t_d= 5, δP = -5, d= 50,θ= 0.01, ν = 10%, P_r =10, we obtained t_d^P =401784 and t_1 =4.2201.*

Example 5.3 *for case IV:We used the following number as the based of parameter P= 500, t_d= 5 , δP = -5, d= 50, θ= 0.01, ν = 10%, P_r =10, we obtained t_1 = 5.05, T_r = 17.97, Q_r = 859.2 and t_2 = 0.11.*

5.1 Sensitivity Analysis

We have analyzed analytically numerically and graphically we have received the following information about this model:

5.1.1 Case I:

1. Increment of deterioration rate increases the regular production rate (Fig. 5).
2. Increment of defective items' production rate decreases the regular production rate while increases the rework time (Data table 1).

5.1.2 Case III:

1. Increment of deterioration rate increases the disrupted regular production rate (Fig.6).
2. Increment of defective items' production rate, increases the disrupted regular production rate while increases the rework time.

5.1.3 Case IV:

1. Increment of deterioration rate decreases the backlog time T_r, whereas increases the backlog rework time t_2 (Fig. 7).
2. Increment of defective items' production rate, increases the rework production time t_1 and backlog rework time t_2, so backlog quantity Q_r also increase, but the backlog time T_r affected less.

Table 1: Effect of v on T_P and t_1.

v	T_P	t_1
0.1	3.3791	3.4129
0.15	3.3786	3.4292
0.20	3.3780	3.4456
0.25	3.3774	3.4619

Table 2: Effect of (θ_1)on various outputs in disrupted system for $(\theta_2 > 0.)$

v	t_1	t_2	T_r	Q_r
0.05	5.52	0.052	1.4627	8538.16
0.1	5.55	0.1043	19.4628	8714.50
0.15	5.58	0.1557	19.4629	8889.91
0.20	5.61	0.2061	19.4630	9064.41

Neelesh Gupta, A. R. Nigwal, U. K. Khedlekar
AN IMPERFECT PRODUCTION SYSTEM WITH REWORK AND
DISRUPTION FOR DELAYING ITEMS CONSIDERING SHORTAGE

RT&A, No 1 (61)
Volume 16, March 2021

.

Table 3: Effect of v on T_d^P and t_1

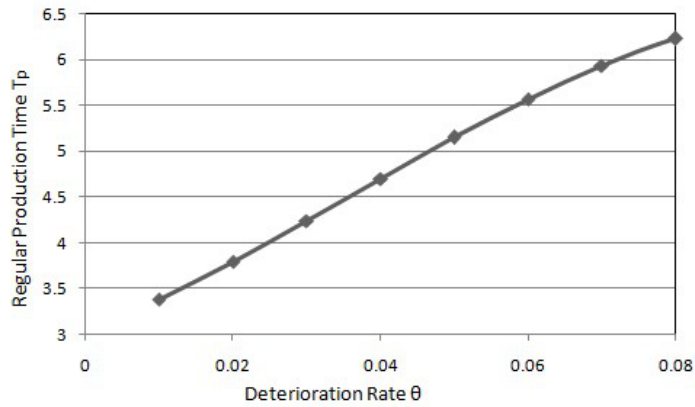| v	T_d^P	t_1
0.1	4.2419	4.2843
0.15	4.2410	4.3046
0.20	4.2400	4.3249
0.25	4.2391	4.3415

Figure 5: Effect of θ on T_P
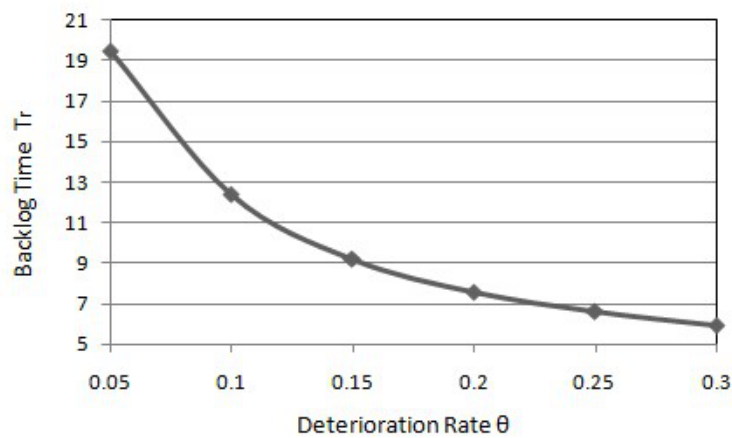

Figure 6: Effect of θ on T_d^P

Figure 7: Effect of θ on T_r

Neelesh Gupta, A. R. Nigwal, U. K. Khedlekar
AN IMPERFECT PRODUCTION SYSTEM WITH REWORK AND
DISRUPTION FOR DELAYING ITEMS CONSIDERING SHORTAGE

RT&A, No 1 (61)
Volume 16, March 2021
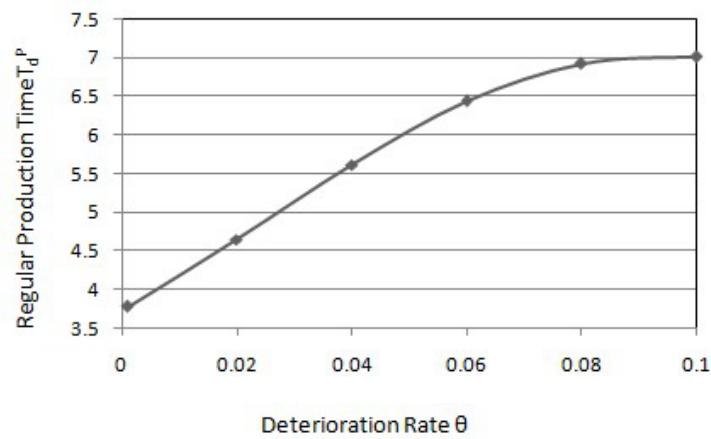
6 Conclusion

In this article we have developed an imperfect production system considering with constant demand rate for deteriorating items. Further we have applied rework process on defective items. Rework process starts after stopping regular production. The model is developed in four different cases, which are (1) the imperfect production and rework, without disruption, (2) the imperfect production and rework with disruption, (3) the imperfect production and rework, without disruption and backlogging and (4) the imperfect production and rework, with disruption and backlogging. we have optimized t_1, T^p, T_d^P, T_r and Q_r for all these above cases. The model is also analyzed by graphically and verified by numerically.

References

[1] Bakker M, Riezebos J., and Teunter R. H. (2012), Review of inventory system with deterioration since 2001. *European Journal of operational Research, vol. 221, 275-284.*

[2] Bhunia A. K., Kandu S., Sannigrahi T, and Goyal S.K. (2009), An application of tournament genetic algorithm in a marketing oriented economic production lot size model for deteriorating items. *International Journal of Production Economics, vol. 119, 112-121.*

[3] Chakrabarti, T., and Chaudhuri, K. S. (1997), An EOQ model for deteriorating items with a linear trend in demand and shortages in all cycles. *International Journal of Production Economics, vol. 49, 205-213.*

[4] Chiu Y.S.P., Liu S. C., Chiu C. L., and Chang H. H. (2011), Mathematical modeling for determining the replenishment policy for EMQ model with rework and multiple shipments, *Mathematical and Computer Modeling, vol. 54, pp 2165-2174.*

[5] Dave U., and Patel L. K. (1981), (T,S_i) Policy inventory model for deteriorating items with time proportional demand, *Journal of the Operational Research Society, vol. 32, pp 137-142.*

[6] Dye C.Y. (2013), The effect of preservation technology investment on a non-instantaneous deteriorating inventory model, *OMEGA, vol. 41, pp. 872-880.*

[7] Ghare P. M.and Schrader G. F.(1963), A model for exponentially decaying inventory system, International Journal of Production and Research, *International Journal of Production and Research, vol. 21, pp 449-460.*

[8] Goyel S. K., and Giri B. C. (2001), Resent trend in modeling of deteriorating inventory, *Europian Journal of Operational Research, vol. 134, pp 1-16.*

[9] Hayak P. A,, and Salameh M. K.(2001), Production lot sizing with the reworking of imperfect quality items produced, *Production Planning and Control, vol. 12, pp 584-590.*

[10] He, Y and He, J. (2010), A production inventory model for deteriorating inventory items with production disruption, *Discrete dynamics in nature and society, vol. 2012, pp 1-14.*

[11] He Y., Wang S. Y. and Lai K. K. (2010), An optimal production inventory model for deteriorating items with multiple market demand, *European Journal of Operations Research, vol. 203, pp 593-600.*

[12] Khedlekar U. K. and Shukla D. (2013),   Simulation of economic production quantity model for deteriorating items, *American Journal of Modeling and Optimization, vol. 1, pp 25-30.*

[13] Khedlekar U. K., Namdev A. and Nigwal A. R.(2018), Production inventory model with disruption considering shortage and time propositional demand. *Yogoslav Jornal of Operational Research, vol. 28, pp. 123-139.*

[14] Khedlekar U. K., Shukla D., and Chandel R.P.S.(2014), Computational study for disrupted production system with time Dependent demand, *Journal of Scientific and Industrial Research, vol. 73, pp 294-301.*

[15]   Papachristos P. and Skori K. (2003),   An inventory model with deteriorating items quantity discount,pricing and time dependent partial backlogging, *International Journal of Production Economics, vol. 83, pp 247-256.*

[16] Parlar, M., and Berkin D. (1991), Future supply uncertainty in EOQ models,   *Naval Research Logistics (NRL), vol. 38, pp 107-121.*

[17] Pervin M., Roy S. K. and Weber G.M (2018), An integrated inventory model with variable holding cost under two levels of trade credit policy, *Numerical Algebra Control and Optimization, vol. 8, pp 169-191.*

[18] Pervin, M., Roy, S.K. and Weber, G.W.(2019), Multi item deteriorating two echelon inventory model with price and stock dependent demand: A trade credit policy, *American Institute of Mathematical Science, vol.15, pp 1345-1373.*

Neelesh Gupta, A. R. Nigwal, U. K. Khedlekar
AN IMPERFECT PRODUCTION SYSTEM WITH REWORK AND
DISRUPTION FOR DELAYING ITEMS CONSIDERING SHORTAGE

RT&A, No 1 (61)
Volume 16, March 2021

[19] Sarkar B, Mandal B. and Sarkar S. (2017), Preservation of deteriorating seasonal products with stock-dependent consumption rate and shortages, *Journal of Industrial and Management Optimization, vol. 13, pp 187-206.*

[20] Shah N. H., Soni H. N. and Patel K. A. (2013), Optimizing inventory and marketing policy for non instantaneous deteriorating items with generalized type deteriorating and holding cost rate, *OMEGA, vol. 41, pp 421-430.*

[21] Rosenblatt, M. J. and Lee, H. L. (1986), Economic production cycle with imperfect production processes, *IIE Transactions, vol. 18, pp 48-55.*

[22] Samanta , G. P and Roy, A.(2004), A production inventory model with deteriorating items and shortages, *Yogeslav Journal of Operation Research, vol. 14, pp 219-230.*

[23] Wee H. M. (1997), A replenishment policy for items with a price dependent demand and a varying rate of deterioration, *Production Planning & control, vol. 8, pp. 494-499.*

Availability and Cost Analysis of Complex Tree Topology of Computer Network with Multi-Server Using Gumbel-Hougaard Family Copula Approach

Kabiru H. Ibrahim

•

Department of Mathematics, Aminu Kano College of Islamic
and Legal Studies Kano, Nigeria
kbrhamis032@gmial.com

Muhammad Salihu Isa

•

Department of Mathematics, Federal University Dutse, Jigawa, Nigeria
salihu.muhd.isa@gmail.com

M. I. Abubakar

•

Department of Mathematics, Federal College
of Education (T) Bichi, Kano, Nigeria
abkidris@yahoo.com

Ibrahim Yusuf

•

Department of Mathematical Sciences, Bayero University, Kano, Nigeria
iyusuf.mth@buk.edu.ng

Ismail Tukur

•

Department of Mathematics, Kano State Polytechnic, Kano, Nigeria.
ismailatukur35@gmail.com

Abstract

In relation to types and advantages of computer network topologies, in this research work, availability and cost analysis of complex computer network is considered to focus on a tree topology network that has four subsystems A,B,C and D and all the subsystems are figured in series and parallel configuration, the subsystem A and B served as computer servers together with two units each and are working 1-out-of-2: G/F policy while C and D subsystems both has three units and are working in 2-out-of-3: G/F scheme, A and B attached to subsystems C and D respectively. The system has two types of failure, degraded (partial failure) or complete failed states. The system is analyzed using supplementary variables techniques and Laplace transform. Copula family and general distribution are employed to restore the complete failed and partial failed states respectively. Computed results have been highlighted by the means of tables and graphs.

Keywords: Availability, Reliability, Sensitivity, (MTTF) Mean time to system failure, Topology, Gumbel-Hougaard family, Cost Analysis**.**

I. Introduction

The paramount of computer network is a needed requirement for improving the quality, efficiency and performance of telecommunications, manufacturing, industries, and hospital equipment. Good computer network system depends on the availability and reliability of the subsystems or units. Clients are connected in some predefined protocol called topologies, accordance of need passing information state topology configuration, where clients are connected to the main server. Among the different types of topology network is tree topology, where one central hub and multiple secondary hubs are used, failed of this central hub amount to complete failure of the system, but the subsystems remain in operational degraded state.

To improve system reliability and availability, implementation of redundant components are required, where some units are working while some remain reserves for immediate action, such operational system style is called k-out-of-n: G/F scheme. In this approach k units must work from the domain n of the system to operate, failure of more than k units results to complete failure of the system. Among many researched from different scholars in computer network topology and reliability theory model that includes, Zhang [1] analyzed on computer network reliability analysis based on intelligent cloud computing method. Saulius and Genadijus [2] investigated reliability of multi-server computer networks. Pradeep and Yogesh [3] studied software reliability growth model for three-tier client server system. Xin et al. [4] focused on reliability analysis of network service model. Potapov et al [5] studied reliability in the model of an information system with client server architecture. Kovalev et al [6] analyzed reliability analysis of distributed computer systems with client server. Fong and Hui [7] studied application of middleware in the three tier client/server database design methodology. Sumit and Anshul [8] studied on an introduction to computer networking. Yunhuai et al [9] investigated opportunity based topology control in wireless sensor network. Geon Yoon, Dae Hyun et al [10] focused on ring topology-based redundancy ethernet for industrial network. Nurul et al [11] studied the performance study of star topology in small internetworks. Ruhimat et al [12] analyzed optimal computer network based on graph topology model. Kudeep et al [13] studied tree topology network environment analysis under reliability approach, nonlinear. Nupur et al [14] focused on an approach to investigating reliability Indices for tree topology. System performance depends on system configuration and repair dynamics. Researchers have adopted different types of failure and repair, a lot of them have considered general repair while many adopted copula [15] which is now considered as the wider and better performance results compared to the general repair to cite few are Abubakar and Singh [16] have examined assessment and performance of industrial system using Gumbel Hougaard copula approach. Kabiru et al. [17] have focused on reliabity assessment of complex system with two subsystems using joint distribution. Ibrahim et al. [18] have analyzed the performance analysis of multi-computer system with three subsystems in series. Muhammad et al [19] studied cost benefit analysis of tree different series parallel dynamo configurations . Pratap et al [20] have examined on the assessment of complex system with two subsystems and multi types failure and repair. Yusuf et al [21] studied performance analysis of multi computer system consisting of active parallel homogeneous.

Copula distributions that couples different types distributions, since it deals with more than one repair of the repairable systems, Gumbel Hougaard family distribution is one among different types of copula family which consider more than one repairs. The authors in the present research study have consider a tree topology system with multi-servers, the system has four subsystems named as A, B, C and D, subsystems A and B stands as servers and are working 1-out-of-2: G/F policy, respectively, while C and D subsystems both are working in 2-out-of-3: G/F scheme, A and B attached to subsystems C and D respectively. The system work in both series and parallel configuration, Gumbel Hougaard family copula distribution employed for computation and

illustration. Lastly, [S_1 , S_2 , S_3, S_4 ,S_5, S_6, S_7, S_8 , S_9 ,S_{10}, S_{11} , S_{12}] represents the states of operation in degraded/partial failure while [S_{13} , S_{14}, S_{15}, and S_{16}] are completely failed states and S_0 is at perfect operational state. The degraded points have repaired by general repair and completely failed states have repaired under Gumbel Hougaard family copula. We invited supplementary variables and Laplace transformation to analyze the system. Measures in reliability among availability, reliability, and MTTF and cost analysis are all treated by the means of tables and graphs.

II.   State Description, Assumption and Notations

Table 1: State Description

State	State Description
S_0	The state S_0 represents a perfect state in which both the subsystems are in good working condition.
S_1	S_1, represents a degraded state with minor partial failure in the subsystem A, due to the failure of the first server of the subsystem A.
S_2	State S_2 represents a degraded state with minor partial failure in the subsystem C, due to the failure of the first unit of the subsystem C.
S_3	state S_3 represents a degraded state with minor partial failure in the subsystem D, due to the failure of the first unit of the subsystem D.
S_4	S_4, represents a degraded state with minor partial failure in the subsystem B, due to the failure of the first server of the subsystem B.
S_5	S_5, represents a degraded state with minor failure, due to the failure of the one unit of subsystems C and D.
S_6	S_6, represents a degraded state with minor failure, due to the failure of the one unit of subsystems D and server of subsystem A.
S_7	This state accounts for a degraded state with major partial failure, due to the failure of first servers of subsystem A and B.
S_8	S_8, represents a degraded state with minor failure, due to the failure of the one unit of subsystem C and a server of subsystem B.
S_9	This state accounts for a degraded state with major partial failure, due to the failure of one units of the subsystem C and D together with a server in subsystem B.
S_{10}	S_{10}, reveals a degraded state with major partial failure, due to the failure of one unit of the subsystem D and a server in subsystems A and B.
S_{11}	S_{11}, reveals a degraded state with major partial failure, due to the failure of one unit of the subsystem C and a server in subsystems A and B.
S_{12}	S_{12}, reveals a degraded state with major partial failure, due to the failure of one unit of the subsystems C and D together with a server in subsystems A and B.
S_{13}	The state S_{13} represent a complete failed state, due to failure of subsystems C and D the system is under repair using copula.
S_{14}	The state S_{14} represent a complete failed state, due to failure of servers in subsystems A and B the system is under repair using copula.
S_{15}	The state S_{15} represent a complete failed state, due to failure of subsystems A and D the system is under repair using copula.
S_{16}	The state S_{16} represent a complete failed state, due to failure of subsystems B and C the system is under repair using copula distribution.

The state description reveals that, S_0 is a state where the system is in a perfect state where both subsystems are in good working condition. S_1, S_2, S_3, S_4, S_5, S_6 and S_8 are the states where the system is in minor partial failure but operational mode. The states S_7, S_9,S_{11}, and S_{12} are in major partial failure in which the system is working under the critical stage, and further failure in any unit in the subsystems might be a cause of complete failure. The statesS_{13}, S_{14}, S_{15}, and S_{16} are the complete failed state of the model. The minor and major failed states will be respire by employing general repair, but the complete failed state will be restored using Gumbel- Hougaard family copula distribution.

Assumption

The following assumptions are taken throughout the discussion of the model:

  (i)   Initially, S_0 is the state where all units in the systems are in its perfect good state.
  (ii) The subsystems A and B are working as servers, with two units each, failure of one unit tends the system to a partial failure (degraded) state and its follows general distribution for repair and if more than one fails then its leads to complete failed state of the system and it restore using copula.
  (iii) Both the subsystems C and D has three units and at least two units must work, if first or second units failed the system function under degraded state and it repaired by general distribution otherwise complete failed state of the entire system.
  (iv) It is assumed that a repaired system works like a new and no damage appears during repair.
  (v)   As soon as the failed unit gets repaired, it performs its task normally.
  (vi) All failure rates are constants and follow a negative exponential distribution

Table 2:   Notations

|	
t :	Time variable on time scale.
s :	A variable for Laplace transform for all expressions.
λ_A / λ_B/λ_C/λ_D:	Failure rates of units of subsystems A, B, C and D
$\varphi(x)$	Repair rates for all unit of subsystems i.e. A, B, C and D
$\mu_0(x)$, $\mu_0(y)$:	Repair rates for complete failed states.
$P_i(x,t)$:	The probability that the system is in S_i state at instant's' for i =0 to 12.
$\bar{P}_i(s)$:	Laplace transformation of state transition probability P (t).
$E_p(t)$	Expected profit during the time interval [0, t).
K_1, K_2:	Revenue and service cost per unit time in the interval [0, t) respectively.
$S_\varphi(x)$	Standard repair distribution function $S_\varphi(x) = \varphi(x)e^{-\int_0^\infty \varphi(x)}$
$L[S_\varphi(x)]$:	$\bar{s}_\varphi(x) = \int_0^\infty e^{-sx} \varphi(x)e^{-\int_0^\infty \varphi(x)}dx$ is the Laplace transform of $S_\varphi(x)$
$\mu_0(x)$ $= C_\theta(u_1(x), u_2(x))$	The expression of joint probability (failed state S_i to good state S_0) according to Gumbel-Hougaard family copula is given as $C_\theta(u_1(x), u_2(x)) = \exp[x^\theta + \{\log \phi(x)\}^\theta]^{1/\theta}$, where, u_1 = $\phi(x)$, and u_2 = e^x, where θ as a parameter, $1 \leq \theta \leq \infty$.
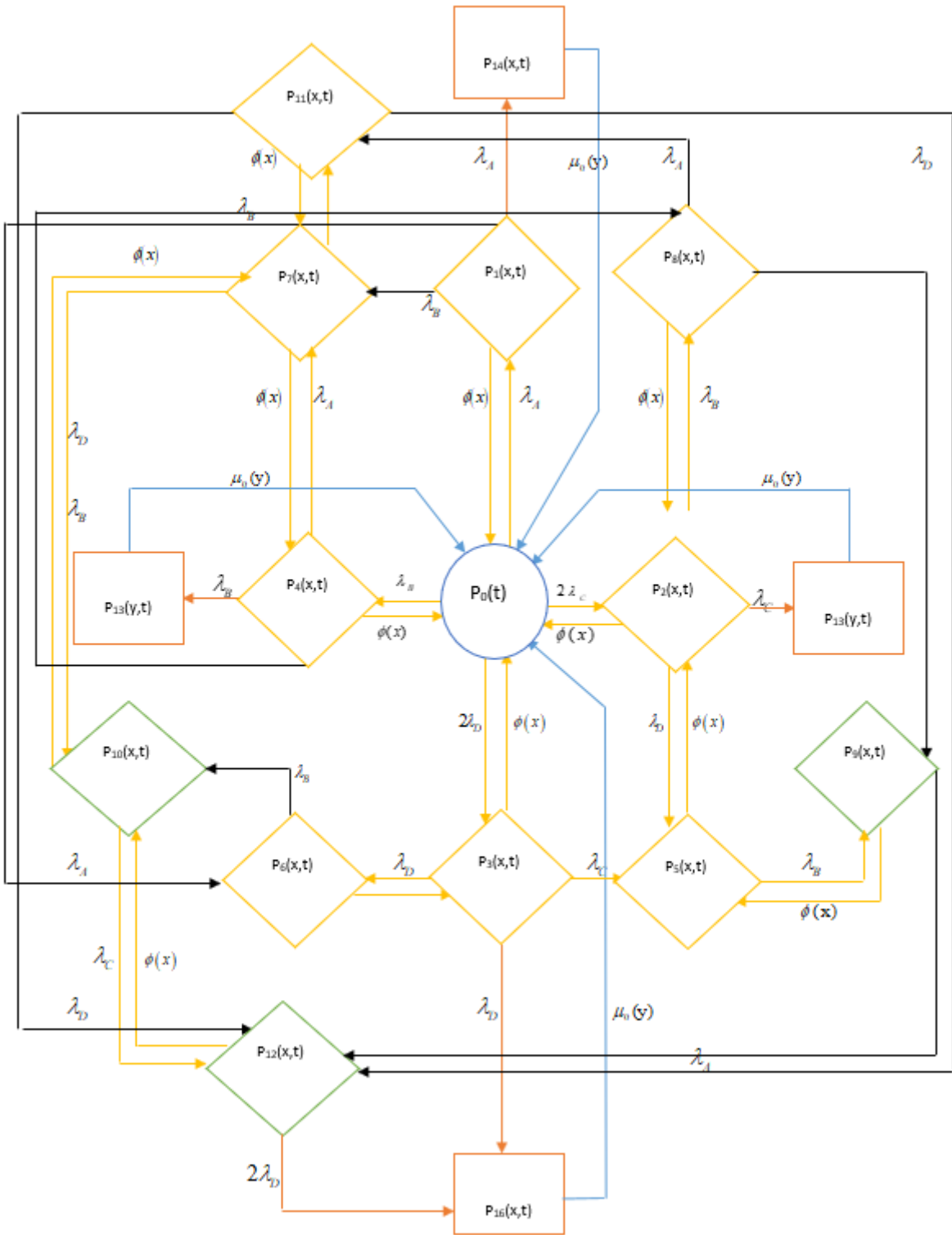
Figure 1: Transition Diagram

III.   Formulation and Solution of Mathematical Model

By the probability of considerations and continuity arguments, the following sets of difference differential equations are associated with the mathematical model:

$$\left(\frac{\partial}{\partial t} + \lambda_A + \lambda_B + 2\lambda_C + 2\lambda_D\right) P_0(t)$$

$$= \int_0^\infty \Phi_1(x) P_1(x,t) dx + \int_0^\infty \Phi_2(x) P_2(x,t) dx + \int_0^\infty \Phi_3 P_3(x,t) dx + \int_0^\infty \Phi_4(x) P_4(x,t) dx$$

$$+ \int_0^\infty \mu_0 P_{13}(y,t) dy + \int_0^\infty \mu_0 P_{14}(y,t) dy + \int_0^\infty \mu_0 P_{15}(y,t) dy$$

$$+ \int_0^\infty \mu_0 P_{16}(y,t) dy \qquad (1)$$

$$\left(\frac{\partial}{\partial t} + \frac{\partial}{\partial x} + 2\lambda_A + \lambda_B + \Phi(x)\right) P_1(x,t) = 0 \qquad (2)$$

$$\left(\frac{\partial}{\partial t} + \frac{\partial}{\partial x} + \lambda_B + \lambda_C + \lambda_D + \Phi(x)\right) P_2(x,t) = 0 \qquad (3)$$

$$\left(\frac{\partial}{\partial t} + \frac{\partial}{\partial x} + \lambda_C + 2\lambda_D + \Phi(x)\right) P_3(x,t) = 0 \qquad (4)$$

$$\left(\frac{\partial}{\partial t} + \frac{\partial}{\partial x} + \lambda_A + 2\lambda_B + \Phi(x)\right) P_4(x,t) = 0 \qquad (5)$$

$$\left(\frac{\partial}{\partial t} + \frac{\partial}{\partial x} + \lambda_B + \Phi(x)\right) P_5(x,t) = 0 \qquad (6)$$

$$\left(\frac{\partial}{\partial t} + \frac{\partial}{\partial x} + \lambda_B + \Phi(x)\right) P_6(x,t) = 0 \qquad (7)$$

$$\left(\frac{\partial}{\partial t} + \frac{\partial}{\partial x} + \lambda_C + \lambda_D + \Phi(x)\right) P_7(x,t) = 0 \qquad (8)$$

$$\left(\frac{\partial}{\partial t} + \frac{\partial}{\partial x} + \lambda_A + \lambda_D + \Phi(x)\right) P_8(x,t) = 0 \qquad (9)$$

$$\left(\frac{\partial}{\partial t} + \frac{\partial}{\partial x} + \lambda_A + \Phi(x)\right) P_9(x,t) = 0 \qquad (10)$$

$$\left(\frac{\partial}{\partial t} + \frac{\partial}{\partial x} + \lambda_C + \Phi(x)\right) P_{10}(x,t) = 0 \qquad (11)$$

$$\left(\frac{\partial}{\partial t} + \frac{\partial}{\partial x} + \lambda_D + \Phi(x)\right) P_{11}(x,t) = 0 \qquad (12)$$

$$\left(\frac{\partial}{\partial t} + \frac{\partial}{\partial x} + 2\lambda_D + \Phi(x)\right) P_{12}(x,t) = 0 \qquad (13)$$

$$\left(\frac{\partial}{\partial t} + \frac{\partial}{\partial y} + \mu_0(y)\right) P_{13}(y,t) = 0 \qquad (14)$$

$$\left(\frac{\partial}{\partial t} + \frac{\partial}{\partial y} + \mu_0(y)\right) P_{14}(y,t) = 0 \qquad (15)$$

$$\left(\frac{\partial}{\partial t} + \frac{\partial}{\partial y} + \mu_0(y)\right) P_{14}(y,t) = 0 \qquad (16)$$

$$\left(\frac{\partial}{\partial t} + \frac{\partial}{\partial y} + \mu_0(y)\right) P_{15}(y,t) = 0 \qquad (17)$$

$$\left(\frac{\partial}{\partial t} + \frac{\partial}{\partial y} + \mu_0(y)\right) P_{16}(y,t) = 0 \qquad (18)$$

Boundary conditions

$$P_1(0,t) = \lambda_A P_0(t) \qquad (19)$$
$$P_2(0,t) = 2\lambda_C P_0(t) \qquad (20)$$
$$P_3(0,t) = 2\lambda_D P_0(t) \qquad (21)$$
$$P_4(0,t) = \lambda_B P_0(t) \qquad (22)$$
$$P_5(0,t) = 4\lambda_C \lambda_D P_0(t) \qquad (23)$$
$$P_6(0,t) = (\lambda_A^2 + \lambda_D^2) P_0(t) \qquad (24)$$
$$P_7(0,t) = (\lambda_A \lambda_C + \lambda_A \lambda_B) P_0(t) \qquad (25)$$
$$P_8(0,t) = (2\lambda_A \lambda_C + \lambda_B^2) P_0(t) \qquad (26)$$
$$P_9(0,t) = (\lambda_B(2\lambda_C \lambda_D) + \lambda_A(\lambda_B \lambda_C + \lambda_B^2)) P_0(t) \qquad (27)$$
$$P_{10}(0,t) = (\lambda_B(\lambda_D^2 + \lambda_A \lambda_B \lambda_C) + \lambda_D(\lambda_A \lambda_C + \lambda_A \lambda_B)) P_0(t) \qquad (28)$$
$$P_{11}(0,t) = (\lambda_A(\lambda_B^2 + \lambda_B \lambda_C) + \lambda_C(\lambda_A \lambda_C + \lambda_A \lambda_B)) P_0(t) \qquad (29)$$

$$P_{12}(0,t) = [\lambda_A \lambda_B(2\lambda_C \lambda_D) + \lambda_A \lambda_D(\lambda_B \lambda_C + \lambda_B^2) + \lambda_C \lambda_B(\lambda_D^2 + \lambda_A \lambda_B \lambda_C)$$
$$+ \lambda_C \lambda_D(\lambda_A \lambda_C + \lambda_A \lambda_B) + \lambda_D \lambda_A(\lambda_B \lambda_C + \lambda_B^2) + \lambda_D \lambda_C(\lambda_A \lambda_C + \lambda_A \lambda_B)] P_0(t) \qquad (30)$$

$$P_{13}(0,t) = 2\lambda_C^2 P_0(t) \tag{31}$$
$$P_{14}(0,t) = \lambda_A^2 P_0(t) \tag{32}$$
$$P_{15}(0,t) = \lambda_B^2 P_0(t) \tag{33}$$
$$P_{16}(0,t) = (4\lambda_D^2 + 2\lambda_D P_{12}(0,t))P_0(t) \tag{34}$$

Solution of the Model

By taking the Laplace transformation of equations (1) to (34) with the help of initial condition $P_0(0) = 1$, one may obtain:

$$(s + \lambda_A + \lambda_B + 2\lambda_C + 2\lambda_D)$$
$$= 1$$
$$+ \int_0^\infty \Phi_1(x)P_1(x,s)dx + \int_0^\infty \Phi_2(x)P_2(x,s)dx + \int_0^\infty \Phi_3(x)P_3(x,s)dx$$
$$+ \int_0^\infty \Phi_4(x)P_4(x,s)dx + \int_0^\infty \mu_0(y)P_{12}(y,s)dy + \int_0^\infty \mu_0(y)P_{14}(y,s)dy$$
$$+ \int_0^\infty \mu_0(y)P_{15}(y,s)dy + \int_0^\infty \mu_0(y)P_{16}(y,s)dy \tag{35}$$

$$\left(s + \frac{\partial}{\partial x} + 2\lambda_A + \lambda_B + \Phi_1(x)\right)\bar{P}_1(x,s) = 0 \tag{36}$$
$$\left(s + \frac{\partial}{\partial x} + \lambda_B + 2\lambda_C + \lambda_D + \Phi_2(x)\right)\bar{P}_2(x,s) = 0 \tag{37}$$
$$\left(s + \frac{\partial}{\partial x} + \lambda_C + 2\lambda_D + \Phi_3(x)\right)\bar{P}_3(x,s) = 0 \tag{38}$$
$$\left(s + \frac{\partial}{\partial x} + \lambda_A + 2\lambda_B + \Phi_4(x)\right)\bar{P}_4(x,s) = 0 \tag{39}$$
$$\left(s + \frac{\partial}{\partial x} + \lambda_B + \Phi_5(x)\right)\bar{P}_5(x,s) = 0 \tag{40}$$
$$\left(s + \frac{\partial}{\partial x} + \lambda_B + \Phi_6(x)\right)\bar{P}_6(x,s) = 0 \tag{41}$$
$$\left(s + \frac{\partial}{\partial x} + \lambda_C + \lambda_D + \Phi_7(x)\right)\bar{P}_7(x,s) = 0 \tag{42}$$
$$\left(s + \frac{\partial}{\partial x} + \lambda_A + \lambda_D + \Phi_8(x)\right)\bar{P}_8(x,s) = 0 \tag{43}$$
$$\left(s + \frac{\partial}{\partial x} + \lambda_A + \Phi_9(x)\right)\bar{P}_9(x,s) = 0 \tag{44}$$
$$\left(s + \frac{\partial}{\partial x} + \lambda_C + \Phi_{10}(x)\right)\bar{P}_{10}(x,s) = 0 \tag{45}$$
$$\left(s + \frac{\partial}{\partial x} + \lambda_D + \Phi_{11}(x)\right)\bar{P}_{11}(x,s) = 0 \tag{46}$$
$$\left(s + \frac{\partial}{\partial x} + 2\lambda_D + \Phi_{12}(x)\right)\bar{P}_{12}(x,s) = 0 \tag{47}$$
$$\left(s + \frac{\partial}{\partial x} + \mu_0(x)\right)\bar{P}_{13}(x,s) = 0 \tag{48}$$
$$\left(s + \frac{\partial}{\partial y} + \mu_0(y)\right)\bar{P}_{14}(y,s) = 0 \tag{49}$$
$$\left(s + \frac{\partial}{\partial y} + \mu_0(y)\right)\bar{P}_{15}(y,s) = 0 \tag{50}$$
$$\left(s + \frac{\partial}{\partial y} + \mu_0(y)\right)\bar{P}_{16}(y,s) = 0 \tag{51}$$

The Laplace transformations of the boundary conditions are:
$$\bar{P}_1(0,s) = \lambda_A\overline{P_0}(s) \tag{52}$$
$$\bar{P}_2(0,s) = 2\lambda_C\overline{P_0}(s) \tag{53}$$
$$\bar{P}_3(0,s) = 2\lambda_D\overline{P_0}(s) \tag{54}$$
$$\bar{P}_4(0,s) = \lambda_B\overline{P_0}(s) \tag{55}$$
$$\bar{P}_5(0,s) = 4\lambda_C\lambda_D\overline{P_0}(s) \tag{56}$$
$$\bar{P}_6(0,s) = (\lambda_A^2 + \lambda_D^2)\bar{P}_0(s) \tag{57}$$
$$\bar{P}_7(0,s) = (\lambda_A\lambda_C + \lambda_A\lambda_B)\bar{P}_0(s) \tag{58}$$
$$\bar{P}_8(0,s) = (\lambda_B^2 + 2\lambda_B\lambda_C)\bar{P}_0(s) \tag{59}$$
$$\bar{P}_9(0,s) = (\lambda_B(2\lambda_C\lambda_D) + \lambda_A(\lambda_B\lambda_C + \lambda_B^2))\bar{P}_0(s) \tag{60}$$
$$\bar{P}_{10}(0,s) = (\lambda_B(\lambda_D^2 + \lambda_A\lambda_B\lambda_C) + \lambda_D(\lambda_A\lambda_C + \lambda_A\lambda_B))\bar{P}_0(s) \tag{61}$$
$$\bar{P}_{11}(0,s) = (\lambda_A(\lambda_B^2 + \lambda_B\lambda_C) + \lambda_C(\lambda_A\lambda_C + \lambda_A\lambda_B))\bar{P}_0(s) \tag{62}$$

$$\bar{P}_{12}(0,s) = [\lambda_A\lambda_B(2\lambda_C\lambda_D) + \lambda_A\lambda_D(\lambda_B\lambda_C + \lambda_B^2) + \lambda_C\lambda_B(\lambda_D^2 + \lambda_A\lambda_B\lambda_C) + \lambda_C\lambda_D(\lambda_A\lambda_C + \lambda_A\lambda_B) +$$
$$\lambda_D\lambda_A(\lambda_B\lambda_C + \lambda_B^2) + \lambda_D\lambda_C(\lambda_A\lambda_C + \lambda_A\lambda_B)]\bar{P}_0(s) \tag{63}$$

$$\bar{P}_{13}(0,s) = 2\lambda_C^2(s)\bar{P}_0(s) \tag{64}$$

$$\bar{P}_{14}(0,s) = \lambda_A^2(s)\bar{P}_0(s) \tag{65}$$

$$\bar{P}_{15}(0,s) = \lambda_B^2(s)\bar{P}_0(s) \tag{66}$$

$$\bar{P}_{16}(0,s) = (2\lambda_D^2 + 2\lambda_D P_{12}(0,t))\bar{P}_0(s) \tag{67}$$

Now solving equations (35) to (51) with the help of equations (52) to (67), yields,

$$\bar{P}_0(s) = \frac{1}{M(s)} \tag{68}$$

$$\bar{P}_1(s) = \frac{1}{M(s)}\left\{\frac{\lambda_A}{S+2\lambda_A+\lambda_B+\Phi(x)}\right\} \tag{69}$$

$$\bar{P}_2(s) = \frac{1}{M(s)}\left\{\frac{2\lambda_C}{S+\lambda_B+2\lambda_C+\lambda_D+\Phi(x)}\right\} \tag{70}$$

$$\bar{P}_3(s) = \frac{1}{M(s)}\left\{\frac{2\lambda_D}{S+2\lambda_D+\lambda_C+\Phi(x)}\right\} \tag{71}$$

$$\bar{P}_4(s) = \frac{1}{M(s)}\left\{\frac{\lambda_B}{S+2\lambda_B+\lambda_A+\Phi(x)}\right\} \tag{72}$$

$$\bar{P}_5(s) = \frac{1}{M(s)}\left\{\frac{4\lambda_C\lambda_D}{S+\lambda_B+\Phi(x)}\right\} \tag{73}$$

$$\bar{P}_6(s) = \frac{1}{M(s)}\left\{\frac{(\lambda_A^2+\lambda_D^2)}{S+\lambda_B+\Phi(x)}\right\} \tag{74}$$

$$\bar{P}_7(s) = \frac{1}{M(s)}\left\{\frac{(\lambda_A\lambda_C+\lambda_A\lambda_B)}{S+\lambda_A+\Phi(x)}\right\} \tag{75}$$

$$\bar{P}_8(s) = \frac{1}{M(s)}\left\{\frac{(2\lambda_B^2+\lambda_B\lambda_C)}{S+\lambda_D+\Phi(x)}\right\} \tag{76}$$

$$\bar{P}_9(s) = \frac{1}{M(s)}\left\{\frac{(\lambda_B(2\lambda_C\lambda_D)+\lambda_D(\lambda_B\lambda_C+\lambda_B^2))}{S+\lambda_A+\Phi(x)}\right\} \tag{77}$$

$$\bar{P}_{10}(s) = \frac{1}{M(s)}\left\{\frac{(\lambda_B(\lambda_D^2+\lambda_A\lambda_B\lambda_C)+\lambda_D(\lambda_A\lambda_C+\lambda_A\lambda_B))}{S+\lambda_C+\Phi(x)}\right\} \tag{78}$$

$$\bar{P}_{11}(s) = \frac{1}{M(s)}\left\{\frac{(\lambda_A(\lambda_B^2+\lambda_B\lambda_C)+\lambda_C(\lambda_A\lambda_C+\lambda_A\lambda_B))}{S+\lambda_D+\Phi(x)}\right\} \tag{79}$$

$$\bar{P}_{12}(s) = \frac{1}{M(s)}\left\{\frac{\begin{array}{c}[\lambda_A\lambda_B(2\lambda_C\lambda_D)+\lambda_A\lambda_D(\lambda_B\lambda_C+\lambda_B^2)+\lambda_C\lambda_B(\lambda_D^2+\lambda_A\lambda_B\lambda_C)\\+\lambda_C\lambda_D(\lambda_A\lambda_C+\lambda_A\lambda_B)+\lambda_D\lambda_A(\lambda_B\lambda_C+\lambda_B^2)+\lambda_D\lambda_C(\lambda_A\lambda_C+\lambda_A\lambda_B)]\end{array}}{S+2\lambda_D+\Phi(x)}\right\} \tag{80}$$

The Laplace transformations of the state transition probabilities that the system is in operational mode. i.e. perfect and partially failed state $(S_0, S_1, S_2, S_3, S_4, S_5, S_6, S_7, S_8, S_9, S_{10}, S_{11}, S_{12})$ at any time are as follows:

$$\bar{P}_{up}(s) = \bar{P}_0(s) + \bar{P}_1(s) + \bar{P}_2(s) + \bar{P}_3(s) + \bar{P}_4(s) + \bar{P}_5(s) + \bar{P}_6(s) + \bar{P}_7(s) + \bar{P}_8(s) + \bar{P}_9(s) + \bar{P}_{10}(s) + \bar{P}_{11}(s) + \bar{P}_{12}(s) \tag{81}$$

$$\bar{P}_{down}(s) = 1 - \bar{P}_{up}(s) \tag{82}$$

Where,

$$M(s) = \left\{(s+\lambda_A+\lambda_B+2\lambda_C+2\lambda_D) - \left(\begin{array}{c}\dfrac{\lambda_A}{s+2\lambda_A+\lambda_B+\varphi(x)} + \dfrac{2\lambda_C}{s+2\lambda_B+\lambda_D+\varphi(x)} + \dfrac{2\lambda_D}{s+2\lambda_D+\lambda_C+\varphi(x)} + \dfrac{\lambda_B}{s+\lambda_A+2\lambda_B+\varphi(x)} \\ + \dfrac{2\lambda_C^2\mu_0(y)}{s+\mu_0(y)} + \dfrac{2\lambda_B^2\mu_0(y)}{s+\mu_0(y)} + \dfrac{2\lambda_A^2\mu_0(y)}{s+\mu_0(y)} + \dfrac{(\lambda_D^2+2\lambda_D P_{12}(0,t))\mu_0(y)}{s+\mu_0(y)}\end{array}\right)\right\} \tag{83}$$

The $\bar{P}_{up}(s)$ and $\bar{P}_{dawn}(s)$ are the system Laplace transform of the state probabilities in operative

and failed state. Then,

$$\overline{P_{up}}(s) = \sum_{i=0}^{12} \overline{P_i}(s) \quad and \quad \overline{P_{dawn}}(s) = 1 - \overline{P_{up}}(s)$$

$$P_{up}(t) = \left\{ \begin{array}{l} 1 + \dfrac{\lambda_A}{s + 2\lambda_A + \lambda_B + \varphi(x)} + \dfrac{2\lambda_C}{s + 2\lambda_B + \lambda_D + \varphi(x)} + \dfrac{2\lambda_D}{s + 2\lambda_D + \lambda_C + \varphi(x)} + \dfrac{\lambda_B}{s + \lambda_A + 2\lambda_B + \varphi(x)} \\[3mm] + \dfrac{4\lambda_C\lambda_D}{s + \lambda_B + \varphi(x)} + \dfrac{\lambda_A^2\lambda_D^2}{s + \lambda_B + \varphi(x)} + \dfrac{\lambda_A\lambda_C + \lambda_A\lambda_B}{s + \lambda_A + \varphi(x)} + \dfrac{\lambda_B^2 + \lambda_A\lambda_C}{s + \lambda_D + \varphi(x)} + \dfrac{\lambda_B(2\lambda_C\lambda_D) + \lambda_D(\lambda_B\lambda_C + \lambda_B^2)}{s + \lambda_D + \varphi(x)} \\[3mm] \dfrac{\lambda_B(\lambda_D^2 + \lambda_A^2) + \lambda_D(\lambda_A\lambda_C + \lambda_A\lambda_B)}{s + \lambda_C + \varphi(x)} + \dfrac{2\lambda_A(\lambda_B^2 + \lambda_B\lambda_C) + \lambda_C(\lambda_A\lambda_C + \lambda_A\lambda_B)}{s + \lambda_D + \varphi(x)} \\[3mm] \dfrac{\lambda_A\lambda_B(2\lambda_C\lambda_D) + \lambda_A\lambda_D(\lambda_B\lambda_C + \lambda_B^2) + \lambda_C\lambda_B(\lambda_D^2 + \lambda_A^2) + 2\lambda_C\lambda_D(\lambda_A\lambda_C + \lambda_A\lambda_B) + \lambda_A\lambda_D(\lambda_B\lambda_C + \lambda_B^2)}{s + \lambda_C + \varphi(x)} \end{array} \right\}$$

(84)

IV. Analytical Study of the Model

I. Availability Analysis

By Setting $\quad S_{\mu_0}(s) = \overline{S}_{\exp[x^\theta + \{\log\varphi(x)\}^\theta]^{1/\theta}}(s) = \dfrac{\exp[x^\theta + \{\log\varphi(x)\}^\theta]^{1/\theta}}{s + \exp[x^\theta + \{\log\varphi(x)\}^\theta]^{1/\theta}}$, $\overline{S}_{\varphi_S}(s) = \dfrac{\varphi_S}{s + \varphi_S}$,

The expression of availability is obtained by taking the inverse Laplace transform of equation (84) together with the values of failure rates, λA=0.01, λB=0.02, λC=0.03, λD=0.04, at $\phi(x) = \theta = x = 1$ and $\mu_0(x) = \mu_0(y) = 2.781$

$$\overline{P_{up}}(t) = \left\{ \begin{array}{l} -0.000007268385466 e^{-1.030000000t} - 0.000001279136863 e^{-1.080000000t} + 0.001158951568 e^{-2.721478824t} \\ -0.009672831318 e^{-1.210427182t} + 0.0008133658410 e^{-1.111354496t} + 0.0001409557370 e^{-1.076073851t} \\ -0.0001619227838 e^{-1.052980075t} + 1.012125757 e^{-0.005985571315t} - 0.001673078923 e^{-1.020000000t} \\ -0.0004724824273 e^{-1.010000000t} - 0.00034152440368^{-1.040000000t} \end{array} \right\} \quad ...(85)$$

Through variation of time t= 0, 1, 2, 3, 4, 5, 6, 7, 8, 9.., units, we get different values of $P_{up}(t)$ with the help of expression (85) as shown in Table 1 and figure 2.

Table 3: Variation of Availability with respect to time (t)

Time(t)	Availability
0	1
1	0.999
2	0.998
3	0.993
4	0.988
5	0.982
6	0.976
7	0.97
8	0.964
9	0.95
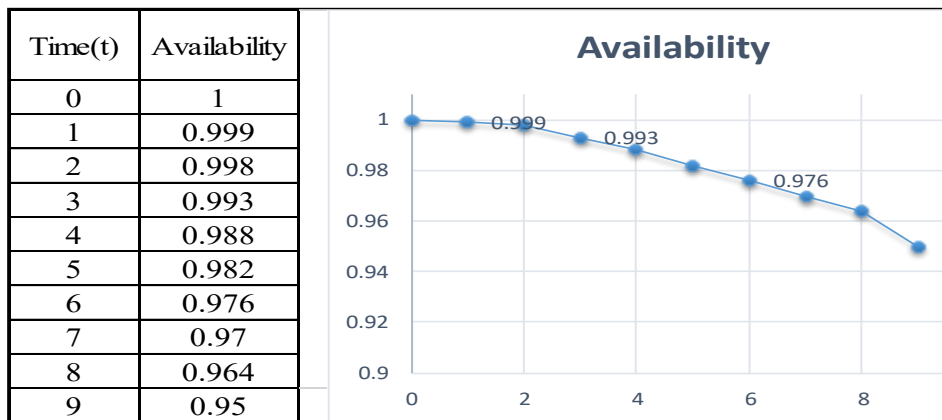
Figure 2: Variation of Availability with respect to time (t)

II. Reliability Analysis

Taking all repair rates to zero with the same value of failure and repair rates in equation (85), i.e $\phi(x)$ and $\mu_0(x)$ and λ_A=0.01, λ_B=0.02, λ_C=0.03, λ_D=0.04, and then taking inverse Laplace transform, we obtained the expression of reliability as:

$$R(t) = \begin{cases} 0.2000000000 e^{-0.05000000000t} - 1.500000000 e^{-0.1200000000t} + 0.8000000000 e^{-0.1500000000t} \\ +0.01133333333 e^{-0.01000000000t} + 0.000287428571 e^{-0.03000000000t} + 0.0001421800000 e^{-0.08000000000t} \\ +0.0203500000 e^{-0.04000000000t} + 2.951145391 e^{-0.1000000000t} + 0.05007500000 e^{-0.02000000000t} \\ +0.06666666667 e^{-0.07000000000t} \end{cases} \quad ...(86)$$

For different values of time t= 0, 1, 2, 3, 4, 5, 6, 7, 8, 9.., units of time, we get different values of Reliability as shown in Table 2. and Figure. 3.

Table 4: Variation of reliability with respect to time (t)

Time(t)	Reliability
0	1
1	0.984
2	0.96
3	0.932
4	0.899
5	0.864
6	0.827
7	0.789
8	0.751
9	0.712
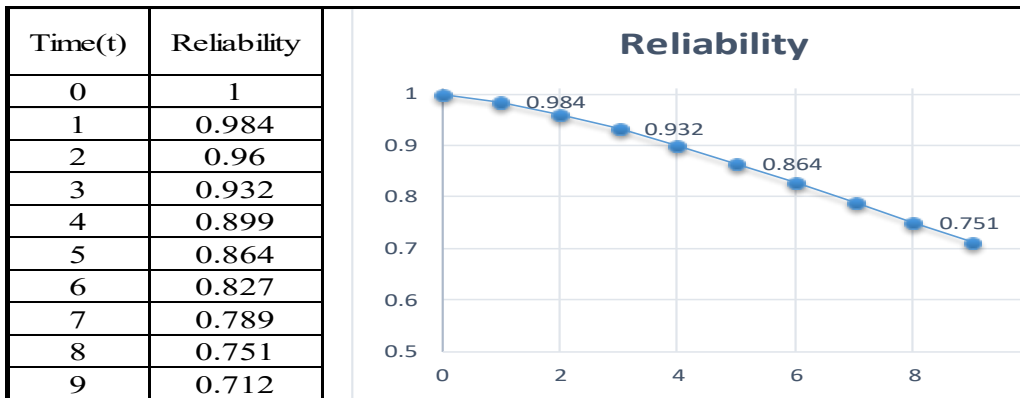
Figure 3: Variation of reliability with respect to time (t)

III. Mean Time To Failure (MTTF) Analysis:

We obtained the expression for MTTF by taking all repairs zero in equation (85), and set the limit of s tends to zero:

$$M.T.T.F. = \lim_{s \to 0} \bar{P}_{up}(s) = \frac{1}{\left\{(s+\lambda_A+\lambda_B+2\lambda_C+2\lambda_D) - \left(\frac{\lambda_A}{2\lambda_A+\lambda_B} + \frac{2\lambda_C}{s+2\lambda_B+\lambda_D} + \frac{2\lambda_D}{s+2\lambda_D+\lambda_C} + \frac{\lambda_B}{s+\lambda_A+2\lambda_B}\right)\right\}} \begin{cases} \frac{\lambda_A}{2\lambda_A+\lambda_B} + \frac{2\lambda_C}{2\lambda_B+\lambda_D} + \frac{2\lambda_D}{2\lambda_D+\lambda_C} + \frac{\lambda_B}{\lambda_A+2\lambda_B} \\ +\frac{4\lambda_C\lambda_D}{\lambda_B} + \frac{\lambda_A^2\lambda_D^2}{\lambda_B} + \frac{\lambda_A\lambda_C+\lambda_A\lambda_B}{\lambda_A} + \frac{\lambda_B^2+\lambda_A\lambda_C}{\lambda_D} + \frac{\lambda_B(2\lambda_C\lambda_D)+\lambda_D(\lambda_B\lambda_C+\lambda_B^2)}{\lambda_D} \\ \frac{\lambda_B(\lambda_D^2+\lambda_A^2)+\lambda_D(\lambda_A\lambda_C+\lambda_A\lambda_B)}{\lambda_C} + \frac{2\lambda_A(\lambda_B^2+\lambda_B\lambda_C)+\lambda_C(\lambda_A\lambda_C+\lambda_A\lambda_B)}{\lambda_D} \\ \frac{\lambda_A\lambda_B(2\lambda_C\lambda_D)+\lambda_A\lambda_D(\lambda_B\lambda_C+\lambda_B^2)+\lambda_C\lambda_B(\lambda_D^2+\lambda_A^2)+2\lambda_C\lambda_D(\lambda_A\lambda_C+\lambda_A\lambda_B)+\lambda_A\lambda_D(\lambda_B\lambda_C+\lambda_B^2)}{\lambda_C} \end{cases}$$

Setting λ_A=0.01, λ_B=0.02, λ_C=0.03, λ_D= 0.04, and varying λ_A, λ_B, λ_C and λ_D respectively as, 0.1, 0.2, 0.3, 0.4, 0.5, 0.6, 0.7, 0.8, 0.9, in (85), we get the variation of M.T.T.F. with respect to failure rates as shown in Table.3 and corresponding Figure.4.

Table 5: Variation of MTTF with respect to failure rate

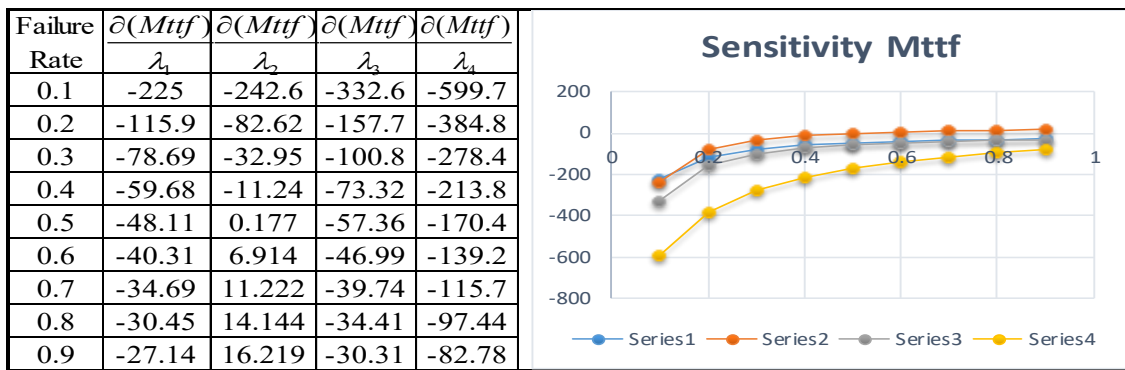| Failure Rate	MTTF λ_1	MTTF λ_2	MTTF λ_3	MTTF λ_4
0.1	38.26	48.74	59.2	104.82
0.2	33.02	34.45	48.26	122.02
0.3	30.94	29.17	43.61	132.97
0.4	29.81	27.18	41.03	141.13
0.5	29.11	26.75	39.38	148.3
0.6	28.63	27.19	38.24	154.82
0.7	28.27	28.16	37.4	160.94
0.8	28.01	29.48	36.75	166.81
0.9	27.79	31.05	36.25	172.49
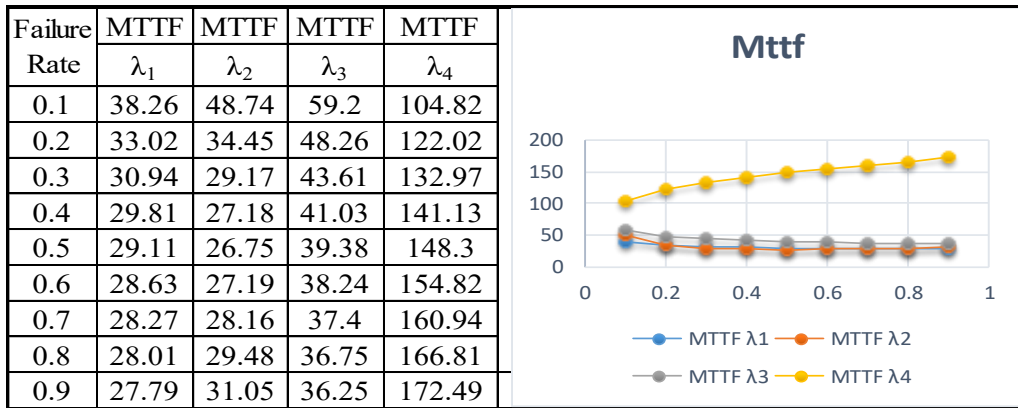
Figure 4: Variation of MTTF with respect to failure rate

IV. Sensitivity analysis of (MTTF):

The computation of sensitivity MTTF is studied through the partial differentiation of MTTF with respect to the failure rates of the system, by introducing the set of parametric variation of the failure rates λ_A=0.01, λ_B=0.02, λ_C=0.03, and λ_D=0.04 from the resulting expression, we calculated the MTTF sensitivity as shown in Table 4 and the corresponding value in Figure.5

Table 6: Sensitivity of MTTF as a function of failure rates

Failure Rate	$\partial(Mttf)$ λ_1	$\partial(Mttf)$ λ_2	$\partial(Mttf)$ λ_3	$\partial(Mttf)$ λ_4
0.1	-225	-242.6	-332.6	-599.7
0.2	-115.9	-82.62	-157.7	-384.8
0.3	-78.69	-32.95	-100.8	-278.4
0.4	-59.68	-11.24	-73.32	-213.8
0.5	-48.11	0.177	-57.36	-170.4
0.6	-40.31	6.914	-46.99	-139.2
0.7	-34.69	11.222	-39.74	-115.7
0.8	-30.45	14.144	-34.41	-97.44
0.9	-27.14	16.219	-30.31	-82.78

Figure 5: Sensitivity of MTTF as a function of failure rates

V. Cost Analysis

The expected profit over the time interval [0, t), can be calculate by the folloewing relation $E_p(t) = K_1 \int_0^t P_{up}(t)dt - K_2 t$. If the service facility of the system is always available, where k_1 is revenue generated and k_2 service cost per unit time. For the same set of the parameter of failure and repair rates in (84), we obtained the expression of cost benefit analysis.

$$E_p(t) = \begin{cases} -0.000007056684918\, e^{-1.030000000t} + 0.0000001184385984\, e^{-1.080000000t} - 0.0004258536050\, e^{-2.721478824t} \\ +0.007991254213\, e^{-1.210427182t} + 0.0007318689436\, e^{-1.111354496t} + 0.0001309907651\, e^{-1.076073851t} \\ +0.0001537757339\, e^{-1.052980075t} - 169.094266083\, e^{-0.005985571315t} + 0.001640273454\, e^{-1.020000000t} \\ +0.0004678043835\, e^{-1.010000000t} + 0.0003283884969\, e^{-1.040000000t} \end{cases} \quad (86)$$

By fixing the revenue K_1= 1 and taking the values K_2= 0.6, 0.5, 0.4, 0.3, 0.2 and 0.1 respectively together with the variation of t =0, 1, 2, 3, 4, 5, 6, 7, 8, 9, Units of time, we obtained the results for expected profit as shown in Table 5 and Figure.6

Table 7: Expected Profit in [0,t) t=0,1 ,2, 3, 4…9

Time (t)	$E_P(t)$: K_2=0.6	$E_P(t)$: K_2=0.5	$E_P(t)$: K_2=0.4	$E_P(t)$: K_2=0.3	$E_P(t)$: K_2=0.2	$E_P(t)$: K_2=0.1
0	0	0	0	0	0	0
1	0.401	0.501	0.601	0.701	0.801	0.901
2	0.802	1.002	1.202	1.402	1.602	1.802
3	1.198	1.498	1.798	2.098	2.398	2.698
4	1.589	1.989	2.389	2.789	3.189	3.589
5	1.974	2.474	2.974	3.474	3.974	4.474
6	2.353	2.953	3.553	4.153	4.753	5.353
7	2.727	3.427	4.127	4.827	5.527	6.227
8	3.095	3.895	4.695	5.495	6.295	7.095
9	3.457	4.357	5.257	6.157	7.057	7.957
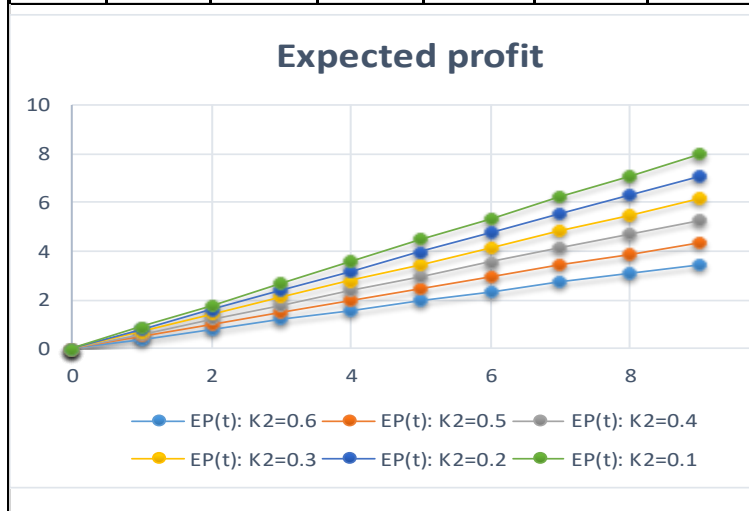
Figure 6: Expected Profit in [0,t) t=0,1 ,2, 3, 4…9

V. Discussion

The performance of the system under the assessment of reliability measures for different values of failure and repair rates. Table.1 and figure 2 shows the information of availability of the complex tree topology with respect to the variation in time when the failure rates are fixed at different values particularly, λ_A=0.01, λ_B=0.02, λ_C=0.03 and λ_D=0.04. The availability of the system decreases slowly, as the probability of failure increases, after sufficient long interval of time the system availability will tend to zero. However, one can simply predict the future behavior of the complex system at any stage for any given set of parametric values.

Table.2 and figure.3 analyzed the reliability of the system when the repair rate setup to zero. The figure shown clearly that the reliability of the system is decreasing faster compare to availability, which evidently proved that when the repairs provided the performance of the system is quite better. Table.3 and figure.4 assess the information of mean time to failure of the system (MTTF) with respect to variation of failure rates. The value change of MTTF is directly propotional to the system

reliability. The computations MTTF for different values of failure rates, λ_A, λ_B, λ_C, and λ_D from the figure the variation in MTTF corresponding to failure rates λ_D is high compared to other failure which indicates that the system will not be affected with higher variations in values λ_D. The MTTF due to λ_A, λ_B, and λ_C will influence the operation of the system.

Table.4 and figure.5 shows the variation of sensitivity MTTF with respect to the values of parameters. which obtained from partial derivative of MTTF with respect to the corresponding failure rate, the variation of sensitivity MTTF corresponding to failure rates λ_D is lower compared to other failure rates.

Table.5 and figure.6 provide the information on how the profit has been generated, by fixing revenue cost per unit time $K_1 = 1$, and varies the service costs $K_2 = 0.6, 05. 0.4, 0.3, 0.2$ and 0.1, if we examine critically from Figure.6 we can reveals that the expected profit increases for low service cost. Which finally shows the Networking system of tree topology system is reliable.

References

[1] Zhang, F. (2019) Research on reliability Analysis of Computer Network Based on Intelligent Cloud Computing Method, *International Journal of Computers and Applications, 41:4, 283-288, DOI: 10.1080/1206212X.2017.1402622.*

[2] Saulius Minkevičius and Genadijus Kulvietis. (2011). Investigation of the Reliability of Multiserver Computer Networks. *International Conference on Analytical and Stochastic Modeling Techniques and Applications, ASMTA 2011: pp 249-256*

[3] Pradeep Kumar and Yogesh Singh. (2010). A Software Reliability Growth Model for Three-Tier Client Server System. *International Journal of Computer Applications, Volume 1 -No. 13, 9-16.*

[4] Xin J., Guo L., Huang N., Li R.,(2013). Network Service Reliability Analysis Model. *Jour. of Chemical Engineering Transactions, 33, 511-516 DOI: 10.3303/CET133308651*

[5] Potapov, V. I., Shafeeva, O.P., Gritsay, A. S ., Makarov, V. V., Kuznetsova, O.P., and Kondratukova, L.K. (2019). Reliability in the Model of an Information System with Client Server Architecture. *Journal of Physics: Conf. Series 1260, 022007. doi:10.1088/1742-6596/1260/2/022007*

[6] I.V. Kovalev, P.V. Zelenkov, M.V. Karaseva, M. Yu. Tsarev, R.Yu.Tsarev. (2015).Computer Model of the Reliability Analysis of the Distributed Comptuer Systems with Architecture "Client-Server".*IOP Conf. Series: Materials Science and Engineering 70, 012009 doi:10.1088/1757-899X/70/1/012009.*

[7] Fong, J., & Hui, R. (1999). Application of Middleware in the Three Tier Client/Server Database Design Methodology. *Journal of the Brazilian Computer Society, 6(1), 50-64.*

[8] Sumit Ahlawat and Anshul Anand (2014).An Introduction to Computer Networking. *International Journal of Computer Science and Information Technology Research, Vol. 2, Issue 2, pp 373-377.*

[9] Yunhuai Liu, Qian Zhang, and Lionel M. Ni (2010) Opportunity Based Topology Control in Wireless Sensor Network" *IEEE Transactions on Parallel and Distributed Systems, VOL.21, NO. 3.*

[10] Geon Yoon, Dae Hyun Kwan Soon Chang Kwon, Yong Oon Park,Young Joon Lee (2006) Ring Topology-based Redundancy Ethernet for Industrial Network. *Siceicase International Joint Conference, pp.1404-1407,18-21.*

[11] Nurul Absar., Mohammad Jahangir Alam and Tasnuva Ahmed. (2014).Performance Study of Star Topology in Small Internet Works. *International Journal of Computer Applications, Volume 107 – No 2, 45-53*

[12] Q . A. A. Ruhimat, G .W Fajariyanto, D. M. Firmansyah and Slamin. (2019).Optimal Computer Network Based on Graph Topology Model. *IOP Conf. Series: Journal of HMPhysics: Conf. Series 1211 (2019) 012007 doi:10.1088/1742-6596/1211/1/012007*

[13] Kudeep Nagiya,Mangey Ram and Ayush Kumar Dua.(2017). A Tree Topology Network Environment Analysis Under reliability Approach, *Nonlinear Studies, 24(1), 199-202.*

[14] Nupur Goyal, Mangey Ram and Ayush Kumar Dua (2016)An Approach to Investigating Reliability Indices for Tree Topology Network.*Cybernetics and Systems,47:7,570-584,DOI: 10.1080/01969722.2016.1209378*

[15] Nelsen, R. B., An Introduction to Copulas, 2nd Edition. Springer, New York, 2006.

[16] M.I. Abubakar and V. V. Singh (2019) Performance Assessment of an Industrial System (African Textile Manufacturers, LTD). Through Copula Approach. *Journal of Operations Research and Decisions. No. 4. Doi:*

10.37190/ord190401

[17] Kabiru H. Ibrahim, V.V. Singh and Abulkareem Lado (2017).Reliability Asssessment of Complex System Consisting Two Subsystems Connected in Series Configuration Using Gumbel-Hougaard Family Copula Distribution. *Journal of Applied Mathematics and Bioinformatics, Vol.7, no.2, 1-27.*

[18] Ibrahim Yusuf, Abdulkareem Lado Ismail, V. V. Singh, U. A. Ali and Nasir Ahmad Sufi. (2020). Performance Analysis of Multi-Computer System Consisting of Three Subsystems in Series Confguration Using Copula Repair Policy. *SN Computer Science (2020) 1:241.* *https://doi.org/10.1007/s42979-020-00258-0*

[19] Muhammad Salihu Isa, U.A.Ali, Bashir Yusuf and Ibrahim Yusuf (2020) cost benefit analysis of tree different series parallel dynamo configurations. Life Cycle Reliability and Safety Engineering (2020) 9:413-423.*https://doi.org/10.1007/s41872-020-00141-0*

[20] Pratap Kumar, Kabiru H. Ibrahim, M.I. Abubakar and V.V. Singh (2020) Probabilistic Assessment of Complex System with Two Subsystems in Series Arrangement With Multi-Types   Failure and Two Types of Repair Using Copula. *Strategic System Assurance and Business Analytics,* *tttps://doi.org/10.1007/978-981-15-3647-2-2*

[21] Yusuf Ibrahim, Sunusi Abdullahi, Ismail Abdulkareem Lado, muhaammmad Salihu Isa, K. Suleiman, Bala Shehu and Ali U.a (2020) performance analysis of multi computer system consisting of active parallel homogeneous. *Annals of optimization Theory and Practice, volume1,no1.pp1-8.* *DOI:10.22121/aotp.2020.239383.1032.*

D. Raghav, D.K. Rawal, I. Yusuf, R. H. Kankarofi, V.V. Singh
RELIABILITY PREDICTION OF DISTRIBUTED SYSTEM WITH
HOMOGENEITY IN SOFTWARE AND SERVER…

RT&A, No 1 (61)
Volume 16, March 2021

Reliability Prediction of Distributed System with Homogeneity in Software and Server using Joint Probability Distribution via Copula Approach

Dhruv Raghav [1], D.K. Rawal [2], Ibrahim Yusuf [3],
Rabiu Hamisu Kankarofi [4], V.V. Singh [5]
•
(1) Department of Computer Science ITS Engg. College,
Greater Noida, India; (2) Department of Mathematics, HIMT Greater Noida,
Uttar Pradesh, India; (3) Department of Mathematical Sciences, Bayero University
Kano Nigeria; (4 & 5) Department of Mathematics, Yusuf maitama Sule
University Kano Nigeria
Email: dhruvragha287@gmail.com [1], diliprawal15@gmail.com [2],
iyusuf.mth@buk.edu.ng [3], rkankarofi@yahoo.com [4], singh_vijayvir@yahoo.com [5]

Abstract

The present paper intends to design and development reliability models for the analysis of distributed hardware-software system. For the determination of reliability and system performance, the study analyzed a distributed system consisting of a single host with two heterogeneous software running on the host and two identical servers configured as series-parallel system. Both client (host), software and server's failure time are to be exponentially distributed while repairs follow two forms of distributions that are general and Gumbel-Hougaard family copula. The system is analyzed using supplementary variable technique with implications of Laplace transforms. The results are presented in tables and graphs. Some important measures of reliability such as availability of system, reliability of the system, MTTF and cost analysis have been discussed. Some particular cases have also been derived and examined to see the practical effect of the model.

Keywords: Distributed System, Clients, Availability, Software, MTTF, Cost Analysis

1 Introduction

Many commercial systems like, military systems, aircraft systems, institutions and industrial setting, are composed of a number of communicating devices that allows distribution, exchange and dissemination of information to various parts, units, sections or department. These are coined as distributed systems, with components running on different processors or in different processes. A distributed system is system consisting of hardware and software devices configured as network. Distributed system is a collection of computers in which each client in the cluster can assist in the execution of various functions. The devices that constitute distributed system are linked through a computer network and distribution middleware. These devices assist the system in providing powerful services, guarantees of performance, fault tolerance, and security. Each distributed system has programs running on many different computers connected via a network, have become very complicated and very difficult to get right. Reliability can be seen as the ability of a system to perform its intended function under stipulated conditions for a specified period of time. To improve distributed system reliability, many researchers have proposed different types of studies/mathematical models and proclaimed better

D. Raghav, D.K. Rawal, I. Yusuf, R. H. Kankarofi, V.V. Singh
RELIABILITY PREDICTION OF DISTRIBUTED SYSTEM WITH
HOMOGENEITY IN SOFTWARE AND SERVER…

RT&A, No 1 (61)
Volume 16, March 2021

performance by their operations. For instance, Wu (2014) discussed the modelling of distributed files systems for practical performance. Vijayalakshmi (2015) analyzed the dependability of homogeneous distributed software hardware systems. Olabiyisi et al. (2011) presented a survey on performance evaluation models for distributed system architecture. Dhulavvagol et al. (2020) discussed the performance analysis of distributed processing system using shard selection techniques on elastic search. Joarder et al. (2016) discussed the incremental repartitioning of shared-nothing distributed databases for scalable OLTP applications. Munoz-Escoi and Juan-Marin (2018) dealt with synchrony in dynamic distributed systems. Ahmed and Wu (2013) presented a survey on reliability of distributed system. Sari and Akkaya (2015) studied fault tolerance mechanism in distributed systems. Mishra and Tripathi (2014) discussed some problems, challenges and issues of distributed software system. Kovalev et al. (2015) presented model on reliability analysis of distributed computer system with architecture client-server.

Inherent in the establishment of reliability requirements in the need to estimate or predict reliability in advance of manufacturing the product. This prediction is a continuing process which takes place at several stages of progression from design through usage. The prediction of system performances is based on system architecture, components arrangements, system configuration, operative environment, ability of handler, regular repair with appropriate repair policies and uses of protection devices to minimize failure effects. Many researchers designed the various types of systems and evaluate their performances employing different types of failure possibilities and maintenance policies. To cite some, them Singh et al. (2010) studied reliability measures for a system which consisting three units at super priority, priority and ordinary unit under preemptive resume repair policy employing supplementary variable approach. Singh et al. (2013) evaluated reliability measures Availability, MTTF and cost benefit analysis for a system consisting two subsystems with controllers in series configuration under k-out-of-n: G/ policy using supplementary variable and copula approach. and A. Kumar and M. Ram (2015) studied reliability measures including sensitivity analysis of a coal handling unit for thermal power plant which consisting two subsystems in series configuration using supplementary variable techniques. M. A, El-Damcese et al (2016) studied reliability and sensitivity analysis of a k-out-of-n: G, warm standby parallel repairable system with replacement at common cause failure using Markov model by taking three different case for analytical results computations A, Kuldeep Nagiya et al. (2017) studied a tree topology network environmental analysis under reliability approach using Markov process and supplementary variable which convert Morkov process to non Morkov process. Ram Niwas and Harish Garg, (2017) analyzed reliability metric including profit function of an industrial system grounded on cost free warranty scheme.

The redundancy improves the system performance of the repairable systems. A frequently used type of redundancy is (k-out-of-n, k ≤ n) system introduces by Birnbaum et al. (1961). A (k-out-of-n:G) which is equivalent to (k+1-out-of-n:F) have analyzed by many researchers which has applied in most of all the systems including industrial, networking systems, mechanical systems, manufacturing systems power plants and transmission and communication systems. Researchers, Rawal et al (2013), Jyoti Gulati et al (2016), Monika Gahlot et al. (2018) have analyzed the performances of the (k-out-of-n:G/F) types of repairable systems by taking different types of failures and two types of repair using copula linguistic approach and concluded that copula repair policy is better over general repair policy. Abdul, K, Lado and Singh (2019) have analyzed a system comprising two subsystems in series configuration with different types of failures and copula repair approach. Afshin Yaghoubi et al (2020) deliberated a closed form of steady state availability of cold standby repairable k-out-of-n: G system using Markov method.

In the architecture of a distributive network system we observed the three subsystems connected in series arrangement namely Clients, Software and Servers. In this model we have consider clients as subsystem 1, Software's subsystem 2 and servers as the subsystem 3. The table 1 presents the states status of the model. In the present study subsystem 1 consists two software, subsystem 2 consists of a client while subsystem 3 comprises of two servers. System failure can occur due the failure of client or the two servers or two software.

D. Raghav, D.K. Rawal, I. Yusuf, R. H. Kankarofi, V.V. Singh
RELIABILITY PREDICTION OF DISTRIBUTED SYSTEM WITH
HOMOGENEITY IN SOFTWARE AND SERVER…

RT&A, No 1 (61)
Volume 16, March 2021
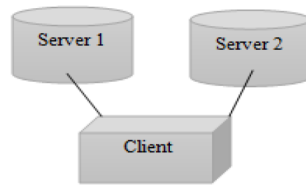
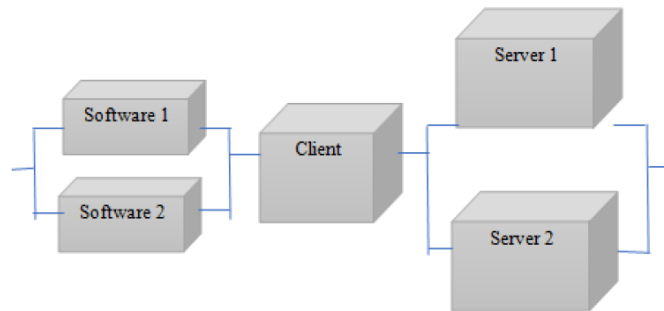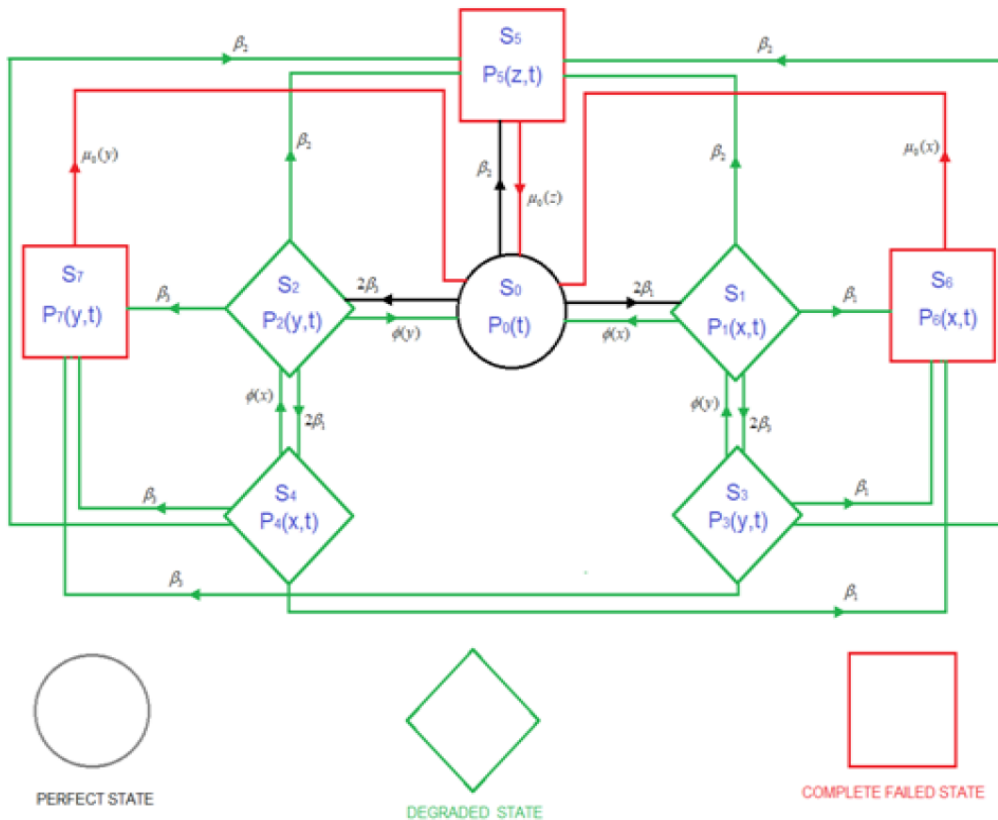Figure 1: Proposed system

$\longrightarrow$ Replicated data

$\longrightarrow$ User traffic

Figure 2: Reliability block diagram of the proposed system

State Structure diagram and State description Table

D. Raghav, D.K. Rawal, I. Yusuf, R. H. Kankarofi, V.V. Singh
RELIABILITY PREDICTION OF DISTRIBUTED SYSTEM WITH
HOMOGENEITY IN SOFTWARE AND SERVER…

RT&A, No 1 (61)
Volume 16, March 2021

State Structure diagram of the Model

Table 1: States of the system table.

State	Subsystem 1	Subsystem 2		Subsystem 3		
	Client	Software 1	Software 2	Server 1	Server 2	System status
S_0	Functional	Functional	Functional	Functional	Functional	Operative
S_1	Functional	Functional	Functional	Failed	Functional	Operative
S_2	Functional	Functional	Failed	Functional	Functional	Operative
S_3	Functional	Failed	Functional	Failed	Functional	Operative
S_4	Functional	Functional	Failed	Functional	Functional	Operative
S_5	Failed	Idle	Idle	Idle	Idle	Down
S_6	Idle	Idle	Idle	Failed	Failed	Down
S_7	Idle	Failed	Failed	Idle	Idle	Down

2 Notations, Assumptions

3.1 Notations

- t: Time variable on a time scale.
- s: Laplace transform variable for all expressions.

- $\beta1/\beta2/\beta3$: Failure rate of Server/ Client /Software.

- $\phi(x)\phi(y)$: Repair rate of Server/ Software

- $\mu_0(x)/\mu_0(y)/\mu_0(z)$:Repair rates for complete failed states of Server/ Client /Software

- $p_i(t)$: The probability that the system is in Si state at instants for =0 to 10

- $\overline{P}(s)$: Laplace transformation of state transition probability

- $P_i(x,t)$: The probability that a system is in state Si for i=1 . . . , the system under repair and elapse repair time is (x, t) with repair variable x and time variable t.

- $P_i(y,t)$: The probability that a system is in state Si for i=1. . . , the system under repair and elapse repair time is (y, t) with repair variable y and time variable t.
- P_i (z, t): The probability that a system is in state Si for i=1. . . , the system under repair and elapse repair time is (z, t) with repair variable z and time variable t.

- $E_p(t)$: Expected profit during the time interval [0, t)
- K_1, K_2: Revenue and service cost per unit time, respectively.
- $\mu_0(x)$: The expression of joint probability (failed state S_i to good state S_0) according to Gumbel-Hougaard family copula definition

$$\mu(x) = c_\theta(u_1, u_2(x)) = exp(x^\theta + \{log\phi(x)^\theta\}^{\frac{1}{\theta}})1 \le \theta \le \infty$$

3.2 Assumption: The undermentioned assumptions are dealt for study of the model.

1. In the initial stage system is good working state with all components
2. The Client is using two similar software's.
3. Both Software's are identical to each other and independent to each other.

D. Raghav, D.K. Rawal, I. Yusuf, R. H. Kankarofi, V.V. Singh
RELIABILITY PREDICTION OF DISTRIBUTED SYSTEM WITH
HOMOGENEITY IN SOFTWARE AND SERVER…

RT&A, No 1 (61)
Volume 16, March 2021

    4. Servers are identical and independent to each other in working context.

    5. Each software failed independent of the other.

    6. Each server failed independent of the other

    7. Servers works simultaneously and independently.

    8. In the degraded mode with minor failure general repair is employed to maintained of servers and software's and clients.

    9. The complete failed state in the system are maintained using copula repair distribution especially Gumbel Hougaard copula distribution.

    10. It assumed that during repair not part of system breakdown/ damage.

Table 1: States of the system

3 Formulation of Mathematical Model

By probability of considerations and continuity arguments, we can obtain the following set of difference differential equations governing the present mathematical model.

$$\left[\frac{\partial}{\partial t} + 2\beta_1 + \beta_2 + 2\beta_3\right]P_0(t) = \int_0^\infty \phi(x)P_1(x,t)dx + \int_0^\infty \phi(y)P_2(y,t)dy$$
$$+ \int_0^\infty \mu_0(y)P_7(y,t)dy + \int_0^\infty \mu_0(x)P_6(x,t)dx + \int_0^\infty \mu_0(z)P_5(z,t)dz$$
(1)

$$\left[\frac{\partial}{\partial t} + \frac{\partial}{\partial x} + \beta_1 + 2\beta_3 + \beta_2 + \phi(x)\right]P_1(x,t) = 0$$
(2)

$$\left[\frac{\partial}{\partial t} + \frac{\partial}{\partial y} + 2\beta_1 + \beta_2 + \beta_3 + \phi(y)\right]P_2(y,t) = 0$$
(3)

$$\left[\frac{\partial}{\partial t} + \frac{\partial}{\partial y} + \beta_1 + \beta_2 + \beta_3 + \phi(y)\right]P_3(y,t) = 0$$
(4)

$$\left[\frac{\partial}{\partial t} + \frac{\partial}{\partial x} + \beta_1 + \beta_2 + \beta_3 + \phi(x)\right]P_4(x,t) = 0$$
(5)

$$\left[\frac{\partial}{\partial t} + \frac{\partial}{\partial z} + \mu(z)\right]P_5(z,t) = 0$$
(6)

$$\left[\frac{\partial}{\partial t} + \frac{\partial}{\partial x} + \mu(x)\right]P_6(x,t) = 0$$
(7)

$$\left[\frac{\partial}{\partial t} + \frac{\partial}{\partial y} + \mu(y)\right]P_7(y,t) = 0$$
(8)

Boundary Conditions: During the operational mode the repair facility is not available than the relation of two consecutive state transition probabilities can be obtain with help of boundary conditions. i.e. $p_{i+1}(0,t) = \sum_i \lambda_i p_i(0,t)$ where j represents the any state. From state transition diagram one can easily have the following relations;

$$p_1(0,t) = 2\beta_1 p_0(t), p_2(0,t) = 2\beta_3 p_0(t), p_3(0,t) = \beta_1\beta_3 p_0(t),$$
$$p_4(0,t) = 4\beta_1\beta_3 p_0(t), p_5(0,t) = \beta_2[1 + 2\beta_1 + 2\beta_3 + 8\beta_1\beta\beta_3]p_0(t),$$
$$p_6(0,t) = \beta_1[2\beta_1 + 8\beta\beta_1\beta_3]p_0(t), p_7(0,t) = \beta_3[2\beta_3 + 8\beta\beta_1\beta_3]p_0(t)$$
(9)

Initials Conditions

$$p_0(0) = 1 and other state probabilities are zero at t = 0$$
(10)

D. Raghav, D.K. Rawal, I. Yusuf, R. H. Kankarofi, V.V. Singh
RELIABILITY PREDICTION OF DISTRIBUTED SYSTEM WITH
HOMOGENEITY IN SOFTWARE AND SERVER…

RT&A, No 1 (61)
Volume 16, March 2021

4 Solution of the Model

Taking Laplace transformation of equations (1)-(9) and using equation (10), we obtain.

$$[s + 2\beta_1 + \beta_2 + 2\beta_3]\overline{P_0}(s) = \int_0^\infty \phi_1(x)\overline{p_1}(x,s)dx + \int_0^\infty \phi_1(y)\overline{p_2}(y,s)dy +$$
$$\int_0^\infty \mu_0(z)\overline{p_5}(z,s)dz + \int_0^\infty \mu_0(y)\overline{p_7}(y,s)dy + \int_0^\infty \mu_0(x)\overline{p_6}(x,s)dx \tag{11}$$

$$\left[s + \frac{\partial}{\partial x} + \beta_1 + 2\beta_3 + \beta_2 + \phi(x)\right]\overline{p_1}(x,s) = 0 \tag{12}$$

$$\left[s + \frac{\partial}{\partial y} + \beta_2 + 2\beta_1 + \beta_3 + \phi(y)\right]\overline{p_2}(y,s) = 0 \tag{13}$$

$$\left[s + \frac{\partial}{\partial y} + \beta_1 + \beta_2 + \beta_3 + \phi(y)\right]\overline{p_3}(y,s) = 0 \tag{14}$$

$$\left[s + \frac{\partial}{\partial x} + \beta_1 + \beta_2 + \beta_3 + \phi(x)\right]\overline{p_4}(x,s) = 0 \tag{15}$$

$$\left[s + \frac{\partial}{\partial z} + \mu_0(z)\right]\overline{p_5}(z,s) = 0 \tag{16}$$

$$\left[s + \frac{\partial}{\partial x} + \mu_0(x)\right]\overline{p_6}(x,s) = 0 \tag{17}$$

$$\left[s + \frac{\partial}{\partial y} + \mu_0(y)\right]\overline{p_7}(y,s) = 0 \tag{18}$$

$$\overline{p_1}(0,s) = 2\beta_1\overline{P_0}(s), \overline{p_2}(0,s) = 2\beta_3\overline{P_0}(s), \overline{p_4}(0,s) = 4\beta_1\beta_3\overline{P_0}(s),$$
$$\overline{P_5}(0,s) = \beta_2[1 + 2\beta_1 + 2\beta_3 + 8\beta_1\beta_3]\overline{P_0}(s), \tag{19}$$
$$\overline{P_6}(0,s) = \beta_1[2\beta_1 + 8\beta_1\beta_3]\overline{P_0}(s), \overline{P_7}(0,s) = \beta_3[2\beta_3 + 8\beta_1\beta_3]\overline{P_0}(s)$$

Solving (11)-(18) with the help of (19) one may get

$$\overline{P_0}(s) = \frac{1}{D(s)} \tag{20}$$

$$\overline{P_1}(s) = \frac{2\beta_2}{D(s)} \frac{(1 - S_\phi(s + \beta_1 + 2\beta_3 + \beta_2)}{(s + \beta_1 + 2\beta_3 + \beta_2)} \tag{21}$$

$$\overline{P_2}(s) = \frac{2\beta_3}{D(s)} \frac{(1 - S_\phi(s + 2\beta_1 + \beta_2 + \beta_3)}{(s + 2\beta_1 + \beta_2 + \beta_3)} \tag{22}$$

$$\overline{P_3}(s) = \frac{4\beta_1\beta_3}{D(s)} \frac{(1 - S_\phi(s + \beta_1 + \beta_2 + \beta_3)}{(s + \beta_1 + \beta_2 + \beta_3)} \tag{23}$$

$$\overline{P_4}(s) = \frac{4\beta_1\beta_3}{D(s)} \frac{(1 - S_\phi(s + \beta_1 + \beta_2 + \beta_3)}{(s + \beta_1 + \beta_2 + \beta_3)} \tag{24}$$

$$\overline{P_5}(s) = \frac{\beta_2[1 + 2\beta_1 + 2\beta_3 + 8\beta_1\beta_3]}{D(s)} \frac{(1 - S_{\mu_0}(s))}{s} \tag{25}$$

$$\overline{P_6}(s) = \frac{\beta_1[2\beta_1 + 8\beta_1\beta_3]}{D(s)} \frac{(1 - S_{\mu_0}(s))}{s} \tag{26}$$

$$\overline{P_7}(s) = \frac{\beta_3[2\beta_3 + 8\beta_1\beta_3]}{D(s)} \frac{(1 - S_{\mu_0}(s))}{s} \tag{27}$$

$$D(s) = s + 2\beta_1 + \beta_2 + 2\beta_3 - \{2\beta_1\overline{S_\phi}(s + \beta_1 + \beta_2 + 2\beta_3)$$
$$+\beta_2(1 + 2\beta_1 + 2\beta_3 + 8\beta_1\beta_3)S_{\mu_0}(s) + 2\beta_3\overline{S_\phi}(s + 2\beta_1 + \beta_2 + \beta_3) +$$
$$\beta_3(2\beta_3 + 8\beta_1\beta_3)S_{\mu_0}(s) + \beta_1(2\beta_1 + 8\beta_1\beta_3)S_{\mu_0}(s)\} \tag{28}$$

D. Raghav, D.K. Rawal, I. Yusuf, R. H. Kankarofi, V.V. Singh
RELIABILITY PREDICTION OF DISTRIBUTED SYSTEM WITH
HOMOGENEITY IN SOFTWARE AND SERVER…

RT&A, No 1 (61)
Volume 16, March 2021

The Laplace transformations of the probabilities that the system is in up (i.e. either good or degraded state) and failed state at any time are as follows:

$$\overline{P}_{up}(s) = \overline{P_0}(s)P_1(s) + P_2(s) + P_3(s) + P_4(s)$$

$$= \frac{1}{D(s)} \left[\begin{array}{l} 1 + 2\beta_1 \frac{(1-S_\phi(s+\beta_1+2\beta_3+\beta_2)}{(s+\beta_1+2\beta_3+\beta_2)} + 2\beta_3 \frac{(1-S_\phi(s+2\beta_1+\beta_2+\beta_3)}{(s+2\beta_1+\beta_2+\beta_3)} \\ +4\beta_1\beta_3 \frac{(1-S_\phi(s+\beta_1+\beta_2+\beta_3)}{(s+\beta_1+\beta_2+\beta_3)} + 4\beta_1\beta_3 \frac{(1-S_\phi(s+\beta_1+\beta_2+\beta_3)}{(s+\beta_1+\beta_2+\beta_3)} \end{array} \right] \qquad (29)$$

$$\overline{P}_{failed}(s) = \overline{P_5} + \overline{P_6} + \overline{P_7} \qquad (30)$$

5 Analytical Study of the model

5.1 Availability of the system for copula repair

When repair follows two types of repair i.e., exponential and general distribution. Setting, the repairs,

$$\overline{S}_{exp\left[x^\theta + \{\log\phi(x)\}^\theta\right]^{\frac{1}{\theta}}}(s) = \frac{exp\left[x^\theta + \{\log\phi(x)\}^\theta\right]^{\frac{1}{\theta}}}{s + exp\left[x^\theta + \{\log\phi(x)\}^\theta\right]^{\frac{1}{\theta}}}, \overline{S}_\phi(s) = \frac{\phi}{s+\phi}$$

in equation (29) and fixing the values of failure rates as,

$, (\beta_1 = 0.04, \beta_2 = 0.04, \beta_3 = 0.04), (\beta_1 = 0.05, \beta_2 = 0.05, \beta_3 = 0.05), (\beta_1 = 0.06, \beta_2 = 0.06, \beta_3 = 0.06), (\beta_1 = 0.07, \beta_2 = 0.07, \beta_3 = 0.07)$ and $\phi = 1, \theta = 1, x = 1$, then taking inverse Laplace transform, one can obtain, the expressions (a, b, c, d) respectively;

- $P_{up}(t) = 0.02105544525e^{(-2777881421t)} - 0.01014421182e^{(-1.293633161t)} + 1.005687563e^{(-0.006785417978t)} - 0.01659879629e^{(-1.120000000t)}$

- $P_{up}(t) = 0.02834810927e^{(-2.800124701t)} - 0.01787925501e^{(-1.359319656t)} + 1.010420311e^{(-0.008855643005t)} - 0.02088916502e^{(-1.150000000t)}$

- $P_{up}(t) = -0.02520769946e^{(-1.180000000t)} + 0.03636839750e^{(-2.825889314t)} - 0.02675858604e^{(-1.421952360t)} + 1.015597888e^{(-0.01045832627t)}$

- $P_{up}(t) = 0.04499933873e^{(-2.855437178t)} - 0.3642027421e^{(-1.481497573t)} + 1.020957837e^{(-0.01136524989t)} - 0.02953980143e^{(-1.210000000t)}$

For, t= 0, 10, 20, 30, 40, 50, 60, 70, 80, 90.. units of time, one may get different values of $P_{up}(t)$ as shown in Table1.

Table 2: Table 1. Availability variation for copula repair

Time(t)	Availability (a) β_j=0.04, j=1, 2,3	Availability (b) β_j=0.05, j=1, 2,3	Availability (c) β_j=0.06, j=1, 2,3	Availability (d) β_j=0.07, j=1, 2,3
0	1.0000	1.0000	1.0000	1.0000
10	0.9397	0.9247	0.9147	0.9112
20	0.8780	0.8464	0.8239	0.8133
30	0.8204	0.7746	0.7420	0.7259
40	0.7666	0.7090	0.6684	0.6479
50	0.7163	0.6489	0.6020	0.5783
60	0.6693	0.5939	0.5422	0.5162
70	0.6254	0.5436	0.4884	0.4607
80	0.5844	0.4975	0.4399	0.4112
90	0.5460	0.4553	0.3962	0.3670
100	0.5102	0.4167	0.3568	0.3276

D. Raghav, D.K. Rawal, I. Yusuf, R. H. Kankarofi, V.V. Singh
RELIABILITY PREDICTION OF DISTRIBUTED SYSTEM WITH
HOMOGENEITY IN SOFTWARE AND SERVER...
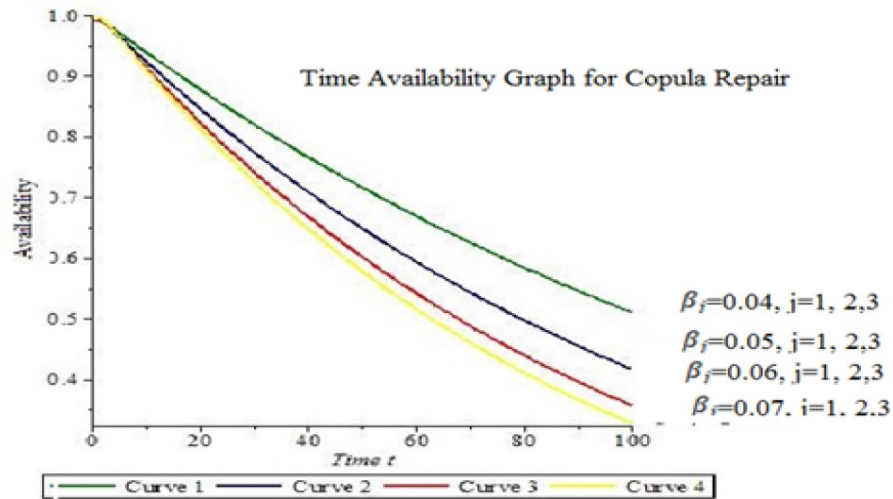
RT&A, No 1 (61)
Volume 16, March 2021

Figure 3: Time v/s. Availability graph for (Copula Repair)

5.2 Availability analysis when the system follows General repair:

If the system follows general repair than the availability of the system can be analyzed by putting $\mu = \Phi$ in equation (61). For the same set of failure rates in Sec (5.1) and taking inverse Laplace transform of resulting expressions one may get availability expressions respect to general repair rates in (a, b, c, d)

- $P_{up}(t) = 0.01149680663e^{(-1.164408188t)} + 0.0120314111e^{(-1.011271752t)} + 0.9853993116e^{(-0002320060097t)} - 10.008927529467e^{(-1.060000000t)}$
- $P_{up}(t) = 0.01347456469e^{(1.326621009t)} + 0.02937122091e^{(-1.026793715t)} + 0.9757788560e^{(-0.006585276132t)} - 0.01862464183e^{(-1.210000000t)}$
- $P_{up}(t) = -0.02918859381e^{(-1..80000000t)} + 0.01027889213e^{(-1.482860719t)} + 0.052669449984e^{(-1.047183349t)} + 0.9662152017e^{(-0.009955931640t)}$
- $P_{up}(t) = 0.004003254503e^{(-1.636498085t)} + 0.08225309992e^{(-1.072910924t)} + 0.9544778674e^{(-0.01059099182t)} - 0.0473422178e^{(-1.240000000t)}$

For different values of the time t from 0, 10. 20, 30, . . . ,100 in interval [0,100] one can obtain the table 2.

Table 3: Table 2. Availability variation for general repair

Time(t)	Availability (a) $\beta_j=0.04$, j=1, 2,3	Availability (b) $\beta_j=0.05$, j=1, 2,3	Availability (c) $\beta_j=0.06$, j=1, 2,3	Availability (d) $\beta_j=0.07$, j=1, 2,3
0	1.0000	1.0000	1.0000	1.0000
10	0.9628	0.9135	0.8746	0.8585
20	0.9407	0.8553	0.7917	0.7722
30	0.9191	0.8008	0.7167	0.6946
40	0.8980	0.7498	0.6488	0.6248
50	0.8774	0.7020	0.5873	0.5620
60	0.8573	0.6572	0.5316	0.5055
70	0.8376	0.6153	0.4812	0.4547
80	0.8184	0.5761	0.4356	0.4090
90	0.7997	0.5394	0.3943	0.3679
100	0.7813	0.5050	0.3570	0.3309

D. Raghav, D.K. Rawal, I. Yusuf, R. H. Kankarofi, V.V. Singh
RELIABILITY PREDICTION OF DISTRIBUTED SYSTEM WITH
HOMOGENEITY IN SOFTWARE AND SERVER…
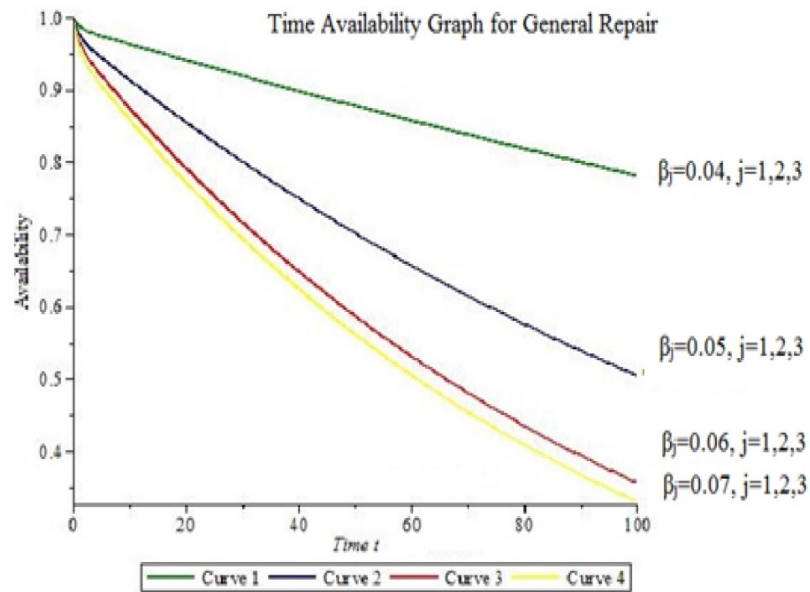
RT&A, No 1 (61)
Volume 16, March 2021

Figure 4: Availability for General Repair

Reliability Analysis:

The system performance of a non-repairable system is known as reliability. Therefor treating all repair of the system to zero in (29) and the inverse Laplace transform of resulting expression give us reliability of system. For the same set of parametric values as in section (7.1) one can obtain the expression (a, b, c, d) as under.

- $R_1(t) = 2.120000000e^{(0.200000000t)} + 2.080000000e^{(1.160000000t)} + 1.040000000e^{(0.1200000000t)}$
- $R_2(t) = -2.150000000e^{(-0.2500000000t)} + 2.100000000e^{(0.2000000000t)} + 1.050000000e^{(-0.1500000000t)}$
- $R_3(t) = 2.120000000e^{(-0.2400000000t)} + 1.060000000e^{(-0.1800000000t)} - 2.180000000e^{(-0.3000000000t)}$
- $R_4() = 1.070000000e^{(-0.21000000000t)} + 2.140000000e^{(-0.2800000000t)} - 2.210000000e^{(-0.3500000000t)}$

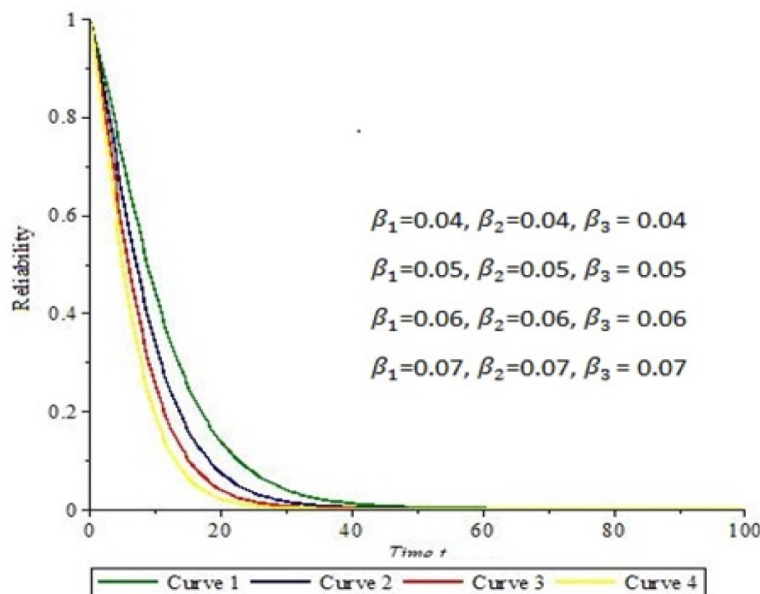The graphical presentation of reliability R(t) variation is shown in figure 5.

Figure 5: Time v/s Reliability Graph for set of values $(\beta1, \beta2, \& \beta3)$

D. Raghav, D.K. Rawal, I. Yusuf, R. H. Kankarofi, V.V. Singh
RELIABILITY PREDICTION OF DISTRIBUTED SYSTEM WITH
HOMOGENEITY IN SOFTWARE AND SERVER…

RT&A, No 1 (61)
Volume 16, March 2021

5.3 Mean Time to Failure (MTTF)

The MTTF is a very important measure of system performance which control failure effect on the system. It deals which unit is more important to get best performance of the system. Mathematically this can be obtained by setting, all repair to zero in equation (29) and then $\lim_{s \to 0} \overline{P}_{up}(s)$ we get expression of MTTF of the system as:

$$MTTF = \lim_{s \to 0} \overline{P}_{up}(s) = \frac{1}{2\beta_1+\beta_2+\beta_3}\left[1 + \frac{2\beta_1}{\beta_1+\beta_2+2\beta_3} + \frac{2\beta_3}{2\beta_1+\beta_2+\beta_3} + \frac{8\beta_1\beta_1}{\beta_1+\beta_2+\beta_3}\right] \qquad (31)$$

Setting, $\beta_2 = 0.04\beta_3 = 0.04$ and varying β_1 as 0.01, 0.02, 0.03, 0.04, 0.05, 0.06, 0.07, 0.08, 0.09 in (31) one may obtain MTTF of the system. Table 2 whose column 2 demonstrates variation of MTTF. with respect to β_1 .

Setting $\beta_1 = 0.04\beta_3 = 0.04$ and varying β_2 as 0.01, 0.02, 0.03, 0.04, 0.05, 0.06, 0.07, 0.08, 0.09 in (31) one may obtain MTTF of the system. Table 2 whose column 3 reveals variation of MTTF. with respect to β_2 .

Setting $\beta_1 = 0.04\beta_2 = 0.04$, and varying β_3 as 0.01, 0.02, 0.03, 0.04, 0.05, 0.06, 0.07, 0.08, 0.09 in (31) one may obtain MTTF of the system. Table 2 whose column 4 establishes variation of MTTF. with respect to β_3 .

Table 4: Table 3.Variation of MTTF with failure rates

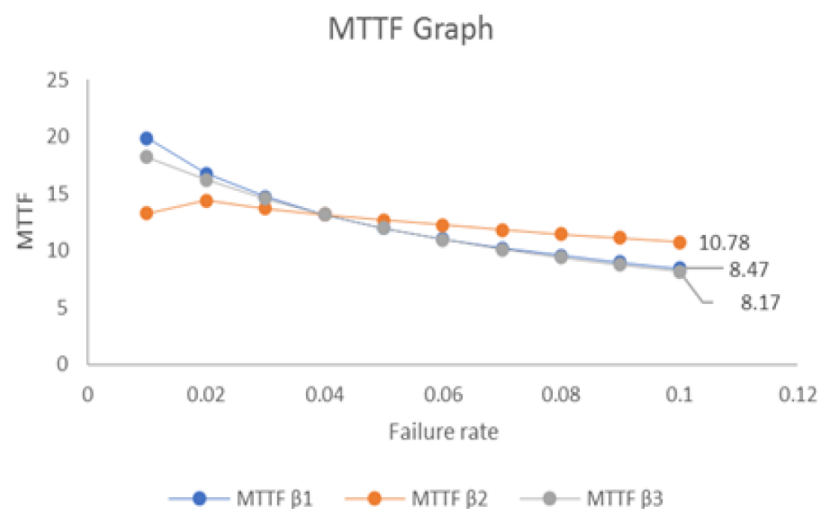| Variation in failure rate	MTTF β_1	MTTF β_2	MTTF β_1
0.01	19.89	13.30	18.25
0.02	16.80	14.40	16.22
0.03	14.71	13.72	14.56
0.04	13.17	13.17	13.17
0.05	11.98	12.68	12.00
0.06	11.02	12.24	11.00
0.07	10.23	11.84	10.14
0.08	9.56	11.47	9.40
0.09	8.98	11.15	8.75
0.01	8.47	10.78	8.17

Figure 6: Failure Rate vs. M.T.T.F.

5.4 Cost Analysis

Cost analysis when the repair follow Gumbel Hougaard family Copula distribution

Let the failure and rates of system be, β_1=0.04, β_2=0.04, β_3= 0.04, ϕ = 1, θ = 1, x = 1, and the service

D. Raghav, D.K. Rawal, I. Yusuf, R. H. Kankarofi, V.V. Singh
RELIABILITY PREDICTION OF DISTRIBUTED SYSTEM WITH
HOMOGENEITY IN SOFTWARE AND SERVER…

RT&A, No 1 (61)
Volume 16, March 2021

facility be always available, then expected profit during the interval [0, t) can be given as the formula,

$$E_p(t) = K_1 \int_0^t P_{up}(t)dt - K_2 t$$

Where K_1 and K_2 are revenue service cost per unit time. Hence the expected profit by the operation of the system for time in interval [0, t) when the system repair follow copula repair is given as;

$$E_p(t) = K_1(-0.007579677e^{-2.77788142t}) + (-0.007841644e^{-1.2936331t}$$
$$-148.213060e^{-.0067854179t} + 0.014820535e^{-1.12000000t} + 148.20) - K_2 t \tag{32}$$

Setting K_1 = 1and K_2 = 0.6, 0.5, 0.4, 0.3, and 0.2 respectively and varying t =0, 10, 20, 30, 40, 50, 60, 70, 80, 90,100 units of time one get Table.

Table 5: Expected profit computation with time variation

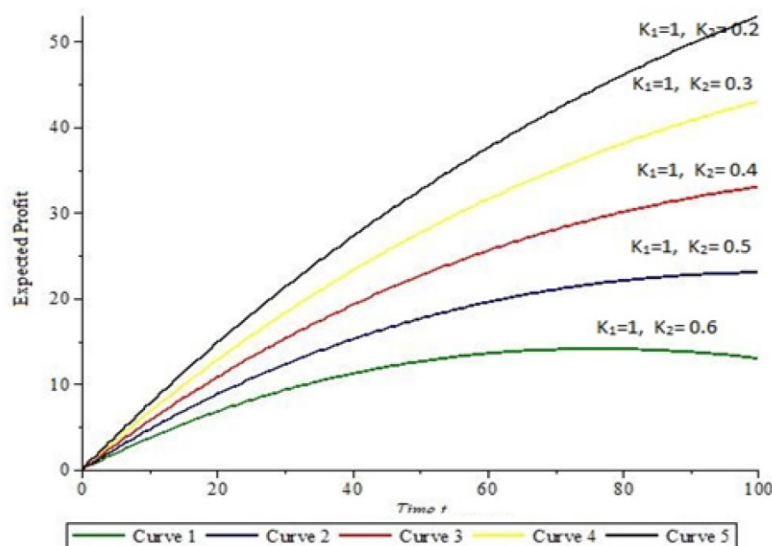| Time t	K_2=0.6	K_2=0.5	K_2=0.4	K_2=0.3	K_2=0.2
0	0	0	0	0	0
10	3.71	4.71	5.71	6.71	7.71
20	6.80	8.80	10.80	12.80	14.80
30	9.30	12.28	15.28	18.28	21.28
40	11.22	15.22	19.22	23.22	27.22
50	12.63	17.63	22.63	27.63	32.63
60	13.56	19.56	26.56	31.56	37.56
70	14.03	21.03	28.03	35.03	40.03
80	14.07	22.07	30.07	38.07	26.07
90	13.72	22.72	31.72	40.72	49.72
100	13.00	23.00	33.00	43.00	53.00

Figure 7: Time vs. Expected Profit

Cost analysis for General Repair: When the repair only follow general repair than expected profit in interval [0,t) can be given by taking $\mu_0 = \theta$. For the same values of failure rates as in copula repair we obtained the expected profit as;

$$E_p(t) = K_1(-0.0101570566e^{-1.3266210t} - 0.0286047923e^{-1.026793715t}$$
$$-148.1758451e^{-0.0065852769t} + 0.0166291445e^{-1.12000000t} + 148.20) - K_2(t) \tag{33}$$

SettingK_1 = 1 and K_2 = 0.6, 0.5, 0.4, 0.3, and 0.2 respectively and varying t =0, 10, 20, 30, 40, 50, 60, 70, 80, 90,100 units of time one get Table.

Table 6: Table 5: Expected profit computation with time variation

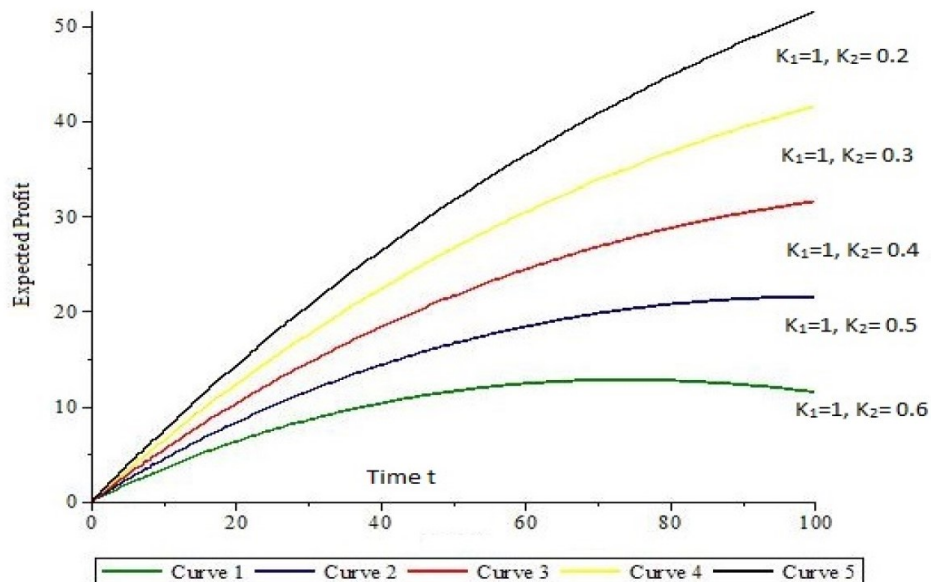| Time t	$K_2=0.6$	$K_2=0.5$	$K_2=0.4$	$K_2=0.3$	$K_2=0.2$
0	0	0	0	0	0
10	3.47	4.47	5.47	6.47	7.47
20	6.31	8.31	10.31	12.31	14.31
30	8.59	11.59	14.59	17.58	20.59
40	10.34	14.34	18.34	22.34	26.34
50	11.59	16.59	21.59	26.59	31.59
60	12.39	18.39	24.39	3039	36.39
70	12.75	19.75	26.75	33.75	40.74
80	12.71	20.71	28.71	36.71	44.71
90	12.28	21.28	30.28	39.28	48.28
100	11.50	21.50	31.50	41.50	51.50

Figure 8: Expected profit as function of time t

6 Result Interpretation and Conclusion

In this paper we have analyzed the system performance based of different types of failures in the associated elements of distributed system via two types of repair employing copula repair approach and general repair. Table1 and Fig.1 provides information availability variation with respect of time. The figure 1 explain that when the failure rates increases than availability deceases. Availability when the failure rates are fixed at $\beta_1 = \beta_2 = \beta_3 = 0.04$, then availability is higher than the values of failure rates $\beta_1 = \beta_2 = \beta_3 = 0.07$. Table 2 and the corresponding Figure 2 presents the availability of system when the repair follows general distribution. By comparing the results from table1 and table 2 we conclude that availability of the system is better when the repair follows copula distribution.

Figure3 presents variation of reliability as non-repairable system. The reliability of system decreases when the failure rates of the subsystems increases. From the Reliability graph it is clear that rate of decrement in reliability values is much high than availability values. One can understand need of regular repair for repairable system to achieving excellent performance. The Figure 4 yields the mean-time-to-failure (MTTF) of the system with respect to variation in failure rates $\beta_1, \beta_2 and \beta_3$ respectively.

D. Raghav, D.K. Rawal, I. Yusuf, R. H. Kankarofi, V.V. Singh
RELIABILITY PREDICTION OF DISTRIBUTED SYSTEM WITH
HOMOGENEITY IN SOFTWARE AND SERVER…

RT&A, No 1 (61)
Volume 16, March 2021

When revenue cost per unit time K_1 is fixed at 1, service costs K_2 = 0.6, 0.5. 0.4. 0.3 and 0.2 the Tables 4 & 5, Figures 5 & 6 presents expected profit incurred by operation of the system. The incurred profit is high when the system repair follows copula distribution. In the both cases it can perceive that as service cost decrease profit increases. Therefor one can conclude that copula repair must be recommended over general repair.

References

1. A. Kumar, M. Ram, (2013), Reliability measures improvement and sensitivity analysis of a Coal Handling unit for Thermal power plant, International Journal of Engineering, Vol 26(9), pp. 1059-1066.
2. Abdul Kareem Lado, V. V. Singh (2019). Cost Assessment of complex repairable system consisting two subsystems in Series configuration using Gumbel Hougaard family copula, International Journal of Quality Reliability and Management, Vol. 36(10), pp1683-1698.
3. Afshin, Yaghoubi, S. T. A Naiki, H. Rostamzadeh, (2020), A close form equation for steady state availability of cold standby repairable k-out-of-n: G system, International Journal of Quality Reliability and Management, Vol 37(1), pp. 145-155.
4. Arif Sari, Murat Akkaya. (2015). Fault Tolerance Mechanisms in distributed systems, Int. J. Communications, Network and System Sciences, 8(12), 471-482.
5. Dhulavvagol, P.M., Bhajantri, V.H and Totad, S.G. (2020). Performance Analysis of Distributed Processing System using Shard Selection Techniques on Elasticsearch, Procedia Computer Science 167, pp. 1626-1635
6. Frances, D. Muñoz-Esco and Rubén de Juan-Marn. (2018). On synchrony in dynamic distributed systems, Open Comput. Sci. Vo. (8), pp.154-164.
7. [7] Joarder Kamal, Manzur Murshed, Rajkumar Buyya, (2016). Workload-aware incremental repartitioning of shared-nothing distributed databases for scalable OLTP applications, Future Generation Computer Systems, Vol. (56), pp 421-435.
8. Jyoti Gulati, V. V. Singh, Dilip Kumar Rawal & C. K. Goel (2016). Performance analysis of complex system in the series configuration under different failure and repair discipline using Gumbel-Hougaard family Copula, International Journal of Reliability, Quality, and Safety Engineering. Vol. 23(2), pp. 1- 21.
9. Kamal Sheel Mishra, Anil Kumar Tripathi. (2014). Some Issues, Challenges and Problems of Distributed Software System, International Journal of Computer Science and Information Technologies, 5 (4), pp. 4922-4925
10. Kovalev, P.V. Zelenkov, M.V. Karaseva, M.Yu. Tsarev, and R.Yu. Tsarev, (2015). Model of the reliability analysis of the distributed Computer systems with architecture, client-server, materials Science and Engineering, Vol. 70(1), pp. 1-10.
11. Kuldeep Nagiya, M. Ram, A. K Dua, (2017). A tree topology network environment analysis under reliability approach, Nonlinear Studies, Vol 24(1), pp. 193-202.
12. M. A. El- Damcese N. H. El Sadany, (2016). Reliability and Sensitivity analysis of the k-out-of-n:G Warm standby parallel repairable system with Replacement at common cause failure using Markov model, Journal of Statistics & Probability, Vol 5 (3), pp. 521-535.
13. Monika Gahlot, V. V. Singh, H. Ismail Ayagi & C.K. Goel (2018). Performance assessment of repairable system in series configuration under different types of failure and repair policies using Copula Linguisticsвђќ, International Journal of Reliability and Safety. Vol.12(4) pp.348-374.
14. Nelsen, R. B. (2006). An Introduction to Copulas (2nd edn.) (*New York, Springer*).
15. Niwas, R. and Garg, H. (2018). An approach for analyzing the reliability and profit of an industrial system based on the cost-free warranty policy, Journal of the Brazilian Society of Mechanical Sciences and Engineering, Vol. 40, pp.1-9.
16. Olabiyisi S.O, Omidiora E.O, Uzoka F.M.E, Mbarika, V and Akinnuwesi B.A. (2011). A Survey of Performance Evaluation Models for Distributed Software System Architecture, Proceedings of the World Congress on Engineering and Computer Science 2010, Vol (1), WCECS 2010, October 20-22, 2010, San Francisco, USA
17. V. V. Singh, Dilip Kumar Rawal & Mangey Ram (2013). Cost analysis of an engineering system involving subsystems in a series configuration," "IEEE Transactions on Automation Science and Engineering, Vol. 10(4),pp. 1124-1130.
18. V.V. Singh, S.B. Singh, Mangey Ram & C. K. Goel (2010). Availability analysis of system having three unit's super priority, priority and ordinary under primitive resume repair policy, International Journal of Reliability and Applications, Vol11(1), pp. 41-53.

D. Raghav, D.K. Rawal, I. Yusuf, R. H. Kankarofi, V.V. Singh
RELIABILITY PREDICTION OF DISTRIBUTED SYSTEM WITH
HOMOGENEITY IN SOFTWARE AND SERVER…

RT&A, No 1 (61)
Volume 16, March 2021

19. Vijayalakshmi, G. (2015). Dependability analysis of homogeneous distributed software hardware systems, International Journal of Reliability, Quality and Safety Engineering, 22(2), 1-19.

20. Waseem Ahmed, Yong Wei Wu. (2013). A survey on reliability in distributed systems, Journal of Computer and System Sciences Vol. 79, pp. 1243-1255.

21. Wu, Y. (2014). Modeling of Distributed File Systems for Practical Performance Analysis, IEEE Transactions on parallel and distributed systems, Vol. 25 (1), pp. 156-166.

A Copula Approach of Reliability Analysis for Hybrid Systems

Naijun Sha

•

University of Texas at El Paso

nsha@utep.edu

Abstract

Copula is a powerful tool to describe dependence among variables and has gained significant attention in many fields of research. In this paper, we study modeling the lifetimes of two fundamental hybrid systems: series-parallel and parallel-series by copula functions to reflect the effect on dependence of working components in the systems. We consider Farlie-Gumbel-Morgenstern (FGM) and Clayton copula functions to represent dependent structures in parallel and series configuration, respectively. A flexible lifetime distribution, the extended exponential distribution, is applied to the components of system. The explicit expressions of the reliability and mean time to failure (MTTF) of both hybrid systems are obtained. For the purpose of illustration, the effect of different degrees on dependence among components is analyzed and presented for various parameter settings in the lifetime distribution.

Keywords: series-parallel system, parallel-series system, copula, extended exponential distribution, reliability analysis

1 Introduction

In a system consisting of several components, most researches of reliability analysis focused on a system with all components being either in series or parallel configuration only. In many real situations, however, it is often seen a "hybrid" setup in which the working components are connected in a way of joining together with both series and parallel. For example, air supply systems generally are modular designed, where the power system consists of a number of semiconductor units combined in a series or hybrid circuit [1, 2]. The hybrid structure on its power transmission path makes hybrid electric vehicles possess the major features of both series and parallel systems, and more plentiful operation modes. Hence such design of vehicles has drawn many interests from many automotive companies [3].

We mainly focus on reliability analysis of two fundamental types of hybrid systems: the series-parallel and parallel-series systems with three components shown in Figure 1 since other more complex-system is some kind of composite of the two systems.

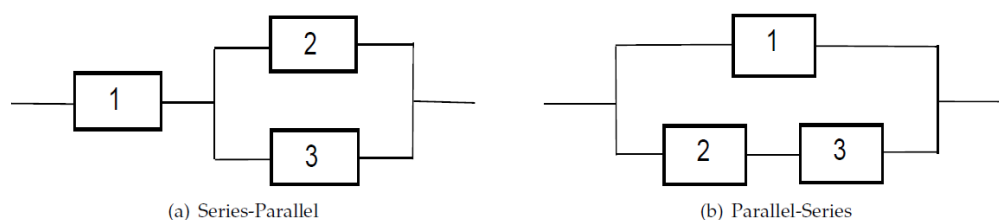(a) Series-Parallel   (b) Parallel-Series

Figure 1: Hybrid Systems of Three Components

In many current literature focusing on system reliability for series or parallel conformation, each component in the system operating or failing is usually assumed to be independent of all the others [4, 5, 6, 7]. However, this assumption may not in line with the actual behavior of system life. In a common environment, components assembled into a system may be subject to the same stress or share the same load. For example, when an aero-engine is operating, the same loads on the blades mounted on one disk to make them rotate together at the same speed [8]. To relax the independent assumption, [9] presented a dependent time failure rate for non-independent components in series systems. In a coherent system including series and parallel systems, [10] and [11] described a multivariate distribution on the lifetimes of dependent components. Due to the difficulty to specify a joint distribution on the dependence situation, an alternative and convenient approach using copula has attracted much attention recently in correlation analysis. Copulas are the mechanisms that allow one to isolate the dependent structure from a multivariate distribution, and different copula functions represent different dependence between variables. The joint distribution of lifetime can be built by modeling dependence among components through a copula function, and hence it makes more convenient and flexible in applications [12]. A number of researchers have focused on employing copulas for modeling dependence in the context of system reliability (see [13, 14, 15, 16, 17], just name a few). Considering the dependence among lifetimes of components depicted by the Clayton copula, [18] investigated a multiple Type-I censored life test of series systems. Using a Gaussian copula to capture the effects of dependence structures on the coherent system reliability, [19] applied and extended the framework to multistate system. In addition, for addressing model uncertainty approximation in a product design space and integrating the model uncertainty into reliability-based design optimization, [20] proposed a copula-based bias modeling approach for reliability and demonstrated by two vehicle design problems.

In this article, we study the system reliability of the two hybrid systems in use of copula function to formalize dependence among components and is organized as follows. Section 2 presents copula functions in modeling the dependent structure of components in the hybrid systems, and Section 3 concentrates on the reliability analysis for the series-parallel and parallel-series systems, respectively. In Section 4, we present numerical and graphical illustrations for the comparisons of system reliability under various dependent situations formalized by copula functions. Lastly we conclude the article with a brief discussion in Section 5.

2 Model by Copula Function

A copula function can capture non-linear association among random variables comprising a vector. The Sklar's Lemma [21] in the case of bivariate variables states: given a bivariate distribution function $H(\cdot,\cdot)$ with two marginals $F(\cdot)$ and $G(\cdot)$, there exists a copula function $C(\cdot,\cdot)$ such that $H(x,y) = C(F(x), G(y))$ for all (x,y) in the domain. In reliability analysis of a system, the dependence structure among the components described by a copula is illustrated as follows. For the hybrid systems displayed in Figure 1, we denote $C_s(\cdot,\cdot)$ and $C_p(\cdot,\cdot)$ as the copulas for the two components in the series and parallel systems, respectively. To make notation simple, let T_i be the lifetime of component i whose density, distribution and reliability/survival functions $f_i(\cdot), F_i(\cdot), \overline{F}_i(\cdot) = 1 - F_i(\cdot)$, and the joint distribution and reliability/survival functions of component i and j are $F_{ij}(\cdot,\cdot), \overline{F}_{ij}(\cdot,\cdot), i, j = 1,2,3$. First, consider the series-parallel system in Figure 1(a), it is obvious that the system life is $T_{sp} = \min(T_1, T_p)$ with the sub-parallel system life $T_p = \max(T_2, T_3)$, and then the system reliability is

$$P(T_{sp} > t) = P(T_1 > t, T_p > t) = P(T_1 > t) + P(T_p > t) - [1 - P(T_1 \le t, T_p \le t)]$$
$$= \overline{F}_1(t) - F_p(t) + C_s(F_1(t), F_p(t))$$
$$= \overline{F}_1(t) - C_p(F_2(t), F_3(t)) + C_s(F_1(t), F_p(t)), t > 0. \tag{1}$$

where

$$F_p(t) = P(T_p \le t) = P(T_2 \le t, T_3 \le t) = C_p(F_2(t), F_3(t)). \tag{2}$$

Likewise, for the the parallel-series system with three components as shown in Figure 1(b), the system life becomes $T_{ps} = \max(T_1, T_s)$ with the sub-series system life $T_s = \min(T_2, T_3)$, and its reliability becomes

$$P(T_{ps} > t) = 1 - P(\max(T_1, T_s) \le t) = 1 - P(T_1 \le t, T_s \le t)$$
$$= 1 - C_p(F_1(t), F_s(t)), t > 0 \tag{3}$$

where

$$F_s(t) = 1 - P(T_2 > t, T_3 > t) = 1 - [P(T_2 > t) + P(T_3 > t) - 1 + P(T_2 \le t, T_3 \le t)]$$
$$= F_2(t) + F_3(t) - C_s(F_2(t), F_3(t)). \tag{4}$$

In reliability, many classic families of distributions such as gamma, Weibull and log-normal, have been studied and applied quite extensively in the literature. Due to the characterizing memoryless property and many other nice properties, exponential distribution has found essential applications in many applied areas such as reliability/survival analysis, operations research and life tests. However, the exponential distribution has a constant failure. In practical situations, observed lifetime data often display varying shapes in the failure rate, and it is desirable that the assumed lifetime distribution has considerable flexibility to capture such characteristics and shapes. Recently, [22] applied an extended exponential distribution to describe dependent components in series and parallel systems. The extended exponential distribution has the distribution, reliability and density functions as follows

$$F(t) = \frac{1 - e^{-\lambda t}}{1 - \bar{\alpha} e^{-\lambda t}}, \overline{F}(t) = \frac{\alpha e^{-\lambda t}}{1 - \bar{\alpha} e^{-\lambda t}}, f(t) = \frac{\alpha \lambda e^{-\lambda t}}{(1 - \bar{\alpha} e^{-\lambda t})^2}, \alpha, \lambda > 0, \bar{\alpha} = 1 - \alpha, t > 0, \tag{5}$$

with α, λ being the shape and scale parameters, and the distribution is denoted by $EE(\alpha, \lambda)$. Obviously $\alpha = 1$ leads to an exponential distribution with scale λ.
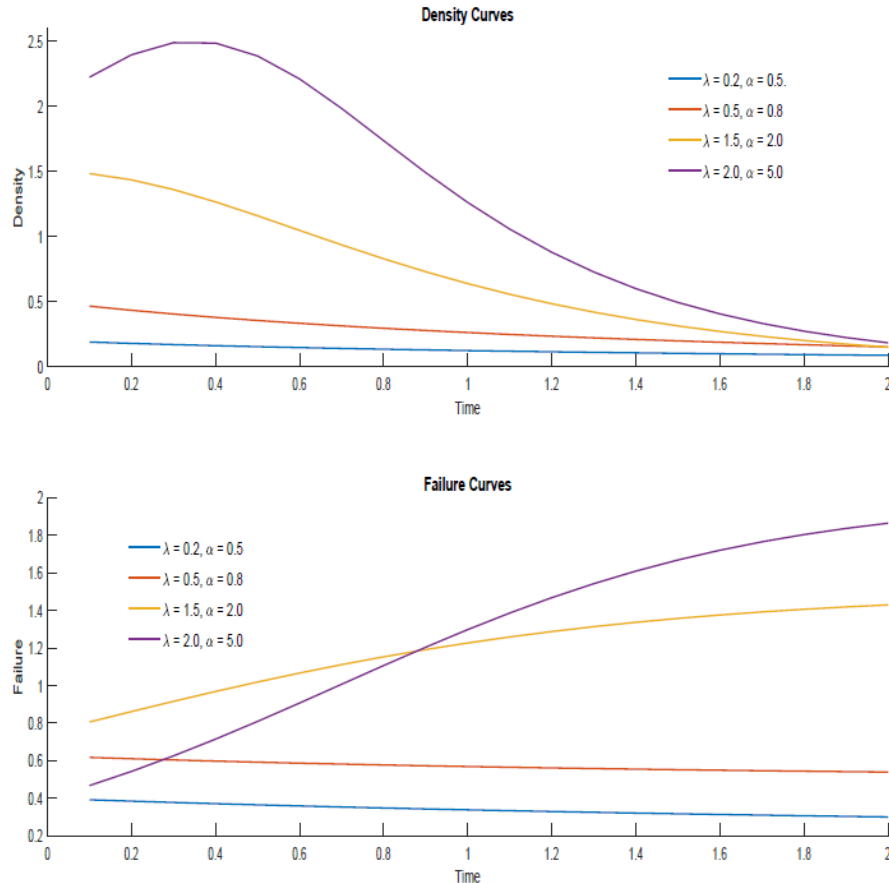

Figure 2: Density and Failure Functions of Extended Exponential Distribution

The density and failure curves of the extended exponential distribution for various settings of parameter values are shown in Figure 2, where one can see that the failures are decreasing over time for $0 < \alpha \leq 1$ while they are increasing for $\alpha > 1$. This extended form of distribution results in a flexible failure function depending on the value of α, called a tilt parameter. More interesting properties and applications of the distriubtion were introduced and discussed recently in [23, 24, 25, 26, 27].

3 Reliability of Hybrid Systems

The reliability analysis of the two hybrid systems is presented in this section. Besides real-time reliability, the mean time to failure (MTTF) is another important measure to explore the effect of dependent components in the system, and so we exhibit the MTTFs $E(T_{sp})$ and $E(T_{ps})$ for the series-parallel and parallel-series systems under various dependent degrees among components.

3.1 Independent Components

For independent components in the system, the applied copulas are $C_p(u, v) = C_s(u, v) = uv$. Then the reliability function for series-parallel system in (??) becomes

$$\overline{F}_{sp}(t) = \overline{F}_1(t) - F_2(t)F_3(t) + F_1(t)F_p(t) = \overline{F}_1(t) - F_2(t)F_3(t) + F_1(t)F_2(t)F_3(t)$$
$$= \overline{F}_1(t)[1 - F_2(t)F_3(t)]. \tag{6}$$

Assuming that each component follows an identical $EE(\alpha, \lambda)$ in (5), we have $F_i(t) = F(t) = \frac{1 - e^{-\lambda t}}{1 - \overline{\alpha} e^{-\lambda t}}, i = 1,2,3$. To make notation simple in the presentation, we omit the time t in the distribution and reliability functions to designate $F = F(t), \overline{F} = \overline{F}(t)$, etc. Then the reliability for the series-parallel system becomes

$$\overline{F}_{sp} = \overline{F}(1 - F^2) = 2\overline{F}^2 - \overline{F}^3. \tag{7}$$

To compute the MTTF of systems, first let $\gamma(k) = \int_0^\infty \overline{F}^k(t) dt, k = 1,2,\cdots$. Taking substitution by $x = 1 - \overline{\alpha} e^{-\lambda t}$, the integrals are calculated as follows

$$\gamma(1) = \int_0^\infty \overline{F}(t) dt = \int_0^\infty \frac{\alpha e^{-\lambda t}}{1 - \overline{\alpha} e^{-\lambda t}} dt = \frac{\alpha}{\overline{\alpha}\lambda} \int_\alpha^1 \frac{1}{x} dx = -\frac{\alpha}{\overline{\alpha}\lambda} \log\alpha, \tag{8}$$

$$\gamma(k) = \int_0^\infty \overline{F}^k(t) dt = \int_0^\infty \left(\frac{\alpha e^{-\lambda t}}{1 - \overline{\alpha} e^{-\lambda t}}\right)^k dt = \frac{\alpha^k}{\overline{\alpha}^k \lambda} \int_\alpha^1 \frac{(1-x)^{k-1}}{x^k} dx$$
$$= \frac{\alpha^k}{\overline{\alpha}^k \lambda} \sum_{r=0}^{k-1} (-1)^r \binom{k-1}{r} \int_\alpha^1 x^{r-k} dx$$
$$= \frac{\alpha^k}{\overline{\alpha}^k \lambda} \left[\sum_{r=0}^{k-2} (-1)^r \binom{k-1}{r} \frac{1 - \alpha^{r-k+1}}{r-k+1} + (-1)^k \log\alpha\right], k = 2,3,\cdots \tag{9}$$

Then the MTTF for the series-parallel system is

$$E(T_{sp}) = \int_0^\infty \overline{F}_{sp}(t) dt = 2\int_0^\infty \overline{F}^2 dt - \int_0^\infty \overline{F}^3 dt = 2\gamma(2) - \gamma(3)$$
$$= \frac{\alpha}{\overline{\alpha}^3 \lambda} \left[\frac{1}{2}\alpha^2 - 2\alpha + \frac{3}{2} - \alpha(\alpha - 2)\log\alpha\right] = \frac{g_{sp}(\alpha)}{2\lambda}. \tag{10}$$

As a special case, when $\alpha = 1$, the MTTF is obtained through the L'Hopital's rule

$$\lim_{\alpha \to 1} g_{sp}(\alpha) = \lim_{\alpha \to 1} \frac{\alpha(\alpha^2 - 4\alpha + 3) - 2\alpha^2(\alpha - 2)\log\alpha}{(1-\alpha)^3}$$
$$= \lim_{\alpha \to 1} \frac{\alpha^2 - 4\alpha + 3 - 2(3\alpha^2 - 4\alpha)\log\alpha}{-3(1-\alpha)^2}$$
$$= \lim_{\alpha \to 1} \frac{-2\alpha + 2 - (6\alpha - 4)\log\alpha}{3(1-\alpha)}$$
$$= \lim_{\alpha \to 1} \frac{-2 - 6\log\alpha - \frac{6\alpha - 4}{\alpha}}{-3} = \frac{4}{3}.$$

Hence $E(T_{sp}) = 2/(3\lambda)$ in the case of exponential lifetime for each component. Similarly, for the parallel-series system, the reliability function in (??) under independent components is

$$\overline{F}_{ps}(t) = 1 - F_1(t)F_s(t) = 1 - F_1(t)[F_2(t) + F_3(t) - F_2(t)F_3(t)]$$
$$= 1 - F_1(t)[1 - \overline{F}_2(t)\overline{F}_3(t)] = \overline{F}_1(t) + F_1(t)\overline{F}_2(t)\overline{F}_3(t). \tag{11}$$

For the identical lifetime distribution $EE(\alpha, \lambda)$ in (5), the reliability becomes

$$\overline{F}_{ps} = \overline{F} + \overline{F}^2 F = \overline{F} + \overline{F}^2 - \overline{F}^3, \tag{12}$$

and the MTTF is

$$E(T_{ps}) = \int_0^\infty \overline{F}_{ps}(t)dt = \gamma(1) + \gamma(2) - \gamma(3)$$
$$= \frac{\alpha}{\alpha^3 \lambda}\left[-\frac{1}{2}\alpha^2 + \frac{1}{2} - (\alpha^2 - 3\alpha + 1)\log\alpha\right] = \frac{g_{sp}(\alpha)}{2\lambda}. \tag{13}$$

By the L'Hopital's rule, the MTTF when $\alpha = 1$ becomes

$$\lim_{\alpha \to 1} g_{ps}(\alpha) = \lim_{\alpha \to 1} \frac{-\alpha^3 + \alpha - 2\alpha(1 - 3\alpha + \alpha^2)\log\alpha}{(1-\alpha)^3}$$
$$= \lim_{\alpha \to 1} \frac{-5\alpha^2 + 6\alpha - 1 - 2(3\alpha^2 - 6\alpha + 1)\log\alpha}{-3(1-\alpha)^2}$$
$$= \lim_{\alpha \to 1} \frac{-10\alpha + 6 - 2(6\alpha - 6)\log\alpha - \frac{2(3\alpha^2 - 6\alpha + 1)}{\alpha}}{6(1-\alpha)}$$
$$= \lim_{\alpha \to 1} \frac{9 - 8\alpha - \frac{1}{\alpha} - (6\alpha - 6)\log\alpha}{3(1-\alpha)}$$
$$= \lim_{\alpha \to 1} \frac{-8 + \frac{1}{\alpha^2} - 6\log\alpha - \frac{-6 + 6\alpha}{\alpha}}{-3} = \frac{7}{3}.$$

Hence $E(T_{sp}) = 7/(6\lambda)$ for independent components with exponential lifetime in the system.

3.2 Dependent Components

First we consider a Farlie-Gumbel-Morgenstern (FGM) copula family which was adopted in [28, 29] to describe relationship of lifetimes for working components in both parallel and series systems. For the sub-parallel system (consisting components 2 & 3) in Figure 1(a) and sub-series system (consisting components 2 & 3) in Figure 1(b), we assume that the dependence structure of components is generated by FGM copulas, given by,

$$C_p(u, v) = uv + \theta_p uv(1 - u)(1 - v), C_s(u, v) = uv + \theta_s uv(1 - u)(1 - v), \tag{14}$$

where $-1 \le \theta_p, \theta_s \le 1$ are the parameters in the copulas used in parallel and series systems. Under the assumption that each component lifetime follows the identical $EE(\alpha, \lambda)$ in (5), i.e. $F_i(t) = F(t) = \frac{1 - e^{-\lambda t}}{1 - \bar{\alpha}e^{-\lambda t}}, i = 1,2,3$, the expression in (2) in series-parallel system becomes with omitting time t is $F_p = C_p(F, F) = F^2(1 + \theta_p \overline{F}^2)$, and so the reliability function is

$$\overline{F}_{sp} = \overline{F} - C_p(F, F) + C_s(F, F_p) = \overline{F} - F^2(1 + \theta_p \overline{F}^2) + FF_p(1 + \theta_s \overline{F}\overline{F}_p)$$
$$= \overline{F} - F^2(1 + \theta_p \overline{F}^2) + F^3(1 + \theta_p \overline{F}^2)\left\{1 + \theta_s \overline{F}[1 - F^2(1 + \theta_p \overline{F}^2)]\right\}$$
$$= \overline{F} - F^2 + F^3 - F^2\overline{F}^3\theta_p + F^3\overline{F}^2(2 - \overline{F})\theta_s + F^3\overline{F}^3(1 - 2F^2)\theta_p\theta_s - F^5\overline{F}^5\theta_p^2\theta_s$$
$$= \overline{A}_1 + \overline{A}_2\theta_p + \overline{A}_3\theta_s + \overline{A}_4\theta_p\theta_s + \overline{A}_5\theta_p^2\theta_s, \tag{15}$$

where

$$\overline{A}_1 = 2\overline{F}^2 - \overline{F}^3, \overline{A}_2 = -\overline{F}^3 + 2\overline{F}^4 - \overline{F}^5, \overline{A}_3 = 2\overline{F}^2 - 7\overline{F}^3 + 9\overline{F}^4 - 5\overline{F}^5 + \overline{F}^6,$$
$$\overline{A}_4 = -\overline{F}^3 + 7\overline{F}^4 - 17\overline{F}^5 + 19\overline{F}^6 - 10\overline{F}^7 + 2\overline{F}^8,$$
$$\overline{A}_5 = -\overline{F}^5 + 5\overline{F}^6 - 10\overline{F}^7 + 10\overline{F}^8 - 5\overline{F}^9 + \overline{F}^{10}. \tag{16}$$

Thus, we have

$$E(T_{sp}) = \int_0^\infty \overline{F}_{sp}(t)dt = A_1 + A_2\theta_p + A_3\theta_s + A_4\theta_p\theta_s + A_5\theta_p^2\theta_s, \tag{17}$$

with

$$A_1 = E(\overline{A}_1) = 2\gamma(2) - \gamma(3) = \frac{\alpha}{\alpha^3\lambda}\left[\frac{1}{2}\alpha^2 - 2\alpha + \frac{3}{2} - \alpha(\alpha - 2)\log\alpha\right], \tag{18}$$

$$A_2 = E(\overline{A}_2) = -\gamma(3) + 2\gamma(4) - \gamma(5) = \frac{\alpha}{\alpha^5\lambda}\left[\frac{1}{12}\alpha^4 - \frac{2}{3}\alpha^3 + \frac{2}{3}\alpha - \frac{1}{12} + \alpha^2\log\alpha\right], \tag{19}$$

$$A_3 = E(\overline{A}_3) = 2\gamma(2) - 7\gamma(3) + 9\gamma(4) - 5\gamma(5) + \gamma(6)$$
$$= \frac{\alpha}{\alpha^6\lambda}\left[\frac{2}{15}\alpha^5 - \frac{11}{12}\alpha^4 + 3\alpha^3 - \frac{13}{3}\alpha^2 + \frac{5}{3}\alpha + \frac{9}{20} - \alpha(\alpha - 2)\log\alpha\right], \tag{20}$$

$$A_4 = E(\overline{A}_4) = -\gamma(3) + 7\gamma(4) - 17\gamma(5) + 19\gamma(6) - 10\gamma(7) + 2\gamma(8)$$
$$= \frac{\alpha}{\alpha^8\lambda}\left[\frac{1}{70}\alpha^7 - \frac{3}{20}\alpha^6 + \frac{13}{15}\alpha^5 - \frac{11}{12}\alpha^4 - \frac{13}{6}\alpha^3 + \frac{137}{60}\alpha^2 + \frac{1}{15}\alpha + \frac{1}{420}\right.$$
$$\left. -\alpha^2(\alpha^2 - 2\alpha - 1)\log\alpha\right], \tag{21}$$

$$A_5 = E(\overline{A}_5) = -\gamma(5) + 5\gamma(6) - 10\gamma(7) + 10\gamma(8) - 5\gamma(9) + \gamma(10)$$
$$= \frac{\alpha}{\alpha^{10}\lambda}\left[-\frac{1}{630}\alpha^9 + \frac{1}{56}\alpha^8 - \frac{2}{21}\alpha^7 + \frac{1}{3}\alpha^6 - \alpha^5 + \frac{1}{5}\alpha^4 + \frac{2}{3}\alpha^3\right.$$

$$-\frac{1}{7}\alpha^2 + \frac{1}{42}\alpha - \frac{1}{504} + \alpha^4\log\alpha\Big]. \tag{22}$$

Note that when $\theta_p = \theta_s = 0$ for the case of independent components, MTTF is the coefficient A_1 which is the same as the expression in (??). Likewise, for the parallel-series system with the expression in (??) being $F_s = 2F - F^2(1 + \theta_s\overline{F}^2)$, the reliability function is

$$\overline{F}_{ps} = 1 - C_p(F, F_s) = 1 - FF_s(1 + \theta_p\overline{F}\overline{F}_s) = 1 - F^2[(1+\overline{F}) - \theta_s F\overline{F}^2][1 + \theta_p\overline{F}^3(1 +$$
$$\theta_s F^2)]$$

$$= \overline{B}_1 + \overline{B}_2\theta_p + \overline{B}_3\theta_s + \overline{B}_4\theta_p\theta_s + \overline{B}_5\theta_p\theta_s^2, \tag{23}$$

where

$$\overline{B}_1 = \overline{F} + \overline{F}^2 - \overline{F}^3, \overline{B}_2 = -\overline{F}^3 + \overline{F}^4 + \overline{F}^5 - \overline{F}^6,$$
$$\overline{B}_3 = \overline{F}^2 - 3\overline{F}^3 + 3\overline{F}^4 - \overline{F}^5, \overline{B}_4 = -\overline{F}^3 + 3\overline{F}^4 - \overline{F}^5 - 5\overline{F}^6 + 6\overline{F}^7 - 2\overline{F}^8,$$
$$\overline{B}_5 = \overline{F}^5 - 5\overline{F}^6 + 10\overline{F}^7 - 10\overline{F}^8 + 5\overline{F}^9 - \overline{F}^{10}. \tag{24}$$

Thus, we have

$$E(T_{ps}) = \int_0^\infty \overline{F}_{ps}(t)dt = B_1 + B_2\theta_p + B_3\theta_s + B_4\theta_p\theta_s + B_5\theta_p\theta_s^2, \tag{25}$$

with

$$B_1 = E(\overline{B}_1) = \gamma(1) + \gamma(2) - \gamma(3) = \frac{\alpha}{\alpha^3\lambda}\Big[-\frac{1}{2}\alpha^2 + \frac{1}{2} - (\alpha^2 - 3\alpha + 1)\log\alpha\Big], \tag{26}$$

$$B_2 = E(\overline{B}_2) = -\gamma(3) + \gamma(4) + \gamma(5) - \gamma(6) = \frac{\alpha}{\alpha^6\lambda}\Big[-\frac{2}{15}\alpha^5 + \frac{5}{4}\alpha^4 - \frac{1}{3}\alpha^3 - \frac{5}{3}\alpha^2$$
$$+\alpha - \frac{7}{60} - \alpha^2(2\alpha - 1)\log\alpha\Big], \tag{27}$$

$$B_3 = E(\overline{B}_3) = \gamma(2) - 3\gamma(3) + 3\gamma(4) - \gamma(5)$$
$$= \frac{\alpha}{\alpha^5\lambda}\Big[-\frac{1}{12}\alpha^4 + \frac{1}{2}\alpha^3 - \frac{3}{2}\alpha^2 + \frac{5}{6}\alpha + \frac{1}{4} + \alpha\log\alpha\Big], \tag{28}$$

$$B_4 = E(\overline{B}_4) = -\gamma(3) + 3\gamma(4) - \gamma(5) - 5\gamma(6) + 6\gamma(7) - 2\gamma(8)$$
$$= \frac{\alpha}{\alpha^8\lambda}\Big[-\frac{1}{70}\alpha^7 + \frac{7}{60}\alpha^6 - \frac{1}{3}\alpha^5 + \frac{37}{12}\alpha^4 - \frac{19}{6}\alpha^3 - \frac{7}{60}\alpha^2 + \frac{7}{15}\alpha - \frac{1}{28}$$
$$-\alpha^2(\alpha^2 + 2\alpha - 1)\log\alpha], \tag{29}$$

$$B_5 = E(\overline{B}_5) = \gamma(5) - 5\gamma(6) + 10\gamma(7) - 10\gamma(8) + 5\gamma(9) - \gamma(10)$$
$$= \frac{\alpha}{\alpha^{10}\lambda}\Big[\frac{1}{630}\alpha^9 - \frac{1}{56}\alpha^8 + \frac{2}{21}\alpha^7 - \frac{1}{3}\alpha^6 + \alpha^5 - \frac{1}{5}\alpha^4 - \frac{2}{3}\alpha^3$$
$$+\frac{1}{7}\alpha^2 - \frac{1}{42}\alpha + \frac{1}{504} - \alpha^4\log\alpha\Big]. \tag{30}$$

Note that the coefficient B_1 is the MTTF when $\theta_p = \theta_s = 0$, corresponding to the case of independent components, whose expression is the same as in (??).

3.3 Different Copulas

For FGM copula family, the Kendall's tau, which measures the "concordance" of bivariate random variables, is $\tau_\theta = 2\theta/9$, resulting in $\tau_\theta \in [-2/9, 2/9]$ for $-1 \le \theta \le 1$. The limited range of dependence restricts the usefulness of this family for application [30]. Since there is usually a stronger correlation of lifetimes among the components in series systems than in parallel systems, it is not appropriate to use FGM copula for modeling an association between component lifetimes in a series system as presented in [28]. [18] used the Clayton copula, a member of Archimedean family, to correlate the lifetimes of components in a series system due to $\tau_\theta = \theta/(\theta + 2) \in [0,1)$ for $\theta \ge 0$, a larger range of dependence. Hence we assume that the dependence structures of components are generated, respectively, by FGM copula in the sub-parallel system (consisting of components 2 & 3) in Figure 1(a) and Clayton copula in the sub-series system (consisting of components 2 & 3) in Figure 1(b). The FGM and Clayton copulas are given by

$$C_f(u,v) = uv + \theta_f uv(1-u)(1-v), C_l(u,v) = (u^{-\theta_l} + v^{-\theta_l} - 1)^{-\frac{1}{\theta_l}}, \tag{31}$$

where $-1 \le \theta_f \le 1$ and $\theta_l \ge 0$ are the parameters in the copulas used in parallel and series systems. From the reliability expression in (??) for the series-parallel system, the system reliability is

$$\overline{F}_{sp}(t) = \overline{F}_1(t) - C_f(F_2(t), F_3(t)) + C_l(F_1(t), F_p(t)), t > 0, \tag{32}$$

with $F_p(t) = C_f(F_2(t), F_3(t))$. For the identical $EE(\alpha, \lambda)$, $F_i = F, i = 1,2,3$ in (5), we have $F_p = C_f(F, F) = F^2(1 + \theta_f\overline{F}^2)$ and $C_l(F, F_p) = (F^{-\theta_l} + F_p^{-\theta_l} - 1)^{-1/\theta_l}$, and the reliability becomes

$$\overline{F}_{sp} = \overline{F} - C_f(F,F) + C_l(F,F_p) = \overline{F} - F^2(1 + \theta_f \overline{F}^2) + C_l(F,F_p) = \overline{C}_1 + \overline{C}_2 \theta_f, \tag{33}$$

where the coefficients

$$\overline{C}_1 = 3\overline{F} - \overline{F}^2 + C_l(F,F_p) - 1, \tag{34}$$

$$\overline{C}_2 = -\overline{F}^2 + 2\overline{F}^3 - \overline{F}^4. \tag{35}$$

Thus, the MTTF of the system

$$E(T_{sp}) = \int_0^\infty \overline{F}_{sp}(t)dt = C_1 + C_2 \theta_f, \tag{36}$$

with

$$C_1 = E(\overline{C}_1) = 3\gamma(1) - \gamma(2) + I_c = \frac{\alpha}{\alpha^2 \lambda}[\alpha - 1 + (2\alpha - 3)\log\alpha] + I_c, \tag{37}$$

$$C_2 = E(\overline{C}_2) = -\gamma(2) + 2\gamma(3) - \gamma(4) = \frac{\alpha}{\alpha^4 \lambda}\left[-\frac{1}{6}\alpha^3 + \alpha^2 - \frac{1}{2}\alpha - \frac{1}{3} - \alpha\log\alpha\right], \tag{38}$$

where the integral $I_c = \int_0^\infty [C_l(F,F_p) - 1]dt$ has no analytic form and a numerical method has to be applied for evaluation. Note that if $\theta_f = \theta_l = 0$, then $F_p = C_f(F,F) = F^2$ and $C_l(F,F_p) = F^3$, and thus the coefficient $C_1 = 3\gamma(1) - \gamma(2) + \int_0^\infty (F^3 - 1)dt = 3\gamma(1) - \gamma(2) + \int_0^\infty [-3\overline{F} + 3\overline{F}^2 - \overline{F}^3]dt = 2\gamma(2) - \gamma(3)$ is the same as A_1 in (18), corresponding to the MTTF in the case of independent components, shown in (??).

Likewise, for the parallel-series system with three components as shown in Figure 1(b), the system reliability in (??) becomes

$$\overline{F}_{ps}(t) = 1 - C_f(F_1(t), F_s(t)), t > 0, \tag{39}$$

where

$$F_s(t) = F_2(t) + F_3(t) - C_l(F_2(t), F_3(t)). \tag{40}$$

Under the identical $EE(\alpha,\lambda)$ lifetime, $F_s = 2F - C_l(F,F)$ with $C_l(F,F) = (2F^{-\theta_l} - 1)^{-1/\theta_l}$, the reliability function is

$$\overline{F}_{ps} = 1 - C_f(F,F_s) = 1 - FF_s(1 + \theta_f \overline{FF}_s)$$
$$= 1 - F[2F - C_l(F,F)][1 + \theta_f \overline{F}(2\overline{F} - 1 + C_l(F,F))] = \overline{D}_1 + \overline{D}_2 \theta_f, \tag{41}$$

where

$$\overline{D}_1 = 2(2\overline{F} - \overline{F}^2) + FC_l(F,F) - 1, \tag{42}$$

$$\overline{D}_2 = 2(\overline{F} - 4\overline{F}^2 + 5\overline{F}^3 - 2\overline{F}^4) + F\overline{F}C_l(F,F)[C_l(F,F) + 4\overline{F} - 3]. \tag{43}$$

It follows that

$$E(T_{ps}) = \int_0^\infty \overline{F}_{ps}(t)dt = D_1 + D_2 \theta_f, \tag{44}$$

with

$$D_1 = E(\overline{D}_1) = 2[2\gamma(1) - \gamma(2)] + I_{d1} = \frac{\alpha}{\alpha^2 \lambda}[2\alpha - 2 + 2(\alpha - 2)\log\alpha] + I_{d1}, \tag{45}$$

$$D_2 = E(\overline{D}_2) = 2[\gamma(1) - 4\gamma(2) + 5\gamma(3) - 2\gamma(4)] + I_{d2}$$
$$= \frac{\alpha}{\alpha^4 \lambda}\left[\frac{1}{3}\alpha^3 - \alpha^2 + 5\alpha - \frac{13}{3} - 2(\alpha + 1)\log\alpha\right] + I_{d2}, \tag{46}$$

where the integrals $I_{d1} = \int_0^\infty [FC_l(F,F) - 1]dt, I_{d2} = \int_0^\infty F\overline{F}C_l(F,F)[C_l(F,F) + 4\overline{F} - 3]dt$ have no closed forms and they could be evaluated by a numerical method for computation. Specifically, $\theta_f = \theta_l = 0$ leads to $C_l(F,F) = F^2$, and then the coefficient $D_1 = 2[2\gamma(1) - \gamma(2)] + \int_0^\infty (F^3 - 1)dt = 2[2\gamma(1) - \gamma(2)] + \int_0^\infty [-3\overline{F} + 3\overline{F}^2 - \overline{F}^3]dt = \gamma(1) + \gamma(2) - \gamma(3)$ is the same as B_1 in (26), corresponding to the MTTF under the situation of independent components, as shown in (??).

4 Illustrations

In this section, we present numerical examples to investigate the performance of reliability and MTTF for each hybrid system under the considered copula functions. Since the lifetimes of components usually appear to be concordance strong correlated in series and weak in parallel system, for the FGM copula applied in both series and parallel systems, we specify a larger positive value for the parameter θ_s and a smaller positive value θ_p to bring about their Kendall's tau values accordingly. Similarly, for the Clayton copula which describes dependence structure for the components in a series system, a larger positive value of θ_l seems appropriate. Therefore we specify parameter values $\theta_p = 0.5, \theta_s = 0.8$ for the case of both parallel and series systems whose

components structures are modeled by FGM copulas, and $\theta_f = 0.5, \theta_l = 1.0$ for the case where the parallel and series systems are modeled by FGM and Clayton copulas, respectively. Additionally, with a fixed scale value λ or tilt value α for the extended exponential distribution, a set of parameter values α and λ are specified to investigate their effects on reliability and MTTF of the hybrid systems. Here we consider two settings: $\lambda = 0.5, \alpha = 0.1, 0.2, \cdots, 1.0$ and $\alpha = 0.5, \lambda = 0.1, 0.2, \cdots, 1.0$ for illustrating purpose.

Reliability curves are displayed in Figures 3 for varying α with fixed λ and in Figure 4 for varying λ with fixed α, respectively. The main findings for both hybrid systems are: First, apparently, the reliability increases as α increases with fixed λ, while the reliability decreases as λ increases with fixed α. Secondly, for any pair of (α, λ): (i) as expected, the highest reliability is for the system with independent components, lower for the dependent components with both modeled by FGM copulas, and the lowest with the parallel modeled by FGM and the series modeled by Clayton copula. (ii) the higher reliability is for the parallel-series than the series-parallel system. Thirdly, it seems that there are larger changes of reliability curves with λ changing than with α changing. Lastly, among the three dependent structures, larger differences of reliability occur in the series-parallel while smaller do in the parallel-series system.

The MTTF curves for the hybrid systems with the two settings of (α, λ) above are shown in Figure 5 and 6, respectively. The main features are summarized as follows: (i) For both hybrid systems, the MTTF increases as α increases with fixed λ, while the MTTF decreases as λ increases with fixed α (this is in accordance with the fact that the MTTF is proportional to λ^{-1} in all cases). It seems, however, that the MTTF decreases much faster as λ increases than that MTTF increases as α increases. (ii) Similar to the situation for reliability, the MTTFs of the hybrid systems are highest for independent components, lower for dependent components with FGM copula modeling both systems, and lowest for dependent components with different copula modeling parallel systems by FGM copula and series by Clayton copula. (iii) The MTTFs for the series-parallel system (shown in Figure 5(a)) are lower than the ones for the parallel-series system (shown in Figure 5(b)) at any α value with fixed λ in either independent or dependent structure of components. The same situation is exhibited at various values of λ with fixed α as shown in Figures 6. (iv) Larger differences of MTTFs can be discerned for the series-parallel system across three dependent structures, and less for the parallel-series system. These are consistent with the exhibitions of the reliability curves in Figures 3 and 4.
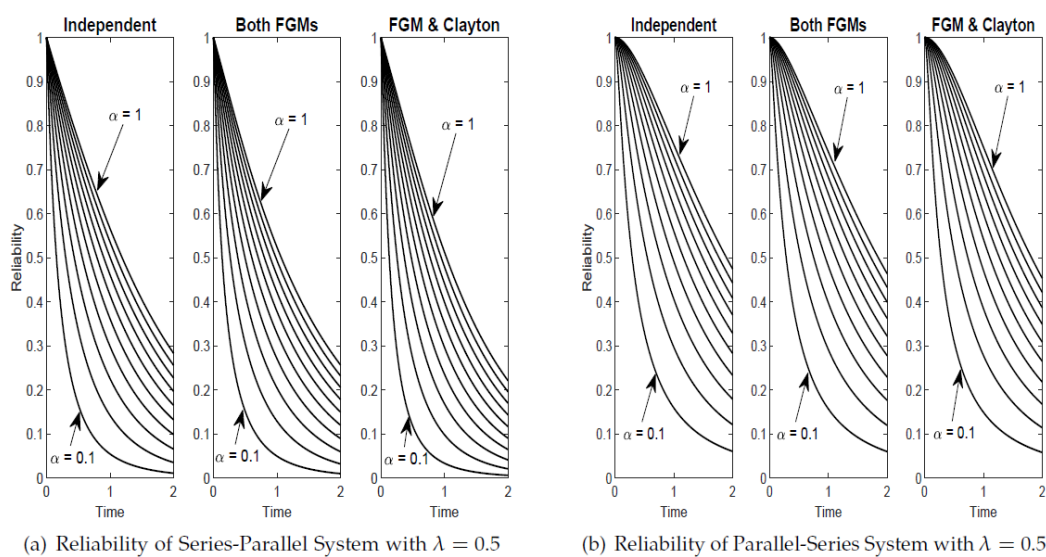

(a) Reliability of Series-Parallel System with $\lambda = 0.5$

(b) Reliability of Parallel-Series System with $\lambda = 0.5$

Figure 3: Comparisons of Reliability in Hybrid Systems

(a) Reliability of Series-Parallel System with $\alpha = 0.5$ (b) Reliability of Parallel-Series System with $\alpha = 0.5$
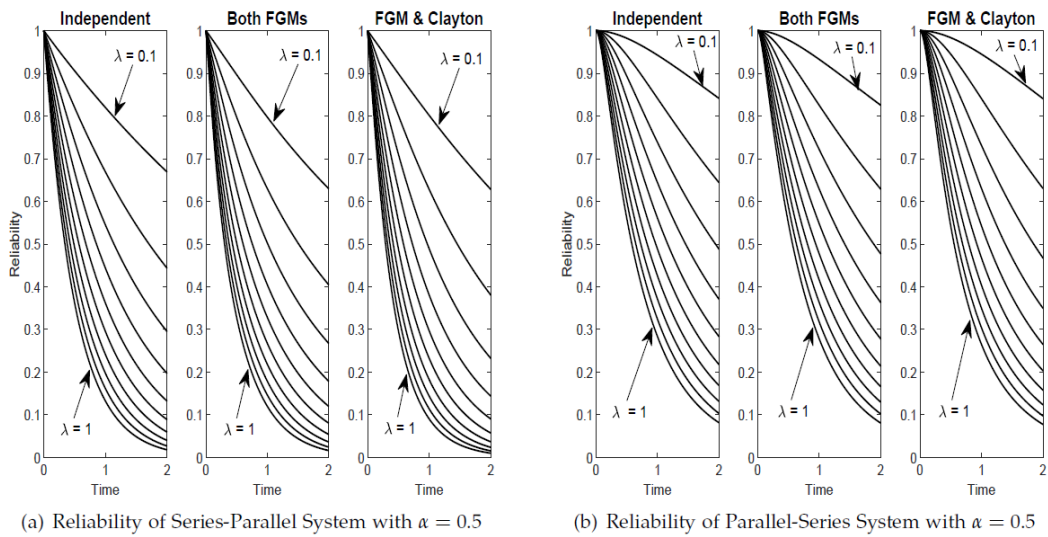
Figure 4: Comparisons of Reliability in Hybrid Systems

(a) MTTF of Series-Parallel System   (b) MTTF of Parallel-Series System
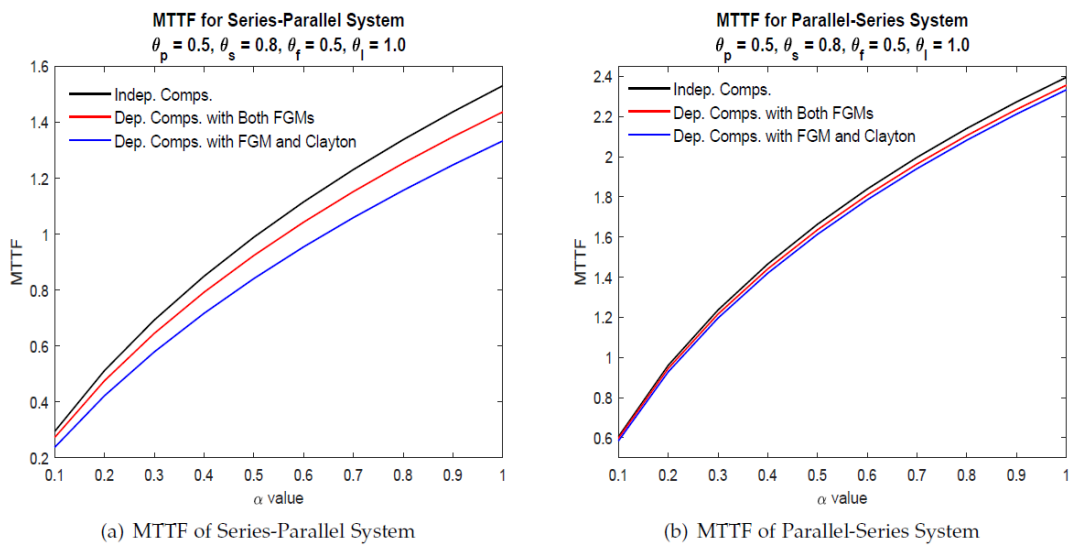
Figure 5: Comparisons of MTTF for Hybrid Systems with $\lambda = 0.5$

(a) MTTF of Series-Parallel System
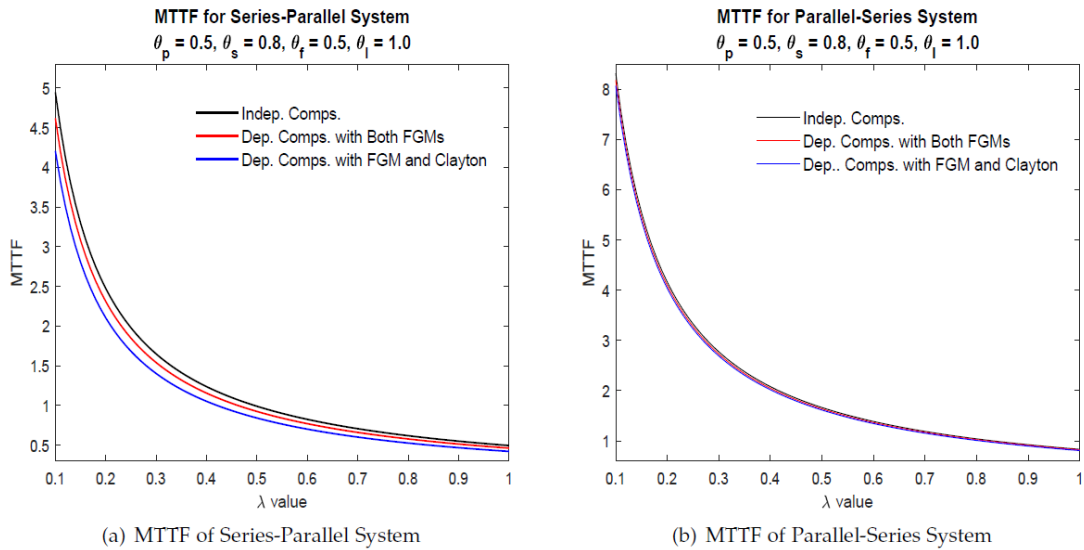
(b) MTTF of Parallel-Series System

Figure 6: Comparisons of MTTF for Hybrid Systems with $\alpha = 0.5$

To further investigate the effect of α and λ values on the system's MTTF under three dependent structures, we display the change rates of MTTF in Tables 1 & 2, where we notice that, for both hybrid systems, the rates are obviously higher for the case of independent components than the ones in the dependent settings in which their changing rates are similar. Furthermore, the change rates are larger in parallel-series system than these in series-parallel system for all cases of dependent structure. These findings are consistent with the curvatures of MTTF displayed in Figures 5 & 6.

Table 1: MTTF Increasing Rate for α with $\lambda = 0.5$

α	0.1	0.2	0.3	0.4	0.5	0.6	0.7	0.8	0.9
				Series-Parallel System					
Independent	2.18	1.81	1.57	1.39	1.26	1.16	1.07	0.99	0.93
Dep. Both FGMs	2.03	1.69	1.47	1.31	1.19	1.09	1.01	0.95	0.89
Dep. FGM & Clayton	1.84	1.57	1.38	1.24	1.13	1.05	0.97	0.91	0.86
				Parallel-Parallel System					
Independent	3.55	2.75	2.29	1.98	1.75	1.58	1.44	1.32	1.23
Dep. Both FGMs	3.49	2.71	2.25	1.95	1.73	1.55	1.42	1.30	1.21
Dep. FGM & Clayton	3.44	2.68	2.24	1.94	1.72	1.55	1.41	1.30	1.21

Table 2: MTTF Decreasing Rate for λ with $\alpha = 0.5$

λ	0.1	0.2	0.3	0.4	0.5	0.6	0.7	0.8	0.9
				Series-Parallel System					
Independent	24.73	8.24	4.12	2.47	1.65	1.18	0.88	0.69	0.55
Dep. Both FGMs	22.11	7.37	3.68	2.21	1.47	1.06	0.79	0.61	0.49
Dep. FGM & Clayton	21.03	7.01	3.50	2.10	1.40	1.00	0.75	0.58	0.47
				Parallel-Parallel System					
Independent	41.59	13.86	6.93	4.16	2.77	1.98	1.49	1.16	0.92
Dep. Both FGMs	40.38	13.46	6.73	4.04	2.69	1.92	1.44	1.12	0.90
Dep. FGM & Clayton	40.34	13.45	6.72	4.03	2.69	1.92	1.44	1.12	0.90

5 Conclusions

In this paper, we have studied reliability analysis of two fundamental hybrid systems: series-parallel and parallel-series, where the lifetimes of dependent components modeled by copula functions. The dependence in parallel and series structures were described by FGM and Clayton copulas to reflect different degree of association, respectively. With the flexible extended exponential lifetime distribution for the components in the system, we obtained the analytic forms of the reliability and mean time to failure (MTTF) of the hybrid systems. Under various parameter settings in the lifetime distribution, the illustrative examples demonstrated that there are higher reliability and longer MTTF for independent components, lower and shorter for FGM dependence in both series and parallel systems, and lowest and shortest for FGM dependence in parallel and Clayton in series. Lastly, in all cases considered, we observed that there are higher reliability and longer MTTF for the parallel-series than the series-parallel system.

References

[1]   Zhang, F. and Shi, Y. (2009). Parameter estimation of the aerospace power supply system using masked lifetime data. *Aerospace Control*, 27(4):96-100.

[2]   Liu, Y. and Shi, Y. (2010). Statistical analysis of the reliability for power supply of spacecraft with masked system life test data, *Aerospace Control*, 28(2):70-74.

[3]   Salmasi, F.R. (2007). Control strategies for hybrid electric vehicles: evolution, classification, comparison, and future trends. *IEEE Transactions on Vehicular Technology*, 56(5):2393-2404.

[4]   Jia, J. and Wu, S. (2009). Optimizing replacement policy for a cold-standby system with waiting repair times. *Applied Mathematics and Computation*, 214(1):133-141.

[5]   Wang, G.J. and Zhang, Y.L. (2011). A bivariate optimal replacement policy for a cold standby repairable system with preventive repair. *Applied Mathematics and Computation*, 218(7):3158-3165.

[6]   Bao, X.Z. and Cui, L.R. (2012). A study on reliability for a two-item cold standby Markov repairable system with neglected failures. *Communications in Statistics: Theory and Methods*, 41(21):3988-3999.

[7]   Jeddi, H. and Doostparast, M. (2015). Optimal redundancy allocation problems in engineering systems with dependent component lifetimes. *Applied Stochastic Models in Business and Industry*, 34(1):84-93.

[8]   Lin, J.W., Zhang, J.H., Yang, S. and Bi, F. (2013). Reliability analysis of aero-engine blades considering nonlinear strength degeneration. *Chinese of Aeronautics*, 26(3):631-637.

[9]   El-Gohary, A.I. (2004). Bayesian estimation of the parameters in two non-independent component series system with dependent time failure rate. *Applied Mathematics and Computation*, 154:41-51.

[10]   Navarro, J., Ruiz, J.M. and Sandoval, C.J. (2007). Properties of coherent systems with dependent components. *Communications in Statistics - Theory and Methods*, 36(1):175-191.

[11] Eryilmaz, S. (2009). Reliability properties of consecutive k-out-of-n systems of arbitrarily dependent components. *Reliability Engineering and System Safety*, 94(2):350-356.

[12] Nelsen, R.B. *An Introduction to Copulas, 2nd Edition*, Springer, New York, 2006

[13] Shih, J.H. and Louis, T.A. (1995). Inferences on the association parameter in copula models for bivariate survival data. *Biometrics*, 51:1384-1399.

[14] Embrechts, P., Linskog, F. and McNiel, A. (2003). Modelling dependence with copulas and applications to risks management. http://www.math.ethz.ch/baltes/ftp/papers.html.

[15] Hong, H., Zhou, W., Zhang, S. and Ye, W. (2014). Optimal condition-based maintenance decisions for systems with dependent stochastic degradation of components. *Reliability Engineering & System Safety*, 121:276-288.

[16] Hao, H. and Su, C. (2014). Bivariate nonlinear diffusion degradation process modeling via copula and MCMC. *Mathematical Problems in Engineering*, 1-11.

[17] Wu, S.M. (2014). Construction of asymmetric copulas and its application in two-dimensional reliability modeling. *European Journal of Operational Research - Stochastics and Statistics*, 238:476-485.

[18] Hsu, T., Emura, T. and Fan, T. (2016). Reliability inference for a copula-based series system life test under multiple type-I censoring. *IEEE Transactions on Reliability*, 65(2):1069-1080.

[19] Zhang, X. and Wilson, A. (2017). System reliability and component importance under dependence: a copula approach. *Technometrics*. 59(2):215-224.

[20] Pan, H., Xi, Z. and Yang, R.J. (2016). Model uncertainty approximation using a copula-based approach for reliability based design optimization. *Structural & Multidisciplinary Optimization*, 54:1543-1556.

[21] Sklar, A. (1959). Functions de repartition a n dimensions et leurs marges. *Publication Institute Statistics University Paris*, 8:229-231.

[22] Barmalzan, G, Ayat, S.M., Balakrishnan, N. and Roozegar, R. (2020). Stochastic comparisons of series and parallel systems with dependent heterogeneous extended exponential components under Archimedean copula. *Journal of Computational and Applied Mathematics*, 380:1-17.

[23] Marshall, A.W. and Olkin, I. (1997). A new method for adding a parameter to a family of distributions with application to the exponential and Weibull families. *Biometrika*, 84:641-652.

[24] Marshall, A.W. and Olkin, I. *Life Distributions*, Springer Verlag, New York, 2007.

[25] Hirose, H. (2002). Maximum likelihood parameter estimation in the extended Weibull distribution and its applications to breakdown voltage estimation. *IEEE Transactions on Reliability*, 9:524-536.

[26] Gupta, R.C., Lvin, S. and Peng, C. (2010). Estimating turning points of the failure rate of the extended Weibull distribution. *Computational Statistics & Data Analysis*, 54(4):924-934.

[27] Cordeiro, G.M. and Lemonte, A.J. (2012). On the Marshall-Olkin extended Weibull distribution. *Statistical Papers*. 54:333-353.

[28] Zhang, Y., Sun, Y. and Zhong, L. (2014). Copula function-based reliability analysis of a series system with a single cold standby unit. *Acta Aeronautica Et Astronautica Sinica*, 35(8):2207-2216.

[29] Zhang, Y., Sun, Y., Li, L. and Zhao, M. (2018). Copula-based reliability analysis for a parallel system with a cold standby. *Communications in Statistics - Theory and Methods*, 47(3):562-582.

[30] Joe, H. *Multivariate Models and Dependence Concepts*, Chapman & Hall, London, 1997